



University  
of Glasgow

Brown, David James (2003) *The nature and origin of breccias associated with central complexes and lava fields of the British Tertiary Igneous Province*. PhD thesis.

<http://theses.gla.ac.uk/4297/>

Copyright and moral rights for this thesis are retained by the author

A copy can be downloaded for personal non-commercial research or study, without prior permission or charge

This thesis cannot be reproduced or quoted extensively from without first obtaining permission in writing from the Author

The content must not be changed in any way or sold commercially in any format or medium without the formal permission of the Author

When referring to this work, full bibliographic details including the author, title, awarding institution and date of the thesis must be given

**The nature and origin of breccias associated  
with central complexes and lava fields of the  
British Tertiary Igneous Province**

**David James Brown**  
**BSc. (Hons.) (Glasgow)**

**A thesis presented for the degree of Ph.D.**

**University of Glasgow**  
**Division of Earth Sciences**

**September 2003**

## Abstract

The British Tertiary Igneous Province (BTIP) contains several large 'breccia' outcrops, classically interpreted as 'vent agglomerates' (Harker 1904; Bailey *et al.* 1924; Richey & Thomas 1930). Re-examination of localities on Ardnamurchan, Mull and Skye provides new evidence that many of these represent mass flow deposits, with implications for the environment and topography of the BTIP at the time of deposition.

At Carraig Mhor, east of Carsaig Bay on the south coast of Brolass, Isle of Mull a sequence consisting of ignimbrite, grading vertically into siltstones and sandstones, is overlain by thick, coarse breccias. The breccias comprise pale igneous clasts (2cm – 1m) with crenulate, angular and rounded shapes, set within a dark, fine-grained, laminated, sedimentary matrix. Complex inter-relationships between clasts and matrix are interpreted as reflecting magma-sediment-water interactions. The breccias are interpreted as peperites and the sequence below provides evidence of local silicic pyroclastic activity during the early stages of formation of the Mull Lava Field.

'Breccias' on the Ardnamurchan Peninsula have previously been interpreted as 'vent agglomerates.' Within them, distinct 'Ben Hiant' and 'Northern' vents have been identified (Richey & Thomas 1930). However, there is no evidence for primary pyroclastic or explosive activity forming these deposits, although clasts of ignimbrite indicate earlier silicic pyroclastic activity. The 'breccias' are typically conglomerates with clasts ranging from rounded to (less commonly) sub-angular, and from 2cm up to 3m in size. Shattered 'megablock' deposits (up to 30m in length) are present locally. Together, these deposits form a stratified sequence containing numerous sedimentary structures. Analysis of clast/matrix relationships and of distribution patterns provides evidence for debris flow/avalanche deposition with increasing clast size, heterogeneity and roundness away from 'source.' The developing heterogeneity of the deposits is strongly linked to the underlying geology and a sedimentary watershed is recognised. Initiation of debris flow/avalanche processes may be linked to the uplift of the Ardnamurchan Central Complex. Locally, ignimbrite clasts indicate well-defined areas of pyroclastic deposition and possible updoming. These ignimbrites have not been found *in situ*, but may be linked to pyroclastic activity similar to that identified at Carraig Mhor on Mull.

Similar debris flow textures are identified on Mull and Skye. Breccias at Coire Mor and Barachandroman on Mull reflect the detachment and breaking up of material from the Mull Lava Field, associated with the emplacement of the Mull Central Complex. Breccias at Loch Ba in Central Mull, and at Srath na Creitheach and Kilchrist, southern Skye, lie within ring-dyke and ring-faulted structures and have been linked to processes of central subsidence. These breccias comprise clasts ranging from sub-angular to (less commonly) sub-rounded, and from 2cm up to 3m in size. Shattered 'megaclast' deposits (typically *ca.* 100m long) are present locally. At Srath na Creitheach, gabbro megablocks rest on a cataclastic basal layer composed of brecciated gabbro. The Srath na Creitheach and Kilchrist deposits form stratified sequences containing various sedimentary structures, including grading, clast imbrication, channels and erosional surfaces. Debris flow textures caused by sector collapse, such as shattered megablocks are recognised, and may be linked to models of caldera subsidence, although evidence is not complete. The reworking of fines from the breccia formed interbedded fine-grained units. The presence of debris flow and avalanche characteristics indicate steep slopes and instability associated with, uplift, faulting and heavy rainfall.

The part of the BTIP represented by Ardnamurchan, Mull and Skye comprised upland areas bordered by lowlands including well-drained lakes and local swamps. Palynological evidence from siltstones interbedded with the Ben Hiant conglomerates indicates upland forests, with Pine and Taxodiaceae, and swamps. The Carraig Mhor peperites demonstrate that, locally, igneous activity reached lake margins. Debris flows and avalanche deposits reflect the steep slopes on the flanks of the uplands with movements prompted by heavy rainfall and local uplift.

## Quotation

**“You're going to find that many of the truths we cling to  
depend greatly on our own point of view”**

***Obi-Wan Kenobi from Star Wars Episode VI: Return of the Jedi***

# Table of Contents

Abstract .....	ii
Quotation .....	iv
Table of Contents .....	v
List of Tables .....	ix
List of Figures .....	x
List of Abbreviations .....	xv
Acknowledgements .....	xvi
Declaration .....	xviii
1 Introduction .....	1-1
2 Breccia lithologies of the British Tertiary Igneous Province .....	2-1
2.1 Introduction .....	2-1
2.2 General Stratigraphy .....	2-1
2.3 Ardnamurchan .....	2-5
2.3.1 Ben Hiant Vents .....	2-7
2.3.1.1 Vent 'Walls' .....	2-7
2.3.1.2 Nature of the Ben Hiant 'agglomerates' .....	2-8
2.3.1.3 Petrology of the Ben Hiant Vents .....	2-10
2.3.1.4 The rhythmic model of eruption .....	2-11
2.3.2 The Northern Vents .....	2-13
2.3.3 Glas Eilean Vent .....	2-13
2.4 Mull .....	2-14
2.4.1 Vent Agglomerates / Breccias .....	2-14
2.4.1.1 Materials .....	2-16
2.4.2 Surface Agglomerates / Breccias .....	2-17
2.4.2.1 Coire Mor .....	2-17
2.4.2.2 Barachandroman .....	2-17
2.5 Skye .....	2-18
2.5.1 Harker's Conclusions .....	2-18
2.5.2 Belig .....	2-18
2.5.3 Srath na Creitheach .....	2-20
2.5.4 Kilchrist .....	2-21
2.5.5 Fionn Choire .....	2-22
3 The classification of volcanoclastic rocks .....	3-1
3.1 Introduction .....	3-1
3.2 Early pyroclastic classifications .....	3-2
3.3 The classification of volcanoclastic rocks by Fisher .....	3-2
3.4 Revision of the classification of pyroclastic rocks .....	3-6
3.5 Classification of volcanoclastic rocks of pyroclastic and epiclastic origins ...	3-10
3.6 Grain size textural classes of volcanoclastic rocks .....	3-13
3.6.1 Conglomerate – closed framework (rounded clasts essential) .....	3-13
3.6.2 Conglomerate – open framework (rounded clasts essential) .....	3-14
3.6.3 Breccia – closed framework (angular clasts essential) .....	3-14
3.6.4 Breccia – open framework (angular clasts essential) .....	3-16
3.6.5 Sandstones (sand sized framework grains predominant) .....	3-18
3.6.6 Mudstones (mud sized grade predominant) .....	3-18

4	Epiclastic deposits in volcanic settings .....	4-1
4.1	Introduction .....	4-1
4.2	Time scales of erosion and transport in volcanic settings .....	4-1
4.3	Epiclastic sediment transport .....	4-2
4.3.1	Particulate sediment transport .....	4-4
4.3.1.1	No interstitial medium required .....	4-4
4.3.1.2	Ice as an interstitial medium .....	4-4
4.3.1.3	Water as an interstitial medium .....	4-5
4.3.1.4	Air as an interstitial medium .....	4-6
4.3.2	Sediment transport by mass movement .....	4-6
4.4	Mass movement transport .....	4-7
4.4.1	Definitions .....	4-7
4.4.2	Mass movement as a function of solid fraction and material type ....	4-9
4.4.3	Mass movement as a function of solid fraction and interstitial fluid ..	4-10
4.4.3.1	Low sediment concentration and air .....	4-10
4.4.3.2	Low sediment concentration and water .....	4-11
4.4.3.3	High sediment concentration and air .....	4-11
4.4.3.4	High sediment concentration and water .....	4-12
4.4.3.5	Discussion .....	4-13
4.4.4	Debris flows and debris avalanches .....	4-13
4.4.4.1	Distinction by velocity and motion type .....	4-14
4.4.4.2	Distinction by sedimentary characteristics .....	4-14
4.5	Origin, transport and deposition of debris flows and avalanches .....	4-16
4.5.1	Debris Flows .....	4-16
4.5.2	Debris Avalanches .....	4-18
4.5.3	Flow Transformations .....	4-21
4.6	Lahars .....	4-22
4.7	Turbidites and coarse-grained deltas .....	4-22
4.8	Environments and landscapes .....	4-26
5	Ardnamurchan .....	5-1
5.1	Regional Geology .....	5-1
5.2	Clast Lithologies .....	5-4
5.3	Ben Hiant .....	5-9
5.3.1	Basal contact of the conglomerates .....	5-10
5.3.2	MacLean's Nose Conglomerate Member .....	5-14
5.3.3	Sron Mhor Lower Conglomerate Member .....	5-14
5.3.4	Ben Hiant Lower Siltstone Member .....	5-15
5.3.5	Sron Mhor Middle Conglomerate Member .....	5-16
5.3.6	Ben Hiant Upper Siltstone Member .....	5-20
5.3.7	Sron Mhor Upper Conglomerate Member .....	5-23
5.3.8	Stallachan Dubha Sandstone Member .....	5-23
5.3.9	Stallachan Dubha Conglomerate Member .....	5-25
5.4	Northern Vents .....	5-25
5.4.1	Conglomerate topography and contact relationships .....	5-25
5.4.2	Allt an Doire Dharaich Area .....	5-28
5.4.3	Fascadale Bay to Swordle Cave .....	5-29
5.4.4	Rubha Carrach .....	5-39
5.5	Clast Count Analysis .....	5-42
5.5.1	Introduction .....	5-42
5.5.2	Methods .....	5-45
5.5.3	The Traverses .....	5-45

5.5.4	Allt an Doire Dharaich to Ardtoe Island .....	5-46
5.5.5	Camphouse to Portban .....	5-47
5.5.6	MacLean's Nose to Swordle Cave .....	5-50
5.5.6.1	MacLean's Nose to East Ben Hiant Gully .....	5-50
5.5.6.2	Tom na Gainmheich to Swordle Cave .....	5-52
5.5.6.3	Analysis of both traverses .....	5-52
5.5.7	Rubha Carrach .....	5-54
5.5.8	Allt na Mi Chomhdhail to Tom na Gainmheich .....	5-56
5.5.9	Rubha Carrach to Swordle Cave .....	5-56
5.5.10	Ben Hiant – Vertical Section .....	5-58
5.5.11	Synthesis .....	5-62
5.6	Photo-statistical analysis of preferred clast orientation .....	5-64
5.6.1	Introduction .....	5-64
5.6.2	Associated problems of clast orientation data .....	5-64
5.6.3	Methodology .....	5-65
5.6.3.1	Preparing and measuring an image for analysis .....	5-65
5.6.3.2	Statistical analysis of clast alignment .....	5-67
5.6.4	Results of photo-statistical analysis .....	5-69
5.6.4.1	Ben Hiant Conglomerate Formation .....	5-69
5.6.4.2	Northern Conglomerate Formation .....	5-75
5.6.5	Summary .....	5-77
5.7	Modes of deposition .....	5-77
5.8	Loch Mudle .....	5-88
5.9	Centre 3 'Breccias' .....	5-90
5.10	Palaeotopography and environments .....	5-92
5.11	Synthesis .....	5-93
6	Mull .....	6-1
6.1	Carraig Mhor .....	6-1
6.1.1	Introduction .....	6-1
6.1.2	Geological Setting .....	6-2
6.1.3	Field Relationships of the Breccias .....	6-2
6.1.4	Basal ignimbrites and sedimentary rocks .....	6-6
6.1.5	Breccia Lithologies .....	6-12
6.1.5.1	Foreshore Intrusions .....	6-12
6.1.5.2	Bulbous projections of igneous material on the foreshore ...	6-15
6.1.5.3	The Lower Blocky Brecciated Lava (LBBL) .....	6-18
6.1.5.4	The Upper Graded Breccia (UGB) .....	6-19
6.1.5.5	Columnar Basalt Lavas .....	6-21
6.1.6	Petrography of the Breccias .....	6-21
6.1.7	Environment of Deposition .....	6-22
6.1.8	Mechanisms of Breccia Formation .....	6-24
6.1.9	Mechanisms of Formation of the Carraig Mhor breccias .....	6-30
6.1.9.1	Variation in Foreshore Magma Injections .....	6-30
6.1.9.2	The origin of the Lower Blocky Brecciated Lava .....	6-30
6.1.9.3	Grading and Transition in Clast Morphology .....	6-31
6.1.10	Conclusions .....	6-34
6.2	Loch Ba .....	6-37
6.2.1	Introduction .....	6-37
6.2.2	Regional geology and setting .....	6-37
6.2.2.1	Centre 1 – The Glen More Centre (Early Caldera) .....	6-37
6.2.2.2	Centre 2 – Beinn Chaisgidle Centre .....	6-38

6.2.2.3	Centre 3 – Loch Ba Centre (Late Caldera) .....	6-38
6.2.3	Loch Ba Breccia Formation .....	6-40
6.2.4	Associated rocks of the Loch Ba Breccia Formation .....	6-44
6.2.4.1	Central Lava Group basalts .....	6-44
6.2.4.2	Rhyolites .....	6-44
6.2.4.3	Dolerites and gabbro .....	6-46
6.2.5	Mode(s) of deposition .....	6-46
6.2.6	Conclusions .....	6-49
6.3	Coire Mor .....	6-50
6.4	Barachandroman .....	6-52
6.5	Salen .....	6-52
7	Skye .....	7-1
7.1	Regional setting .....	7-1
7.2	Srath na Creitheach .....	7-4
7.2.1	Introduction .....	7-4
7.2.2	Previous Research .....	7-4
7.2.3	Srath na Creitheach Breccia Formation .....	7-6
7.2.4	Modes of deposition .....	7-16
7.2.5	Conclusion .....	7-21
7.3	Kilchrist .....	7-21
7.3.1	Introduction .....	7-21
7.3.2	Previous Research .....	7-21
7.3.3	Further Research .....	7-24
7.3.4	Conclusion .....	7-31
8	Discussion: Palaeotopography, environments and modes of formation .....	8-1
8.1	Modes of formation .....	8-1
8.1.1	Epiclastic deposits in the British Tertiary Igneous Province .....	8-1
8.1.2	Peperite formation in the British Tertiary Igneous Province .....	8-13
8.2	Palaeoenvironments of the British Tertiary Igneous Province .....	8-15
8.3	Palaeotopography of the British Tertiary Igneous Province .....	8-19
8.4	Magmatic Processes in the British Tertiary Igneous Province .....	8-21
9	Conclusions .....	9-1
9.1	Debris flows and avalanches .....	9-1
9.2	Peperites .....	9-3
9.3	Palaeoenvironments and topography .....	9-4
9.4	Ignimbrites and silicic intrusions .....	9-6
10	Appendix A: Ignimbrites .....	10-1
11	Appendix B: Samples List .....	11-1
12	Appendix C: Statistics .....	12-1
13	Appendix D: Optical Mineralogy and Cathodoluminescence .....	13-1
14	References .....	14-1

## List of Tables

Table 2.1	A composite stratigraphy for the pre-Palaeogene geology of the Hebridean area of the British Tertiary Igneous Province .....	2.2
Table 3.1	Classification of Volcaniclastic Rocks .....	3.3
Table 3.2	Genetic classification of pyroclastic flows .....	3.8
Table 3.3	Non-genetic classification of volcaniclastic rocks .....	3.10
Table 4.1	Classification of sediment transport processes .....	4.3
Table 4.2	Classification of slope processes by solid fraction and interstitial fluid. ....	4.11
Table 4.3	Key sedimentary characteristics distinguishing sub-aerial debris flow and debris avalanche deposits .....	4.15
Table 5.1	Fabric data of Ben Hiant Conglomerate Formation and Northern Conglomerate Formation mass flow deposits .....	5.73
Table 6.1	Lithostratigraphic subdivisions of the Mull Lava Field Sequence .....	6-3
Table 8.1	Summary of palynological analysis of material collected from interbedded units of the Ben Hiant Conglomerate Formation .....	8.16

## List of Figures

Figure 2.1	Sketch map depicting the distribution of, and inferred relation ships between the Palaeogene lava fields in the Hebridean area of the BTIP .....	2.4
Figure 2.2	Sketch map of the Inner Hebrides area of the BTIP, showing the location of the central complexes and the main structural elements...	2.6
Figure 2.3	Simplified geological map of the Ardnamurchan Central Complex...	2.8
Figure 2.4	Map of the Ben Hiant 'Vent Complex' of Richey & Thomas (1930).	2.9
Figure 2.5	Diagrams to illustrate in section the inferred stages in the early eruptive history of a volcano of the Ben Hiant group (after Richey 1938) .....	2.12
Figure 2.6	Simplified geological map of the Mull Central Complex .....	2.15
Figure 2.7	Simplified geological map of the Skye Central Complex .....	2.19
Figure 3.1	Geometric relations of the three main types of pyroclastic deposit.....	3.7
Figure 3.2	Classification scheme of pyroclastic fall deposits .....	3.8
Figure 3.3	Example of ballistic bombs .....	3.15
Figure 3.4	Welded ignimbrites with eutaxitic textures defined by fiamme .....	3.17
Figure 4.1	Sediment transport by rolling, sliding and saltation .....	4.6
Figure 4.2	Classifications of mass movement on steep slopes .....	4.10
Figure 4.3	Models of surging cohesionless debris flows .....	4.18
Figure 4.4	Debris avalanche transport model .....	4.19
Figure 4.5	Transport and depositional processes in debris avalanches .....	4.20
Figure 4.6	Schematic diagram illustrating genetic relationships of volcanic phenomena and the generation of debris avalanches, debris flows and hyperconcentrated flows .....	4.23
Figure 4.7	Characteristics of low and high concentration turbidity currents and their deposits .....	4.23
Figure 4.8	Schematic diagram of two varieties of steep face, coarse grained deltas .....	4.25
Figure 5.1	Simplified geological map and summary diagram of the Ardnamurchan Central Complex .....	5.3
Figure 5.2	Photomicrographs of clast lithologies from the Ardnamurchan conglomerates .....	5.6
Figure 5.3	Photomicrographs of clast lithologies from the Ardnamurchan conglomerates .....	5.7
Figure 5.4	Photomicrographs of clast lithologies from the Ardnamurchan conglomerates .....	5.8
Figure 5.5	Simplified geological map of the Ben Hiant area, Ardnamurchan ....	5.10
Figure 5.6	Schematic diagram of cliff section of the Ben Hiant Conglomerate Formation .....	5.11
Figure 5.7	Vertical log located north east of David's Gully towards MacLean's Nose, Ardnamurchan .....	5.12
Figure 5.8	Vertical log located south west of David's Gully towards MacLean's Nose, Ardnamurchan .....	5.13
Figure 5.9	Basal contact of BHCF conglomerate overlying lava at a low angle.	5.17
Figure 5.10	The MacLean's Nose Conglomerate Member .....	5.17

Figure 5.11	The Sron Mhor Lower Conglomerate Member .....	5.17
Figure 5.12	The Ben Hiant Lower Siltstone Member .....	5.18
Figure 5.13	The Sron Mhor Middle Conglomerate Member .....	5.18
Figure 5.14	The Ben Hiant Upper Siltstone Member: General features .....	5.19
Figure 5.15	The Ben Hiant Upper Siltstone Member: Photomicrographs and CL images .....	5.22
Figure 5.16	The Sron Mhor Upper Conglomerate Member .....	5.24
Figure 5.17	The Stallachan Dubha Sandstone Member and Stallachan Dubha Conglomerate Member .....	5.24
Figure 5.18	Basal contacts of conglomerate in the Northern Conglomerate Formation .....	5.27
Figure 5.19	Hummocky topography and basalt/conglomerate relationships in the Northern Conglomerate Formation .....	5.27
Figure 5.20	Fine grained lithologies and sedimentary structures from conglomerates in the Allt an Doire Dharaich area, Northern Conglomerate Formation .....	5.28
Figure 5.21	Clast lithologies in the Northern Conglomerate Formation .....	5.31
Figure 5.22	Location map and lithoclast dominated flow units in the Northern Conglomerate Formation .....	5.32
Figure 5.23	Distribution of calcareous sandstone megablocks in the Northern Conglomerate Formation .....	5.33
Figure 5.24	Vertical log of the Rubha na h-Acairseid sandstone and laminated siltstone dominated conglomerate flow units .....	5.33
Figure 5.25	Channel structures in the Rubha na h-Acairseid area .....	5.35
Figure 5.26	Conglomeratic dykes and stratification in the Rubha na h-Acairseid area .....	5.36
Figure 5.27	Kilmory Bay stacks, displaying flow units and lateritic horizons ....	5.37
Figure 5.28	Sedimentary features from Rubha a' Gharaidh Leith .....	5.38
Figure 5.29	Chaotically arranged shale clasts and layers in conglomerate from Swordle Cave .....	5.38
Figure 5.30	Topography and intrusions of the Rubha Carrach area .....	5.41
Figure 5.31	Sedimentary structures from the Rubha Carrach cliff section .....	5.43
Figure 5.32	Vertical log and reconstruction of faulting in the Rubha Carrach conglomerates .....	5.44
Figure 5.33	Map of traverses and sample sites on the Ardnamurchan Peninsula ..	5.46
Figure 5.34	Allt an Doire Dharaich to Ardtoe Island Clast Count Analysis .....	5.48
Figure 5.35	Camphouse to Portban Clast Count Analysis .....	5.49
Figure 5.36	MacLean's Nose to East Ben Hiant Gully Clast Count Analysis .....	5.51
Figure 5.37	Tom na Gainmheich to Swordle Cave Clast Count Analysis .....	5.53
Figure 5.38	MacLean's Nose to Swordle Cave Clast Count Analysis .....	5.55
Figure 5.39	Rubha Carrach Clast Count Analysis .....	5.57
Figure 5.40	Allt na Mi Chomhdhail to Tom na Gainmheich Clast Count Analysis .....	5.59
Figure 5.41	Rubha Carrach to Swordle Cave Clast Count Analysis .....	5.60
Figure 5.42	Ben Hiant-Vertical Section Clast Count Analysis .....	5.61
Figure 5.43	Calculation of clast alignment statistics of mass-flow deposits .....	5.66
Figure 5.44	Diagrammatic representation of measurement of clast orientation ...	5.67
Figure 5.45	Three-dimensional view of an idealised block of a mass flow unit ...	5.70
Figure 5.46	Simplified geological map showing photo-statistical sample points in the Ben Hiant Conglomerate Formation .....	5.70
Figure 5.47	Photographs of vertical side view exposure faces .....	5.72

Figure 5.48	Rose diagrams of Ben Hiant Conglomerate Formation exposures displaying clast alignment and directional fabric strength values ( <i>R</i> ).	5.74
Figure 5.49	Upwards decrease in angle of imbrication, common in volcanoclastic mass flow deposits .....	5.75
Figure 5.50	Simplified geological map showing sample points in the Northern Conglomerate Formation .....	5.76
Figure 5.51	Rose diagrams of Northern Conglomerate Formation exposures displaying clast alignment and directional fabric strength values ( <i>R</i> ).	5.76
Figure 5.52	Typical front view deposit within the Northern Conglomerate Formation .....	5.77
Figure 5.53	Inferred vertical vent wall contact at Richey's Gully .....	5.79
Figure 5.54	Sedimentary watershed in the area around Beinn nan Losgann-Loch Mudle, Ardnamurchan .....	5.81
Figure 5.55	Highly brecciated megaclast or crackle breccia .....	5.82
Figure 5.56	Graded-stratified hyperconcentrated flow deposits .....	5.85
Figure 5.57	Transition from debris avalanche to proto-debris flow to debris flow.....	5.87
Figure 5.58	Peperite lithologies from the Loch Mudle area .....	5.89
Figure 5.59	Net veining textures in the 'Centre 3 breccias' .....	5.91
Figure 5.60	Schematic reconstruction of modes of formation of Ben Hiant Conglomerate Formation and Northern Conglomerate Formation deposits in Ardnamurchan .....	5.95
Figure 6.1	Location map of Carsaig Bay, south coast of Broilass, Ross of Mull, NW Scotland .....	6.3
Figure 6.2	Geological map and cross section through Morvern and the Isle of Mull .....	6.4
Figure 6.3	View of Carraig Mhor coastal section, showing relationships between sedimentary rocks, lavas, breccias and intrusions .....	6.4
Figure 6.4	Schematic diagram of Carsaig Bay cliff section, illustrating field structures and spatial relationships .....	6.5
Figure 6.5	Detailed schematic diagram of Carraig Mhor foreshore platform ....	6.7
Figure 6.6	Detailed log of the Carraig Mhor foreshore platform .....	6.8
Figure 6.7	Ignimbrite and sedimentary units from the Carraig Mhor foreshore platform .....	6.10
Figure 6.8	Shallow intrusion features from Carraig Mhor foreshore platform....	6.13
Figure 6.9	Variations in intrusive contacts and jigsaw fit textures from Carraig Mhor .....	6.14
Figure 6.10	Composite sill features from the Carraig Mhor foreshore platform ...	6.16
Figure 6.11	Bulbous projections of igneous material displaying irregular margins and complex relationships with sediment host .....	6.16
Figure 6.12	Clast types in the Carraig Mhor breccias .....	6.17
Figure 6.13	The Upper Graded Breccia Unit (UGB) .....	6.20
Figure 6.14	Photomicrographs of Carraig Mhor breccias displaying fracture and clast textures .....	6.23
Figure 6.15	Diagrammatic representation of andesite-sandstone interaction at Turnberry, Scotland .....	6.26
Figure 6.16	Diagrammatic representation of coal-magma interaction .....	6.26
Figure 6.17	Diagrammatic representation of peperite formation .....	6.29
Figure 6.18	Diverse injections of magma into sediment from Carraig Mhor foreshore .....	6.32
Figure 6.19	Diagrammatic representation of mode of formation of Carraig Mhor	

	breccias .....	6.33
Figure 6.20	Simplified geological maps of stages of the Mull Central Complex ..	6.39
Figure 6.21	Simplified geological map of the area around Loch Ba, Mull .....	6.41
Figure 6.22	Typical example of Loch Ba Breccia Formation deposits .....	6.41
Figure 6.23	Sedimentary features from the Loch Ba Breccia Formation .....	6.43
Figure 6.24	Fractured and shattered basalt megablocks in the Loch Ba Breccia Formation .....	6.45
Figure 6.25	Photomicrograph of matrix of fine grained clast supported breccia from the lower breccia unit of the Loch Ba Breccia Formation .....	6.46
Figure 6.26	Simplified geological map of the area around Coire Mor, Eastern Mull .....	6.51
Figure 6.27	Field photographs of textures within the Coire Mor breccias .....	6.51
Figure 6.28	Simplified geological map of the area around Barachandroman, South Mull .....	6.53
Figure 6.29	Field photographs of textures within the Barachandroman breccias ..	6.53
Figure 6.30	Simplified geological map of the area around Salen, Eastern Mull ...	6.55
Figure 6.31	Field photographs of textures within the Salen breccias .....	6.55
Figure 7.1	Simplified geological map depicting centres of the Skye Central Complex .....	7.2
Figure 7.2	Map of Loch na Creitheach volcanic vent .....	7.7
Figure 7.3	Typical textures of the Srath na Creitheach Breccia Formation .....	7.7
Figure 7.4	Sandstone features in the Srath na Creitheach Breccia Formation ....	7.9
Figure 7.5	Gabbro-breccia relationships from the Srath na Creitheach Breccia Formation .....	7.11
Figure 7.6	Schematic logs (a) and (b) of Srath na Creitheach Breccia Formation deposits .....	7.14
Figure 7.7	Example of intensely shattered and fractured gabbro slab east of slab 7.....	7.15
Figure 7.8	Schematic reconstruction of gabbro slab textures in the Srath na Creitheach Breccia Formation .....	7.15
Figure 7.9	Evolution of the Rum Caldera .....	7.17
Figure 7.10	Possible hummocky topography of gabbro slabs in the Srath na Creitheach Breccia Formation .....	7.20
Figure 7.11	Geological map of the Kilchrist area, Skye .....	7.22
Figure 7.12	Channel feature in the Kilchrist breccias, SW of Creagan Dubh .....	7.25
Figure 7.13	Sedimentary features from the Kilchrist breccias .....	7.26
Figure 7.14	Photomicrograph displaying sedimentary textures in the Kilchrist breccias .....	7.28
Figure 7.15	Cnoc nam Fitheach to Meall Coire Forsaidh Clast Count Analysis, Kilchrist, Skye .....	7.29
Figure 8.1	Schematic block diagram showing a reconstruction of the palaeogeography of the Ardnamurchan area during the early Tertiary .....	8.9
Figure 8.2	Schematic block diagram showing a reconstruction of the palaeogeography of the Loch Ba area during the early Tertiary .....	8.10
Figure 8.3	Schematic block diagram showing a reconstruction of the palaeogeography of the Srath na Creitheach area during the early Tertiary .....	8.11
Figure 8.4	Schematic block diagram showing a reconstruction of the	8.12

Figure 8.5	palaeogeography of the Kilchrist area during the early Tertiary ..... 8.12
	Simplified cross section showing the relationships of the Ben Hiant Conglomerate Formation with country rock lithologies ..... 8.20

## List of Abbreviations

Where possible, abbreviations are used throughout the text, however reference can be made to this section.

ACC	Ardnamurchan Central Complex
AMS	Anisotropy of Magnetic Susceptibility
BHCF	Ben Hiant Conglomerate Formation
BHLSM	Ben Hiant Lower Siltstone Member
BHUSM	Ben Hiant Upper Siltstone Member
BTIP	British Tertiary Igneous Province
BTVP	British Tertiary Volcanic Province
CL	Cathodoluminescence
IDI	Isotropic Dispersive Inflation
LBBF	Loch Ba Breccia Formation
LBBL	Lower Blocky Brecciated Lava
MCC	Mull Central Complex
MHWS	Mean High Water Springs
MLWS	Mean Low Water Springs
MNCM	MacLean's Nose Conglomerate Member
MORB	Mid Ocean Ridge Basalt
NCF	Northern Conglomerate Formation
PHP	Palaeogene Hebridean Province
RLSC	Rubha na h-Acairseid Laminated Siltstone-dominated Conglomerate
RMGC	Rubha na h-Acairseid Microgranite-dominated Conglomerate
RPS	Rubha na h-Acairseid Pebbly Sandstone
RSstC	Rubha na h-Acairseid Sandstone-dominated Conglomerate
SCC	Skye Central Complex
SDCM	Stallachan Dubha Conglomerate Member
SDSM	Stallachan Dubha Sandstone Member
SMLCM	Sron Mhor Lower Conglomerate Member
SMMCM	Sron Mhor Middle Conglomerate Member
SMUCM	Sron Mhor Upper Conglomerate Member
SNCBF	Srath na Creitheach Breccia Formation
UGB	Upper Graded Breccia

## Acknowledgements

This research was funded by a University of Glasgow 2001 Scholarship and a Mineralogical Society Postgraduate Bursary, both of which are gratefully acknowledged.

My principal supervisor, Dr. Brian Bell, has been an incredible source of encouragement and inspiration throughout the PhD. Always willing to provide ideas and comments as well as excellent observations in the field, Brian has patiently sifted through my seemingly endless piles of text and 'dioramas' with diligence and a keen eye. Brian's advice throughout has been well placed and his style and level of supervision most appreciated. His help in the field, including incorporating me into the Ardnamurchan and Mull trips when much of my research was carried out, has been invaluable. I have particularly enjoyed his company both in the department and in the field where we realised our mutual appreciation of curry and rhubarb crumble (not at the same time). The dodgy jokes were numerous! Thank you Brian for all your help.

My second supervisor, Dr. Colin Braithwaite, has been a wonderful part of my supervising 'team.' Colin's boundless enthusiasm and ideas have been a great help, and his sedimentary input was much needed and appreciated. Colin suggested the traverses and statistical analyses that advanced the research so much, sorted out my epiblastic terminology issues, and always reviewed my text drafts with great detail. His time and effort has been hugely appreciated.

Dr. Chris Burton has always made me feel incredibly welcome in the department, and signed all those claim forms without looking! Dr. Tim Dempster must be thanked for inviting me on the Spain trip in my first year, which was invaluable in my breccia education, and for all his thought-provoking questions. Thanks must also go to Dr. Geoff Tanner for his kind words and all that he has taught me. My time in the department has been greatly eased by Dr. Jeff Harris. Always amusing, always educational and completely mad he has continually put a smile on my face and plied me with fine wines!

Kenny Roberts has worked tirelessly to resolve my numerous computer problems and provide me with loads of stuff. His help in sorting out the Laptops Direct people was hugely appreciated. John Gilleece has done an excellent job turning out numerous thin sections for me, often at short notice, and to an exceptional standard. Our nights working along the top shelf in the Sonachan were memorable (just!).

An essential part of my fieldwork in Ardnamurchan could not have been carried out without the help of Graham McLeod. Graham was the best field assistant imaginable, driving me to numerous localities, carrying rocks, following me up perilous cliff sections and helping me with the clast counts. His assistance, questions, time and effort were hugely appreciated and I could always trust his opinions in the field. Despite his constant moaning and getting me addicted to coffee (!), the memories of salmon curry, field singing, and the caravan will live forever.

Throughout my PhD I have had the honour of working in the field with Dr. Henry Emeleus of the University of Durham. Henry's time, advice and observations have been greatly received and I am forever indebted to him for suggesting that trips to Portban and Rubha Carrach might be useful. I feel very privileged to have worked with such a kind and intelligent man. Dr. John Faithfull of the Hunterian Museum also gave up much of his time to help me in the field on Mull, providing endless enthusiasm and helpful suggestions. Dr. Dave Jolley of the University of Sheffield carried out palynological analysis on some of my samples and their results have been extremely helpful, considerably broadening the scope of my thesis.

In my three years I have been able to work (and socialise!) alongside a fantastic bunch of postgraduates. Stewart Clark has been my partner in crime for most of this period as well as a great flat mate for the last year and a half. Stew, I'll never forget the Oblomov bush incident, the infamous Aberdeen night out, the silly hats, 'Shaft,' the wine do's and above all, rocking to 'Sweet

Child.' Cheers mate! Simon Passey has been a great mate over the years and his dancing and chat up techniques have been legendary to watch. Thanks also Simon for always being there for a good chat, loads of technical help, all the Cheesy Pop nights, 'Dambusting' and above all taking on the roles of 'Simon Danger Powers' and 'Sir Bobby' like no other man could Have It! Being an old git, 'Big Dave' Parkinson should have been a terrific role model for all us young whippersnapper PhD students. However, he has not! Thanks Dave for teaching me all about the wildlife of the Serengeti and how it preys on Stirling residents attempting to travel on the Glasgow Underground. "RC NOW!" Thanks must go to Will Goodwin for all the curry, liqueur, cigars and great company and Jurgen 'JJ' Jacob for being South African, saying 'classique' a lot and for generally being a great guy. Kathy Keefe, Jenny England, Liz Campbell, Liam Reinhardt, Cristina Persano, Claire Pannell, Laiq Rahman, Sarah Stewart, Sally Alexander and Alison Bowdler-Hicks have all been fantastic friends over the years. Thanks in particular to Kathy and Jenny for being so supportive, and Liam for being mad and Irish.

Over this time I have been lucky enough to live with some great flatmates. Torquil MacLeod has been a great flatmate and friend and the Lang's, Pewter Pot, Truffle and Scottish Women's Rugby team nights will never leave me. With Torquil comes Ruth Debenham, who is a fantastic mate and an endless source of mobile phone tips and accessories! Kirsty Milton replaced Torquil in the flat (what an act to follow) and has been a great friend over the years. Cheers Kirsty for your support, discovering 'Bouzo' and converting to rock!

Thanks must also go to Deborah Smith for being my text buddy, producing *the Cheesy Pop CD* and for being such a great laugh.

I'd like to thank all my old undergraduate mates, in particular Esther MacRae (*nee*. Campbell), Martin Gratton, Jen and Graeme Dobbin and Gordon (El Presidente) Ross for all the great times, for staying in touch and all your support.

Of all my mates though, the Barrhead lads must be thanked the most. Over the years you have always been there for me and provided an endless source of entertainment, friendship and Tennent's. I may not be around so much but I'll always be at home with you guys. Cheers to Charlie Bisland, Alister Gemmell, 'Big Gonads' Reilly, Julie McManus, Alan Thomson, Kenny McGuire, Jamie McLaren, Caroline Eason, Alison Cartwright, Garron Crangle, Mark Pignatelli and Davie Hayes, as well as 'Uncle' Ken Campbell and Dave Murray.

All the staff of the RC must be thanked for dealing with us reprobates for the last three years, along with the makers of Sprite, Irn-Bru and Tennent's for various reasons!

The staff of the Sonachan Hotel, in particular Davie, Helen and Eilidh must also be thanked for their wonderful hospitality and tremendous food. The bold Lawrence was always a constant source of amusement.

I would also like to thank the naked Carraig Mhor waterfall chicks, for considerably brightening up an otherwise dull day in the field!

Above all, three people have helped me through this thesis, and ensured its successful completion. I must thank my parents James and Morag, although it is a completely inadequate gesture, for all their support and love over the years. They have given selflessly to ensure my education, health and happiness and I am forever indebted to them. Mum and Dad, I love you and thank you for everything you have ever done for me.

Finally, I must thank Kate Dobson. Kate, you rescued me from my lowest ebb and made me feel alive again. You have helped me with proof reading, shown me tricks on the computer, kept me working hard and put up with my bad moods and computer induced tempers. You never fail to make me smile, have always been there when I felt down, and inspired me to keep on going. You are my best friend, my love. Thank you.

## Declaration

The material presented in this thesis is the result of my own independent research, between October 2000 and September 2003. All previously published or unpublished work by other researchers quoted in this thesis is given full acknowledgement in the text.



David J. Brown

September 2003

# 1 Introduction

The lava fields and exhumed central complexes of the British Tertiary Igneous Province (BTIP) offer a rare opportunity to observe and interpret rocks formed in shallow intrusive through to surface environments associated with basaltic and rhyolitic volcanoes on a rifted continental margin. A wide variety of coarse, clastic rocks and associated deposits are preserved within the central complexes of Ardnamurchan, Arran, Mull, Rum and Skye in Scotland and Carlingford and Slieve Gullion in Northern Ireland. Coarse, clastic deposits are also preserved in the lava fields of Eigg, Mull (including Ardnamurchan) and Skye. These breccias (and conglomerates) are described only briefly in the literature and their origins are poorly understood. Modes of origin are thought to include: intrusive breccia formation above crystallising plutons due to gas escape, the formation of primary pyroclastic deposits in the vicinity of explosive vents, and the development of epiclastic deposits derived from poorly consolidated primary volcanic rocks in the vicinity of vents, or by mass movement. Furthermore, the spatial, genetic and temporal relationships between these rocks and the intrusions of the central complexes are often uncertain. As a result, the original structural level of such fragmental rocks at the time of their formation is unclear.

This project sets out to document a broad spectrum of lithologies in the lava fields and exhumed central complexes of NW Scotland and to classify and explain their origins. From this work, a model will be developed which will relate the various types of breccias and associated rocks to their level and mode of formation, providing new and exciting insights into the evolution of the BTIP.

The NW European continental margin was characterised in the Palaeogene by dramatic igneous activity, which resulted in a series of lava fields, intrusive centres, dyke swarms and sill complexes in the west coast of Scotland. This activity began at *ca.* 60.5 Ma and continued to *ca.* 55 Ma. Following the impact of the proto-Iceland plume at the base of the lithosphere and associated crustal thinning, fissure systems developed (now represented by the dyke swarms) and three lava fields were created on Eigg (including Muck), Mull (including Ardnamurchan and Morvern) and Skye (including Canna) (Bell & Williamson 2002). The lavas are interbedded with a variety of pyroclastic and epiclastic deposits including fluvial and lacustrine units, indicating the intermittent formation of the lava

fields, and environments ranging from upland forests to estuarine conditions (Jolley 1997). This was followed by the emplacement of the central complexes, which are the shallow cores of volcanoes (Emeleus 1982). Controlled by major fault lineaments, the central complexes comprise a series of ring intrusions, stocks and plutons and are of basic and silicic composition (Bell & Williamson 2002).

Associated with these rocks are a series of coarse, clastic deposits. These breccias and conglomerates display a variety of geometries ranging from small exposures only a few metres thick to outcrops of *ca.* 10km<sup>2</sup>. Typically, they comprise heterogeneous clasts set within a matrix of fine, similar comminuted material in both clast and matrix supported relationships. Clasts range from rounded to angular and typically range in size from 2cm to 50cm across, with larger clasts up to 5m. Rarer blocks, or megablocks, are identified which are up to several hundreds of metres across. Interbedded with the breccias are numerous pyroclastic, epiclastic and sedimentary units. The origin of these units is also unclear. In the study area of NW Scotland substantial exposures of breccia associated with the BTIP crop out at: Ben Hiant and the Achateny Valley of Ardnamurchan; Loch Ba, Sgurr Dearg, Coire Mor and Barachandroman on Mull; throughout Rum; and at Belig, Kilchrist and Srath na Creitheach on Skye.

Previous research has favoured an explosive origin for these deposits and therefore pyroclastic nomenclature has been adopted. Classic research on Skye, Mull and Ardnamurchan by Harker (1904), Bailey *et al.* (1924) and Richey & Thomas (1930) respectively, suggested an explosive, pyroclastic origin for these breccias and the term 'vent agglomerate' was used widely. This reflected the explosive breakthrough of overlying country rocks by magmatic and gaseous agents followed by the collapse of material into a crater. This definition was accepted and little research has been carried out on the breccias since. Modern geology however, has seen a substantial leap in our knowledge and understanding of breccia forming processes, as we are now able to observe and accurately measure active volcanic settings. Consequently, a wide variety of pyroclastic, epiclastic and autoclastic modes of fragmentation and deposition are now recognised as forming breccias. Following this new impetus, re-examination of breccia localities at Kilchrist, Skye (Bell, B. R. 1985) and Coire Dubh, Rum (Troll *et al.* 2000, Donaldson *et al.* 2001) suggested an epiclastic mode of deposition, involving processes of mass movement and sub-aerial reworking. Therefore, the need for a more comprehensive re-assessment of breccia lithologies throughout the BTIP is now required.

The objectives of this study are primarily to accurately describe and determine the nature and origin of breccia lithologies associated with central complexes and lava fields of the BTIP. As a result of this work, models can be developed to explain surface and near surface processes of breccia formation within the BTIP. Furthermore, these interpretations have implications for palaeoenvironments and palaeotopography during the formation of the BTIP. These studies were carried out by means of extensive fieldwork in conjunction with petrography and laboratory research. The following field localities were studied in detail: The 'Ben Hiant Vent' and 'Northern Vents' (Richey & Thomas 1930) of Ardnamurchan; Barachandroman, Carraig Mhor, Coire Mor, Loch Ba and Salen on Mull; and Kilchrist and Srath na Creitheach on Skye. Other localities on Ardnamurchan, Mull and Skye were not investigated due to time and weather constraints whilst the breccias of Rum were not considered due to recent research on them (Troll *et al.* 2000, Donaldson *et al.* 2001). The location, geological history and description of these lithologies are contained within the main text.

To achieve these objectives extensive fieldwork was carried out at the localities outlined above. Detailed observations and descriptions were made of the breccias and associated lithologies, comprising mapping, logging and accurate sketching. This enabled the spatial nature of the breccias and associated lithologies to be determined and schematic diagrams of these complex field relationships to be produced. Numerous textures within the breccias were also recorded. Conventional petrological means were applied, in the field and laboratory, to the measurement of clast and grain compositions. Where possible, the breccias (and/or conglomerates) were analysed in a series of horizontal and vertical traverses. These traverses were carried out in numerous 10m transects where information was recorded on clast type, clast size, clast roundness and the proportion of matrix. These data enabled trends within the breccias to be analysed and displayed pictorially. Simple statistics were also performed to establish the strength of these relationships. Further statistical analysis was conducted on the orientation of clasts within breccias enabling further conclusions to be reached about their mode of deposition. Representative material was sampled for petrographic analysis. Interbedded sandstone and siltstone lithologies from the conglomerates of Ben Hiant, Ardnamurchan were sampled for palynological analysis, to determine their environmental information. Rarer clasts from these interbedded units were subject to cathodoluminescence in order to investigate their mineralogy and petrogenesis. Finally, clasts of ignimbrite and *in situ* ignimbrite were

sampled from various localities in the BTIP. This material will be used in future research to date silicic pyroclastic events from the early Tertiary.

This data can then be used to:

- Draw conclusions about the local history of the BTIP in the context of its regional geology.
- Accurately document the spatial relationships of the breccias and their associated lithologies.
- Suggest modes of formation, transportation and deposition for the breccias.
- Develop a picture of surface and near surface processes relating to breccia formation within the BTIP.
- Identify areas of uplift and subsidence in the BTIP.
- Draw conclusions about sediment recycling associated with the breccia.
- Compare and contrast the various lithologies.
- Suggest environments and topography at the time of deposition.
- Explore the influence of caldera formation on these deposits.
- Interpret the role of silicic pyroclastic and intrusive events in the Palaeogene.

Chapter 2 is a brief description and summary of the geological setting and history of research on the breccia lithologies of the BTIP. Chapter 3 is a review and explanation of the classification of volcanoclastic rocks, whose terminology has been adopted in this study. A review of epiclastic deposits, their terminology and associated modes of fragmentation, transportation and deposition follows in Chapter 4. Processes relating to epiclastic agents and their nomenclature are used throughout this study. Chapters 5, 6 and 7 provide detailed descriptions and interpretations of the breccias and associated lithologies of Ardnamurchan, Mull and Skye respectively. In each case, the lithologies are

described before going on to suggest modes of deposition and, where appropriate palaeoenvironment and palaeotopography. Chapter 8 compares and contrasts the various lithologies and their implications on the development of the BTIP. The wider roles of palaeoenvironment, palaeotopography and magmatic/tectonic influences are also discussed. Conclusions are presented in Chapter 9. Appendix A is a brief outline of the significance of ignimbrites associated with the breccias and their potential for further resolving the chronology of the BTIP. Appendix B is a Samples List of relevant material collected throughout the thesis. Appendix C is additional statistical data from clast analyses. Appendix D details the optical microscopy and cathodoluminescence equipment used in the thesis.

In summary, this research will hopefully provide exciting new insights into the formation of breccias, their spatial, genetic and temporal relationships with central complexes and lava fields, and the evolution of the BTIP.

---

## **2 Breccia lithologies of the British Tertiary Igneous Province**

### **2.1 Introduction**

The islands and peninsulas along the western coast of Scotland have long been recognised as the sites of intensive igneous activity during the early Tertiary (Palaeogene) Period. This area is known by a number of names such as the British Tertiary Igneous Province (BTIP), the British Tertiary Volcanic Province (BTVP) and the Palaeogene British Province (PBP). This area includes the islands of Skye, Rum, Mull and Arran and also the Ardnamurchan peninsula, as well as smaller islands (see Fig. 2.1) and Slieve Gullion, Mourne and Carlingford in Northern Ireland. This review will concentrate on the research, which has been undertaken on the Inner Hebrides, in particular Ardnamurchan, Mull and Skye.

The BTIP comprises plateau lava fields, central complexes and linear dyke swarms. Associated with the central complexes, interpreted as the sub-volcanic roots of basaltic volcanoes, and the lava fields, are various coarse, clastic deposits of breccia. This review will briefly summarise the regional geology of the BTIP and outline previous interpretations as to the nature and origin of these breccias.

### **2.2 General Stratigraphy**

The majority of rocks in the Hebridean area of the BTIP are pre-Palaeogene in age and will be reviewed below. A composite stratigraphy for the pre-Palaeogene geology of the Hebridean area of the BTIP is summarised in Table 2.1 below.

To the west of the Moine Thrust (Figure 2.2), the Caledonian Foreland is dominated by Lewisian (Archaean) gneisses which form much of the Outer Hebrides and are the oldest rocks in the British Isles. They are intensely metamorphosed and folded, and typically comprise dark and light banded mafic and quartzo-feldspathic materials. Lewisian rocks are exposed on Skye, Raasay and Rum. These are unconformably overlain by Torridonian (late Proterozoic) red sandstones and conglomerates formed in ancient river systems, which crop out on Skye, Raasay and Rum, and fill the Lewisian landscape. To the east of

the Moine Thrust, are the rocks of the Moine Supergroup, which were thrust north-eastwards over the Lewisian and Torridonian rocks.

Mesozoic	Cretaceous sandstone and chalk
	Jurassic sandstones, mudstones and limestones
	Triassic conglomerates, breccias and sandstones
Palaeozoic	Permian sandstones
	Carboniferous sandstones, mudstones, limestones and lavas
	Devonian sandstones
	Cambro-Ordovician dolostones and sandstones
Precambrian	Dalradian schists
	Moine schists, psammities and pelites
	Torridonian sandstones
	Lewisian gneisses

**Table 2.1 - A composite stratigraphy for the pre-Palaeogene geology of the Hebridean area of the British Tertiary Igneous Province**

Originally sandstones and mudstones, the Moine rocks were metamorphosed and folded, and comprise low to high grade schists, psammities and pelites. Moine rocks crop out on Ardnamurchan, Morvern and Mull. Small outcrops of Dalradian schists and slates are exposed on the east of Mull and on Arran. Cambro-Ordovician dolostones and limestones are exposed in Southern Skye, whilst Devonian sandstones, Carboniferous sedimentary rocks and lavas, and Permian sandstones, breccias and conglomerates are common on the Isle of Arran.

Also preserved in NW Scotland are strata of Mesozoic age, deposited in large sedimentary basins. Triassic deposits typically comprise conglomerates and breccias, red marls and

sandstones. A more detailed stratigraphy of the Jurassic rocks is provided as reference is made to their lithostratigraphic units in Chapter 5. The Jurassic deposits comprise a lower marine series, followed by estuarine deposits, after which marine conditions were re-established. This lower marine series (Lias Group and Bearreraig Sandstone Group) includes the Broadford Beds Formation (sandstones and limestones), the Pabay Shale Formation and Scalpay Sandstone Formation and the Raasay Ironstone Formation of the Lias Group and a sequence of sandstones and mudstones of the Bearreraig Sandstone Group. Estuarine deposits of the Great Estuarine Group include concretionary sandstones, and these are overlain in places by Upper Jurassic sandstones and mudstones (Oxfordian and Kimmeridgian) (Hudson & Trewin 2002). The Cretaceous is characterised by thin deposits of glauconitic sandstone and chalk.

During the early Tertiary (Palaeogene), the NW European continental margin was the site of intense volcanic activity, comprising flood lava sequences, shallow intrusive centres, dyke swarms and sill complexes. The magmatism has been attributed to the impact of the proto Iceland plume at the base of the lithosphere, causing ocean floor spreading between NW Europe and East Greenland, and between West Greenland and Baffin Island. The location of lava fields was controlled by crustal thinning in the Mesozoic (Thompson & Gibson 1991), whilst the location of the central complexes was affected by ancient lineaments, such as Caledonian age faults. Within the BTIP there are four flood lava fields: i) The Antrim Lava Field, ii) The Eigg Lava Field, iii) The Mull Lava Field; and, iv) The Skye Lava Field.

Figure 2.1 depicts the lava fields of the Hebridean sector of the BTIP. Sub-aerial facies lavas dominate all three and they are typically transitional between alkali olivine and tholeiitic basalts. More evolved equivalents are rare. The lavas were erupted from fissure systems (now represented by dyke swarms and vents fed by the central complexes) (Walker, G. P. L. 1993a,b).

Interbedded with the lavas are a series of pyroclastic and epiclastic deposits, as well as fluviatile and lacustrine sedimentary facies, and palaeosols. Environments at the time comprise upland forests, through swamps, to estuarine and lacustrine settings (Jolley 1997).

The central complexes comprise foci of intrusive activity underlying now eroded volcanic edifices, and their locations are depicted in Figure 2.2. Age relationships between the

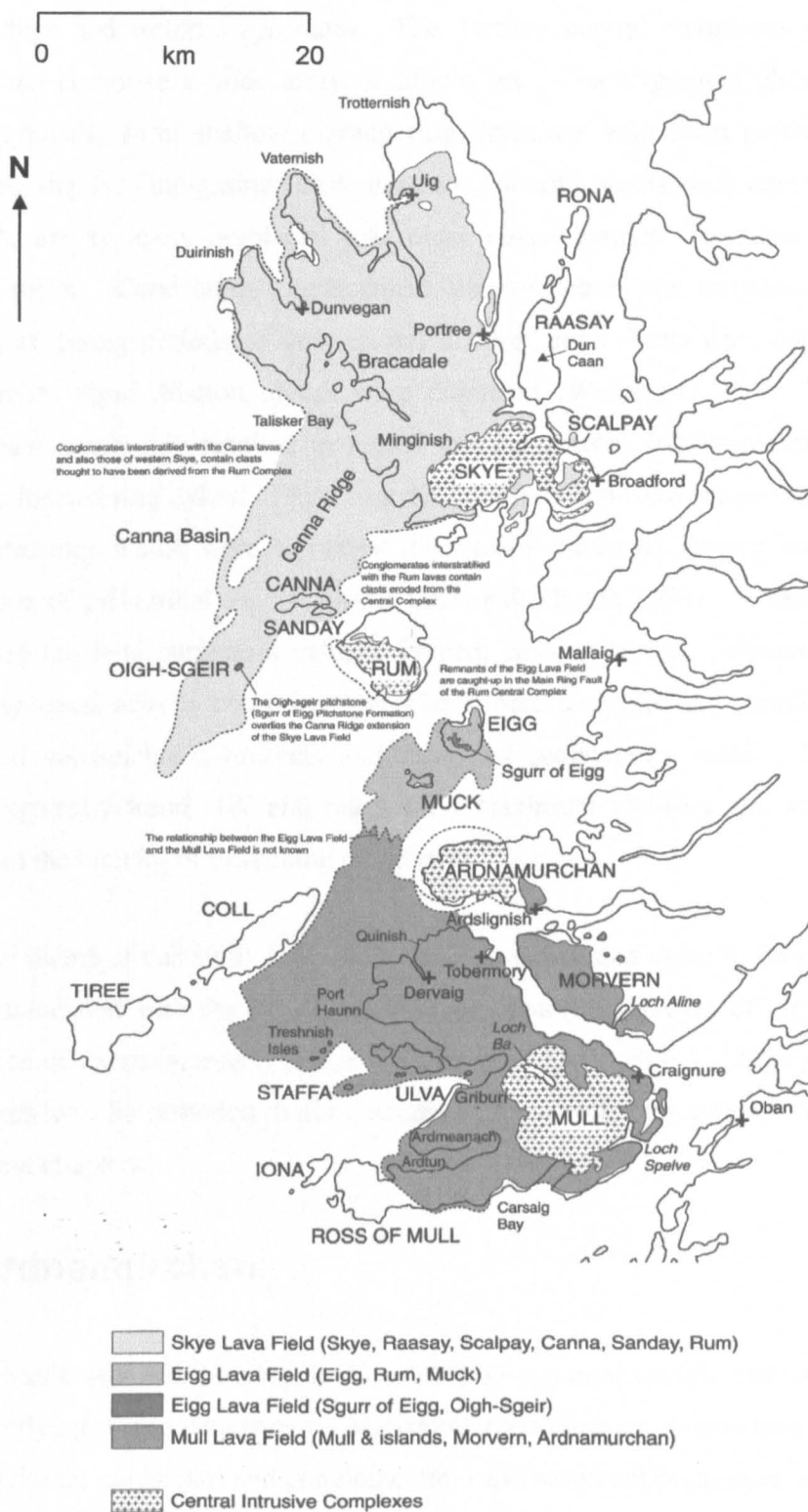


Figure 2.1 – Sketch map depicting the distribution of, and inferred relationships between the Palaeogene lava fields in the Hebridean area of the BTIP (from Bell & Williamson 2002).

older flood lava fields and the central complexes may be deduced from intrusive relationships and isotopic age dates. The Tertiary central complexes are up to 15km across, and comprise a wide array of lithologies. Coarse-grained ultrabasic and basic masses typically form shallow dipping ring intrusions with focal points at only a few kilometres depth. Fine-grained basic intrusions of cone sheets, with common focal points at depth, are typically emplaced into older coarse-grained intrusions or surrounding country rocks. Cone sheet emplacement was related to the intrusion of linear dyke swarms, as during periods of slow crustal dilation, cone sheets were emplaced, whereas during more rapid dilation, dykes were dominant (Walker, G. P. L. 1993b). Silicic magmatism commonly resulted in nested granitic plutons, whilst intermediate material typically formed ring dykes. These ring dykes of hybrid, mixed magma material are steep sided intrusions which were emplaced into steep, outwardly dipping fractures, causing subsidence of cylindrical shaped blocks (Butler & Hutton 1994). Where these fractures penetrated the land surface, a caldera formed, causing surface volcanic activity. This surface volcanic activity comprised pyroclastic breccias, tuffs and ignimbrites as well as associated volcanoclastic breccias and reworked sedimentary rocks. The linear dyke swarms typically trend NW and reach their maximum intensity and associated crustal dilation in the vicinity of the central complexes.

The main theme of this study is to understand the nature and mode of formation of breccia masses associated with the lava fields and the central complexes of the BTIP. A brief description of the main breccia deposits of Ardnamurchan, Mull and Skye and their history of research will be provided, before studies of these outcrops are dealt with in detail in subsequent chapters.

## 2.3 Ardnamurchan

The peninsula of Ardnamurchan is dominated by a central complex intruded into plateau lavas overlying a thin sequence of Mesozoic strata (Jurassic limestones, sandstones and shales; Triassic sandstones and conglomerates) and basement psammites and pelites of the Moine Supergroup (Fig 2.3).

The most detailed study of the Ardnamurchan Palaeogene igneous rocks is presented by Richey & Thomas (1930). Three centres of intrusive activity were recognised: (i) Centre 1 (oldest); (ii) Centre 2; and (iii) Centre 3 (youngest).



**Centre 1.** Richey & Thomas (1930) identified a series of volcanic vents, mainly filled with agglomerates and traversed by cone sheets. The outermost cone sheets are inclined inwards at shallow angles (15-20°) whilst those towards the interior are steeper, up to *ca.* 40°.

**Centre 2.** Richey & Thomas (1930) identified abundant basic cone sheets forming an outer set, which surround a gabbroic complex of ring intrusions. A linear vent is also present at Glas Eilean.

**Centre 3.** Richey & Thomas (1930) identified a suite of gabbroic ring dykes surrounding more silicic masses such as tonalite and quartz-monzonite.

### **2.3.1 Ben Hiant Vents**

The Ben Hiant Vents of Richey & Thomas (1930) are filled predominantly with ‘agglomerates,’ which are inter-stratified with thin layers of ashy material and sheets of columnar jointed andesitic pitchstone. Richey & Thomas (1930) recognised two vents: NE and SW, with remnants of their bounding walls still visible. A composite mass of intrusive dolerite forms the central peak of Ben Hiant and cuts out what was originally a considerably larger mass of fragmental rock. The country rocks to the ‘agglomerates’ comprise plateau lavas, Mesozoic sedimentary rocks and basement (Moine) psammites and pelites.

#### **2.3.1.1 Vent ‘Walls’**

The ‘agglomerates’ of the NE Vent have reasonably well exposed contacts with plateau basalt lavas. Richey & Thomas (1930) suggested that these contacts are inclined at 35-50° towards the interior of the ‘agglomerate’ mass and that the lavas adjacent to the contact are locally brecciated. The SW Vent also has steeply dipping contacts with its country rocks. At MacLean’s Nose, the ‘agglomerates’ have a steeply inclined contact, with Moine psammites and pelites. This ‘agglomerate’ – Moine contact can be traced to the NE where it gives way to a more complicated section involving plateau lavas and Mesozoic sedimentary rocks. Continuing NE, the contact is displaced by a fault, before coming into contact again with the Moine rocks. It then swings to the NW, exposing a vertical junction with plateau basalt lavas. The main dolerite intrusions of Ben Hiant have removed any

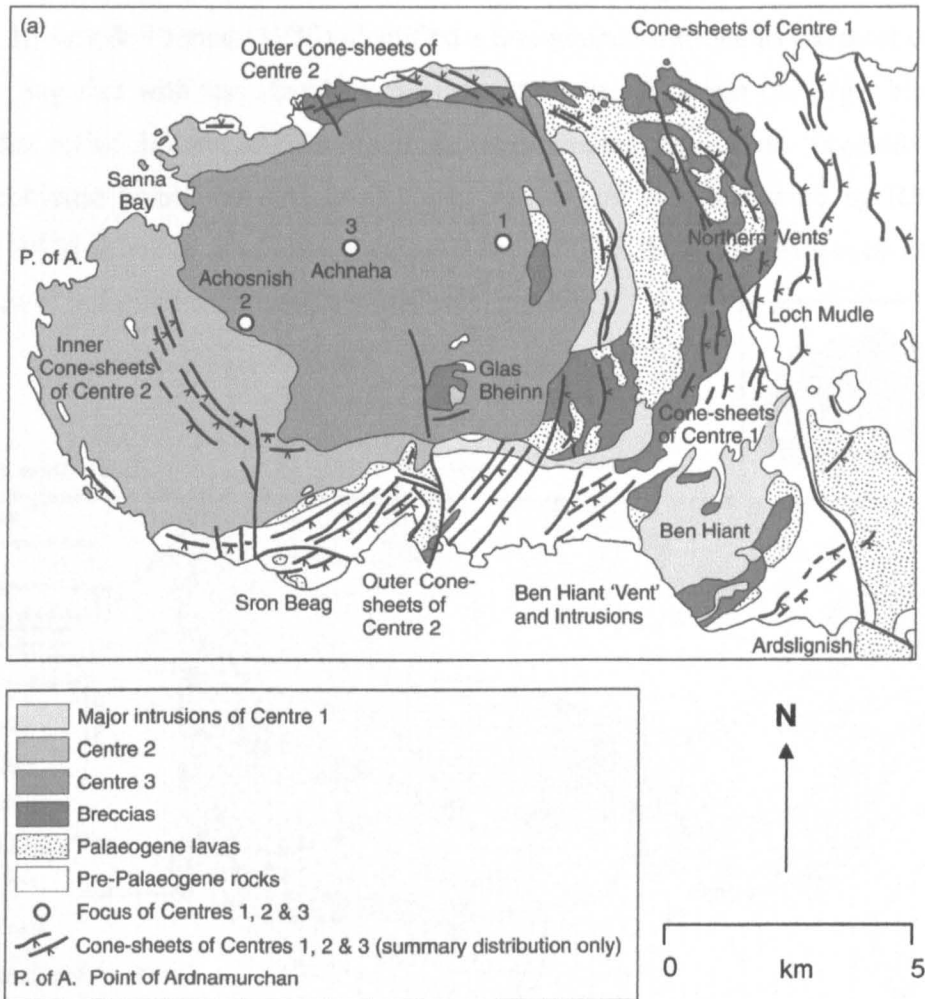


**Figure 2.3 – Simplified geological map of the Ardnamurchan Central Complex (from Bell & Williamson 2002)**

further evidence of the nature of the contact. Richey & Thomas (1930) concluded that the NE Vent preceded the SW Vent (Fig. 2.4).

### 2.3.1.2 Nature of the Ben Hiant 'agglomerates'

The Ben Hiant 'agglomerates' are described by Richey & Thomas (1930) as consisting of angular fragments of a variety of lithologies which range in size from a few mm to 40cm, together with larger 'bombs' of unspecified size. The blocks within the agglomerate are set within a fine matrix of ashy material. The agglomerates rarely show signs of bedding and any evidence of stratification is due to the presence of thin layers, up to 1.5m thick, of ashy material (Richey & Thomas 1930).



Richey & Thomas (1930) described the matrix component of the agglomerate as altered, fine-grained, ashy material, together with a significant proportion of comminuted block lithologies. Similar ashy material forms distinctive beds, which occur throughout the entire thickness of the agglomerate mass on Ben Hiant. These ashy beds, typically 30-50cm thick, have sharp bases; however, many of them grade upwards into typical agglomerate. The vertical interval between individual ashy beds is approximately 5m and they appear to be either horizontal or inclined gently towards the interior of the agglomerate mass (Richey & Thomas 1930).

Within the agglomerate mass there are sheets of columnar jointed andesitic pitchstone (three separate outcrops within the SW Vent, see Figure 2.4), interpreted by Richey & Thomas (1930) as lava flows. These sheets of pitchstone are inclined at shallow angles towards the interior of the agglomerate mass.

### **2.3.1.3 Petrology of the Ben Hiant Vents**

In summary, Richey & Thomas (1930) suggested that the agglomerates contain much in the way of silicic fragments and that trachyte, rhyolite and dacite form the bulk of the material, thus pointing to the former existence of silicic extrusive and intrusive rocks. The most common rock type is a microporphyritic (bostonitic) trachyte, which consists of short microliths of alkali feldspar within a groundmass of feldspar and glass. From MacLean's Nose, Richey & Thomas (1930) identified examples of flow banded rhyolite, displaying phenocrysts of orthoclase (1-2mm) in a groundmass predominantly of feldspar and displaying a sub-spherulitic structure. Richey & Thomas (1930) also identified examples of 'big-feldspar basalt' with phenocrysts up to 2.5cm in length.

Richey & Thomas (1930) suggested that the ashy layers represent bedded tuffs. The bedded tuffs are extremely fine-grained and are dominated by broken crystals of plagioclase and augite derived from the plateau basalts. Small grains of quartz and mica derived by comminution from the subjacent Moine rocks are also abundant (Richey & Thomas 1930).

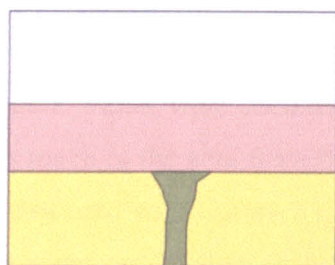
The pitchstones are dark brown to black vitreous microporphyritic rocks. They contain microphenocrysts of plagioclase and augite (1-2mm) set in a pale brown glass with microliths of plagioclase and augite, and traces of magnetite and apatite.

#### 2.3.1.4 The rhythmic model of eruption

Since Richey's observations in the 1930 memoir, he developed his ideas in a paper from 1938, to produce a model of eruption for the Ben Hiatt Vents. Richey (1938) suggested that there was an extreme rarity of fragments of country rocks within the vents, except near the vent walls where blocks of plateau basalts had fallen into the vent. Richey (1938) concluded that each of the vents erupted through the country rock in a series of explosions, leaving a crater filled in by volcanic materials. He observed that the succession of agglomerates and tuff extended from sea level to a height of 350m before abutting against the intrusive dolerite, and so suggested that the crater must have been at least 350m in depth. The succession of agglomerates and tuff is well displayed and documented, and Richey (1938) claimed that each repetition in the succession represented a distinct volcanic eruption, estimating that some 50 eruptions were involved.

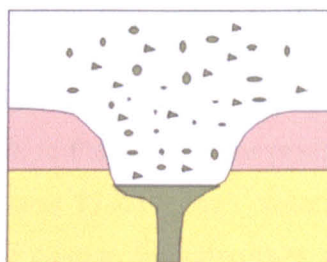
From the various field relationships and petrographical analysis of the agglomerate and tuff, Richey (1938) suggested a two-stage model for the mode of eruption (Fig 2.5). Firstly, he suggested the initial formation of a great crater by explosive shattering of the overlying basaltic lavas, which was then followed by its filling with material from a series of explosive eruptions. Following this initial eruption, he assumed that trachytic magma solidified in the pipe, sealing the vent.

Richey (1938) suggested that below the solidified plug of trachyte, gas would accumulate in the upper part of the magma column, and eventually as pressure built up would escape explosively. Therefore, the plug and any debris collected above would be shattered and agglomerate would be spread over the crater floor. Richey (1938) then suggested that, following this eruption, the top of the magma column would be below the level of the crater floor and gas erosion of the Moine wall rocks of the pipe would occur, explaining the occurrence of Moine material in the tuff. This fine-grained eroded material and other basaltic particles would be projected into the air before settling to form a bed of tuff, forming after the main eruption. This cycle of agglomerate and tuff accumulation then repeats, Richey (1938) suggesting *ca.* 50 cycles were involved.



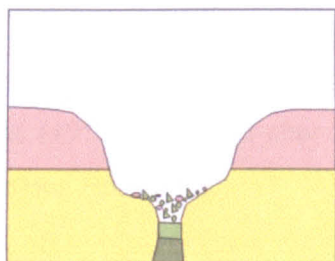
1) Prelude to Great Initial Eruption

Magma in pipe reaches base of basaltic plateau and spreads laterally. Gas pressure at top of magma column increases



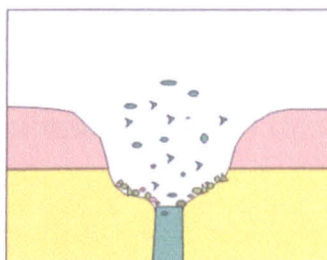
2) Great Initial Eruption

Great Explosion Crater blown out of the basaltic plateau



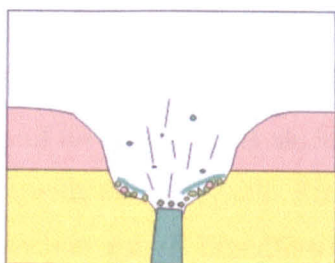
3) Period of Repose After Initial Eruption

Top of magma column solidifies. Top of pipe gets choked with debris. Below solidified plug, gas pressure increases at top of magma chamber.



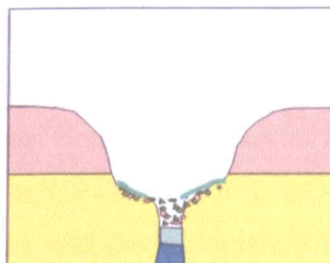
4) Recurrent Cycle: Activity, First Stage

Plug is shattered by explosive gases, and is blown out together with other debris. Bed of agglomerate collects on vent floor.



5) Recurrent Cycle: Activity, Second Stage

Strong gas phase causes comminution of materials and erosion of walls of the pipe. Bed of tuff collects on vent floor.



6) Recurrent Cycle: Period of Repose

Top of magma column solidifies. Top of pipe gets choked with debris. Below solidified plug, gas pressure increases at top of magma chamber.

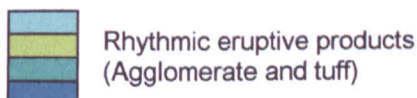
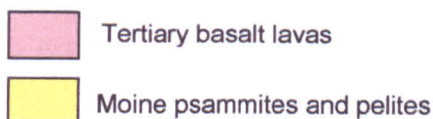


Fig. 2.5 – Diagrams to illustrate in section the inferred stages in the early eruptive history of a volcano of the Ben Hiant group (after Richey 1938).

### 2.3.2 The Northern Vents

The Northern Vents were identified as an irregular outcrop of agglomerates and tuff occupying much of the area from Ben Hiant, north to the coast of the peninsula (Fig. 2.3), and are associated with Centre 1 (Richey & Thomas 1930). Their eastern boundary lies abruptly against pre-Tertiary rocks whereas their western boundary lies against Tertiary basalt lavas and is quite indistinct. Richey & Thomas (1930) suggested that the vent explosions shattered the basalt lavas. The Northern Vent agglomerates contain much basaltic debris, but also Mesozoic sedimentary rocks, Moine schists, psammites and pelites. Blocks of porphyritic, silicic lithologies are identified, and Richey & Thomas (1930) suggested their presence indicates that the vent explosions were due to silicic magma, as they cannot be linked with the shattering of any exposed country rock. Richey & Thomas (1930) described abundant microporphyrific (bostonitic) clasts, suggesting a link to the Ben Hiant Vent.

A number of examples of unusual masses of Mesozoic sedimentary rock are seen within the agglomerate. At Achateny Water a block of calcareous sandstone measuring 30m in both directions, containing unusual fossils, and with vertical bedding is exposed. Smaller blocks (~5m) are found in the adjacent agglomerate, although nowhere in the preserved part of the Mesozoic sequence to the east of the vent, is this lithology preserved. The sandstone is thought to be of Bearreraig Sandstone Formation (formerly Inferior Oolite) age (Richey & Thomas 1930). This is again the case at Ardtoe Island where there is a large strip of brecciated black shale. There are only limited exposures of the agglomerate in contact with its outer wall. Richey & Thomas (1930) identified agglomerate with a vertical junction against Broadford Beds limestone, with the agglomerate containing many fragments of the limestone, and a low angle contact with the Pabay Shale Formation. Brecciation of the outer walls however is rare. Richey & Thomas (1930) suggested evidence for recurrent explosions in the Northern Vents from a number of tuff filled fissures traversing older tuff and agglomerate.

### 2.3.3 Glas Eilean Vent

Located at Kilchoan Bay, on the promontory of Glas Eilean is a narrow outcrop of volcanic breccias. Richey & Thomas (1930) suggested they represent a linear vent 1km in length extending parallel to adjacent cone sheets of Centre 2 in a north easterly direction. The

breccias are fault bounded to the NW with Tertiary basalt lavas and to the SE by Moine rocks.

Fragments within the vent material comprise blocks of Moine psammite and pelite, Jurassic sandstone and limestone, together with various basic igneous lithologies, possibly of cone sheet origin. The matrix forms vein-like features (up to 0.5m across) with fine-grained margins against the blocks. It is composed of comminuted block material in association with pumiceous and shard-like fragments of glass of silicic composition. Paithankar (1967) suggested this material formed a network of veins emplaced as pyroclastic material during rapid volatile loss and was responsible for the brecciation of block lithologies.

## 2.4 Mull

Mull is dominated by Tertiary basaltic lavas and intrusive rocks, Mesozoic sedimentary rocks, and pre-Mesozoic rocks such as Moine schists. Its intrusive complex comprises numerous cone sheets and ring dykes, together with significant outcrops of breccia or agglomerate. Three distinct centres form the central complex: 1, the Early Caldera (or Glen More Centre); 2, the Beinn Chaisgidle Centre and 3, the Late Caldera (Loch Ba Centre) (Skelhorn 1969) (Fig. 2.6). The Mull Memoir (Bailey *et al.* 1924) suggested that two types of breccia or agglomerate are present. The majority are vent agglomerates similar in formation to those reviewed from Ardnamurchan, and a second type of surface agglomerates which are thought to accumulate on the lavas. This section will review both types.

### 2.4.1 Vent Agglomerates / Breccias

Bailey *et al.* (1924) suggested these rocks are derived from explosive vents later than the plateau lavas and erupted through them, thus causing brecciation. In general, they contain fragments of the lavas, plutonic rocks such as gabbro, Mesozoic sedimentary rocks and Moine schists/gneisses. Bailey *et al.* (1924) noted that gneiss fragments seem to be restricted to the more peripheral vents and suggested that the lack of gneiss fragments from the central vents indicated that the 'gneissic floor' beneath the caldera areas was already relatively quite depressed at the time of these explosions. Alternatively, the gneiss fragments may have been cleared from the vent (Bailey *et al.* 1924). Large quantities of

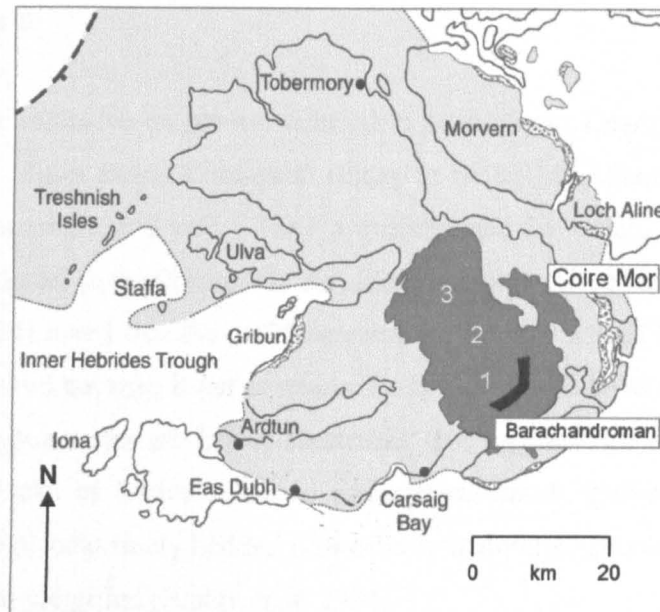


Figure 2.6 – Simplified geological map of the Mull Central Complex (after Bell & Williamson 2002).

silicic rock fragments such as rhyolite were identified throughout the vents, and the agglomerates are thought to have formed from the shattering of country rock by explosions from silicic magma (Bailey *et al.* 1924). Bailey *et al.* (1924) suggested two periods of explosive activity in the history of Central Mull. The first of these is responsible for the series of vents from Beinn Bheag, through Sgurr Dearg, to the southern face of Ben Buie. The second explosive period is responsible for the agglomerate vent exposed along the northern margin of the Ben Buie gabbro to the west of Loch Airdeglais. Breccias are also recognised in the Loch Ba area and are interpreted to be associated with the Loch Ba Ring

Dyke by Lewis (1968). The formation of the Loch Ba breccias is thought to represent the last of the repeated explosions of Mull's eruption history.

#### 2.4.1.1 Materials

The first of these explosive events are referred to as the Sgurr Dearg Vents (Bailey *et al.* 1924) (Fig. 2.6). From Beinn Chreagach Bheag to Beinn Mheadhon there are extensive outcrops of agglomerate and tuff. They are dominated by basalt, rhyolite and Moine fragments of moderate to small size, the rhyolite containing microphenocrysts of feldspar. Bailey *et al.* (1924) noted that the tuff frequently grades into a well bedded volcanic grit and mudstone but did not map it out as regular beds. The basalt lavas surrounding the vent walls of these agglomerates are highly shattered. The agglomerate of Sgurr Dearg itself contains large blocks of Moine material, granophyre, basalt, gabbro, rhyolite, Triassic sandstone and other local finely bedded sedimentary materials. Blocks of earlier intrusive lithologies are also identified (Bailey *et al.* 1924).

In the Glas Bheinn and Loch Spelve area, Bailey *et al.* (1924) described three small vent areas, which comprise finely bedded sandstones, dipping at high angles, derived from the attrition of granophyre. The agglomerates of Ben Buie are dominated by granophyre, gabbro and Moine clasts. Bailey *et al.* (1924) suggested these agglomerates were formed when part of the Ben Buie layered gabbro subsided as a result of the dropping of a ring faulted caldera.

The area around Loch Ba is dominated by the Loch Ba ring dyke, where there is subsidence of the central block about a large ring fault (Bailey *et al.* 1924). The ring fault is *ca.* 8km in diameter and is dominated by a mixed magma intrusion (Sparks 1988). Within the ring fault are outcrops of breccia, comprising fragments of basalt, gabbro, felsite and granophyre. Bailey *et al.* (1924) proposed an explosive vent origin, but Lewis (1968) suggested they were formed by the breaking up of the wall rocks by gas streaming off the subjacent silicic magma. Transport of entrained fragments would lead to the admixture of the various rock types, and continued erosion of the walls by this gas fluidised system would provide 'room' for the later emplacement of the silicic magma. This breccia has therefore been interpreted as pyroclastic and not cataclastic in origin (Lewis 1968).

## 2.4.2 Surface Agglomerates / Breccias

Bailey *et al.* (1924) identified two distinct masses of surface 'agglomerate or breccia,' located outwith the Mull Central Complex. The first is located in the Coire Mor district to the west of Craignure, whereas the second is located on the western shore of Loch Spelve at Barachandroman (Fig. 2.6). Both are located along the course of the Coire Mor Syncline.

### 2.4.2.1 Coire Mor

The Coire Mor outcrop is a coarse breccia containing fragments of Moine gneiss, granophyre, gabbro, basalt and Mesozoic sandstone. The basalt is derived from the lavas and includes examples of big feldspar basalt, whilst the gabbro and granophyre are of Centre 2 origin. Fragments of a dark grey rhyolite with microphenocrysts of feldspar are identified, and these were interpreted as lava contemporaneous with the agglomerate (Bailey *et al.* 1924). These rhyolites are similar in nature to the vent materials described in Section 2.4.1.1. The agglomerates are interpreted as having accumulated on the contemporaneous land surface and not in a vent, as Bailey *et al.* (1924) recognised that the agglomerate is contained in the centre of a syncline of lavas, and that the lavas and agglomerate are distinctly conformable. Richey (1961) subsequently noted that the rocks are not bedded and are similar to agglomerate within the central complex of Mull and suggested that a vent broke through the syncline.

### 2.4.2.2 Barachandroman

This outcrop (Fig. 2.6) comprises a largely unbedded assemblage of angular fragments of basalt, quartzite (thought to be baked Triassic sandstone) and less common fragments of Moine schist and Mesozoic sedimentary rocks, locally overlying a large thickness of baked quartz sandstone and mudstone (Bailey *et al.* 1924). The breccia rests upon basaltic lavas, which dip under the breccia at 25°. Large blocks of basalt, detached from the lava field, are identified in the breccia and Bailey *et al.* (1924) suggested that the lavas were broken up under subaerial decay at the time the breccias were accumulating on top on them. Bailey *et al.* (1924) described considerable deformation of bedding of some strata at the base of the breccia, and proposed that the sand and mud had formed underwater on an inclined surface, before slipping towards the bottom of the hollow.

## 2.5 Skye

The Skye Central Complex comprises the Cuillin (oldest), Srath na Creitheach, Western Red Hills and Eastern Red Hills Centres (Bell & Harris 1986) (Fig. 2.7). These comprise a range of typically gabbroic and granitic intrusions, which are associated with a series of breccia outcrops. Early work on Skye was carried out in considerable detail by Harker (1904) who described the breccias as vent agglomerates. Subsequent revisions of these interpretations have been made.

### 2.5.1 Harker's Conclusions

Harker (1904) described in detail the agglomerates, tuffs and breccias of Skye. Furthermore, he comments on the relationships between the agglomerates of Belig, Srath na Creitheach and Kilchrist and the gabbro and granite intrusions of the Skye Central Complex. Harker (1904) suggested that the agglomerates were explosive in origin and were much older than the gabbro and granite intrusions of the Skye Central Complex. This requires the existence of an earlier suite of plutonic gabbros and granites (whose fragments comprise the breccia), which are nowhere exposed by erosion. Harker (1904) proposed that the unexposed gabbro and granite are petrographic 'prototypes' which correspond to the later intrusions. Richey (1932) however, found evidence in the Belig area of a number of cone sheets, which cut the gabbro but not the agglomerates. Therefore, this suggested the agglomerates were intermediate in age between the Cuillin gabbro and the Red Hills granites (Richey 1932, Bell, J. D. 1966).

### 2.5.2 Belig

Harker (1904) described an area of volcanic agglomerate and tuff in the upper parts of Coire Choinnich and Coire na Selig, which forms the north western part of Belig (Fig. 2.7). The 'agglomerate' forms a lenticular mass with a maximum vertical extent of 350m. The agglomerate contains fragments ranging from a few cm to 50cm in size, set in a dark grey to dirty green matrix of comminuted block material. The fragments are predominantly of basalt and gabbro, although granite fragments are common. Harker (1904) described the agglomerate as locally fining to a silicic grey tuff devoid of fragments, particularly where the outcrop thins out towards the west.

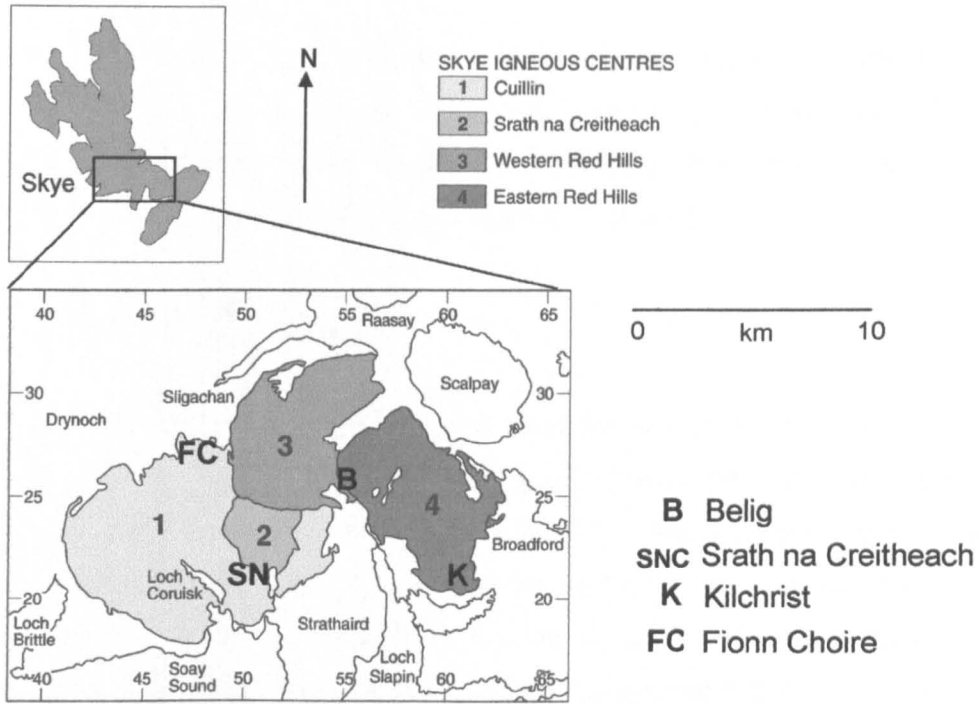


**Figure 2.7 – Simplified geology map of the Skye Central Complex. Grid references are indicated (after Bell & Williamson 2002).**

J. D. Bell (1966) interpreted the Belig rocks as having formed inside vents or underground, and following Fisher's classification (1960) suggested they should be referred to as breccias. Bell (1966) subdivided the Belig 'vent' into three separate larger outcrops, together with smaller patches due to disruption by later intrusions. The largest mass forms the higher parts of Coire Choinnich and the northern slopes of Belig, a second mass outcrops at the headwater of Eas a' Chait, and a third as a strip between the gabbro and granite in Coire na Seilg. The Belig and Coire na Seilg masses have vertical southern contacts with granite and gabbro respectively. The breccia typically contains rounded and sub-angular blocks in a fine-grained matrix. The Belig mass shows considerable variation in the size and composition of the blocks, as well as the ratio of blocks to matrix. In the other masses the grain size is more regular. Bell (1966) noted the variable shape of clast types. Gabbro clasts are typically sub-angular with rounded edges and occasionally are well rounded, whereas granite clasts are sub-angular. The sedimentary blocks are irregular and angular and, locally, their bedding is distorted giving the whole block a shattered appearance. Bell (1966) recognised that gabbro clasts dominate the centre of the Belig mass, typically with basalt and Mesozoic sedimentary clasts in the SE and Torridonian sandstone in the west. Bell (1966) suggested that the largest blocks in the Belig mass are slabs of gabbro and basalt, which are cut by cone sheets and which may have slid into the vent.

Bell (1966) suggested that the breccias were formed by the explosive effects of gas, mainly water vapour, streaming from underlying silicic magma, by a process referred to as 'gas streaming.' This eruptive stage disrupted the overlying rocks, and the fragments were fluidised, becoming more mixed and rounded as they moved.

### 2.5.3 Srath na Creitheach

A large mass of breccia is exposed in the Srath na Creitheach area on the slopes of Druim Hain and Blaven (Fig. 2.7). Harker (1904) identified these deposits as vent agglomerates and defined a lenticular shaped vent of approximately 1.5km in diameter and a thickness of 100m. In addition, a narrow strip extends for another 1.5km just below the gabbro of Druim Hain. The vent contains large, angular fragments of various sizes, which are dominated by gabbro and basalt, and are set in a fine-grained dull green matrix. In places the agglomerate becomes a fine textured 'tuff' composed of dark and light grey bands. The tuff is distributed irregularly with varying dips, and Harker (1904) suggested that it was broken up by another explosive outburst from below, or an uneven settling down.

Jassim (1970) and Jassim & Gass (1970) carried out subsequent research on this area. Jassim & Gass (1970) identified a Loch na Creitheach volcanic vent, which has an area of approximately 2km<sup>2</sup> and a faulted contact with the Cuillin gabbro. The subsequent emplacement of the Red Hills granites has destroyed the vent's circular shape, and only a semi-circular mass remains. The outer contact is believed to be vertical, and a zone of crushing ranging from 5 to 15m wide, is found. Jassim & Gass (1970) described pyroclastic debris ranging from coarse agglomerates to well-bedded, fine-grained tuffs, and large, generally concordant slabs of gabbro 'interbedded' with the pyroclastic material. The agglomerate is dominated by sub-rounded to sub-angular blocks of basalt and gabbro, whereas the tuffs are composed of fine-grained, similar comminuted material. The tuffs are well bedded and display alternating fine and coarse *ca.* 2mm bands, which commonly display bomb sag features. Jassim & Gass (1970) identified twelve large gabbro slabs ranging in length from 40 to 900m within the agglomerate mass. Typically these are brecciated and are both mineralogically and chemically identical to gabbro from the main Cuillin mass.

Jassim & Gass (1970) suggested that the agglomerates were formed when a vent burst through overlying basaltic and gabbroic material, by a gaseous explosive agent. Collapse

of the vent walls would then have occurred, enlarging the vent and further explosive activity then produced within the caldera, agglomerates and finely bedded tuffs. At times large gabbro slabs became detached from the caldera wall and slid into the vent. The whole vent structure was then subjected to subsidence of some 750-1000 metres along marginal ring fractures. Finally, the region was intruded by the Red Hills granites.

#### 2.5.4 Kilchrist

The largest area of breccia in Skye crops out on the Holy ground of Kilchrist, approximately 4km SW of Broadford (Fig. 2.7). It is bounded to the north by a later granite intrusion forming the Red Hill, Beinn Dearg Bheag. Harker (1904) identified these rocks as vent agglomerates and described a mass of unstratified, heterogeneous material ranging in size from small fragments to blocks 30cm in diameter, set within a fine-grained, dull, dark green matrix. The matrix is typically basaltic in composition, which Harker (1904) interpreted as volcanic dust thrown up by the eruptions. Fragments include: Torridonian sandstone and shale; Cambrian limestone and quartzite; Jurassic limestone, sandstone and siltstone; Tertiary basalt, dolerite, rhyolite, tuff (including ignimbrite), granite, pitchstone, gabbro, and coarse and fine-grained pre-existing polygenetic pyroclastic material. Harker (1904) also noted that a partial ring of a later granophyre intrusion surrounds the vent. This was re-interpreted as a hybrid (mixed magma) intrusion by Bell, B. R. (1982).

Ray (1962) described three acid breccia bodies, which were described by Bell & Harris (1986) as intrusive, brecciated porphyritic rhyolite stocks. Bell, B. R. (1985) and Bell & Harris (1986) suggested that the volcanic products were not vent fillings but instead the results of surface or near surface volcanism and associated epiclastic (surface) processes within a subsiding caldera. Bell (1985) described the agglomerates as being preserved in a ring faulted mass, intercalated with thin volcanoclastic sandstones and *in situ* extrusive ignimbrites. Evidence of stratification is limited but Bell (1985) described a 0.5m thick bed of lateritised material indicative of subaerial weathering.

### 2.5.5 Fionn Choire

The majority of agglomerates and breccias described so far on Skye are predominantly basic in composition. In one area in the Cuillin Hills, however, a group of rhyolitic and trachytic breccias are preserved. Located at Fionn Choire (Fig. 2.7), Harker (1904) divides them into three main groups. The first, and lowest of these consists mainly of trachytic lavas, the second is of rhyolitic tuffs and breccias, and the third is of rhyolitic lavas. The trachytic lavas are overlain by a group of rhyolitic tuffs, which coarsen in places to a rhyolitic breccia, composed of angular to sub-angular clasts (*ca.* 2cm of rhyolite) set within a grey to light green matrix. These are overlain by flow banded rhyolite lavas which Harker (1904) described as ‘dovetailing’ with the overlying basalt lavas. The trachytic lavas are underlain by amygdaloidal basalt lavas that dovetail with the trachyte lavas, which die out eastwards. Harker (1904) suggested that the more evolved materials were erupted contemporaneously with the basaltic lavas.

## 3 The classification of volcanoclastic rocks

### 3.1 Introduction

Volcanoclastic is a non-genetic term for any fragmental aggregate of volcanic parentage, irrespective of origin (Cas & Wright 1987). There have been several attempts in the literature to successfully categorise volcanoclastic rocks, though only in more recent years have classifications encompassing all volcanoclastic material been produced. Much of the earlier research was focused primarily on pyroclastic rocks and/or pyroclastic fragments (Wentworth & Williams 1932). Pyroclastic material was widely defined as rocks produced by explosive or aerial ejection of material from a volcanic vent (Wentworth & Williams 1932), but if this definition is to be used, certain materials cannot be considered. This includes:

1. Fragments produced in volcanic vents but which are not ejected from the vent
2. Fragments formed during the breaking up of a moving lava flow
3. Fragments that originate by the weathering and erosion of solidified lava flows or consolidated pyroclastic deposits

This definition is clearly inadequate and so wider classification schemes were created which incorporate the previously omitted material (Fisher 1960, 1961; Wright *et al.* 1980; Cas & Wright 1987). These schemes are based on the primary origin of the fragments, their grain-size and textures, thus producing genetic and lithological classifications. In some cases however, a purely descriptive category is only possible where the volcanoclastic origin is doubtful or unknown.

The classification and understanding of volcanoclastic rocks are essential in determining the nature and origin of breccias associated with central complexes and lava fields of the BTIP, and as a means of classifying field observations. Therefore, the purpose of this chapter is to briefly introduce these classification schemes, in order to use them as a basis for future research.

## 3.2 Early pyroclastic classifications

One of the earlier rock classifications was the largely unaccepted scheme of Grabau (1924), who included pyroclastic rocks as one of five major subdivisions of all rock types. The pyroclastics were then further subdivided by grain size, adopting the terms rudyte (>2.5mm), arenyte (0.5mm-2.5mm) and lutyte (<0.5mm), and using the prefix 'pyro'. Grabau's pyrordyte corresponded in grain-size to other rudytes (conglomerate and breccia), pyrarenyte corresponded to other arenytes (sandstone), and pyrolutytes corresponded to other lutytes (mudstone). Grabau (1924) also recognised that pyroclastic rocks could be reworked by erosional agents and prefixed hydro (water), anemo (wind) and atmo (weathering) to distinguish between these processes. This classification suffered however, due to its use of the term rudite (or rudyte), as a rudite or rudaceous rock is defined as a general term applied to sedimentary rocks having a grain size of 2mm or more (Allaby & Allaby 1990). Therefore, it is inappropriate to use this term to encompass all aspects of volcanoclastic rocks, which are considerably more diverse in origin, formation and texture.

Wentworth & Williams (1932) defined pyroclastic fragments primarily on grain size and adopted the terms blocks and bombs (>32mm), lapilli (4-32mm), coarse ash (0.25-4mm) and fine ash (<0.25mm). The size ranges for pyroclastic fragments however were not precisely defined and later authors preferred the application of a scheme to reflect the terminology used in standard sediments (Seegerstrom 1950; Thorarinsson, 1954).

Fisher (1960, 1961) equated pyroclastic fragments with typical sedimentary classification, and was able to relate both pyroclastic and epiclastic (those formed by surface processes) fragments. Coarse blocks and bombs were equated to boulder sizes (>256mm), fine blocks and bombs corresponded to cobble sizes (64-256mm) and lapilli corresponded to pebble sizes (2-64mm). Coarse ash was equivalent to sand sizes (2-1/16mm) and finally fine ash was equivalent to silt and clay sizes (<1/16mm).

## 3.3 The classification of volcanoclastic rocks by Fisher

Fisher (1961) expanded this classification to include the origin of particles, as well as their size (Table 3.1) and it incorporated particles formed by pyroclastic, epiclastic and autoclastic processes. Fisher (1961) also suggested a secondary classification whereby,

tuff, for example, can be subdivided based upon its transporting agent (fluvial, glacial, aeolian), its environment of deposition (lacustrine or marine), and its composition (crystal, lithic or vitric).

Predominant grain size (mm)	Autoclastic	Pyroclastic	Epiclastic	Equivalent non-genetic terms
256	Flow breccia Autobreccia	Pyroclastic breccia	Epiclastic volcanic breccia	Volcanic breccia
64		Agglomerate	Epiclastic volcanic conglomerate	Volcanic conglomerate
	Intrusion breccia	Lapillistone		
2	Tuffisite	Coarse tuff	Epiclastic volcanic sandstone	Volcanic sandstone
1/16		Fine tuff	Epiclastic volcanic siltstone	Volcanic siltstone
1/256			Epiclastic volcanic claystone	Volcanic claystone

**Table 3.1 - Classification of Volcaniclastic Rocks (from Fisher 1961)**

Fisher (1961) identified three key volcaniclastic terms: autoclastic, pyroclastic and epiclastic. The autoclastic rocks are referred to as fragmental rocks which may be produced in volcanic vents, by friction in flowing lava, or by internal gas explosions in lavas after they have ceased flowing (Fisher 1961). The pyroclastic fragments are produced by volcanic explosions and are extruded as discrete particles from vents. The term primary is used to indicate that the material has not been transported from its place of deposition, before being lithified. Epiclastic is defined as “a term applied to mechanically deposited sediments (gravel, sand, mud) consisting of weathered products of older rocks. Detrital material from pre-existent rocks” (American Geological Institute 1957). Fisher (1961) therefore defined epiclastic volcanic rocks as those derived by weathering and erosion of

lithified or solidified volcanic rocks. Non-genetic names were applied to the classification (Fisher 1961). These names, based upon their grain size, are needed for volcanoclastic rocks with fragments of unknown origin. Volcanic sandstone, for example, is a rock containing volcanic particles of sand size, regardless of the origin of the fragments.

Fisher (1960) earlier defined a classification of volcanic breccias based on the terms autoclastic, pyroclastic and epiclastic. Autoclastic volcanic breccia is formed by the fragmentation of semi-solid and solid lava during confinement beneath the surface, or by relatively slow movement of unconfined lava flows. These processes are sub-divided into flow and volcanic intrusion breccia. Fisher (1960) defined flow breccia as a rock formed by the fragmentation of an advancing and congealing lava flow, including a'a (spiny fragments) and block (smooth polyhedral blocks) breccia. Volcanic intrusion breccia can be formed by the movement of magma under confinement within the lithosphere by:

1. Internal brecciation within a moving solid or semi-solid igneous mass;
2. Brecciation along the solidified flanks of an intrusion by friction;
3. Brecciation and mixing with the material which the magma intrudes;
4. Explosions caused by groundwater coming into contact with magma;
5. Brecciation by the process of fluidisation – a process causing brecciation and rounding of fragments by streaming gases (Reynolds 1954);
6. Gas streaming and collapse in breccia pipes (Gates 1950).

Fisher (1960) also included peperite breccia, formed from the shallow intrusion of fluid magma into unconsolidated or poorly consolidated sediments (Scrope 1858; Kokelaar 1982; Busby-Spera & White 1987; White *et al.* 2000) and friction breccia formed within rising magma or between a body of magma and its wall rock. The term friction has been used for volcanic rocks brecciated by faulting (Stearns & MacDonald 1947), but Fisher (1960) suggested the use of the term volcanic fault breccia to distinguish between primary brecciation by movement of magma, and secondary brecciation by fault movement.

Fisher (1960) recognised pyroclastic breccia as formed by explosions and ejection of liquid and/or solid fragments from volcanic sources, including Vulcanian, pyroclastic flow and hydrovolcanic breccia. He suggested Vulcanian explosions produced angular lithic fragments and typically formed thin, small volume stratified ash deposits containing large ballistic bombs and blocks. The same author grouped under the name 'pyroclastic flow breccia', all those breccias formed by extrusion of solid-liquid-gas mixtures. Three main types were recognised by Williams (1956), comprising a Pelean type formed by flank eruptions or dome collapse, a Krakatoan type initiated by low pressure explosions, and a fissure type formed by upwelling of magma through fissures. Hydrovolcanic breccias originate by steam explosions as a result of hot lava coming in contact with water or ice, in phreatic explosions and steam explosions resulting from lava flowing from land into water, from non-ice areas onto or against ice, or from lava extruded beneath water or ice. Phreatovolcanic breccias, formed by the contact of hot lava or magma with surface water which has seeped underground (Williams 1941), are also included.

Vent agglomerate and vent breccia were also identified by Fisher (1960). Vent agglomerate comprises large (>64mm) pyroclastic fragments (including bombs) located within a vent, and is of pyroclastic origin. Vent breccia is composed of angular debris in vents, but is not necessarily of pyroclastic origin, as vents can be filled by volcanic debris derived from the sides of vents by collapse, explosion, landslide or reworking by water.

Fisher (1960) identified epiclastic volcanic breccia as fragments produced by any type of rock fragmentation, which are transported by epigene geomorphic agents or by gravity transfer. He also recognised laharic breccia formed by lahars. A lahar is a mudflow containing debris and angular blocks of chiefly volcanic origin (Van Bemmelen 1949) and can be caused as a result of volcanic eruptions with associated heavy rainfall, or the collapse of a crater lake. The second form of epiclastic volcanic breccia is termed water-laid volcanic breccia. This is composed of angular to sub-angular volcanic rock fragments that originate from a volcanic region undergoing rapid erosion and may originate in either active or non-active volcanic regions, and are transported and deposited in any standing body of continental or marine water. Finally, Fisher (1960) proposed the term volcanic talus breccia. This is composed of angular, volcanic fragments, formed by mass movement. They accumulate around the lower slopes of volcanic cones and within craters, by avalanche or landslide, due to oversteepening of slopes.

Epiclastic volcanic breccias can be formed by a variety of mechanisms, on which there exists a substantial body of literature. This summary focuses on their various morphological characteristics, origin, transportation and deposition, and therefore emphasises that epiclastic breccias have their own independent classification system. This shall be reviewed in Chapter 4.

### 3.4 Revision of the classification of pyroclastic rocks

Whilst Fisher (1960, 1961) identified pyroclastic deposits primarily by size as tuff, lapillistone and pyroclastic breccia and agglomerate, with the breccia containing subdivisions of vulcanian, pyroclastic flow and hydrovolcanic origin, pyroclastic deposits have now been defined in more detail, recognising features such as composition and geometric relations. Wright *et al.* (1980) therefore introduced a more comprehensive classification for pyroclastic deposits.

Three types of component are present in pyroclastic deposits, including: juvenile vesiculated fragments (pumice, scoria), crystals and lithics (Sparks & Walker 1973). Lithics are sub-divided into non-vesiculated juvenile fragments (cognate lithics), country rock which has been explosively ejected during eruption (accessory lithics), or clasts picked up locally during transport (accidental lithics).

Sparks & Walker (1973) recognised three main pyroclastic deposits:

1. Pyroclastic fall deposits are produced when material is explosively ejected from a vent, producing an eruption column high into the atmosphere which expands, then falls back down under the influence of gravity and wind direction. The geometry and size of the deposits reflect the eruption column height, wind velocity and direction (Wilson *et al.* 1978). Fall deposits are typically bedded, of uniform thickness and are well sorted (Fig. 3.1a)
2. Pyroclastic flow deposits involve the lateral movement of pyroclastic material as a gravity controlled, hot, high concentration gas/solid dispersion, which may in some cases be partly fluidised (Sparks 1976). These unstratified deposits are topographically controlled and fill valleys and depressions (Fig. 3.1b). Carbonised wood may also be present.

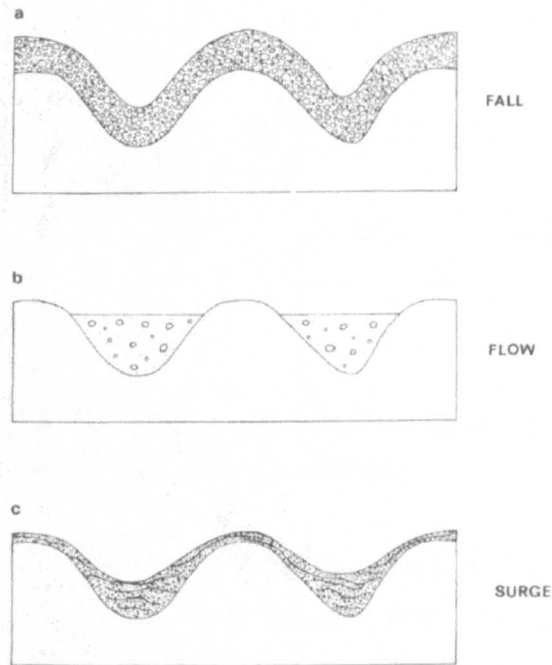
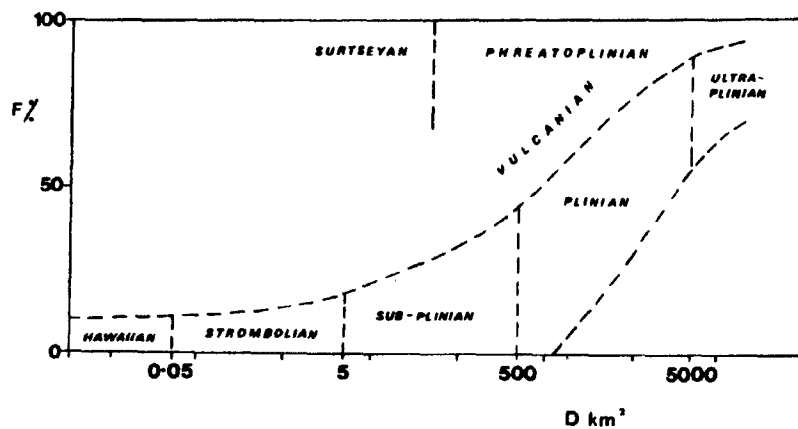


Figure 3.1 - Geometric relations of the three main types of pyroclastic deposit overlying the same topography (from Wright *et al.* 1980).

3. Pyroclastic surge deposits involve the lateral movement of pyroclasts as expanded, turbulent, low concentration gas/solid dispersions. The geometry of the deposits typically reflect topography, and tend to preferentially accumulate in depressions (Fig. 3.1c). They are characterised by sedimentary bedforms (cross bedding, dunes and antidunes, planar lamination, pinch and swell structures, and chute and pool structures) and are well sorted (Sparks 1976).

Using these definitions of pyroclastic deposits, Wright *et al.* (1980) proposed a classification whereby two quite different systems are needed. The first of these is to interpret the genesis of the deposit (which links to a volcano's history, behaviour and eruptive mechanisms), whereas the second is lithological and is primarily descriptive, describing features such as grain size.

Wright *et al.* (1980) suggested the following genetic classification. For pyroclastic fall deposits the classification scheme of Walker, G. P. L. (1973) is adopted (Fig. 3.2). This is



**Figure 3.2 - Classification scheme of pyroclastic fall deposits (after Walker, G. P. L. 1973). F=weight percentage of deposit finer than 1mm. D=dispersal of fall deposit.**

a quantitative scheme and is based on the accurate mapping of the distribution of a fall deposit and the analysis of grain sizes. Small volume, effusive Hawaiian and Strombolian eruptions are compared for example with large volume, explosive Plinian eruptions.

Wright *et al.* (1980) sub-divided pyroclastic flows into the categories of essential fragment (the degree to which they are vesiculated and subsequently their density), eruptive mechanism, type of pyroclastic flow (e.g. pumice, scoria, block and ash etc.) and the type of deposit produced (Table 3.2). Wright *et al.* (1980) suggested that the term 'nuée ardente' as applied to the Pelean eruptions of 1902 (Lacroix 1903) should be avoided altogether, preferring the term block and ash flows (Perret 1937).

Pyroclastic surges are sub-divided by the type of essential fragment and eruptive mechanism, to include base, ground and air fall surges. Base surges are stratified and laminated deposits containing juvenile vesiculated fragments (typically pumice), ash and crystals. Ground surges are typically less than 1m thick and are composed of ash, juvenile vesiculated fragments, crystals and lithics. They are enriched in denser components, show unidirectional bedforms, carbonised wood and small fumarole pipes. Ash-cloud surges are stratified deposits found at the top and as lateral equivalents of flow units of pyroclastic flows. They show unidirectional bedforms, pinch and swell structures and can occur as separated lenses.

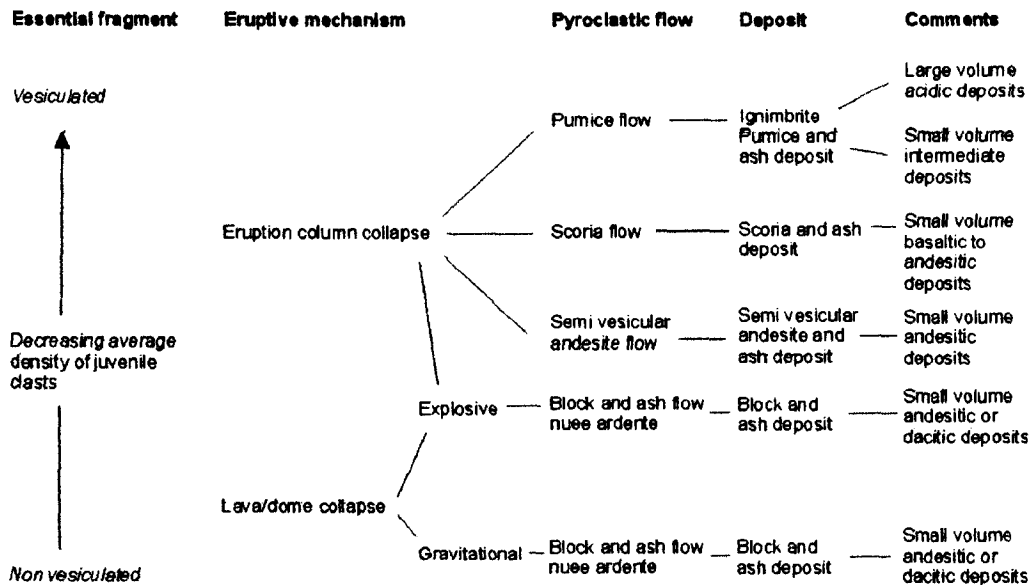


**Table 3.2 - Genetic classification of pyroclastic flows (after Wright *et al.* 1980)**

In addition, Wright *et al.* (1980) proposed a lithological classification. These lithological features are primarily descriptive, but can be indicative of certain modes of origin, and include:

1. The grain size limits of the pyroclastic deposits and their overall grain size distribution
2. The constituent fragments of the deposit
3. The degree and type of welding

Both 1) and 2) can be used as indicators of origin. The system of Fisher (1961) is adopted by Wright *et al.* (1980) as the basis for the classification of the grain size limits of pyroclastic fragments (Table 3.1). Welding is a post-depositional process involving the sintering together of hot vesicular fragments and vitreous shards under compaction (Sparks & Wright 1979), typically associated with ignimbrites (the rock or deposit formed from pumiceous pyroclastic flows, irrespective of the degree of welding or volume (Sparks *et al.* 1973)). In zones of dense welding, glass shards and larger (10-40mm), flattened pumice fragments (fiamme) define a planar foliation, or eutaxitic texture, indicative of significant compaction.

### 3.5 Classification of volcanoclastic rocks of pyroclastic and epiclastic origins

The classification of modern and ancient volcanoclastic rocks of pyroclastic and epiclastic origins by Cas & Wright (1987) provides an incredibly detailed classification focusing more specifically on textural and compositional relations, and also the nomenclature of quench-fragmented and autobrecciated volcanoclastics. The problems associated with the use of the terms 'agglomerate' and 'vulcanian' are also discussed. The classification schemes of Walker, G. P. L. (1973) and Wright *et al.* (1980) are adopted by Cas & Wright (1987) for pyroclastic rocks.

Cas & Wright (1987) recognised that features such as devitrification, recrystallisation, new mineral growth during diagenesis, low grade metamorphism, deformation and weathering may greatly modify original textures and mineralogy, and therefore, it can be extremely difficult to make a genetic classification or apply terminology.

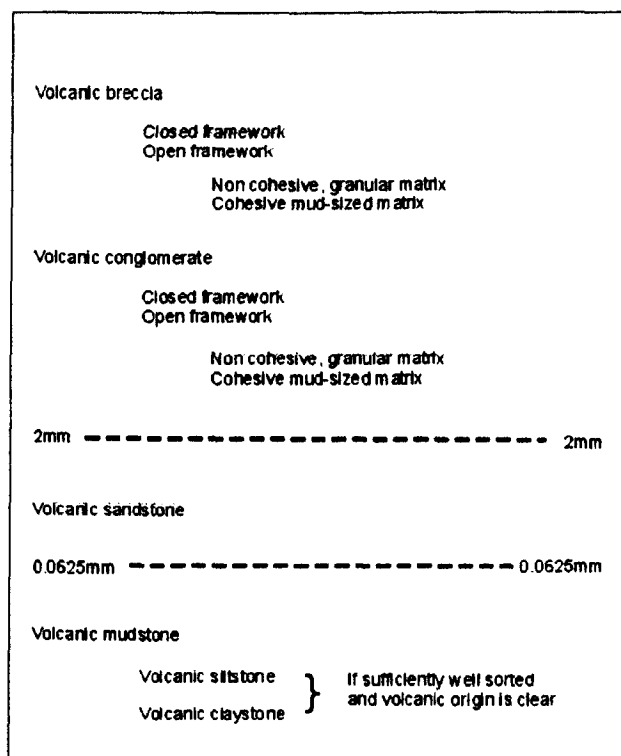


Table 3.3 - Non-genetic classification of volcanoclastic rocks (from Cas & Wright 1987)

Consequently, Cas & Wright (1987) proposed that genetic terminology should not be applied to volcanoclastic rocks until a complete study of their characteristics, such as textural and compositional features, geometry and palaeogeography, are made. Following Fisher's lead (1961), Cas & Wright (1987) therefore suggested an initial non-genetic terminology should be used and this data is presented in Table 3.3.

Cas & Wright (1987) sub-divided the descriptive properties of volcanoclastic deposits into two categories, textural and compositional, and commented on their use. Textural characteristics include:

1. *Coherent igneous texture versus fragmental texture.* Cas & Wright (1987) suggested intrusive or extrusive porphyritic rocks should have an even distribution of crystals, set in a fine-grained groundmass which lacks any clastic texture. Should this be present then the rock may have undergone fragmentation origins, such as quenching in a peperite or by epiclastic fragmentation caused by collapse.
2. *Welding.* Evidence of welding, such as eutaxitic texture and pumice lenticle foliation, is typically a good indicator of pyroclastic origin, although pumice and other juvenile clasts can be aligned by sedimentary processes, or flattened by deformation (Cas & Wright 1987).
3. *Grain size.* This is ambiguous, as coarse material deposited for example in a mudflow can then be reworked by fluvial or marine systems.
4. *Sorting.* This is relatively useful in distinguishing types of pyroclastic deposits. Typically pyroclastic falls are well sorted, whilst flows and surges are poorly sorted. Reworking of volcanoclastic material may produce sorting (Cas & Wright 1987).
5. *Shape.* Cas & Wright (1987) recognised that grain shape is one of the more useful characteristics for determining origin, although it is still subject to later reworking or mass flow processes. Highly fragmented material can be distinctive for explosively ejected detritus, and glass shards are diagnostic of explosive fragmentation during eruption. Shaped bombs, breadcrust bombs and irregular spatter fragments are typical of the explosive eruption of basaltic magma, and they form the criteria for the use of the term agglomerate, to be discussed later. Large, irregular blocks though, may have many fragmentational and depositional origins.

6. *Angularity or rounding.* Angularity itself does not mean close proximity to the vent or indeed primary volcanic origin or depositional origin (Cas & Wright 1987). Rounded clasts typically indicate post-eruptive reworking or represent accidental lithics.
7. *Framework type.* A rock can have either an open or closed framework (Cas & Wright 1987) (matrix or clast supported), which does not indicate origin, but instead transport conditions.

Compositional characteristics include:

1. *Compositional affinities.* Cas & Wright (1987) suggested that volumetrically, the majority of basaltic products are lavas, while the majority of silicic products are pyroclastic materials.
2. *Compositional homogeneity.* This is used to assess the amount of reworking of a volcanoclastic deposit. Cas & Wright (1987) suggested that if a deposit is relatively homogeneous then there has not been much mixing of source materials.
3. *Clastic components.* Whilst a large amount of glass shards, pumice or scoria indicates a pyroclastic origin, it does not necessarily indicate pyroclastic deposition. However, Cas & Wright (1987) noted that should crystal and lithic contents increase, whilst compositional homogeneity decreases, then epiclastic fragmentation and deposition origins become more possible.

By assessing the characteristics outlined above, Cas & Wright (1987) proposed a classification scheme whereby the origins of volcanoclastic material are related to a grain size and textural classification, and this is reviewed in Section 3.6, below.

Cas & Wright (1987) highlighted significant problems with nomenclature in the literature on volcanoclastic rocks. Agglomerate is a coarse pyroclastic deposit composed of a large proportion of rounded, fluidally shaped, volcanic bombs (generally >64mm). Evidence of true volcanic bombs, such as shaped or breadcrust types or bomb sags must be present for this term to be used. True agglomerate is also a good indicator of proximity to a vent. Many geologists, however, have wrongly applied this term to any type of volcanic breccia, and then made suggestions about proximity to vent which may be completely wrong.

Further confusion arises over the consequences of redeposition on nomenclature. Pyroclastic and epiclastic deposits are distinguished based on their modes of fragmentation and final deposition. Pyroclastic deposits have a pyroclastic mode of formation and of deposition (i.e. fall, flow or surge), whereas epiclastic deposits can be both fragmented and deposited by normal surface processes such as weathering. Therefore, where pyroclastic deposits are reworked or redeposited, or both, by epiclastic agents, then genetic terms such as agglomerate and tuff can no longer be used, as it is essentially now a different rock. Such a deposit would then become a volcanic breccia, sandstone or mudstone (dependent on grain size). If evidence of its pyroclastic fragmentation still remains, then qualifying terms such as tuffaceous breccia or tuffaceous mudstone may be used (Cas & Wright 1987).

### 3.6 Grain size textural classes of volcanoclastic rocks

Cas & Wright (1987) sub-divide volcanoclastic rocks into six broad categories, based on the textures present:

- |                                    |                                  |
|------------------------------------|----------------------------------|
| a) Conglomerate – closed framework | b) Conglomerate – open framework |
| c) Breccia – closed framework      | d) Breccia – open framework      |
| e) Sandstones                      | f) Mudstones                     |

Within each section are specific examples of how the various textural classes can form.

#### 3.6.1 Conglomerate – closed framework (rounded clasts)

1. *Epiclastic reworking in fluvial and shoreline conditions.* These have a heterogeneous clast composition, display sedimentary structures and well rounded clasts and are found in the context of sedimentary successions.
2. *Epiclastic mass flow redeposition in subaqueous conditions.* These have a heterogeneous composition with a range of disorganised to stratified facies.

3. *Pumice and scoria concentration zones in ignimbrites and scoria pyroclastic flow deposits.* Typically less than 2m thick, they are compositionally homogeneous, clast supported by pumice or scoria, intercalated with ignimbrites, and form sheet to lensoidal deposits.
4. *Fines depleted ignimbrite.* These display a homogeneous composition. They have a crystal rich matrix if the magma is porphyritic. Thicknesses can be greater than 10m and the deposits are usually massive, although occasional bedding is found.

### **3.6.2 Conglomerate – Open framework (rounded clasts)**

5. *Epiclastic reworking and mass flow redeposition.* All deposits are set in a granular matrix and share characteristics similar to 1 and 2.
6. *Cohesive pebbly mud flows and lahars.* These pebbly mudstones are tens of metres thick, are typically massive, and clast composition ranges from heterogeneous to homogeneous. There is no evidence of hot state emplacement, such as hot blocks and no gas segregation structures are present.
7. *Non-welded ignimbrite and scoria flow deposits.* These compositionally homogeneous and internally massive flows are tens of metres thick and gas segregation pipes may be identified.

### **3.6.3 Breccia – Closed framework (angular clasts)**

8. *Epiclastic redeposition and mass wastage, including gravitational collapse and caldera margin collapse.* These vary from homogeneous to heterogeneous in composition and range from poorly stratified to graded. Typically they display local lobate geometries, although are more extensive for redeposited facies. If large scale collapse has occurred they can be hundreds of metres thick. Associated epiclastic facies may contain sedimentary structures.
9. *A'a lavas.* These are compositionally homogeneous and have an irregular and spinose clast morphology. The margins are often brecciated but the interior is massive, and overall such units are less than 10m thick.

10. *Block lavas and autobrecciated lavas*. These are similar to a'a lavas except that the clasts are angular blocks rather than spines. They are intermediate or silicic in composition and can have thicknesses of up to 100m or more.
11. *Lava dome/flow front talus deposits*. As for 10, except there is diffuse layering in scree slope talus deposits.
12. *Agglutinates*. These are of homogeneous composition, typically basaltic spatter fragments rapidly accumulated and partially welded together, displaying fluidal clast shapes. They have variable thicknesses of up to tens of metres and are typically interbedded with massive lavas.
13. *Agglomerates*. A coarse pyroclastic deposit composed of a large proportion of rounded, fluidally shaped, volcanic bombs (generally >64mm) (Fig. 3.3).

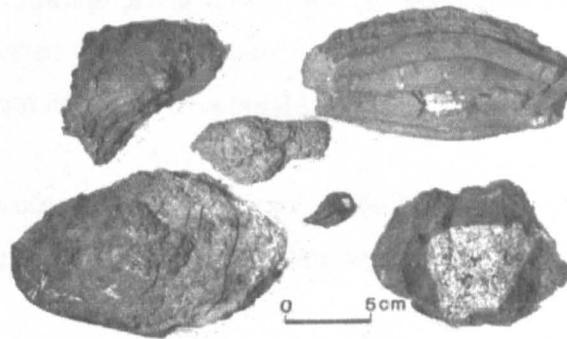


**Figure 3.3 – Example of ballistic bombs, some with included xenoliths, from Mt Leura, Australia. Note their shaped nature gained during flight (from Cas & Wright 1987).**

14. *Quench-fragmented lavas and shallow intrusives (hyaloclastites)*. These are compositionally homogeneous with very angular to splintery clasts. They contain coarse blocks to finely aggregated glassy aggregates and may be crystal rich if the magma is porphyritic. There is a 'jigsaw' style fitting together of clasts where there has been little redistribution from the site of fragmentation, the clasts shattering as they enter water or wet sediment.
15. *Hydrothermal explosion breccias*. The range of clast types and morphology in these rocks is very diverse. The clasts are usually altered and set in a matrix of

hydrothermally altered clays. They can be associated with surge deposits and accretionary lapilli may also occur.

16. *Hydraulic fracture breccias*. Where fluid pressure exceeds the tensile strength of a rock, hydraulic fracture breccias are formed. This fluid then propagates a crack and fractures it in a tensile manner. Typically, these breccias are compositionally homogeneous to partially heterogeneous, containing angular to splintery altered clasts.
17. *Pumice fall deposits (Subplinian, Plinian and Ultraplinian)*. These typically 10 to 25m thick deposits have a homogeneous clast composition, are massive to diffusely layered and show no cross-stratification.
18. *Scoria fall deposits (Hawaiian, Strombolian)*. The basic equivalent of 17.
19. *Lithic concentration zones and ground layers of violent ignimbrites*. Typically less than 1m thick these ignimbrites have a varied clast composition and are gradational upwards into matrix supported and lithic poor breccia. They are interbedded with other ignimbrite facies and underlain by a basal layer of sand grain size.
20. *Co-ignimbrite breccias (lag breccias and ground breccias)*. As for 19, but the clasts are coarser and the deposits thicker (approximately 20m).
21. *Fines depleted ignimbrite*. As for 4, but the pumice clasts are angular.

### **3.6.4 Breccia – Open framework (angular clasts essential)**

22. *Glacial till and moraines (diamictites)*. These heterogeneous deposits are of variable thickness and are massive to crudely bedded with clasts ranging from angular to sub-rounded, set in a matrix of fine rock powder. Fluvio-glacial structures are common.
23. *Glacial dropstone deposits*. Similar to 22, but they are thinner and the matrix is usually coarser. They are contained within lacustrine and marine facies, and the deposits as a whole may be reworked. The dropstones may display impact sags.
24. *Epiclastic reworking and/or mass flow redeposition with granular matrix*. As for 5, but the clasts are angular to sub-rounded.

25. *Cohesive debris flows and lavas.* As for 6, but the clasts are angular to sub-rounded.

26. *Ignimbrite and other, denser pyroclastic flow deposits (block and ash flows, and scoria flows).* Lithic and crystal populations are typically homogeneous and thickness can vary from <5m to hundreds of metres in ignimbrites, whereas denser clast flow deposits are several tens of metres thick. Gas segregation pipes are present and in the case of welded ignimbrites, a eutaxitic texture is developed (Fig. 3.4).

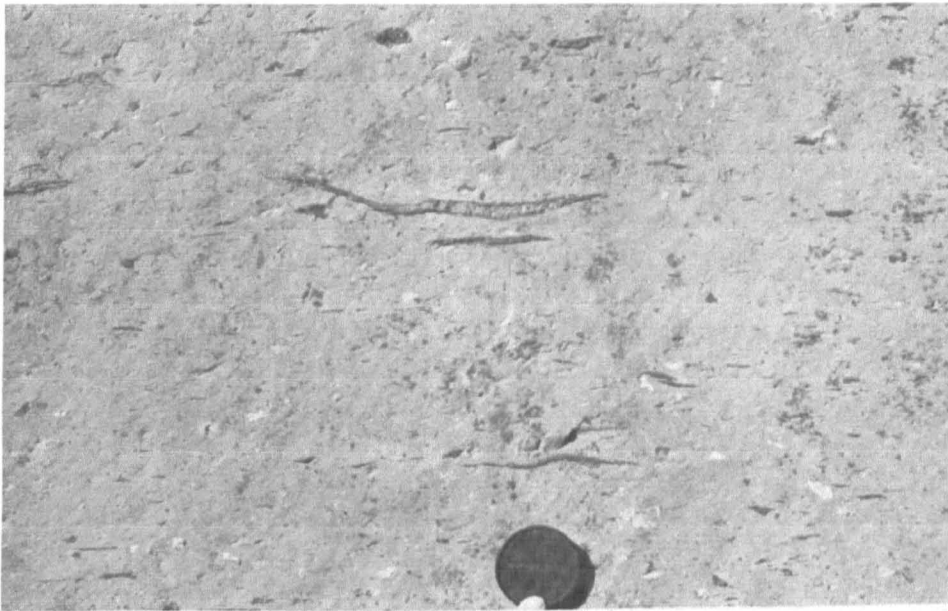


**Figure 3.4 - Welded ignimbrites with eutaxitic textures defined by fiamme from La Piedad, Central Mexico (from Cas & Wright 1987).**

27. *Co-ignimbrite breccias and proximal ignimbrites.* As for 18 and 20, but they are matrix supported.

28. *Near vent base surge deposits.* Base surge deposits that are typically heterogenous and contain ballistics and impact sags. Internally, they show massive, bedded and cross bedded structures.

29. *Ground or ash-cloud surge deposits.* Their composition is dependent on the composition of the parent pyroclastic flows and their lithic content. Ground and ash-cloud deposits are typically bedded and less than 2m thick.

30. *Giant pumice beds*. Such pumice beds are relatively homogeneous with pumice clasts up to several metres across, set in a matrix of lacustrine (or marine) origin. Clasts may display radial jointing or chilled margins.

### **3.6.5 Sandstones (sand sized framework grains predominant)**

31. *Epiclastic reworked sandstones*. These sandstones have abundant sedimentary structures including hummocky or high angle cross bedding. Body and trace fossils may be present.
32. *Epiclastic mass flow redistribution sandstones*. These typically demonstrate mass flow facies characteristics (Chapter 4) and body and trace fossils can be present.
33. *Weathered and/or devitrified lava/dykes*. These generally display a granular texture and have a massive character. They have an even distribution of phenocrysts and may display relict flow banding, set within a fibrous to granitic groundmass of quartz and feldspar.
34. *Fine-grained ignimbrites*. These ignimbrites are massive and eutaxitic textures may be present if originally welded. They are gradational into other ignimbrite facies.
35. *Air-fall ashes and tuffs*. Typically less than 1m thick, such ashes and tuffs are compositionally homogeneous and finely laminated.
36. *Base surge deposits*. As for 28, but finer grained.
37. *Ground and ash-cloud surge deposits*. As for 29, but finer grained.

### **3.6.6 Mudstones (mud sized grade predominant)**

38. *Epiclastic mudstone*. As for 31 and 32.
39. *Fine-grained ignimbrite*. As for 34.
40. *Air-fall ashes and tuffs*. As for 35.
41. *Surge deposits*. As for 36 and 37.

The classification of Cas & Wright (1987) is very detailed and comprises the most extensive review of volcanoclastic rocks. Its framework provides an easily applicable scheme based on grain size and textural characteristics, which can then be applied to suggest modes of origin. Furthermore, the influence of surface reworking and deposition is also considered. Consequently, this scheme was applied in the initial assessment of the nature and origin of breccia lithologies from the BTIP. Although this scheme can be successfully applied as a first stage in the identification and assessment of volcanoclastic rocks, more specialised classifications are required for epiclastic deposits. The role of epiclastic deposits on volcanic edifices has generally been underestimated and recent research has recognised their importance and identified a wide range of characteristics and complex modes of fragmentation, transportation and deposition. These processes are reviewed in Chapter 4, below.

## **4 Epiclastic deposits in volcanic settings**

### **4.1 Introduction**

Volcanic eruptions are short-lived events and represent only a small proportion of the life history of a volcano, most of which is represented by dormant periods. In these circumstances it should not be surprising if an abundance of volcanic debris is produced as a result of erosion from the steep slopes of volcanoes by a wide variety of transport mechanisms not directly related to volcanism. In the volcanic context these are collectively referred to as epiclastic deposits. The purpose here is to review such deposits and set out the characteristics that differentiate them from those resulting from pyroclastic and autoclastic igneous processes normally thought to dominate volcanic settings.

Epiclastic deposits form as a result of weathering, erosion, transportation and deposition of sediments in both subaerial and subaqueous environments. They are equally active in volcanic and non-volcanic settings, as debris is exposed to chemical, physical and occasionally biological weathering. For example, physical processes such as gravitational collapse; mass wasting; mass flows; the effects of waves on marine and lacustrine shorelines; running water from rivers; moving ice, and freezing and thawing, may all be available in volcanic settings to produce material for transport and deposition. Similar deposits are associated with turbidites and coarse-grained deltas, and these will be briefly considered. This review will examine the characteristics of the various epiclastic deposits that result from these processes, ranging from rockfalls and landslides, through debris avalanches, debris flows and grain flows, to sheet and stream flows, focusing on criteria for their recognition. The definition and use of the term 'lahar' will be reviewed. Epiclastic deposits provide valuable information on the landscapes and palaeoenvironments associated with volcanic settings.

### **4.2 Time scales of erosion and transport in volcanic settings**

In volcanic areas such as those around stratovolcanoes and rhyolitic centres, whose lifespan may comprise millions of years, there are lengthy periods of repose between eruptions. During these intervals of quiescence, surface erosion occurs at a very high rate.

As these periods are of far greater duration than the eruptive phases, the high rates of removal are capable of eliminating much of the surface relief of the volcanic piles. Known erosion rates in volcanic settings are summarised by Francis (1983), ranging from 0.1-1.0 m/ka for erosion downcutting in high relief areas, to 1-2km/Ma in the Andes. Francis (1983) noted that the high ratio of loose volcanic debris in these settings and the loss of vegetation cover accelerates erosion rates, and suggests that 1-2Ma are necessary to remove the proximal near-vent area of a stratovolcano. Such rates compare favourably with the calculation of erosion rates for Mount Rainier in the Cascade Range by Mills (1976). Here the dissection of landforms suggests rates of 1.1m/ka, whilst those calculated from river sediment load are 3-4m/ka. This equates to an interval of 1-3Ma for total erosion of the 3km stratovolcano. High erosion rates in times of quiescence provide significant volumes of volcanic debris that may become involved in epiclastic processes.

The studies of Vessel & Davies (1981) demonstrate both the greater duration of epiclastic processes, and their rejuvenation by eruptive periods. Their study of the Fuego volcano in Guatemala revealed four cyclic phases of activity. Phase 1, lasting 80-125yrs, was an inter-eruption phase, and was characterised by river erosion and delta reworking with low sediment deposition. This was followed by phase 2, lasting less than a year and marked by the eruption of lava and by pyroclastic deposition. Phase 3 was a two-year fan-building period, with deposition dominated by debris flows and coarse fluvial sediments, reflecting heavy rainfall. Alluvial fans are common on the flanks of stratovolcanoes. Finally, phase 4 lasting only 20-30yrs, was a phase of flood prone stream braiding in response to entry to the system of large volumes of volcanoclastic sediment. The periods of epiclastic activity clearly outlasted the eruptive phases, and it should be of no surprise that volcanic settings offer such potential for the production of volcanic debris.

These studies have been applied to stratovolcanoes and therefore, caution should be exercised when making comparisons to the BTIP. Eruptions in the BTIP were continental flood basalts, which form a gentler topography than stratovolcanoes and therefore erosion rates would be less. Given the relatively rapid eruption of the BTIP there may also have been insufficient time for such significant amounts of erosion.

### **4.3 Epiclastic sediment transport**

The transport of sediment in both volcanic and non-volcanic settings takes place in one of

two ways: as discrete particles or by mass movement. In particulate movement, each particle behaves individually, whilst in mass movement a large group of particles behave as one and move en masse so that particle freedom is restricted and collisions are rare. Transportation can also be divided by the degree of involvement of an interstitial medium such as ice, water or air. In a few cases, air is present but does not actively entrain particles (Cas & Wright 1987). A summary of sediment transport processes is shown in Table 4.1.

Epiclastic	Nearest primary volcanic analogue
<b>1 Sediment transport not dependent on an interstitial medium</b>	
particulate	
(a) particle free fall	air-fall
(b) particle creep	
mass-movement	
(c) rock fall	
(d) slides	
(e) avalanches	nuées ardentes, block and ash flows
(f) grain flow	
<b>2 Sediment transport in which ice is an essential interstitial medium</b>	
particulate	
(a) ice rafting	
(b) glaciers	
mass-movement	
(c) glaciers	
(d) permafrost creep	
<b>3 Sediment transport in which water is an essential interstitial medium</b>	
particulate	
(a) traction (bed load, saltation)	
(b) suspension	
(c) in solution	
mass-movement	
(d) fluvial torrent flow, sheet flood	
(e) subaqueous granular mass flow (e.g. turbidity currents)	
(f) mud flows, debris flows	lahars
(g) slumps	
(h) soil creep	
<b>4 Sediment transport in which air is an essential interstitial medium</b>	
particulate	
(a) traction	} windblown
(b) suspension	
	surges, eruption columns, plumes
mass-movement	
(c) air-lubricated rock avalanches	pumice, scoria, ash, block and ash flows

Table 4.1- Classification of sediment transport processes (from Cas & Wright 1987)

Particulate sediments may be involved in transport processes that include particle creep, traction, saltation, and suspension by water and/or wind. Although systems may be large individual motions are typically relatively small-scale, resulting in deposits that range from gravels to clays. Processes characteristically produce a range of distinctive structures under the general heading of 'cross-lamination' although products of particle creep are

generally structureless. By contrast, mass movements cover smaller areas but their collective motion is large-scale, producing a series of distinct, identifiable, coarse-grained deposits, many of which lack structure. This thesis sets out to document a number of coarse-grained 'breccias' in the British Tertiary Igneous Province (BTIP) that are attributable to processes of mass movement. The discussion of epiclastic deposits will briefly review processes of particulate movement before emphasising those of mass movement.

### **4.3.1 Particulate sediment transport**

Particulate sediment transport can be sub-divided by the involvement of an interstitial medium. This can be by ice, water, air or where no interstitial medium is required at all.

#### **4.3.1.1 No interstitial medium required**

Here there is no interstitial medium required to drive sediment movement, and the only force acting on the sediment is that of gravity. Obviously, air is present between particles, otherwise there would be a vacuum, but this air does not contribute to the motion of the particle. Two methods of transport can occur: particle free fall and particle creep. In particle free fall, a fragment is dislodged from a raised position and falls downslope. Typical examples are dislodgement of particles or blocks from cliff faces. Particle creep is the slow, downslope movement of individual particles, by the influence of gravity, although rainfall and wind are periodic causes of movement. Particles roll or slide downslope in small increments, almost unrecognisable to the eye and produce no discernible structure. It is common where unconsolidated debris lies on slopes (Cas & Wright 1987).

#### **4.3.1.2 Ice as an interstitial medium**

Sediment particles are trapped within or on top of large bodies of ice that provide solid-state grain support and transport the sediment. Sediment transport by ice may involve glaciers and ice rafting. Glaciers are large, mobile masses of ice in which flow, laterally or downslope is driven by gravity. They are capable of transporting substantial volumes of sediment. This may be eroded from the substrate at the base and margins of the glacier, or derived from material falling on to the surface of the ice and carried forward. Sediment particles drop out of the ice as it melts and produce diamictite deposits consisting of

unsorted debris ranging from clay size particles to large blocks. Glaciers develop at high latitudes and altitudes, and as volcanism can occur independent of climate, even in low latitudes the high slopes of volcanoes are commonly associated with glaciers. In ice rafting, an iceberg (calving from a glacier flowing into the sea or a lake) that is carrying sediment, begins to melt and gradually deposits its sediment load. Boulders that it releases form dropstones and may be found in otherwise fine-grained deposits, commonly deforming underlying sediment layers. In high latitudes volcanic terrains bordering marine environments commonly provide dropstones of volcanic origin (Lisitzin 1962).

#### **4.3.1.3 Water as an interstitial medium**

This occurs where sediment is immersed in water, on the bed of a river or in the sea. In particulate sediment, transport occurs in three ways traction, saltation, and suspension. Bed-load transport produces a group of structures such as ripples, dunes, cross-stratification, and planar lamination. These form when any fluid flows over a bed of cohesionless grains and initiates their movement. Traction involves the rolling or sliding of particles along the bed, whilst saltation indicates transport in a series of bounces or small hops (see Fig. 4.1). This can be caused by the impact of particles falling back to the bed, or by turbulence at flow velocities high enough to temporarily suspend particles. Based on the mean flow velocity, water depth, and the mean sediment size, a well-defined suite of sedimentary structures is created. Suspension involves particles supported above the bed by fluid turbulence, and is typically restricted to fine-grained material. Clay- or silt-size particles are carried in suspension (see Fig. 4.1) and are deposited as currents wane to produce suspension fall out muds. Where freshwater carrying clays in suspension mixes with seawater, deposition may be aided by flocculation. Coarser particles may also be carried in suspension if flow velocities are high. These processes all occur in rivers and lakes and on shorelines associated with volcanic settings. For more detailed discussion the reader is referred to Allen (1970, 1982) or Leeder (1982).

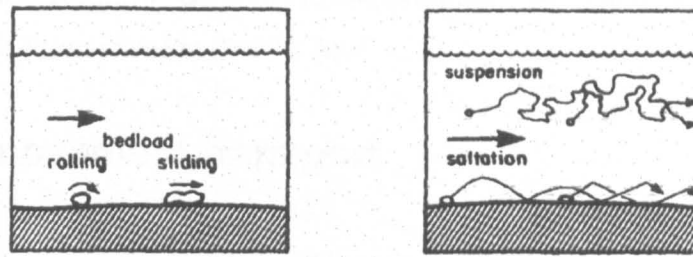


Fig. 4.1 - Sediment transport by rolling, sliding and saltation (jumping). Smaller grains may also be lifted into suspension (from Cas & Wright 1987)

#### 4.3.1.4 Air as an interstitial medium

Transport by air is provided by wind. Sediment is carried as bedload and in suspension as in water. The processes are similar to those in water, except that because the density and viscosity of air are lower, particles are less buoyant. Higher flow velocities are required to move material of equivalent sizes and wind cannot move coarse granular material. Transport processes are responsible for structures such as ripples and large-scale dunes. In volcanic settings, wind transport can be a strong influence on newly erupted pyroclastic ash.

#### 4.3.2 Sediment transport by mass movement

Sediment transport by mass movement, like particulate sediment transport, can be divided on the basis of the nature of the interstitial medium (Table 4.1). However, this is a simplistic classification and the extensive literature on such deposits suggests that the situation is more complex. Much of the literature concerning these deposits is based on fluid mechanics and flow dynamics of their movement (e.g Takahashi 1978; Innes 1983; Coussot & Meunier, 1996). These are problems to be solved, by experimentation, mathematical and engineering analysis, that are beyond the scope of the present work. The emphasis here is on the geological characteristics of these deposits focusing on textural, lithological and structural characteristics and their origin, transport and deposition, exemplified in work by Fisher & Schmincke (1984); Glicken (1991); Smith & Lowe (1991); Yarnold (1993); Coussot & Meunier (1996); Schneider & Fisher (1998); Bertran & Texier (1999). Many of the distinctions suggested by these authors are difficult to recognise and there is much overlap and transition between the major processes and

products of mass movement. Given these complications, the simple classification used in Section 4.3.1 will be reviewed in detail below.

## 4.4 Mass movement transport

A number of systems of classification differentiating flows and mass movements may be found in the literature (Beverage & Culbertson 1964; Varnes 1978; Hansen 1984; Pierson & Costa 1987). The distinguishing criteria vary from author to author but include: triggering mechanism, sediment composition, solid fraction, physical flow processes and others. The scientific background of the author often has a strong influence on the nature of the resulting classification. Geologists, geographers, engineers or physicists, may use different terms to describe the same features. As a result, it is commonly difficult to cross-reference schemes and many classifications are over-complicated. Some basic definitions are required for the major mass movement processes. These will be followed by two recent classification schemes that provide simple conceptual views of flow and mass movements, using practical, identifiable criteria.

### 4.4.1 Definitions

Streamflows represent flow of a Newtonian fluid. Flow is turbulent except for a thin layer near the bed, and turbulence is the principle sediment support mechanism (Pierson & Costa 1987).

Hyperconcentrated flows are flows intermediate between dilute, turbulent, 'normal' streamflow, and viscous, non-turbulent debris flows (see below). Introduced by Beverage & Culbertson (1964), the term describes flows where debris is supported by buoyancy, grain interactions and some turbulence. Hyperconcentrated flows were defined as having a sediment concentration between 40 and 80 wt. %, compared to <40 wt. % for streamflow and >80 wt. % for debris flows.

A number of definitions exist for the term debris flow. Generally debris-flows can be described as large volumes of viscous and highly concentrated water-debris mixtures that flow along a channel-bed (Coussot & Meunier 1996). Other definitions include the rapid mass movement of granular solids, water and air moving as a single phase system (Costa & Williams 1984); and strongly transient flows of heavily debris-laden slurry, separated by

periods of relatively low flow rate or zero flow (Johnson 1970). Debris flows occur both subaerially and subaqueously in settings where slopes are relatively steep and fine-grained water-saturated sediments and coarse debris are available, creating unstable conditions. They can be triggered by heavy rainfall or ice melt on the surface (Fisher & Schmincke 1984; Cas & Wright 1987) or subaqueously by storms.

Debris avalanches are rapid granular mass movements originating in rocky or granular mass ruptures on steep slopes (Coussot & Meunier 1996). Cas and Wright (1987) view these avalanches as mobile, fluidal flows characterized by close packing of blocks and fragments that jostle, bump, push, collide and fragment each other in transit. Kessler & Bedard (2000) describe them as large, dislodged rock mass flows that move rapidly down generally high slopes. They result from large volume landslides (Pierson & Costa 1987).

Rockfalls are directly related to particle free fall as described in section 4.3.1.1, where rock matter is dislodged and moves rapidly downslope under gravity (Cas and Wright 1987).

A slide represents a dislodged mass of rock that maintains contact with and shears over the substrate, moving as a coherent mass under the influence of gravity. Slides are initiated on relatively steep slopes and vary widely in scale (Cas & Wright 1987).

Granular mass flows reflect the downslope flow of a volume of cohesionless grains containing interstitial water. They are typically sub-aqueous and flow into lakes and oceans. As movement of the grains is initiated by gravity, mixing between sediment and water occurs. The sediment mass expands and fluid turbulence is created in the interstitial spaces within the flow, providing grain support (Nardin *et al.* 1979; Allen 1982). Subaqueous granular mass flows, where turbulence plays an essential grain support role, are called turbidity currents and their deposits are turbidites. Turbidity currents produce a sequence of structures reflecting changing flow regime as the current decelerates. Their regular succession of structures was first recognised by Bouma (1962) and is now known as the Bouma sequence. Such deposits are common in the sedimentary record including volcanic settings. They are found in deep lakes, in particular in caldera lakes with steep erodible margins, in streams and in deltas, and in marine settings marginal to volcanic provinces (Sigurdsson *et al.* 1980; Wright & Mutti 1981; Carey & Sigurdsson 1984; Lajoie 1984). Turbidites are an important and extensive subject in their own right, and are briefly reviewed in section 4.6.

#### **4.4.2 Mass movement as a function of solid fraction and material type**

Cousot & Meunier (1996) proposed a classification of the common mass movements and flows on steep slopes on the basis of the proportion of the flow represented by solids and the type of material involved. It is recognised that sediment concentrations progressively increase when flows vary from pure water, to stream flows transporting particulate solids, to hyperconcentrated flows, and to debris flows and landslides/debris avalanches. The solid fraction can be expressed as a percentage by volume or weight. The nature of the material is important because the behaviour in water of cohesive fine particles such as clays is quite different to that of non-cohesive coarse sands or pebbles. The classification is presented in the form of an ellipse (Fig. 4.2) although the limits it defines are strictly conceptual and qualitative. From this we can determine (approximately) that a flow containing roughly equal proportions of solid and water, with both cohesive and granular material is classed as a debris flow. A flow of similar solid fraction percentage, but with more cohesive material, is a mudflow. A flow containing a high solid fraction of granular material following failure is a debris avalanche, and a high solid fraction flow of cohesive material following failure is a landslide.

This classification provides a method of determining the nature of mass movement on the basis of two simple and identifiable criteria. It is quick and easy to use and ideal for a first approximation in identifying mass movement processes. However, there are many more criteria that may be used to successfully classify mass movement processes. Several features in coarse-grained mass movement deposits are shared with other deposits. These include clast size, shape, and sorting, and clast to matrix ratio. The relative influence of these factors needs to be resolved.

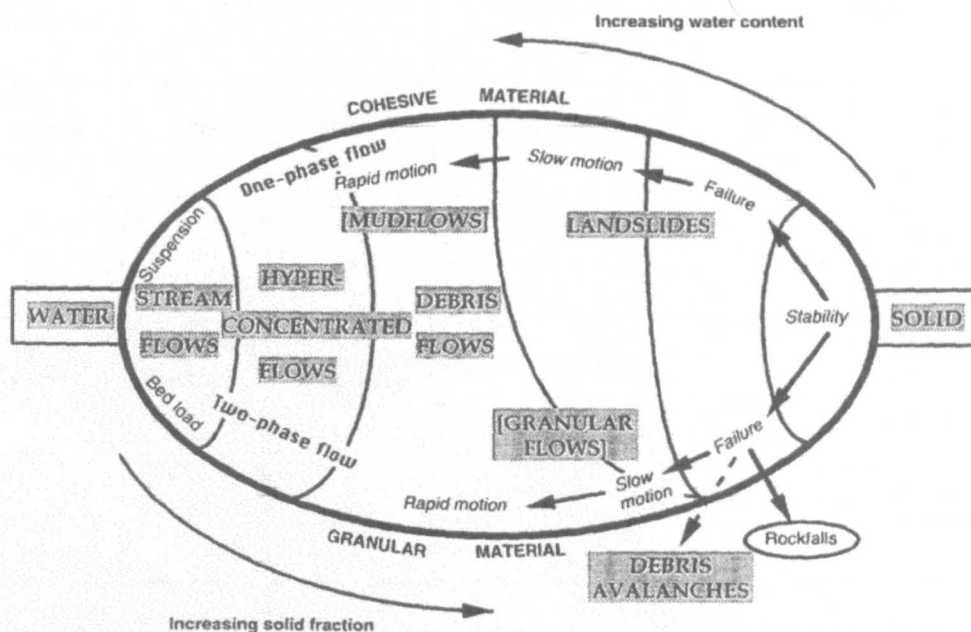


Fig. 4.2 – Classifications of mass movement on steep slopes as a function of solid fraction and material type (from Cousot & Meunier 1996).

#### 4.4.3 Mass movement as a function of solid fraction and interstitial fluid

Bertran & Texier (1999) proposed a system (Table 4.2), based on Varnes (1978) and Pierson & Costa (1987), whereby mass movements are classified as a function of solid fraction and interstitial fluid content, indicating the rheological behaviour of the flow. The latter is reflected in important morphological and microstructural characteristics of the deposits. This scheme is again simple, but provides a good conceptual framework for identification of mass movement processes.

##### 4.4.3.1 Low sediment concentration and air = rockfall

These conditions produce rockfall deposits where rock clasts fall from a cliff as individual particles or a dispersed assemblage and come to rest after rolling, bouncing or sliding onto talus. Talus is coarse and poorly sorted, with a clast-supported openwork structure, characterised by an absence of, or at most very crude stratification. The clast fabric is

Sediment concentration	Low		Intermediate	High	
	Air	Water	Water + fines	Air	Water + fines
Main interstitial fluid					
Process	Rockfall	Streamflow	Hyperconcentrated flow	Grain flow Rock avalanche	Debris flow (liquefaction) Solifluction Earth slide/flow (distinct sliding planes)

**Table 4.2 – Classification of slope processes by solid fraction and interstitial fluid (from Bertran & Texier 1999)**

random or displays only a weak preferred orientation parallel to the slope (Bertran & Texier 1999). Rockfalls typically form scree slopes.

#### **4.4.3.2 Low sediment concentration and water or water and fines = overland flow**

Overland flow deposits are essentially stream flow deposits (but of much smaller-scale) formed from waters carrying only a small amount of sediment, and confined within a thin layer of only a few millimetres. Such flows are often referred to as runoff. The deposits are usually moderately sorted with random to weakly oriented clast fabric (Bertran & Texier 1999).

#### **4.4.3.3 High sediment concentration and air = grain flows and rock avalanches**

Grain flows are dry, cohesionless flows of debris on steep talus slopes. They are characterised by lateral levees, fine-grained channel bottom deposits and elongated frontal lobes. They are typically stratified, with inverse grading, strong imbrication of clasts, and slope-parallel preferred orientation, although these features disappear in distal parts of the lobes. A fine-grained layer, ranging from 1-2 mm to decimetres in thickness, is present at the base of the deposits (Bertran & Texier 1999).

Rock avalanches (Siebert 1984; Glicken 1991) are flows of extremely large volumes of rock ( $>10^3\text{m}^3$ ) that disintegrate during sliding or collapse (Hsu 1975). Deposits are tongue or fan-shaped and mantle the underlying topography. Accumulation is concentrated in the distal part of the avalanche, and the surface of the deposit is hummocky. The main diagnostic criteria include the presence of megablocks (1m up to 100m), angular clasts, commonly with a jigsaw fit, and inverse grading. A basal layer commonly has an abundant homogeneous fine-grained cataclastic matrix with distinct sliding planes and lacks jigsaw fit clasts.

#### **4.4.3.4 High sediment concentration and water or water and fines = debris flows, solifluction, earth slides and flows**

In the event of liquefaction by higher pore pressures the debris moving on steep slopes becomes a debris flow. Bertran & Texier (1999) describe these as initiated by the removal of loose debris accumulated in gullies or by the transformation of landslides into slurry following a rainstorm. They form crudely stratified deposits characterised by coarse openwork or matrix-supported lenses resembling diamicton deposits. The clast fabric shows weak to moderate preferred orientation.

Periglacial solifluction occurs in high latitudes, where there is only partial liquefaction of debris and no distinct sliding planes. It involves the slow downslope displacement of sediments at velocities ranging from 1 to 10cm a year. This is caused by frost creep, due to alternation of frost heaving (growth of ice lenses) and resettlement of the soil (melting of ice), or by gelifluction, where high pore water pressures during thaw result in a loss of soil strength and subsequent flow. Massive or crudely stratified diamicton deposits are formed.

Finally, where there is only partial liquefaction of debris, but distinct sliding planes are present, motions are referred to as earth slides and earth flows. These are mass displacements where movement is concentrated along basal and internal shear planes. The sliding mass typically remains coherent but may break into a few blocks or disintegrate. Slides are typified by slickensided slip planes and may show internal deformation of former bedding in the form of folds, stretching or boudinage.

#### 4.4.3.5 Discussion

Bertran & Texier's (1999) scheme represents a simple breakdown of the characteristics of mass movement processes and deposits. Using criteria easily identifiable in the field, it may be used to distinguish the main processes of mass movement. It is clear however, that many characteristics, for example the presence of coarse poorly-sorted angular clasts with little or no stratification, are shared by many of these deposits (Smith & Lowe 1991; Yarnold 1993) and more detailed approaches are therefore required to be confident of field recognition. Whilst these schemes are suitable for the identification of deposits resulting from rockfalls, streamflows, slides and solifluction, there is a particular need for clarity regarding debris flows and debris avalanches.

#### 4.4.4 Debris flows and debris avalanches

Debris flows have long been recognised as instigated by failure of unsorted, typically mud-bearing gravelly sediment mantling a fan catchment and resulting from the rapid addition of water in the form of rainfall or snowmelt (Pack 1923; Woolley 1946). They are noted from mountainous regions around the globe, spanning all climates (Blair & McPherson 1994) and numerous workers have studied their initiation, transport mechanics and occurrence (Johnson 1970; Takahashi 1978; Innes 1983; Pierson & Costa 1987; Coussot & Meunier 1996). They are common in volcanic settings and are associated with the term 'lahars' (Fisher & Schmincke 1984). In volcanic areas, enormous volumes of sediment are transported downslope by mass flow processes, and their deposits dominate volcanoclastic sedimentary sequences (Smith 1986). Since the eruption that triggered collapse of the north flank of Mount St. Helens on 18th May 1980 (Voight *et al.* 1981) much attention has been paid to the role of debris avalanches in the history of volcanoes. Many ancient deposits have been recognised as being produced by debris avalanches and their significance in volcanoclastic sequences has become clearer (Ui 1983; Siebert 1984; Glicken 1986, 1991; Ui & Glicken 1986; Palmer *et al.* 1991; Smith & Lowe 1991; Yarnold 1993). Deposits of debris flows and debris avalanches are common in volcanic settings, yet they share a coarse-grained, angular, unsorted and poorly stratified appearance and this means that they are difficult to differentiate. A number of schemes and comparisons have been outlined in response to this problem.

#### 4.4.4.1 Distinction by velocity and motion type

Coussot & Meunier (1996) separate debris flows and debris avalanches/landslides on the basis of velocity and motion type. Debris flows move at rates of  $0.5\text{-}10\text{ms}^{-1}$ , whereas debris avalanches move at  $>10\text{ms}^{-1}$  (Johnson 1970; Kobayashi 1992). However, this distinction cannot be applied to ancient deposits. The role of water is negligible in debris avalanches, but in debris flows pore-water pressures facilitate the motion of the granular material and water may initiate colloidal interactions between clay particles (Pierson & Costa 1987). The motion within avalanches and landslides originates at internal fractures, faults or slip surfaces. The mass generally undergoes relatively little deformation and preserves the initial structure of material within the final deposit. Within debris flows, however, the initial structure is highly deformed and is commonly entirely lost.

#### 4.4.4.2 Distinction by sedimentary characteristics

Yarnold (1993) provided an excellent comprehensive review of sedimentary characteristics important in distinguishing debris flow and debris avalanche deposits (Table 4.3). These data will be summarised here. For clarity, Table 4.3 contains selected references citing examples of and commenting on, the various diagnostic features used.

Debris flows are commonly restricted to channels but may locally move as sheets. They are typically  $<5\text{m}$  thick. Their internal fabric may show coarse-tail normal grading, reverse-to-normal or reverse grading, or no grading. Clasts are matrix-supported and commonly show a preferred alignment of their long axes parallel to the direction of flow. The matrix materials are typically products of surface weathering incorporated into the flows. Flows are derived from heterogeneous debris and can mix with surface materials and flows from other sources, producing mixed populations of rounded and angular clasts. In a volcanic context this debris is predominantly of volcanic origin, but other clasts available on the landscape can be included. Heterogeneous rock types and particles are randomly mixed, except for the coarsest clasts that dominate the frontal part of the flow during runout. Fracturing of clasts is rare except where inherited from source. Maximum clast size is typically  $<10\text{m}$ . Flows have limited erosional power and show only minor local scouring. Slip surfaces are rare and margins experience only weak diffuse shear, forming striae at contacts. Flows commonly display flat or convex upper surfaces and can be flanked by levees.

Deposit type	Debris-flow deposits; nonvolcanic, dry climate (Bull, 1972, 1977; Nilasa, 1962; Johnson, 1984; Harvey, 1984)	Rock-avalanche deposits; nonvolcanic, dry climate (Longwell, 1951; Yarnold and Lombard, 1989; Krieger, 1977)
Form and size	Flows commonly restricted to channels with ribbon-like plan-view geometries (Gascoyne, 1978); locally move as "sheets" but tend to break into finger-like lobes or cease movement after traveling relatively short distances (Eisbacher and Chague, 1984); deposits of individual flows typically <5 m thick	Unconfined flows may display sheet- or tongue-like geometries with long dimensions as much as 15 km (Watson and Wright, 1969); deposits of individual flows may range from a few meters to several hundred meters in thickness (Harrison and Falcon, 1937)
Internal fabric	Individual flows may display no grading or reverse, reverse-to-normal, or coarse-tail normal grading; large clasts typically matrix-supported; clasts also commonly display a preferred alignment of their long axes parallel to the direction of flow (Smith, 1986)	Large-volume lobes are typically nongraded or display apparent reverse grading resulting from concentrated comminution in the lower portion of lobes (Cruden and Hung, 1986); such lobes range from clast- to matrix-supported (Shaller, 1991); fabric data from smaller volume lobes is lacking.
Clast roundness	Flows are commonly derived from heterogeneous colluvium or alluvial deposits and can coalesce and intermix with flows from separate sources to produce clast populations with rounded, angular, or mixed clasts	Consist of predominantly angular to subangular fragmental debris, with the exception of (usually minor) foreign materials that originally mantled the parent block or that were entrained during runout; shape characteristics of "primary" fragments may vary to some degree with rock type or even clast size (Hewitt, 1988)
Clast fracturing	Intense fracturing of constituent materials is uncommon, except where inherited from source	Indurated materials within large-volume flows are commonly intensely fractured, forming zones of "jigsaw" and "crackle" breccia; the intensity of fragmentation varies with rock type and position within lobes; debris within smaller volume lobes can also exhibit considerable fracturing (Mudge, 1965)
Maximum clast size	Typically <10 m in long dimension; maximum clast size correlates strongly with bed thickness (Nemec and Steel, 1984)	Highly shattered but discernible blocks many tens of meters to over 100 m in maximum dimension are associated with some lobes (Harrison and Falcon, 1937; Mudge, 1965); unfractured fragments in excess of 10 m have been observed
Matrix characteristics	Commonly dominated by pedogenic mud; may contain lightweight fragments (for example, wood) and bubble vesicles (Costa, 1988)	Matrix materials within dry lobes typically dominated (>80%-90% by vol.) by cataclastically generated granules and coarse- to medium-grained sand
Clast mixing	Caterpillar-track-like cycling tends to randomly intermix various rock types and particle shapes incorporated into flows, except for coarsest clasts, which may maintain a frontal position during runout	Thorough mixing probably atypical of most dry flows (Eisbacher and Chague, 1984); large-volume lobes tend to preserve the relative position of materials within their parent blocks during runout (Shreve, 1968); such lobes commonly exhibit distinct monolithologic domains in which clasts and matrix are of identical composition
Substrate deformation	Flows associated with limited erosive power; locally exhibit minor to moderate scouring (Johnson, 1970), commonly entirely depositional (Gascoyne, 1978; Hooke, 1987)	Large-volume flows commonly associated with vigorous scouring and bulldozing; may even deform subjacent sediments to depths of 5 m or more; degree of deformation dependent upon properties of flow, runout course, and substrate
Slip surfaces	Flow margins generally experience diffuse shear that does not result in intense comminution; weak striae may form along contacts (Middleton and Hampton, 1976)	Commonly contain discrete internal slip surfaces with intervals of gouge on the order of 10 cm thick; basal contacts locally exhibit striations and zones of pulverization
Surface topography	Individual flows typically display flat or broadly convex surfaces; may be flanked by levees	Large-volume flows commonly display large hummocks, ridges, and debris cones in addition to lateral ridges (Pfeifer, 1978); hummocky surfaces have also been described for smaller volume lobes (Mudge, 1965)

Table 4.3 - Key sedimentary characteristics distinguishing subaerial debris flow and debris avalanche deposits (from Yarnold 1993).

Where unconfined, debris avalanches may form sheet or tongue-like deposits up to 15km in length. Individual flows range from a few metres to several hundred metres thick. Flows vary from clast- to matrix-supported and are typically reverse graded or ungraded due to comminution in the lower parts of flows. They are composed primarily of angular to sub-angular fragments, the shape of which may vary with rock type or clast size. Blocks and clasts within flows are often intensely fractured and display zones of jigsaw or crackle breccia. Highly fractured but discernible blocks many tens of metres in diameter are common and blocks up to 100m are found. Unfractured blocks in excess of 10m have been observed. The matrix is composed primarily (80-90 vol. %) of cataclastically-generated granules and coarse- to medium-grained sand, produced through fracturing and

grinding associated with the avalanche event. Mixing of clasts is rare and the relative positions are preserved during runout. Monolithic domains in which clast and matrix compositions are identical are preserved. Large volume flows are associated with scouring and bulldozing and may deform underlying sediments. The flows contain discrete internal slip surfaces with layers of cataclastic gouge, and the basal contact layer commonly shows intense pulverisation. The surface topography of avalanches may include hummocks and ridges, up to 50m high.

The key characteristics separating debris flow and avalanche deposits are therefore textural. Debris flow deposits are poorly sorted, with angular to rounded clasts of heterogeneous material set in a fine-grained matrix. Clasts are rarely fractured and deposits are often reverse or reverse-to-normal graded. Debris avalanches are of larger volume and consist of coarse, angular, homogeneous clasts in a matrix of cataclastically generated coarse sand grade material. Highly fractured megablocks and jigsaw pattern clasts may be present. Surfaces of flows are characterised by large hummocks. For recent deposits, this distinction is readily applicable in the field.

## **4.5 Origin, transport and deposition of debris flows and avalanches**

It is important to consider the origin, transport and deposition of debris flows and debris avalanches in order to identify and explain some of their distinguishing characteristics. Numerous studies of the origins, transport and deposition of these deposits are documented from various localities (Palmer *et al.* 1991; Smith & Lowe 1991; Pierson 1995; Coussot & Meunier 1996; Blair & McPherson 1998; Schneider & Fisher 1998; Kessler & Bedard 2000; Reubi & Hernandez 2000).

### **4.5.1 Debris flows**

Debris flows are flowing liquefied slurry. They are initiated by the addition of water (e.g. through rainfall, lake collapse or snow and ice melt) to poorly sorted sediment, but at what point do they begin to flow? Debris flows contain approximately 50 to 75% sediment by volume (Pierson 1985) and such mixtures are 10<sup>4</sup> to 10<sup>5</sup> times more viscous than water (Johnson 1984). These mixtures possess finite yield strength and this must be overcome by applied stress before deformation (i.e. flow) is possible (Pierson 1995). This stress is

applied by the addition of water to the sediment mass and when the yield strength is overcome, the mass flows as a single viscous, plastic material. In cohesive or muddy debris flows, the fine fraction is sufficiently large (>10%) for the fine particle-water mixture to form an interstitial fluid that facilitates grain movement and assists flow. In cohesionless, or granular, debris flows, the fine fraction is low enough for direct grain-to-grain contacts to influence mass movement (Coussot & Meunier 1996; Kessler & Bedard 2000).

Movement in debris flows begins in a basal zone of maximum shear stress where laminar flow, sliding and rolling of clasts occurs. Further up in the flow, in an area of lower shear, the rest of the material is rafted along as a semi-rigid plug (Kessler & Bedard 2000). In cohesionless debris flows with large clast concentrations, inverse grading is observed (Shultz 1984). The means by which inverse grading develops are not well understood. Bagnold (1954) states that dispersive forces act normal to flow boundaries during movement of concentrated dispersions. The transfer of momentum from grain to grain or from close grain encounters during flow, supports individual grains throughout the flowing bed. Bagnold's equations show that the dispersive force acting on a particle is proportional to the rate of shear, suggesting that when particles are sheared together, the larger particles will drift towards the zone with least shear (Johnson 1970). As the upper part of a flow is subject to lower shear stress, larger clasts are concentrated here and hence inverse grading is produced (see Fig. 4.3). As this concentration of boulders and coarse cobbles reaches the flow front, they become interlocked and this inhibits flow movement. As a result clasts are pushed laterally to form levees, and may reorient their long axes from a slope-perpendicular to a slope-parallel trend (Blair & McPherson 1998), forming a vague clast imbrication.

Debris flows are initiated when applied shear stress exceeds the yield strength of the material involved, movement ceases when the shear stress falls below this limit. Deposition occurs en masse as a large plug of material and the flow essentially 'freezes' (Johnson 1970; Smith 1986).

## 4.5.2 Debris Avalanches

Debris avalanches are very rapid, inertial granular flows resulting from large volume landslides, and are important in volcanic settings where they result from sector collapse of steep structurally unstable volcanic cones or flanks (Siebert 1984). Rocky or granular mass-ruptures initiate collapses. These can include large-scale rockfalls or slides (Cousot & Meunier 1996), or faulting that delimits large-scale blocks (Glicken 1986). Models have been developed to explain transportation of debris avalanches.

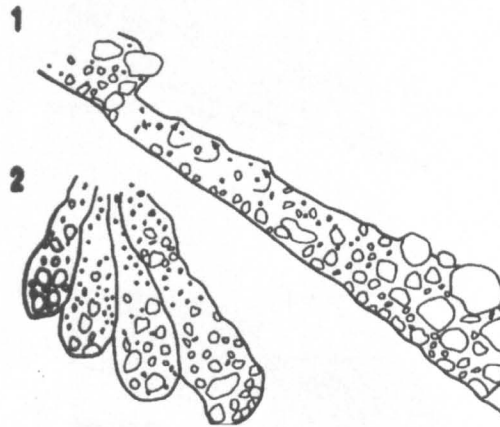


**Figure 4.3 - Models of surging cohesionless debris flows showing examples of potential vertical size distribution within flow. 1) Large clasts are supported at the top of the flow in the proximal zone and a more chaotic class distribution is observed further back in the flow. 2) Shows abrupt facies changes along lateral transects (from Kessler & Bedard 2000).**

Reubi & Hernandez (2000) proposed a model based on a typical debris avalanche deposit in the Maronne Valley of the Cantal Volcano in France (see Fig.4.4). In response to gravity instability, gigablocks are delimited by normal faults and begin to slide, producing large scarp structures with positive topographic relief. During the slide, basal friction produces shear that fragments the moving mass. This stress is stronger at the base of the mass and a layer of fine particles develops, whilst the main part of the avalanche is brecciated and fragmented but not dispersed. The basal layer may temporarily develop turbulent behaviour and pick up and mix with clasts from the source edifice, but this is not always the case. Downslope the avalanche transforms from a slide into a flow and the

middle and upper zones become heavily brecciated, but remain coherent, moving as a rigid sheet. The characteristic relief is formed from the scarps created during the slide and is preserved as hummocky deposits. These are easily identifiable in modern deposits, but may be difficult to recognise in outcrops of ancient rocks or to differentiate from irregular erosion surfaces (Smith & Lowe 1991).

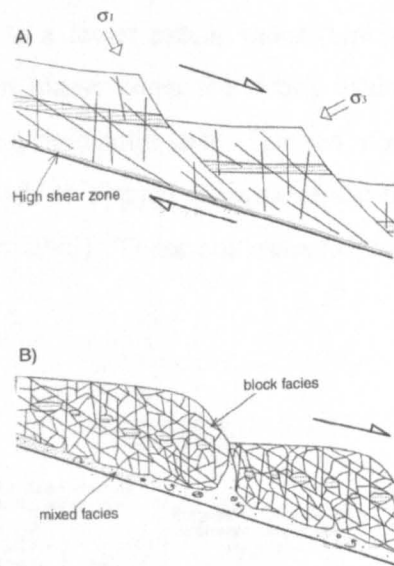


**Figure 4.4 - Debris avalanche transport model: A) Sliding stage B) Flow stage (from Reubi & Hernandez 2000)**

Schneider & Fisher (1998) proposed an alternative transport model based on the same Cantal Volcano. This focused on the production of fractured clasts, megaclasts and jigsaw textures within debris avalanche deposits. They suggest that a megaclast is completely fragmented by a dense network of cracks. These are rapidly opened and 'injected' or filled by the matrix (which they express as 'inflation'), which surrounds large clasts and blocks. Crack widths increase from the centres to the edges of clasts, indicating inflation contemporaneous with intraclast matrix injection. This inflation typically produces sub-spherical clasts and megaclasts. Where cracks are completely opened a jigsaw pattern is preserved. Schneider & Fisher (1998) call this process 'Isotropic Dispersive Inflation' (IDI).

Fracture of the material may result from pre-avalanche mass failure or brecciation (Glicken 1991). Ui *et al.* (1986) suggested that it might occur during transport of the avalanche mass because of interactions between clasts or with the substratum at the base of the avalanche. Matrix is produced by grinding of the clasts and typically results in deposits where clasts are homogeneous and are separated by material of the same composition (Smith & Lowe 1991). Schneider & Fisher (1998) suggest that the geometry of the clasts and megaclasts, the lack of clast rotation and imbrication, and the occurrence of IDI, indicate that debris avalanches are not turbulent during transport.

Debris avalanches are rigid sliding masses that behave as dilatant fluids. This fluidisation, most commonly by air and to a lesser extent water (Glicken 1991), allows the mass to move. Deposition occurs en masse when the debris avalanche transforms from a non-turbulent fluidised mass, into a rigid solid state. Friction, observed from shear structures at the base of the avalanche leads to a rapid slowing of the mass, which dilates, stops and solidifies (Schneider & Fisher 1998). These processes are summarised in Figure 4.5.

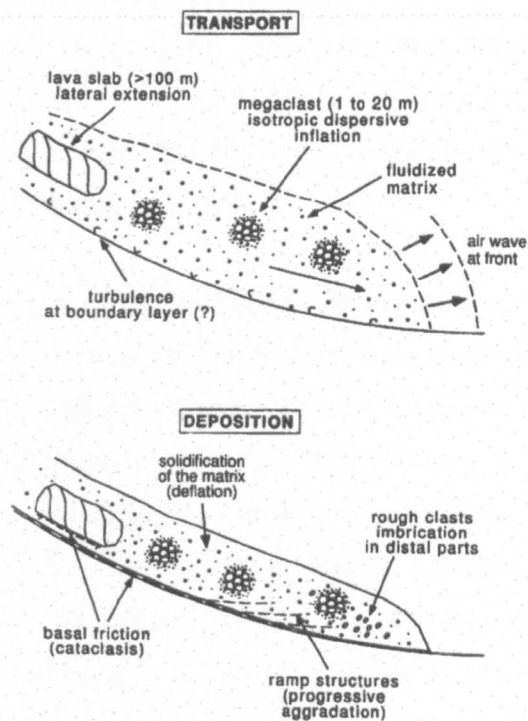


Figure 4.5 - Transport and depositional processes in debris avalanches of the Cantal Volcano, France (from Schneider & Fisher 1998)

### 4.5.3 Flow transformations

Flow transformations are defined as changes in flow behaviour between laminar and turbulent states (Fisher 1983). Surface transformations from the addition of fluid (dilution) or sediment (bulking) are common in mass movement events, especially in volcanic settings, and flows may develop from one style to another. They are particularly relevant to this review as different deposits can result from the same event.

Dilution occurs when flows mix with water, commonly in stream channels or small ponds and lakes. Dilution of a debris flow to form a hyperconcentrated flow was observed following a debris flow event on Mount St. Helens in 1982 (Pierson & Scott 1985). Mixing of turbulent streamwater diluted the flow front to form a hyperconcentrated flow. Downstream the passage of the hyperconcentrated flow was followed by the undiluted part of the debris flow, and therefore a two-stage deposition was recorded, with a lower hyperconcentrated flow deposit grading upwards into a debris flow deposit.

The process of bulking involves the addition of loose sediment into a flow. Large volume dilute stream or overland flows, generated by eruption-induced snowmelt, rainfall or lake collapse, can bulk up with loose sediment and transform to debris and/or hyperconcentrated flows (Pierson & Scott 1985). Bulking explains the appearance and heterogeneity of rounded to sub-rounded clasts found in many debris flow deposits, particularly downslope (Smith & Lowe 1991).

Flow transformations are also responsible for the link between debris flows and debris avalanches. Debris flow deposits typically form downslope of or laterally adjacent to debris avalanches, where avalanche deposits become diluted or water-rich portions of the avalanche separate out and continue as debris flows (Palmer *et al.* 1991). Large volume debris flow deposits, containing clasts metres in diameter that have moved several kilometres, imply the mobilisation of large volumes of material at source. A simple explanation for this would be mass failure of a volcano slope, and hence generation of a debris avalanche. This could then be transformed, by dilution after runout, to a debris flow. The processes of flow transformation are summarised in Figure 4.6 (Smith & Lowe 1991), illustrating the various stages required for the initiation of debris flows, avalanches, hyperconcentrated flows and normal streamflow in a volcanic environment.

## 4.6 Lahars

The term 'lahar' originated in Indonesia where it described a volcanic breccia transported by water (van Bemmelen 1949), but in geological literature it has become synonymous with a volcanic debris flow. It has been applied both to the flowing debris-water mixture (the event) and to the deposit (Fisher & Schmincke 1984). It has been used to describe any poorly sorted volcanoclastic sedimentary deposit, irrespective of whether there is direct evidence of debris flow deposition. Particular writers have restricted it to deposits emplaced at high temperatures as a direct result of volcanism (Neall 1976; Smith 1986). This indifference has seen a wider use of the term recommended and adopted, whereby a lahar is "a general term for a rapidly flowing mixture of rock debris and water (other than normal streamflow) from a volcano." A lahar is an event; it can refer to one or more discrete processes, but does not refer to a deposit (Smith & Fritz 1989). This definition successfully recognises the complexity of volcano-hydrologic events, and recognises that some aspects of these processes are unique to volcanic areas, but are not always directly related to eruptions.

## 4.7 Turbidites and coarse-grained deltas

Subaqueous granular mass flows in which turbulence plays the major grain support role are called turbidity currents and their deposits are turbidites. In turbidity currents with low sediment concentrations particle interaction is minimal and particles are sorted according to their hydraulic properties. When sedimentation begins the heaviest particles settle first, producing a well-defined upward-fining sequence. Turbidity currents produce a sequence of structures reflecting changing flow regime as the current decelerates (Bouma 1962), and this is now known as the Bouma sequence (Fig. 4.7). It reflects a transition from massive graded beds, through plane-lamination, climbing ripples and laminated mud to pelagic mud deposition. Complete Bouma sequences are rare; depending on features such as initiation point, flow distance and sediment load. Proximally, basal divisions (a and b) are typically present, whereas distal turbidites frequently preserve upper divisions (c, d and e). In turbidity currents with high sediment concentrations (where much larger clasts can be supported), particle freedom is inhibited and size grading is poorly developed, or absent. Reverse grading may be developed in the basal region of these deposits by the process of

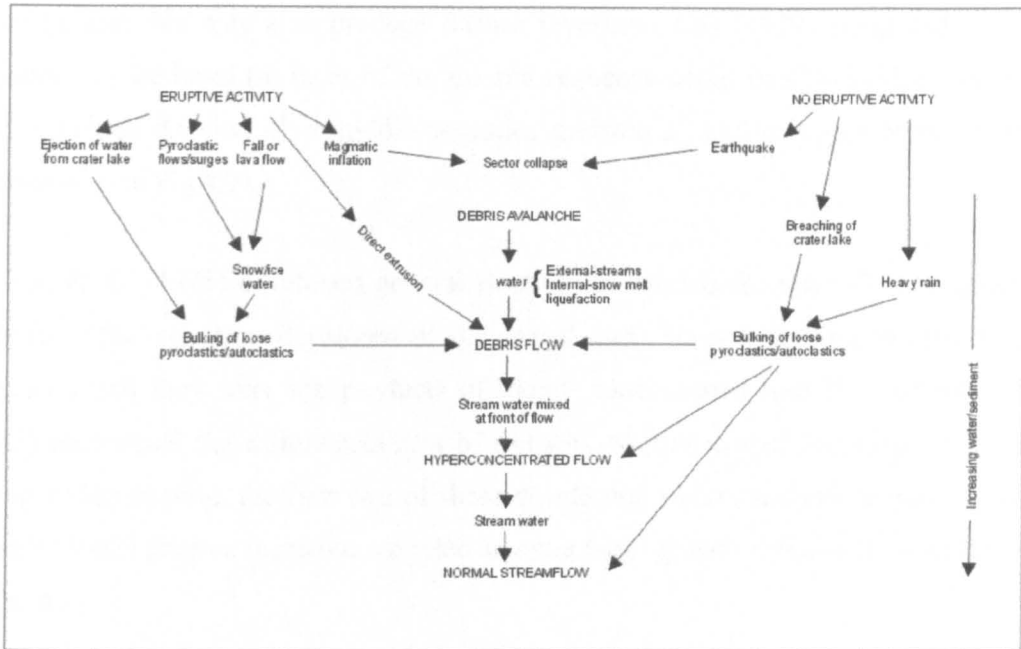
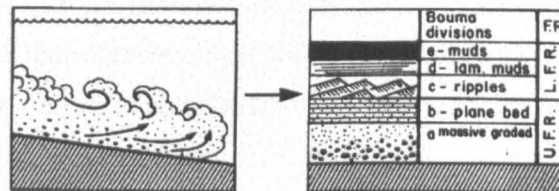


Figure 4.6 - Schematic diagram illustrating genetic relationships of volcanic phenomena and the generation of debris avalanches, debris flows and hyperconcentrated flows. Principal processes of sediment transport and deposition are vertically arranged in the centre according to the ratio of sediment to water in the moving flow; dilution or bulking determines their relationship. Processes that may release large volumes of water, or sediment, or both, are listed near the top of the diagram. Paths drawn along the margins of the chart indicate the types of flow phenomena that may be expected to result, depending on the degree of dilution or bulking (from Smith & Lowe 1991).

(a) Low concentration turbidity currents



(b) High concentration turbidity currents

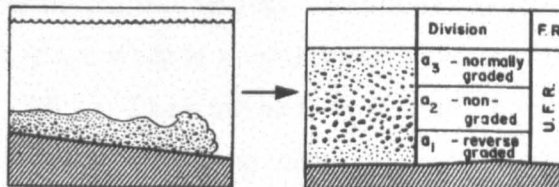


Figure 4.7 - Characteristics of low and high concentration turbidity currents and their deposits (after Cas & Wright 1987). F.R.=Flow Regime. U.F.R.=Upper Flow Regime.

shearing, and this may also produce diffuse layering. Cas (1979) suggested that these variations in the basal (a) layer of the Bouma sequence could be sub-divided into a basal reverse graded division a<sup>1</sup>, a middle ungraded division a<sup>2</sup>, and an upper normally graded division a<sup>3</sup> (see Fig.4.7).

Walker, R. G. (1975) developed general Bouma-like models for mass flow conglomerate deposits. The common development of normal and reverse grading in such deposits suggested that they were the products of highly concentrated turbidity currents. Lowe (1982) recognised the different effects of traction, traction carpet and suspension fallout during sedimentation, the first two of these developing in coarse sand to gravel deposits. Lowe's (1982) scheme therefore included an extra basal gravelly, planar to cross laminated division.

Turbidite deposits have been identified in many volcanic settings. They have been found in deep lakes, in particular caldera lakes with steep erodible margins, in streams and in deltas, and in marine settings marginal to or incorporating volcanic provinces (Cas 1979; Sigurdsson *et al.* 1980; Wright & Mutti 1981; Carey & Sigurdsson 1984; Yarnold 1993). Here the focus has been on the general characteristics of mass movement processes. Turbidites are intimately associated with mass flow deposits, and the sequence of reverse grading to no grading to normal grading is also known in debris flows. Many examples cited have referred to sub-aerial deposits (Glicken 1991; Smith and Lowe 1991; Pierson 1995; Bertran & Texier 1999). However, similar deposits can also be generated sub-aqueously, and it should therefore be expected that turbidites might be associated with coarse clastic rocks. For a more detailed review of turbidites see Cas (1979) and Walker, R. G. (1984).

Deltas are common in marine volcanic settings. An alluvial delta is a prism of sediment deposited by an alluvial system, whether a solitary river or an alluvial fan, into a body of standing water (Nemec 1990). When sediment crosses the land-water boundary it is transported and deposited down the steep delta face slope, where mass movement processes such as debris flows, avalanches and turbidity currents occur. Figure 4.8 illustrates some of these deposits in two typical deltaic settings. It is important, therefore, when analysing mass movement deposits, to know that they are commonly associated with the alluvial systems of deltas.

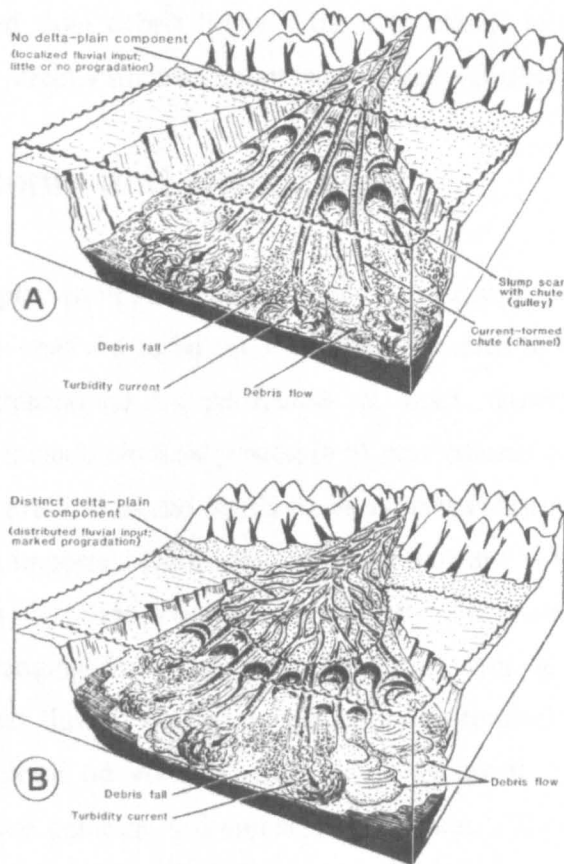


**Figure 4.8 – Schematic diagram of two varieties of steep face, coarse-grained deltas: A) a conical underwater delta and B) a Gilbert-type delta (from Nemec 1990).**

The coarsest debris of deltas tends to accumulate in the toe zone where debris falls or avalanches and debris flows are common. Most features of these are common to subaerial and subaqueous mass movements although there are subtle differences. Debris falls dominate on slopes of conical underwater deltas. Slopes are steepened by deposition and become unstable, causing failure, rockfalls and avalanches. As the debris falls, larger clasts outpace smaller ones and come to the front of the flow where they are partially overridden by fine material, producing normal grading. Subaqueous debris falls have much in common with subaerial rockfalls, except that on delta slopes, those on slopes derived from accumulated sediment produce more rounded, sorted material, whilst rockfalls from rocky headwalls produce immature, angular material (Nemec 1990). Subaqueous debris

flows share the same features of dispersive pressure, causing reverse grading, as subaerial systems (Pierson 1986). Lastly, turbidity currents are among the most important mechanisms of sediment transport and deposition on steep slopes of coarse-grained deltas. They may be derived from debris flows if these accelerate to a speed high enough to become turbulent, or directly from sediment laden stream effluent (Nemec 1990).

## **4.8 Environments and landscapes**

Epiclastic processes play an important role in volcanic settings. Volcanic edifices provide substantial sources of material to be used in these processes by weathering and erosion. Sediment can be transported by particulate or mass movement by a number of mechanisms. These include physical processes of gravitational collapse or mass wasting, rockfalls, landslides, avalanches and debris flows as well as transport by flowing water or by ice. Gravity is an important component of all of these and is linked to the typical high steep volcanic slopes. Volcanoes occur independently of climate and thus are associated with environments ranging from high altitude or high latitude snow and ice caps, to marine, lacustrine and fluvial systems in temperate to tropical settings. Many of the processes that take place on volcanic edifices are subaerial, but subaqueous deposits including turbidites are common volcanoclastic associates. Alluvial fans are widespread reflecting the high relief of most volcanoes, together with coarse-grained deltas at land-water interfaces. It is clear therefore that a wide range of environments and landscapes are found in volcanic regions, and within these a vast spectrum of processes is in operation. These environments and landscapes can be inferred from their deposits, providing a composite view of the palaeolandscape and perhaps climate of the area under investigation.

## 5 Ardnamurchan

As outlined in Chapter 2, areas of the Ardnamurchan Peninsula thought to represent volcanic centres have been referred to as the 'Ben Hiant' and 'Northern' vents (Richey & Thomas 1930). The deposits within these areas were identified as explosive vent agglomerates, and cross-cutting relationships suggested that they were emplaced before Centres 1, 2 and 3 (Richey & Thomas 1930). This chapter describes the lithologies of the deposits within these areas, concentrating on stratigraphical relationships, the characteristics of the deposits including clast-matrix relationships, and structures. A series of transects, involving analyses of clast compositions and shapes, and matrix proportions have been used to determine regional trends within these deposits. These will be reviewed before examining the environments and modes of deposition.

Analyses suggest that these deposits were not formed by explosive, pyroclastic processes but by epiclastic deposition. The 'vent agglomerates' or 'breccias' are typically conglomerates with clasts ranging from rounded to (less commonly) sub-angular, and from 2cm up to 3m in diameter. Shattered 'megaclasts' up to 30m in length are present locally. The deposits form a stratified sequence containing numerous sedimentary structures. Analyses of clast-matrix relationships and patterns of distribution provide evidence of the depositional mechanism with clast size, heterogeneity and roundness of clasts increasing away from the 'source.' The developing heterogeneity of the deposits is strongly linked to the underlying geology and a sedimentary watershed can be recognised. It is suggested that the bulk of these deposits were formed by debris flow/avalanches. The following descriptions provide evidence for this hypothesis, which will be discussed in more detail later in this chapter.

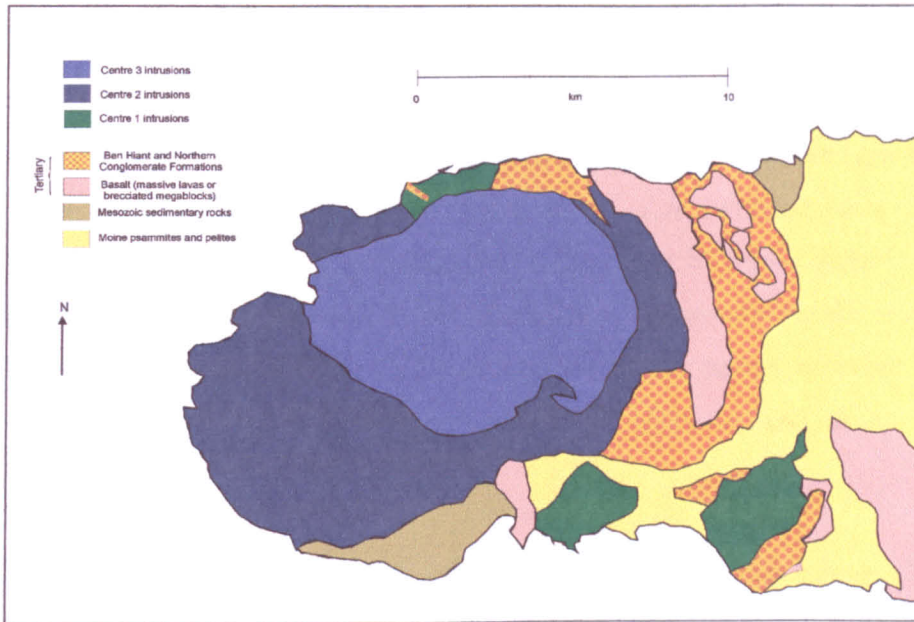
### 5.1 Regional Geology

The Ardnamurchan Peninsula is dominated by a central igneous complex intruded into plateau lavas that overlie a thin sequence of Mesozoic strata (Jurassic limestones, sandstones and shales; Triassic sandstones and conglomerates) and basement psammites and pelites of the Moine Supergroup. Richey & Thomas (1930) present the most detailed study of the Ardnamurchan Palaeogene igneous rocks. Three centres of intrusive activity were recognised: (i) Centre 1 (oldest); (ii) Centre 2 and (iii) Centre 3 (youngest) (Fig. 5.1).

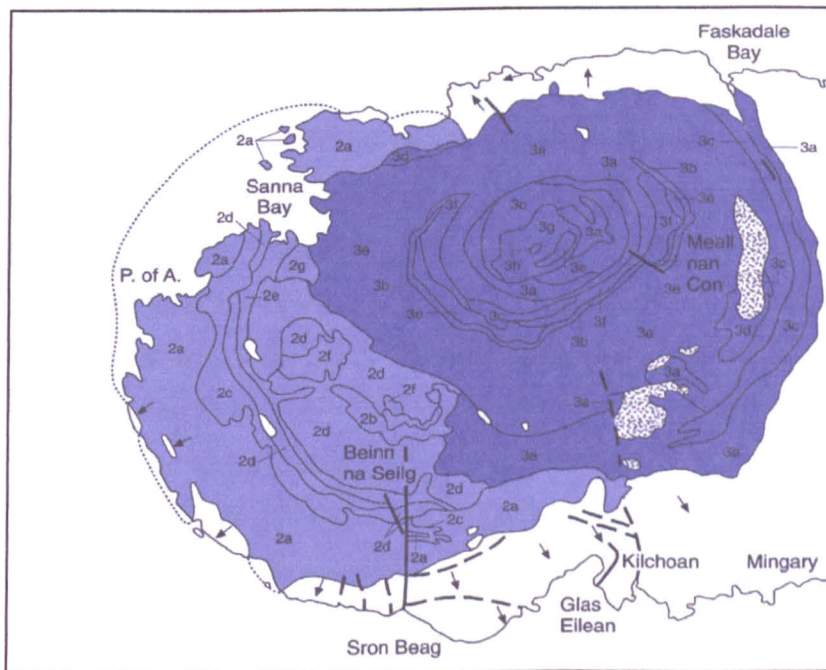
*Centre 1.* Here Richey & Thomas (1930) identified a series of volcanic vents, mainly filled with agglomerates and traversed by cone sheets. The outermost cone sheets are inclined inwards at shallow angles (15-20°) whereas those towards the interior are steeper, up to *ca.* 40°. Richey & Thomas (1930) described the Ben Hiant and Northern Vents as agglomerates, comprising sub-rounded to sub-angular blocks of material, set within a fine-grained matrix. The Ben Hiant Vent was noted as composed primarily of trachytic material and basalt with little to no country rock fragments, and a vertical vent wall was identified at several localities. Richey (1938) suggested the agglomerates were formed by a rhythmic series of eruptions. The Northern Vents was described as containing rhyolitic and trachytic material similar to that at Ben Hiant and therefore, Richey & Thomas (1930) suggested a link between the two. Blocks of Mesozoic sedimentary rock are common in the Northern Vents deposits (Richey & Thomas 1930).

*Centre 2.* Richey & Thomas (1930) identified abundant basic cone sheets forming an outer set surrounding a complex of gabbroic ring intrusions. A linear vent is also present at Glas Eilean. Four phases of intrusive activity can be recognised (Emeleus 1982). The first phase involved the intrusion of an outer suite of 'older' basic cone sheets. Towards Kilchoan, the density of cone sheets is very high, and multiple and composite cone sheets are recognised. The first major intrusion of Centre 2 is the Hypersthene Gabbro, which cuts the older suite of cone sheets. This gabbro displays excellent modal layering, and augen, and upward pointing finger structures, north of Sanna Bay, indicate post-cumulus modifications. A steep sided hybrid intrusion is located interior to the Hypersthene Gabbro. It comprises dolerite veined by microgranite and felsite and complex relationships between the dolerite and silicic material indicate magma mingling. A third phase of intrusive activity is indicated by the emplacement an inner suite of basic cone sheets, inclined at 70°, forming a focal point below Aodann. Finally, a series of ring intrusions of quartz gabbro were emplaced.

*Centre 3.* Richey & Thomas (1930) identified a suite of gabbroic ring dykes surrounding more acidic masses such as tonalite and quartz-monzonite. This is thought to be one of the best preserved developments of ring-dyke structures in the world. The largest intrusion in Centre 3 is the Great Eucrite, an olivine bytownite gabbro which forms the distinctive topography of Centre 3. The innermost part of the Great Eucrite is composed of masses of amphibole-rich tonalite and a central, biotite-rich quartz monzonite, formed from the interaction between the evolving basic magma and partially melted country rock.



B)



## Centre 2

- 2a Hypersthene gabbro
- 2b Old gabbro
- 2c Quartz-dolerite with granophyre
- 2d Quartz-gabbros
- 2e Eucrites
- 2f Granophyre & felsite
- 2g Fluxion gabbros

- Cappings and screens
- Pre-Centre 2 rocks

P. of A. Point of Ardnamurchan

## Centre 3

- 3a Quartz gabbros
- 3b Quartz-dolerite with granophyre
- 3c Fluxion gabbros
- 3d Other gabbros
- 3e Eucrites
- 3f Biotite-eucrite
- 3g Tonalite
- 3h Quartz-monzonite

- Faults
- Prevalent dip direction in Mesozoic sedimentary sequence

**Figure 5.1 – Simplified geological map and summary diagram of the Ardnamurchan Central Complex.** a) Simplified geological map of the Ardnamurchan Central Complex (after Edinburgh Geological Society 1976). b) Summary diagram of Centres 2 and 3 (after Bell & Williamson 2002).

## 5.2 Clast Lithologies

The 'breccias' or conglomerates of the 'Ben Hiant' and 'Northern' vents are typically clast supported with sub-rounded to sub-angular clasts set in a fine-grained sand-silt grade matrix of comminuted material (Figs. 5.2a, 5.2b, 5.2c). Clast lithologies include: aphyric basalt, porphyritic basalt, amygdaloidal basalt, plagioclase megacrystic basalt, scoriaceous basalt, microgranite, trachyte, ignimbrite, Moine psammites and pelites, quartzite, various sandstones including a distinctive calcareous sandstone, siltstones and shales. These lithologies will be briefly described.

The typical aphyric basalt is a transitional alkali olivine-tholeiite rock, comparable with those of the Mull lava field. It is dark grey to black with occasional reddened olivine microphenocrysts approximately 0.5mm in diameter. Some aphyric clasts are spheroidally weathered and reddened, others are bleached pale grey-green. Vesicles ranging from 0.5mm to 1mm are common, and have locally been stretched by flow. Chloritic alteration is widespread and some altered glass is present. The pyroxene present is typically a titaniferous augite and ophitic textures are common (Fig. 5.2d). Porphyritic basalt is common, with lath shaped plagioclase phenocrysts up to 2 mm in diameter, and rarer olivine. In the Fascaidale area, a dark green-brown basalt with phenocrysts of plagioclase up to 0.5cm diameter is recognised (Fig. 5.2e). The amygdaloidal basalt is typically grey-green in appearance. The amygdales are typically flow-aligned and range in size from 0.5mm to 1cm. They are predominantly filled by chlorite and epidote (Fig. 5.2f). Large blocks of plagioclase megacrystic basalt are common. The rock is dark grey to black and fine-grained with closely packed white-beige phenocrysts of plagioclase ranging in size from 0.5 to 3cm, typically 1cm (Fig. 5.3a). This lithology is also recognised on Mull. Scoriaceous basalt is typically reddened with a pitted, scoriaceous texture and a low density.

Spectacular clasts of rhyolitic ignimbrite weather pink-brown to grey, with purple to grey flow banding. These contain orthoclase phenocrysts 1-3mm in length, and occasional microphenocrysts, typically 1mm in length, of quartz and light green pyroxene. Flow bands range from 0.1 to 0.5mm thickness and surround and drape the orthoclase phenocrysts. Some bands consist of fine-grained randomly aligned plagioclase laths. The centres of these are typically coarser. Fiamme up to 5cm in length include devitrified quartz rich examples (Fig. 5.3b).

The microgranite has a pink to dirty brown weathered appearance but is typically pale grey. It is medium- to coarse-grained with crystals generally up to 3mm in size. Orthoclase phenocrysts up to 5mm across are common (Fig. 5.3c). The groundmass is composed of quartz and feldspar crystals with a spherulitic texture (Fig. 5.3d, 5.3e) that are locally replaced by patchy brown carbonate, which also displays spherulitic textures (Fig. 5.3f). Spherulitic textures are indicative of rapid cooling and may suggest an origin as a high level stock or on the margins of a granitic intrusion, which was then exhumed and incorporated in the conglomerate.

The trachyte is typically pale grey, although rare examples are black and mottled. It is generally fine-grained but locally has a microporphyritic texture. The phenocrysts, up to 2mm in size, are typically plagioclase, and are set in a groundmass of plagioclase, quartz, orthoclase and small brown euhedral pyroxene crystals (Fig 5.4a). Grains of magnetite are responsible for the black mottled appearance. Some feldspars and pyroxenes have grown in a skeletal fashion, forming needle-shaped crystals up to 2mm in length (Fig. 5.4b). This morphology suggests rapid growth. Vesicles up to 2mm in length are typically almond-shaped and aligned, indicating a flow texture. They are filled with quartz, chlorite and epidote.

Moine psammites are typically grey to pink. They are metamorphosed quartz- and feldspar-rich sandstones with well-rounded grains 1-2mm in diameter (Fig. 5.4c). Micas are weakly aligned and the rocks have generally undergone low-grade metamorphism. Clay-rich grey Moine pelites are also present. These are layered on a scale of 0.5cm to 3cm, producing alternating pink and grey bands.

White to grey quartzite clasts are present. These are of uncertain origin but may represent Moine lithologies. Examples of an impure quartzite are also found at Rubha Carrach, with dark *ca.* 2mm thick layers.

Various sandstones are identified throughout the sequence. These range from grey to buff to light brown, and all are fine-grained. No bedding has been identified. Sandstones are typically arkosic or quartz arenites, containing, sub-rounded to rounded grains of quartz and plagioclase, typically less than 1mm in diameter. Pressure-dissolution is common and they are well compacted but any remaining primary pore space is filled with calcite.

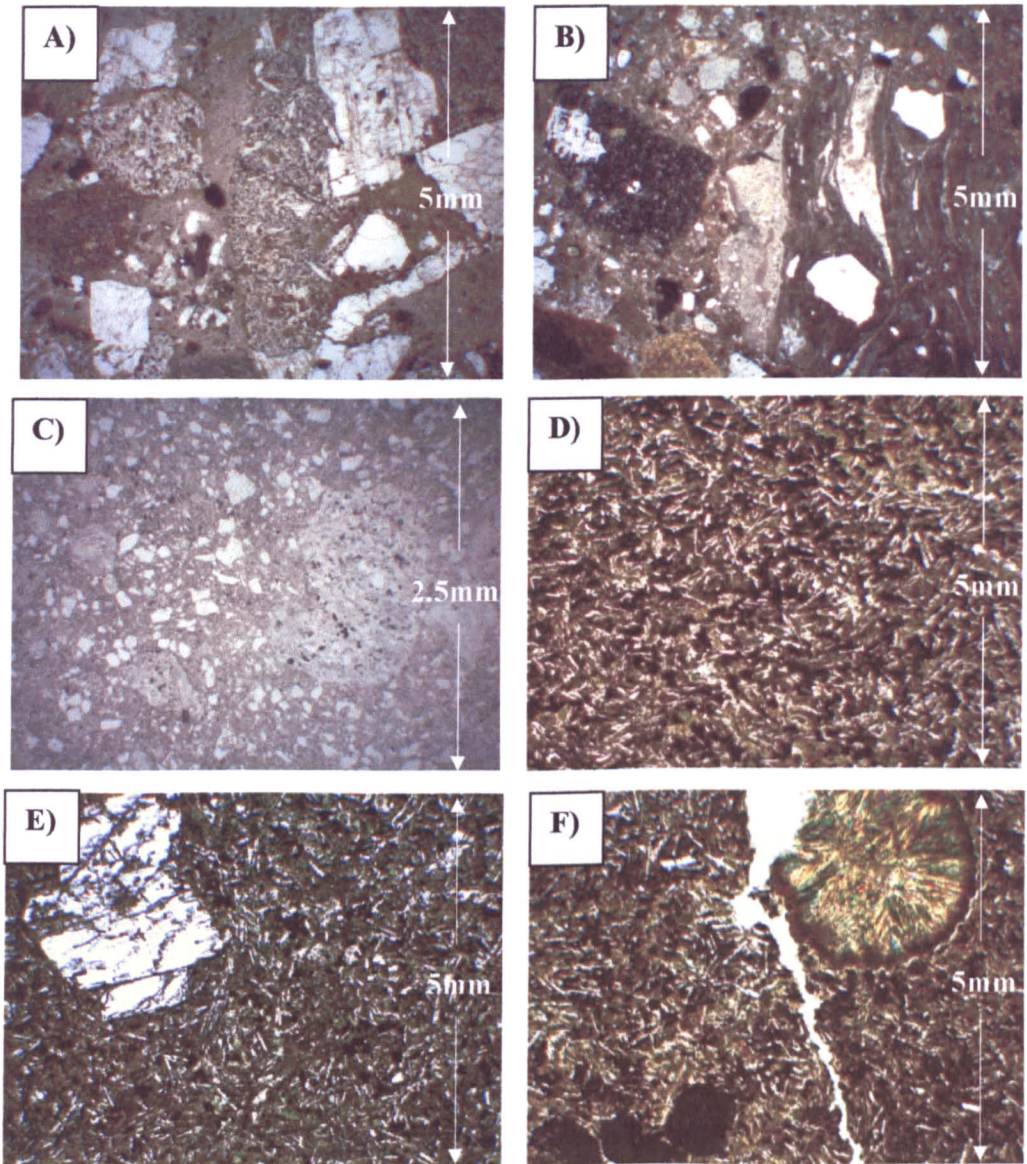
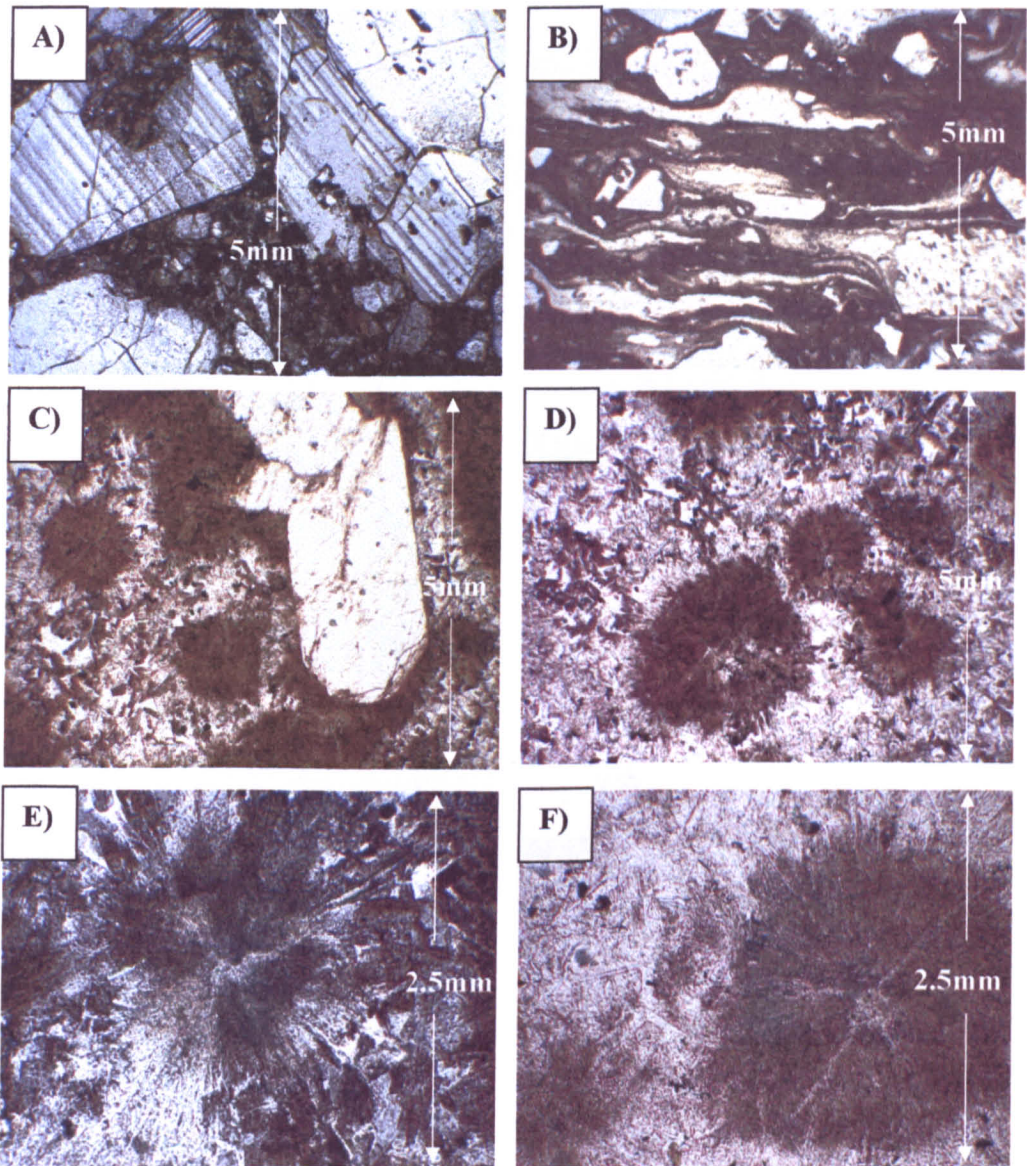
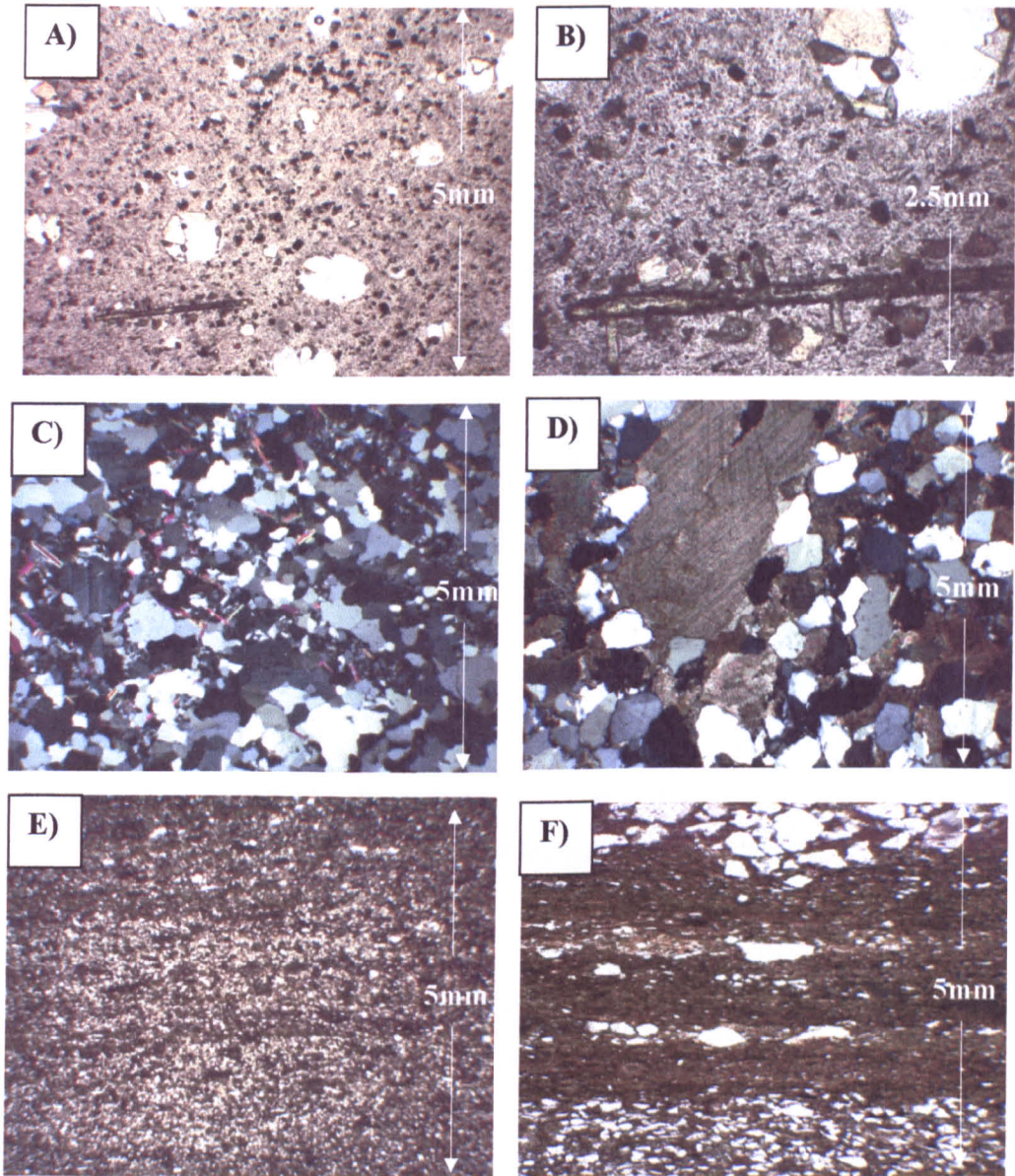


Figure 5.2 – Photomicrographs of clast lithologies from the Ardnamurchan conglomerates. A) Typical clast supported conglomerate displaying sub-rounded to sub-angular clasts of basalt and feldspar crystal fragments in a fine-grained matrix (ppl). B) Conglomerate displaying small clasts of basalt and ignimbrite (ppl). C) Grey matrix composed of quartz, feldspar and basalt fragments (ppl). D) Aphyric alkali olivine basalt clast (xpl). E) Porphyritic basalt clast with phenocryst of plagioclase feldspar (*ca.* 2mm across) (xpl). F) Amygdaloidal basalt clast. Vesicles are filled with epidote (xpl).



**Figure 5.3 – Photomicrographs of clast lithologies from the Ardnamurchan conglomerates. A) Plagioclase megacrystic basalt clast. Phenocrysts can be up to 5cm (xpl). B) Ignimbrite clast showing well developed flow banding and feldspar phenocrysts (ppl). C) Microgranite clast showing feldspar phenocrysts in a quartz and feldspar groundmass (xpl). D) Microgranite clast displaying spherulitic texture (xpl). E) Quartz and feldspar crystals displaying spherulitic texture in microgranite clast (xpl). F) Calcite replacing quartz and feldspar spherules in microgranite clast (xpl).**



**Figure 5.4 – Photomicrographs of clast lithologies from the Ardnamurchan conglomerates. A) Trachyte clast displaying feldspar phenocrysts (ppl). B) Enlarged view of trachyte showing elongate pyroxene crystallite (ppl). C) Moine psammite clast comprising compacted, rounded quartz grains and fine laths of muscovite (xpl). D) Calcareous sandstone clast. This sandstone is well compacted and there is little primary pore space. All remaining pore space is filled with calcite cement. Note the large grain of calcite in the upper centre of the view (xpl). E) Well sorted siltstone clast comprising grains of quartz and feldspar. F) Laminated siltstone (ppl). Laminae comprising quartz and feldspar grains are *ca.* 1mm thick. Finer muddy laminae are present (ppl).**

The calcareous sandstone is grey to light red with a pitted surface due to its calcareous component. It consists of sub-rounded to sub-angular quartz grains, typically 0.5-1mm in diameter. Grains of calcite up to 3mm in diameter may represent crinoid ossicles. It is well compacted with significant pressure dissolution. Any remaining pores have been filled with calcite cement (Fig. 5.4d).

Locally clasts include a dark grey to black siltstone with discontinuous light grey layers no more than 1mm thick. This is composed of sub-rounded to sub-angular silt-size (0.1-0.2mm) quartz grains in a muddy matrix but coarser layers are predominantly of quartz (Fig. 5.4e).

Clasts of black shale and laminated siltstone with 1-2mm thick laminae are present in some areas. Locally these are baked becoming pale yellow to grey-green (Fig. 5.4f).

### 5.3 Ben Hiant

The Ben Hiant 'Vent' covers an area of approximately 5km<sup>2</sup> (Fig. 5.5). The best exposures of conglomerates are to be found in the cliff section from Richey's Gully (NM541622) to the headland of MacLean's Nose (NM533616). The cliff section begins at a break in slope *ca.* 120m above sea level, and continues near vertically to *ca.* 240m. Tracks and gullies allow detailed examination of the section. The conglomerates within the section form a stratified sequence, the Ben Hiant Conglomerate Formation (BHCF) and a number of structures whose characteristics will be described in detail. These features are outlined in a schematic diagram, Figure 5.6, which is centred on a gully cut by numerous dykes (David's Gully) located at NM53656191. A distinctive laurel tree (David's Tree) is included for reference. The figure outlines the main components of the conglomerates. The complex, stratified sequence referred to here as the Ben Hiant Conglomerate Formation (BHCF) can be sub-divided into a number of members, ranging from siltstones to coarse conglomerates, listed in Figure 5.6 and shown in vertical logs, Figures 5.7 and 5.8.

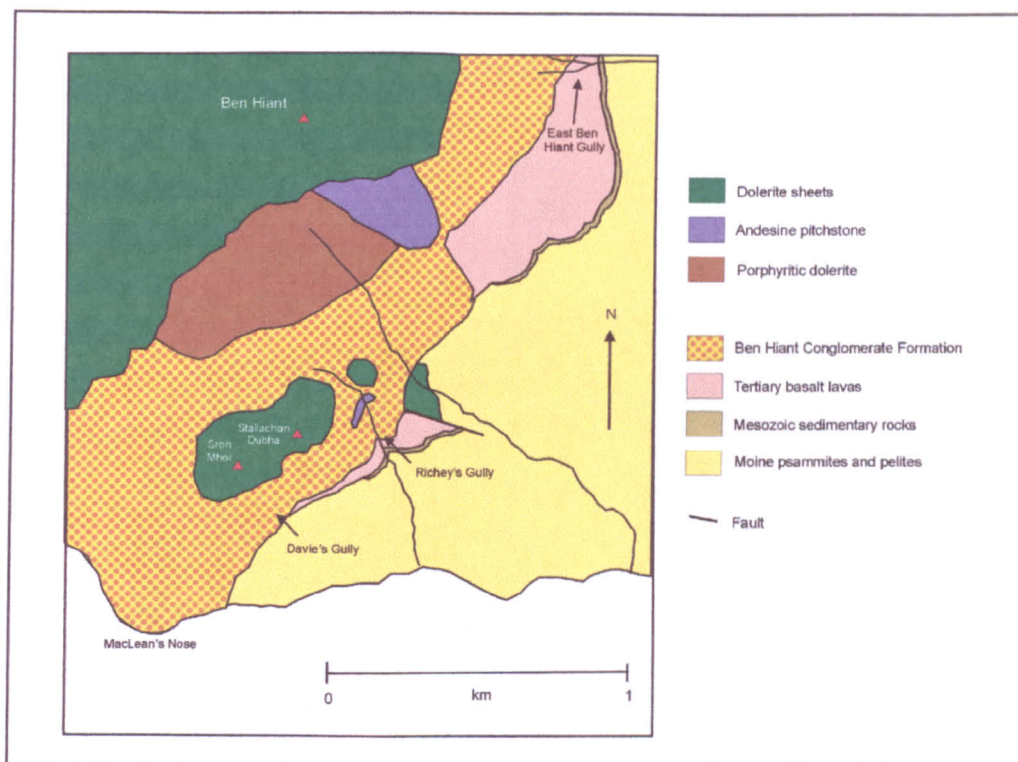


**Figure 5.5 – Simplified geological map of the Ben Hiant area, Ardnamurchan (after Edinburgh Geological Society 1976).**

### 5.3.1 Basal contact of the conglomerates

The conglomerates of Ben Hiant lie unconformably on both Moine psammites and pelites and Tertiary basalt lavas. The boundary shows an onlap relationship rising from sea level at MacLean's Nose to ~240m to the north. The contacts vary from horizontal to gently inclined, and in places are near vertical. The contact with the Moine can only be seen at low tide at MacLean's Nose. The conglomerate overlaps the deformed, banded pink and white psammites, and dark grey pelitic layers of the Moine at a low angle. The lavas form a low line of cliffs on the flanks of Ben Hiant and are up to 30m thick with rubbly tops and bottoms to individual flows. Outcrop surfaces typically show reddish-brown spheroidal weathering. The upper surface of the lava sequence seen in Figure 5.9, is uneven and has been filled by the conglomerate suggesting an irregular palaeotopography.

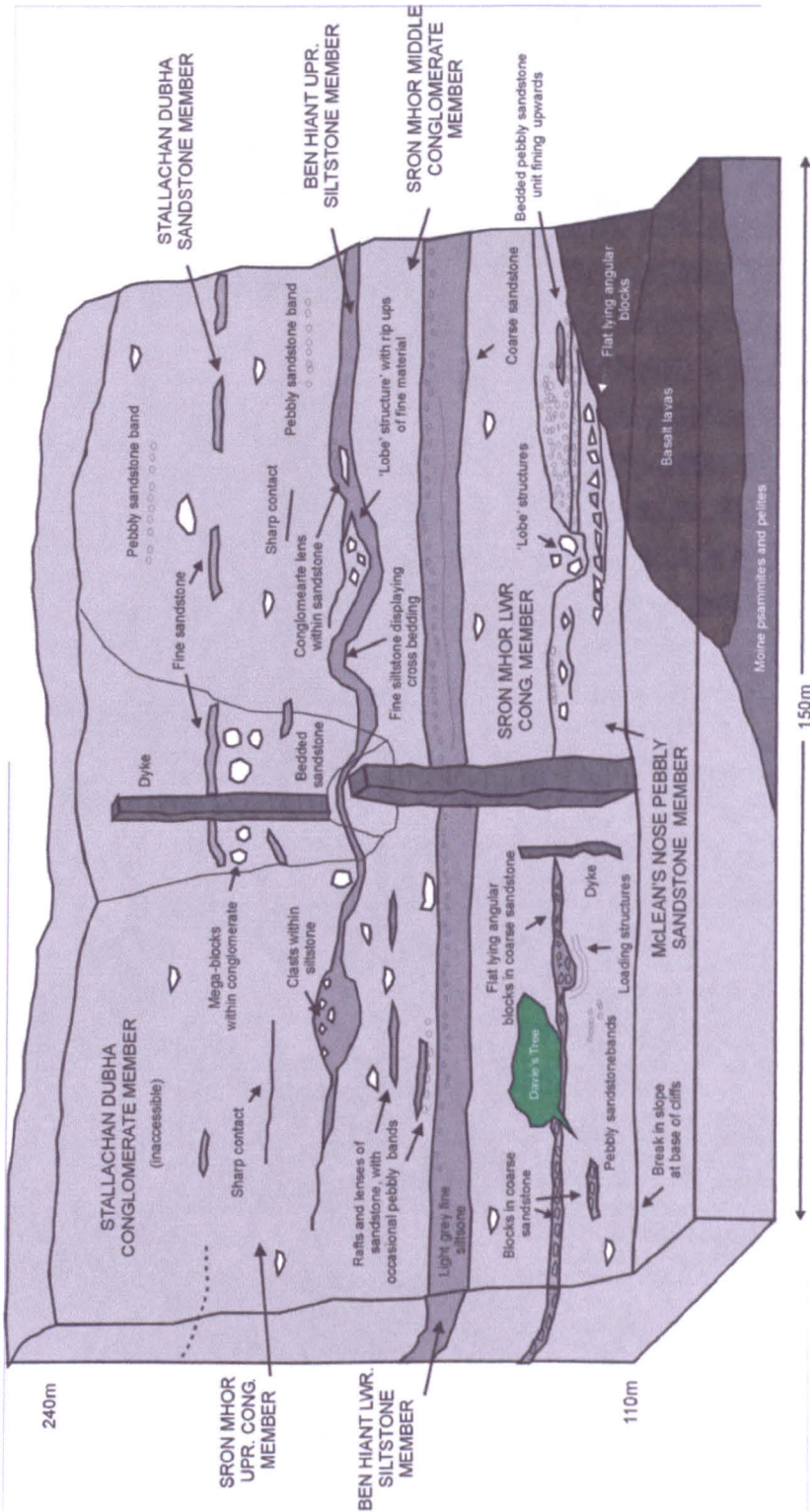
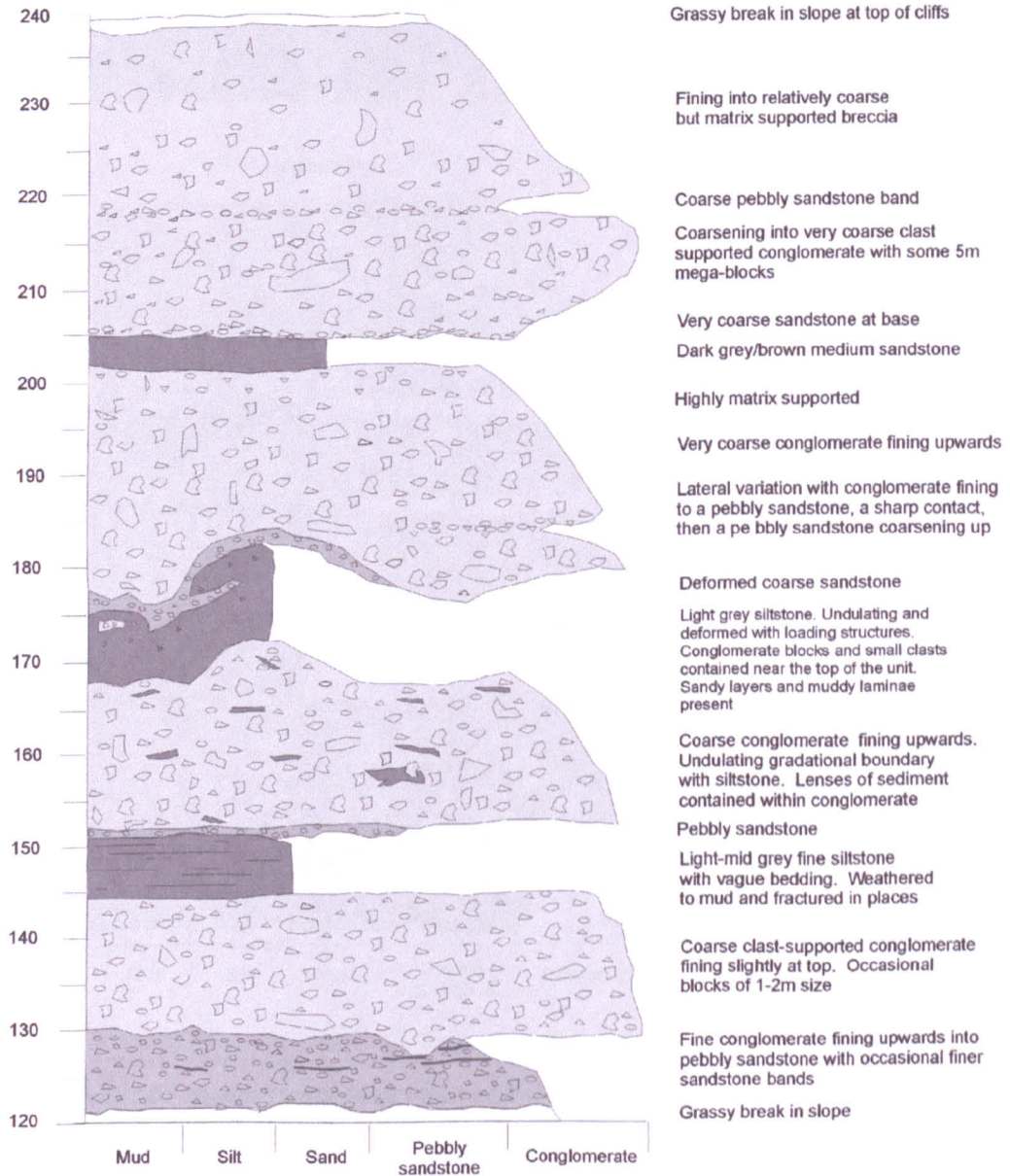
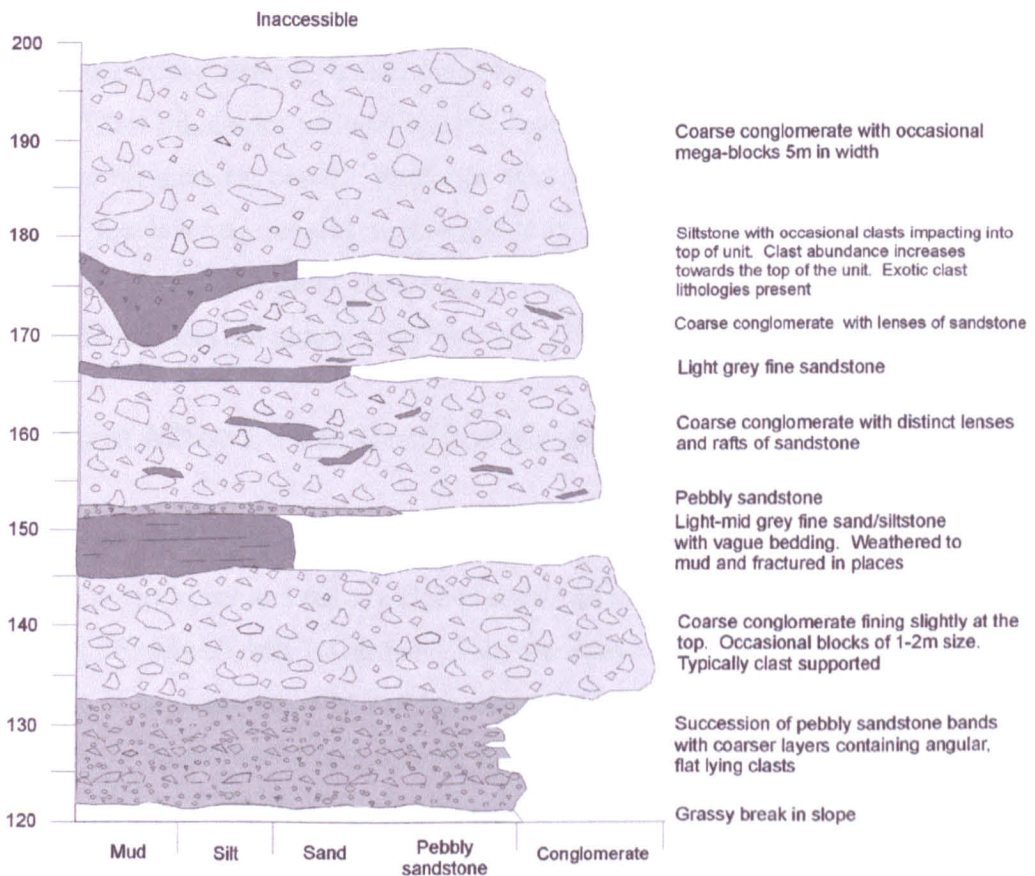


Figure 5.6 – Schematic diagram of cliff section of the Ben Hiant Conglomerate Formation (NM53656191). Height values shown are metres above sea level.



**Figure 5.7- Vertical log located north east of David's Gully towards MacLean's Nose, Ardnamurchan (NM53706194). Height values shown are in metres above sea level.**



**Figure 5.8 – Vertical log located south west of David’s Gully towards MacLean’s Nose, Ardnamurchan (NM53616191). Height values shown are in metres above sea level.**

### 5.3.2 MacLean's Nose Conglomerate Member

A succession of pebbly sandstones and fine-grained conglomerates overlies the lavas. These extend from approximately 120 to 130m above sea level. The unit is poorly exposed due to vegetation and access to the west of the section is poor. The MacLean's Nose Conglomerate Member (MNCM) is approximately 10m thick and contains a series of blue-grey pebbly sandstones and fine-grained conglomerates 10cm to 2m thick. These dip gently into the cliff face (134/7° SSW). There is much lateral variation within this unit. In the eastern part of the section it grades upwards from a fine-grained conglomerate to a pebbly sandstone, with occasional finer-grained sandstone bands, 20cm thick, whereas in the west no coarsening or fining is observed. Clasts in the MNCM typically range from 2 to 15cm across and are sub-rounded to sub-angular, with rarer angular clasts. All clasts are held in a highly weathered, fissile sand grade matrix, which forms approximately 25% of the unit. Clast lithologies include: aphyric basalt, porphyritic basalt, amygdaloidal basalt, plagioclase megacrystic basalt, ignimbrite, trachyte and various sandstones. Figure 5.10a illustrates the layering present within the unit. Locally, coarse clast-supported layers contain flat lying, sub-angular blocks up to 15cm in length set in a coarse, sandy matrix. Three of these layers are indicated in Figure 5.10b.

### 5.3.3 Sron Mhor Lower Conglomerate Member

Overlying the MNCM is a dark brown to black, coarse, poorly sorted conglomerate. The rock is clast-supported and set in a fine-grained matrix of basaltic material that forms 30% of the unit. Fining slightly towards the top, the Sron Mhor Lower Conglomerate Member (SMLCM) is approximately 15m thick extending to 145m above sea level. Clasts are typically sub-rounded to sub-angular and range from 2 to 75cm in diameter, with scattered blocks of 1-2m (Fig. 5.11a). Clast lithologies include aphyric basalt, porphyritic basalt, amygdaloidal basalt, plagioclase megacrystic basalt, ignimbrite, trachyte and various sandstones and siltstones. The larger clasts or 'megablocks' are commonly of aphyric basalt, or plagioclase megacrystic basalt, and appear shattered or fractured (Fig. 5.11b). Locally, the base of the SMLCM is irregular and fills 'channel-like' depressions up to 1m deep, causing loading and deformation in the bedding of the underlying MNCM. Coarse blocks are concentrated towards the bases of these structures. No bedding is apparent within the unit and blocks are chaotically organised within the conglomerate mass, often oriented vertically with their long axes at right angles to the base of the unit.

### 5.3.4 Ben Hiant Lower Siltstone Member

The Ben Hiant Lower Siltstone Member (BHLSM) is blue to light/mid grey and is generally massive with only vague traces of bedding. Approximately 8m thick, it extends to ~155m above sea level. Crumbly, fissile, and heavily fractured, it is highly weathered in places forming mud. In common with other fine-grained rocks in this section, it is easily eroded and forms a gently sloping 'ramp', contrasting with the commonly near vertical faces of the exposed conglomerate units. Both upper and lower surfaces show relatively planar contacts (Fig. 5.12a). Locally at the top, a 50cm thick sandstone contains pebbles up to 2cm in diameter.

In thin section, silt-size grains are typically sub-rounded to sub-angular and consist of quartz and lithic fragments (typically basalt) less than 0.05mm in size. Finer-grained patches of clay-grade material can be identified although they are irregular and do not form layers. Rare grains of heavily altered, zoned plagioclase approximately 3mm across are present (Fig. 5.12b).

A palynological analysis of this material yielded a large amount of organic matter, with a low percentage of inertinite (i.e. fusain, charred wood). It contains a large quantity of pollen, including *Inaperturopollenites hiatus*, which is derived from Upland Taxodiaceae trees, probably *Metasequoia* or *Glyptostrobus*. The *Metasequoia* type pollen is the dominant flow top vegetation throughout the lava field time and is comparable to modern coniferous trees (Jolley 1997). There is no evidence of any marine/estuarine influence. There are large amounts of Pine type grains, *Pityosporites*, which represent input from upland sources. *Pityosporites* are typically seen next to bounding faults, or in proximal drainage system areas. The pollen flora indicate an environment of deposition in a floodplain/lake setting with much of the surrounding vegetation being upland Pine and Taxodiaceae forest (D. Jolley, pers. comm).

### 5.3.5 Sron Mhor Middle Conglomerate Member

The normally graded Sron Mhor Middle Conglomerate Member (SMMCM) is dark brown to black and comprises a coarse, poorly-sorted, clast-supported conglomerate set in a dark, fine-grained matrix of basaltic material, that forms 30% of the unit. It varies from approximately 15 to 25m in thickness, extending to 175m above sea level at its maximum extent. Clasts are typically sub-rounded to sub-angular, and 2 to 75cm across, with scattered megablocks, commonly fractured, of 1-2m. Clast lithologies include: aphyric basalt, porphyritic basalt, amygdaloidal basalt, plagioclase megacrystic basalt, trachyte, ignimbrite and various sandstones. A number of lenticular bodies of mid-dark grey sandstone and siltstone are inclined at low angles within the unit (Fig. 5.13). These vary from 10 to 50cm in length (in section), but are never more than 20cm thick. One such lens, laterally continuous for 3m, forms a distinct linear feature within the SMMCM (Figure 5.6, 5.7 & 5.8). The upper surface of the SMMCM is irregular, with a relief of up to 10m

A palynological analysis of siltstone lenses within the conglomerate yielded a large amount of organic matter, with low percentages of inertinite (i.e. fusain, charred wood). It contained a large quantity of pollen, dominated by Pine type grains, *Pityosporites*. The pines indicate input from upland sources, often near bounding faults, and represent proximal drainage systems. There are large amounts of *Inaperturopollenites hiatus*, which is derived from Upland Taxodiaceae trees, probably *Metasequoia* or *Glyptostrobus*, that represent the dominant flow top vegetation in the early Tertiary (Jolley 1997). No marine or estuarine pollen is recognised. The pollen flora is derived from a floodplain/lake setting with much of the surrounding vegetation being a pine forest (D. Jolley, pers. comm). The pines represent input from upland sources, often near bounding faults, and represent proximal drainage systems.

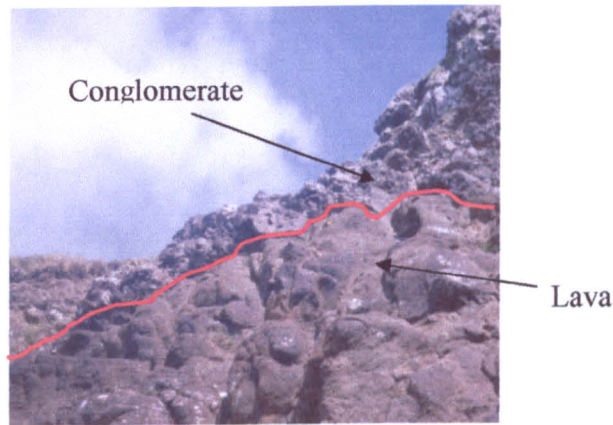


Figure 5.9 – Basal contact of Ben Hiant Conglomerate Formation overlying lava at a low angle (NM53806193).

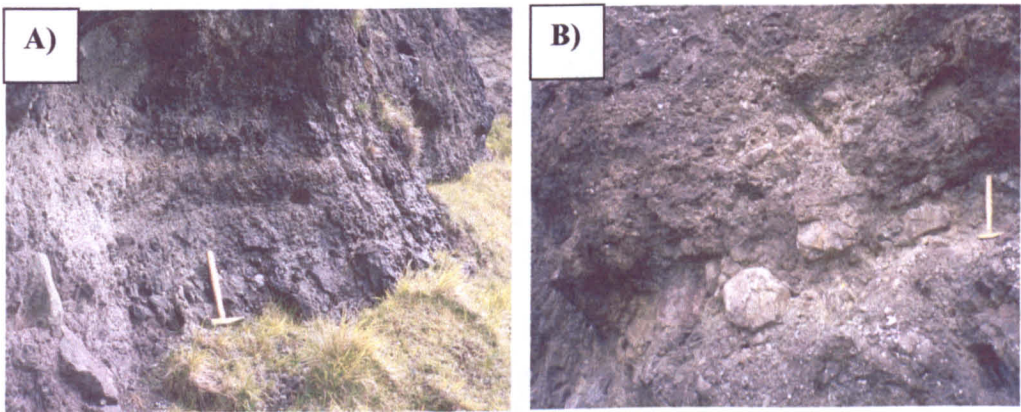


Figure 5.10 – The MacLean's Nose Conglomerate Member: a) Gently dipping fine conglomerates and pebbly sandstones (NM53706194). b) Coarse, flat lying angular blocks within the MacLean's Nose Conglomerate Member (NM53616191).

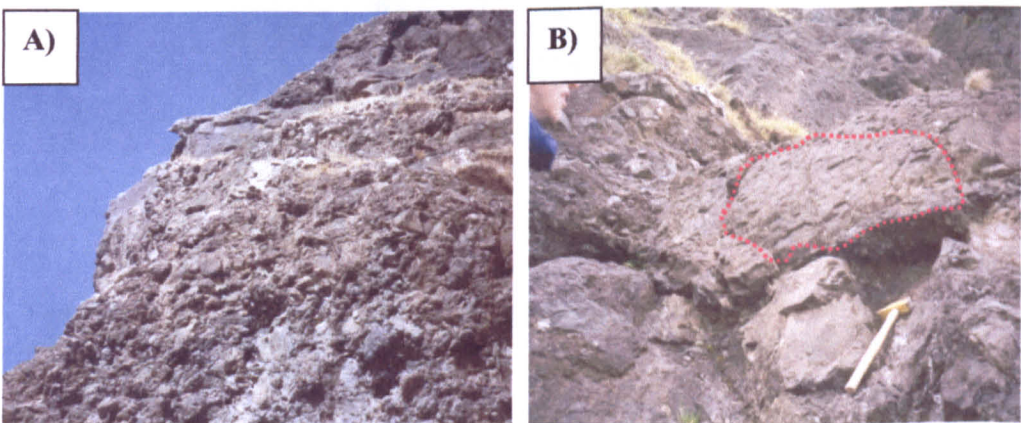
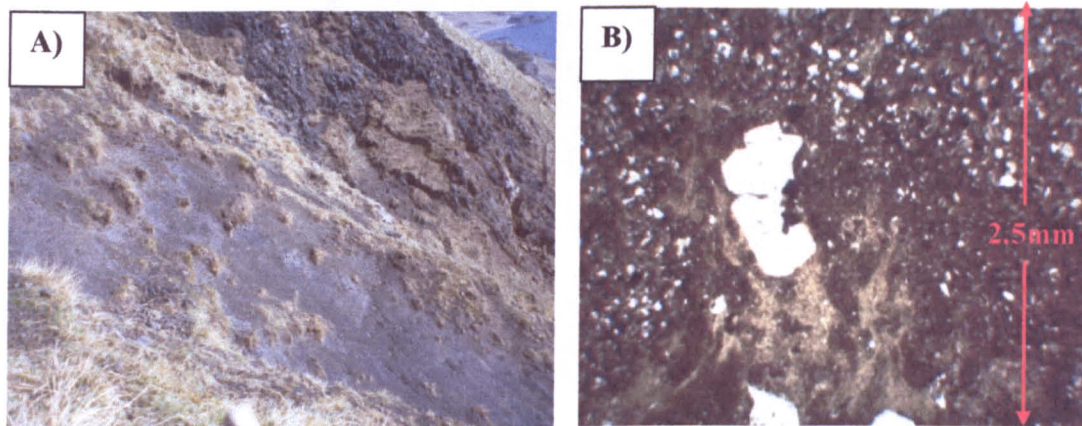


Figure 5.11 – The Sron Mhor Lower Conglomerate Member (NM53706195): a) Clast morphologies and textures. The Sron Mhor Lower Conglomerate Member is typically clast supported with large, sub-rounded clasts. b) Shattered megablock of basalt within the unit.



**Figure 5.12 – The Ben Hiant Lower Siltstone Member (NM53706196): a) General view of unit. The siltstone weathers to a blue-grey mud and displays a fine lamination. b) Photomicrograph (ppl) showing general composition and large feldspars surrounded by chlorite.**



**Figure 5.13 – The Sron Mhor Middle Conglomerate Member (NM53706197). Lens of dark grey siltstone in the Sron Mhor Middle Conglomerate Member. Large blocks of basalt have slid into the siltstone.**

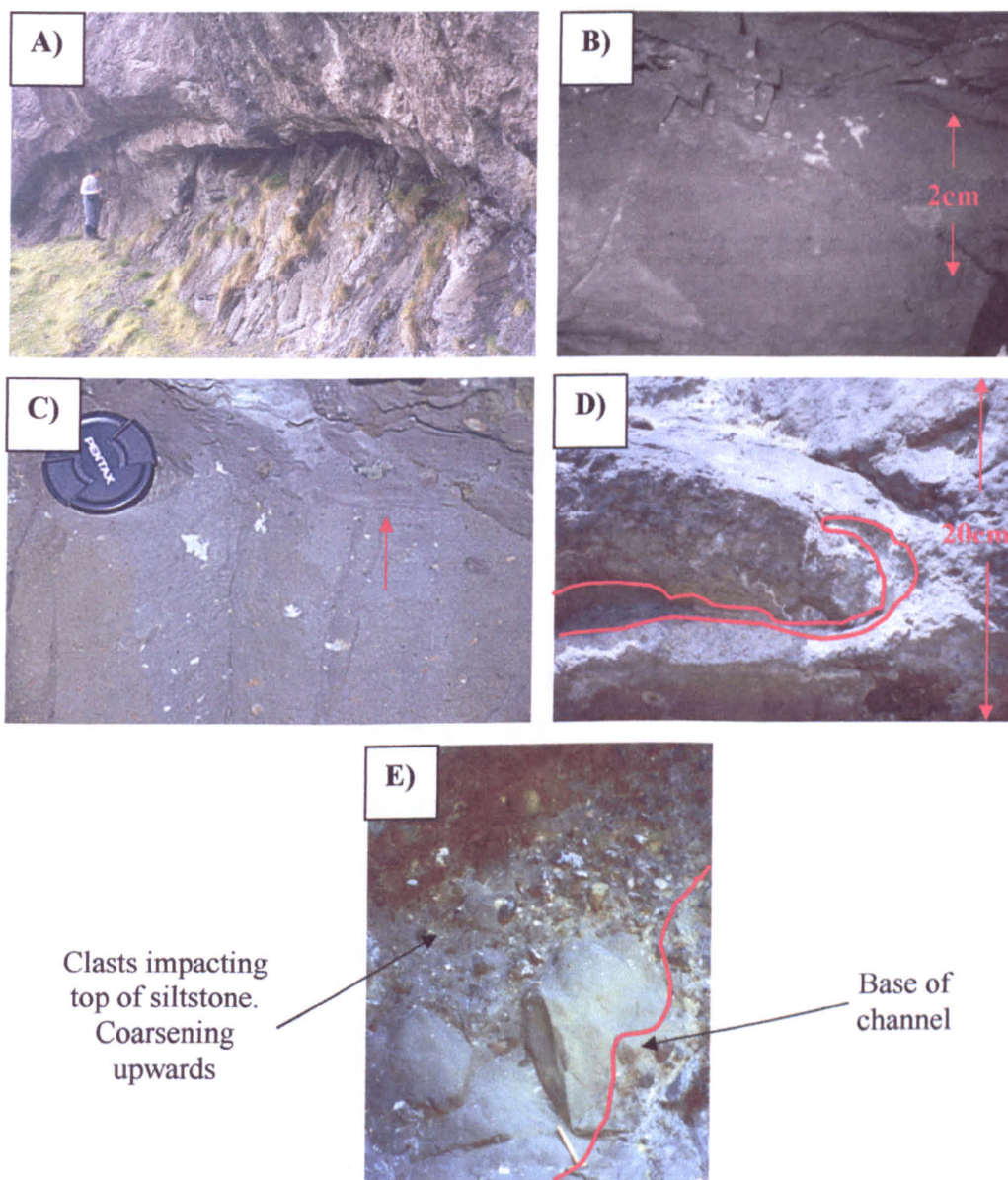


**Figure 5.14 – The Ben Hiant Upper Siltstone Member (NM53706197): General features.** a) Platform and overhang topography of the Ben Hiant Upper Siltstone Member. b) Small sandy layers. c) Muddy laminae (indicated by arrow) and small clasts of calcified crumbly, white sandstone. d) Deformation of underlying siltstone by conglomerate lobe. e) Channel within the Ben Hiant Upper Siltstone Member showing increasing clast abundance upwards.

### 5.3.6 Ben Hiant Upper Siltstone Member

The Ben Hiant Upper Siltstone Member (BHUSM) is light grey and ranges from 1m up to 10m in thickness. It extends to 180m above sea level in the cliff, forming a distinct in-weathered platform and overhang (Fig. 5.14a). Both the lower and upper surfaces are irregular, and soft-sediment deformation structures are present within the unit. Bedding defines a series of channels, the floors of which form the thickest part of the unit. The BHUSM is typically coarser than the BHLSM, with occasional sandy layers up to 2cm thick (Fig. 5.14b). Siltstones of varying thickness with muddy laminae (Fig. 5.14c) are present. Small-scale faults are present locally. Clasts, typically 1-2cm across, of a crumbly, fine-grained white sandstone (Fig. 5.14c) are present throughout the unit but have not been recorded elsewhere. Lenses of conglomerate and pebbly sandstone are locally present within the siltstone (Fig. 5.14d). West of David's Gully (Figures 5.6, & 5.8), is a distinct 'channel' containing pebbly siltstone *ca.* 10m thick, which fills the underlying topography. This tapers laterally to less than 1m in places, and is inclined at a steep angle, locally nearly vertical, to the SMMCM beneath. Clasts of the white sandstone and other lithologies are present within the channel, increasing in abundance towards the top and producing a gradational boundary with the overlying conglomerate (Fig. 5.14e). Locally, a fine-grained conglomerate/pebbly sandstone overlies the BHUSM, but in places there is a highly deformed inter-fingering with the siltstone boundary.

In thin section the BHUSM resembles the BHLSM, being composed primarily of quartz grains, mud and lithic fragments, typically basalt. Grains are generally angular but vary to sub-rounded, and are well-sorted. Many show pressure dissolution boundaries. No lamination is observed (Fig. 5.15a).

The fine-grained white sandstone clasts within the BHUSM consist of tightly packed sub-rounded to sub-angular grains of calcite up to 0.5cm in size, each of which is an aggregate of tightly packed sub-rounded grains (Fig. 5.15b). Plagioclase laths up to 0.5cm in size are also present, forming approximately 20% of clasts. The texture resembles that of a sand-size clastic sediment with little primary pore space due to compaction. The large feldspars show a blue-pink luminescence. Inspection by cathodoluminescence (CL) reveals three to four generations of calcite (Fig. 5.15c). A variety of grains of different chemistry can be recognised. These include areas of fine-grained calcitised material, typically showing duller luminescence; fragments of calcareous siltstone; and glassy shards, some containing vesicles.

This suggests there may have been a lithic sandstone, which was formed from recycling of sandstone, siltstone and volcanoclastic glassy material. The large feldspar crystals may have been phenocrysts from porphyritic lava (Fig. 5.15d). The rock was then eroded before deposition as clasts in the BHUSM.

Palynological analysis of the BHUSM has yielded a large amount of organic matter, with minor percentages of inertinite (i.e. fusain, charred wood). It contains a large quantity of pollen, with abundant *Inaperturopollenites hiatus*, which is derived from Upland Taxodiaceae trees, probably *Metasequoia* or *Glyptostrobus*. Grains of *Nyssapollenites kruschi* sub-species. *analepticus* (Nyssaceae, *Nyssa*) and a grain of *Cupuliferoidaepollenites liblarensis* (Fagaceae, probably *Castanea* type) have also been identified. The *Nyssa* type pollen is very common throughout the NE Atlantic Palaeogene, but only really occurs in any numbers high up in the sequence in the Staffa Group interbasaltics of the Mull Lava Field (D. Jolley, pers. comm.). The plant from which it is derived is comparable to swamp cypress trees and grew in lowland, swampy conditions (Jolley 1997), more stable than the riparian environments commonly represented. The same argument can also be applied to the *Castanea* type trees. The *Metasequoia* type pollen is analogous to modern coniferous trees and is common throughout the lava field time (Jolley 1997).

No freshwater lake or marine/estuarine pollen is identified. The dominant material is *Pityosporites*, a Pine type grain, which commonly found in upland areas. They are usually associated with bounding faults, and located in proximal drainage system areas (D. Jolley, pers. comm). At Ardslnish, material taken from a coal in the sediments at the bottom of the lava pile also contains *Nyssa* types in number (Simpson 1961), and a few other thermophilic species that are only seen on Mull. This assemblage is comparable to that in the BHUSM material.

These data therefore provide evidence that the BHUSM was deposited in swampy, lacustrine conditions, with no marine/estuarine influence. An environment of lowland swamps surrounded by Upland Taxodiaceae and Pine forests is suggested (D. Jolley, pers. comm.). This material is comparable, with sediments at the bottom of the Ardnamurchan lava pile, and interbasaltic horizons, suggesting a time of deposition closely linked to the lava field. The presence of this material both above and below conglomerates indicates cyclic deposition of material in high and low energy environments.

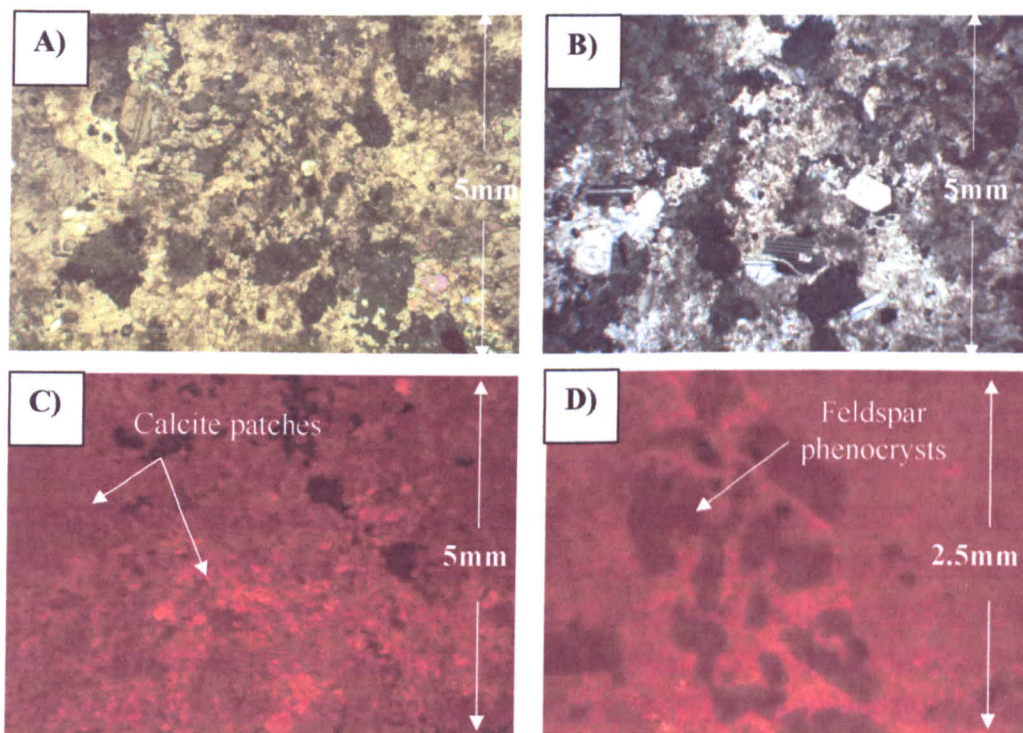


**Figure 5.15 – The Ben Hiant Upper Siltstone Member: Photomicrographs and CL images.**  
 a) Photomicrograph showing typical composition of channelised siltstone (ppl). b) Calcareous white sandstone clast containing large feldspars and aggregate of tightly packed sub-rounded to sub-angular grains, each of which contains a further aggregate of tightly packed sub-rounded grains (xpl) c) CL image showing areas of different calcite (defined by variable luminescence) in calcareous white sandstone. These represent aggregates of sub-rounded calcified grains d) CL image of feldspar crystals within lithic fragment of calcareous white sandstone.

### 5.3.7 Sron Mhor Upper Conglomerate Member

The Sron Mhor Upper Conglomerate Member (SMUCM) is dark brown to black and is a coarse, poorly sorted, clast supported conglomerate with a dark, fine-grained matrix of basaltic material that forms *ca.* 30% of the unit. The unit is 20m thick and its top is approximately 200m above sea level. It is generally unbedded and sub-rounded to sub-angular clasts 2cm to 75cm across are chaotically arranged. Larger blocks of 1-2m are typically shattered and locally blocks up to 5m are present. Clast lithologies include: aphyric basalt, porphyritic basalt, amygdaloidal basalt, plagioclase megacrystic basalt, ignimbrite and various sandstones. A 5m thick section near the base of the unit includes two discrete beds of normally-graded pebbly sandstone (Figure 5.7) that are laterally continuous for approximately 10m before tapering out (Fig. 5.16a). At the same level, west of this locality, there is a sharp contact representing another break in deposition extending laterally for 5m (Fig. 5.16b). The top of the unit is finer-grained, particularly towards the eastern end of the section. At the top, (Figure 5.7) it is transitional to a matrix-supported (approximately 45%) fine-grained conglomerate.

### 5.3.8 Stallachan Dubha Sandstone Member

The Stallachan Dubha Sandstone Member (SDSM) is dark grey to brown and forms a series of discontinuous lenses no more than 3m thick and 15m long in section, at approximately 200m above sea level. It is a fine- to medium-grained sandstone and is heavily weathered and fractured on the exposed surface, breaking easily into small flakes (Fig. 5.17a).

A palynological analysis of this material yielded a moderate quantity of pollen, dominated by Pine type grains, *Pityosporites*, which represent input from upland sources. These are usually seen next to bounding faults, or in proximal drainage system areas. There are large amounts of *Inaperturopollenites hiatus*, which is derived from Upland Taxodiaceae trees, probably *Metasequoia* or *Glyptostrobus*. *Metasequoia* pollen was an important flow top flora in the early Tertiary and is similar to modern coniferous trees (Jolley 1997). No marine or estuarine influence is recognised from the analysis. The pollen flora is derived from a floodplain/lake setting with much of the surrounding vegetation being an Upland Pine and Taxodiaceae forest (D. Jolley, pers. comm).

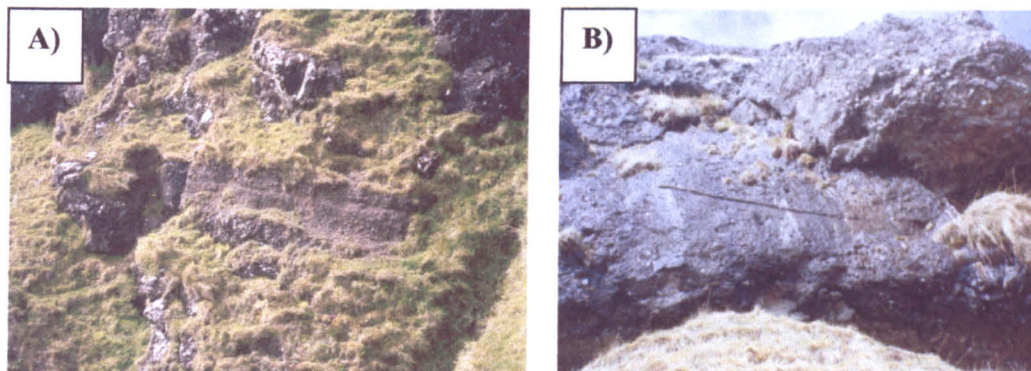


**Figure 5.16 – The Sron Mhor Upper Conglomerate Member (NM53706198): a) Normally graded 2.5m thick conglomerate unit fines to a pebbly sandstone. There is a depositional break forming a planar horizon before the deposition of another 22.5m thick normally graded conglomerate is deposited. b) Sharp depositional break (*ca.* 5m across)**

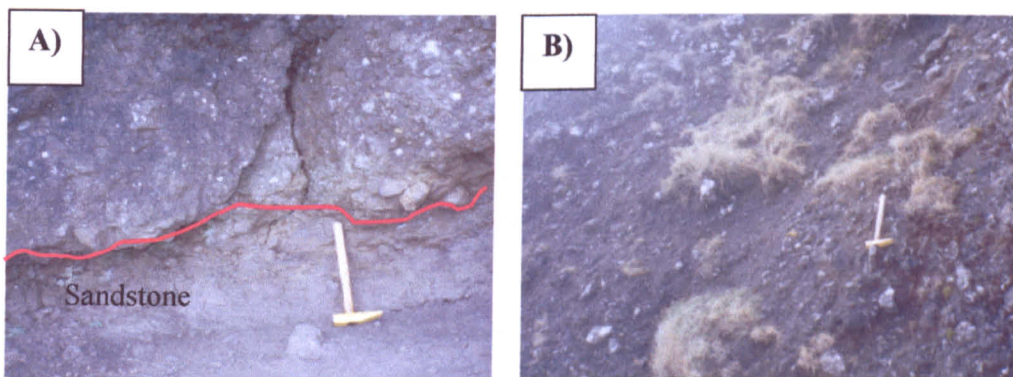


**Figure 5.17 – The Stallachan Dubha Sandstone Member and Stallachan Dubha Conglomerate Member (NM53706198). a) The Stallachan Dubha Sandstone Member is a laterally discontinuous fine-grained *ca.* 50cm thick dark grey-brown sandstone. b) The Stallachan Dubha Conglomerate Member is a poorly stratified *ca.* 35m thick, matrix supported unit.**

### 5.3.9 Stallachan Dubha Conglomerate Member

The Stallachan Dubha Conglomerate Member (SDCM) is reddish-brown to grey and consists of coarse, matrix-supported lithoclasts set in a light to dark brown matrix of basaltic material, that comprises approximately 45% of the rock (Fig. 5.17b). The unit is approximately 35m thick, and continues to 240m above sea level, terminating at a break in slope. Clasts are sub-rounded to sub-angular and range from 2cm to 50cm across, with a few blocks up to 1m or, more rarely 5m. Clast lithologies include aphyric basalt, porphyritic basalt, amygdaloidal basalt, plagioclase megacrystic basalt, various sandstones and siltstone. Localised variations are recorded in Figure 5.7, where pebbly sandstone is found at the base of the unit and coarsens up over 10 m to a clast-supported conglomerate, overlain by a 50cm thick pebbly sandstone band extending laterally for 2m, at 220m above sea level. Above this the SDCM continues to fine upwards.

## 5.4 Northern Vents

The Northern Vents cover an area of approximately 10km<sup>2</sup> on the Ardnamurchan Peninsula. The topography of this area is considerably lower and more undulating than that around Ben Hiant, and there are few vertical sections through the conglomerates. A number of outcrops are present along the northern coastal section at Rubha Carrach, in the section from Fascadale Bay to Swordle Cave, and at other localities. These allow compositional, morphological and size trends to be identified, (reviewed in Section 5.5). Due to the dispersed nature of the outcrops the conglomerates are not easily divisible into members, but as a group they will be referred to as the Northern Conglomerate Formation (NCF). Clast characteristics are similar to those of the Ben Hiant Conglomerate Formation described in Section 5.3. The relationship of the conglomerates with the Tertiary lavas and country rocks will also be examined.

### 5.4.1 Conglomerate topography and contact relationships

Northern Conglomerate Formation (NCF) deposits are best exposed in the U-shaped valley of the Achateny water. Here they are bounded to the east by Moine psammities and pelites and locally Mesozoic rocks, and to the west by various Centre 2 and 3 intrusive rocks. They are cut by numerous Centre 1 cone sheets. The poorly exposed and highly vegetated valley drains to the north. The Moine rocks east of the valley form a series of 'highlands,'

including the ridge of Beinn Bhreac, topographically above the Tertiary rocks of the Achateny valley. The unconformable contact of the conglomerate with Moine rocks is rarely exposed, but can be seen at Tom na Gainmheich (NM54456774). Although small, this outcrop reveals the uneven Moine topography on which the conglomerate, dominated by Moine psammites lithoclasts, was deposited (Fig. 5.18a). At a small roadside quarry, north east of Kilmory (NM53707051) conglomerate overlies heavily fractured Mesozoic shale, identified as Pabay Shales by Richey & Thomas (1930). The contact surface dips at 111/11° W, cutting across bedding in the shales, and the conglomerate here contains approximately 50% shale clasts (Fig. 5.18b). Few contacts are exposed west of the Achateny valley, but these reveal intrusive boundaries with Centre 2 gabbro, dolerite and granophyre intrusions.

The published Geological Survey map of the area suggests that the conglomerates have a complex relationship with Tertiary basalt lavas. The 'lavas' of this area, however, differ from those south east of Loch Mudle, on Ben Hiant, and on the Morvern Peninsula. These latter occurrences are characterised by typical, 'stepped' plateau lava topography. At Loch Mudle, approximately 15 flows of varying thickness can be identified, extending from 130 to 280m above sea level. Inter-lava lithologies such as shale, and reddened weathering surfaces are present and at the base of the whole sequence red and grey mudstones are identified. Rubbly tops and bottoms are also present at Ben Hiant and a 5m thick red mudstone unit is preserved at the base of the sequence. None of these features are present in the lavas associated with the NCF. The 'lavas' form low, hummocks, locally surrounded by conglomerate within the floor of the Achateny valley and there is no evidence of a stepped topography. Dolerite cone sheets in this area form steeper ridges (Fig. 5.19a). The lavas are intensely fractured and shattered, with no evidence of features such as columnar jointing (Fig. 5.19b), as in outcrops near Kilmory Church (NM53206992). Distinct flows cannot be identified or traced and no outcrop is more than 30m in length. Lava can be seen lying both above and below the conglomerate (Fig. 5.19c) and there is no regular outcrop pattern. Together, these features suggest that the 'lavas' are large blocks, or 'megablocks' of basalt contained within the conglomerate. The fact that they are lithologically similar to rocks of the local lava field indicates that they were probably derived from these by the processes that eroded and deposited the conglomerates.

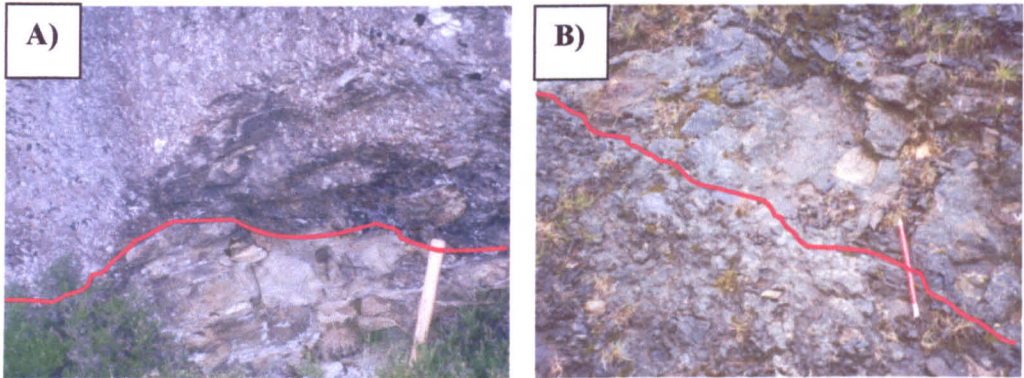


**Figure 5.18 – Basal contacts of conglomerate in the Northern Conglomerate Formation. a) Fine conglomerate lying unconformably on Moine rocks at Tom na Gainmheich. The conglomerate is dominated by Moine clasts (NM54456774). b) Conglomerate overlying Lower Lias shale at a low angle, north east of Kilmory. Conglomerate is dominated by shale and sandstone (NM53707051).**

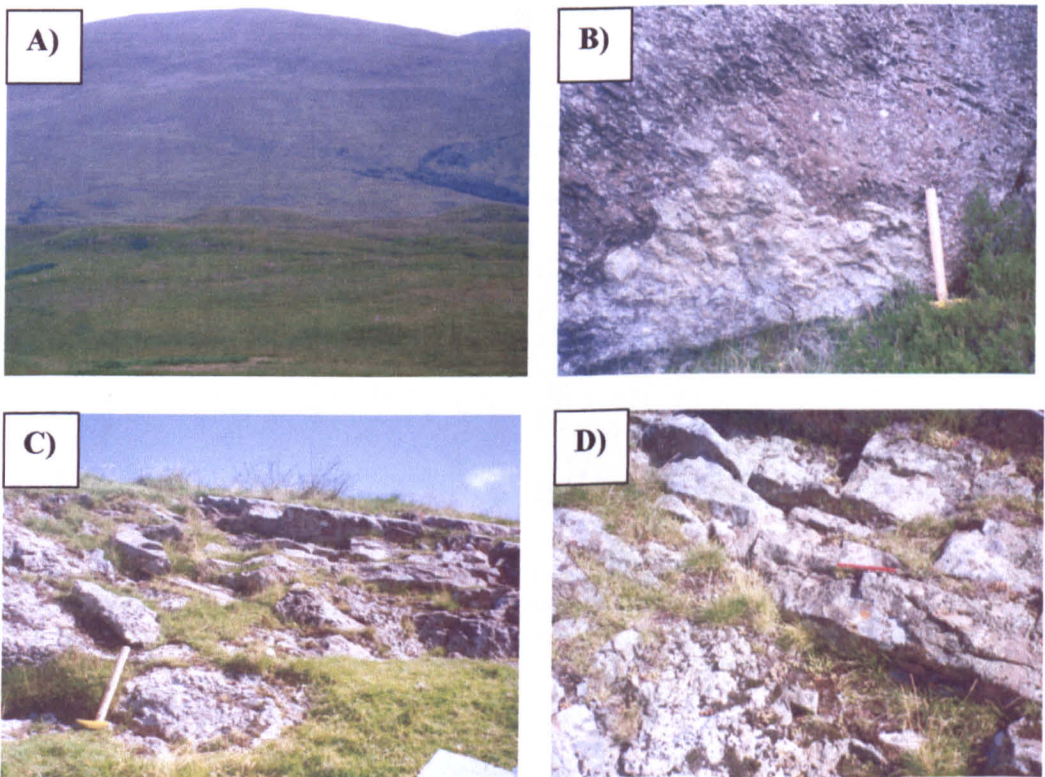


**Figure 5.19 – Hummocky topography and basalt/conglomerate relationships in the Northern Conglomerate Formation. a) Achateny valley, showing low hummocky topography in the foreground (NM5368). b) Shattered megablocks of basalt overlying conglomerate forming a low angle, undulating contact (NM54386816). c) Relationship of conglomerate (foreground) and shattered basalt blocks (background) (NM53136804). d) Enlarged view showing fractured basalt megablock resting on conglomerate (NM53136804).**

## 5.4.2 Allt an Doire Dharaich Area

The Allt an Doire Dharaich stream section and nearby roadside localities at Braehouse and Allt na Mi Chomhdhail, are typical southern outcrops of the Northern Vents. These conglomerates are dark brown to black and matrix-supported. They are fine-grained and locally form poorly-sorted pebbly sandstones (Fig. 5.20a) with chaotically arranged clasts set in a dark brown, matrix of basaltic sand. Clasts are typically sub-angular, less commonly sub-rounded, ranging from 2 to 10cm in length with occasional blocks up to 30cm. No megablocks have been identified. Clast lithologies include only aphyric basalt, porphyritic basalt, Moine psammite, quartzite and infrequent sandstone. Certain localities display vague bedding with channel-like structures present. A 10m thick section in the Allt Mhic an t-Saoir at NM53436833 comprises two ‘flows’ or units. The upper slightly coarser unit fills a gently inclined channel (Fig. 5.20b).

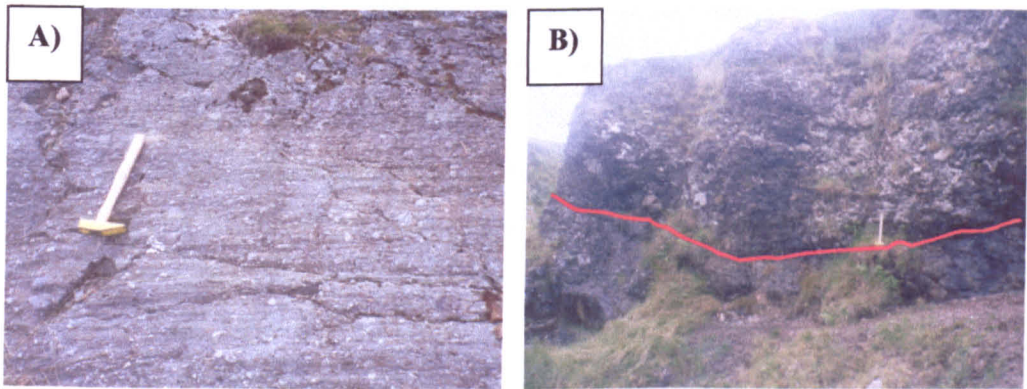


**Figure 5.20 – Fine-grained lithologies and sedimentary structures from conglomerates in the Allt an Doire Dharaich area, Northern Conglomerate Formation (NM52706777). a) Fine-grained nature of conglomerate/pebbly sandstone at Braehouse. Lineations in this figure are glacial striae and not bedding b) Channel structure in stream section at Allt an Mhic an t-Saoir (NM53436833).**

### 5.4.3 Fascaidale Bay to Swordle Cave

The deposits that crop out along the north coast are typically coarse-grained and clast supported, comprising sub-rounded lithoclasts of a wide range of rock-types, including Mesozoic sedimentary rocks and Palaeocene silicic igneous lithologies. The distribution of both is strongly linked to the underlying geology and the silicic lithoclasts commonly form local concentrations. Considerable variation in lithology, size, and shape is found between Fascaidale Bay and Swordle Cave and is discussed in Section 5.5, below.

At Meall Buidhe Mor and Fascaidale Bay, the clast-supported conglomerates are dominated by sub-rounded to rounded lithoclasts (2 – 20cm; rarely up to 1m) of scoriaceous and orthoclase-phyric basalt. These apparently unbedded deposits display a distinctive pink and green coloration on weathered surfaces and because they are highly resistant to weathering, give rise to craggy exposures (Fig 5.21a).

The nature of the conglomerates changes along a traverse from west to east, characterised in the Portban, Ardtoe Island and Kilmory area, where large quantities of Mesozoic sedimentary lithoclasts are present, and the conglomerates display numerous sedimentary structures. At Rubha na h-Acairseid, numerous blocks of reddish-brown, calcareous sandstone are present. These blocks of sandstone are typically sub-rounded, 20–50cm across (Fig. 5.21b), and rarely much larger, with one example measuring 30m by 25m (Fig. 5.21c). Smaller blocks, up to 5m across, of identical material surround this megablock. These have bedding planes and bedding structures with random orientations, different from those within the megablock. No comparable sandstone is found *in situ* within the Mesozoic sequence preserved to the east of the NCF outcrop, although Richey & Thomas (1930) suggest a Bearreraig Sandstone Group (formerly Inferior Oolite) age.

Scattered blocks of fossiliferous sandy limestone occur within the conglomerates. These resemble rocks from the Bradford Beds of the Lower Jurassic and contain numerous belemnites and oysters, tentatively identified as *Ostrea*. Blocks are typically sub-rounded to sub-angular and approximately 10 to 20cm across (Fig. 5.21d). Locally, sub-angular clasts (2 – 10cm) of yellow, green and grey thermally altered shale are relatively common and form clast-supported conglomerates. The overall nature of this tightly packed and chaotically arranged shale-dominated conglomerate deposit suggests derivation by shattering of a larger pre-existing outcrop (Fig. 5.21e). Similar shales crop out at Mingary

Castle on the south coast of the peninsula, where sills and cone sheets are the obvious source of heat responsible for the thermal alteration. A similar model may explain the presence of thermally altered lithoclasts of (Pabay) shales within NCF conglomerates.

The area around Rubha na h-Acairseid is difficult to analyse in detail due to strong tides which cover the best exposures for most of the day, and the presence of multiple minor intrusions. Despite limited inland exposure, an idea of the stratigraphy can be developed and three distinct conglomerate units with characteristic lithologies can be mapped (Fig. 5.22). The apparently conformable relationships of these conglomerates and the presence of features such as normal grading and channel structures, suggest flow processes were responsible for their deposition.

Each conglomerate comprises more than one 'lobe' or 'flow', with distinctive lithoclast assemblages. The lowest of these units, the Rubha na h-Acairseid Microgranite-dominated Conglomerate (RMGC), crops out on a wave-cut low tide platform and is at least 10m thick. It is dominated by sub-rounded clasts (2 - 20cm; rarely up to 1m) of microgranite, with occasional aphyric basalt and scoriaceous basalt clasts, together with rare blocks of sandstone. This unit is more matrix-supported and slightly finer-grained than other deposits in this area. The boundary is difficult to define precisely, but overlying the RMGC is the *ca.* 8m thick Rubha na h-Acairseid Sandstone-dominated Conglomerate (RSstC), which crops out on low rocky and grassy platforms around Rubha na h-Acairseid. The RSstC is clast-supported, with sub-rounded lithoclasts 2-50cm across and rarer megablocks > 2m, comprising *ca.* 75% of the deposit. Approximately two thirds of the total clasts comprises sandstone with the remaining one third of calcareous sandstone. The calcareous sandstone typically forms large megablocks and their distribution is illustrated in Figure 5.23. At the top of the sequence is the Rubha na h-Acairseid Laminated Siltstone-dominated Conglomerate (RLSC). The RLSC is *ca.* 5m thick and clast supported (*ca.* 70% of the deposit), composed primarily of sub-angular, typically laminated siltstone and thermally altered shale clasts (*ca.* 50%), and rarer sub-rounded sandstone (*ca.* 35%) lithoclasts, 2 to 30cm across, with larger blocks up to 1m. A vertical log for this section (at NM52297075) is illustrated in Fig. 5.24.

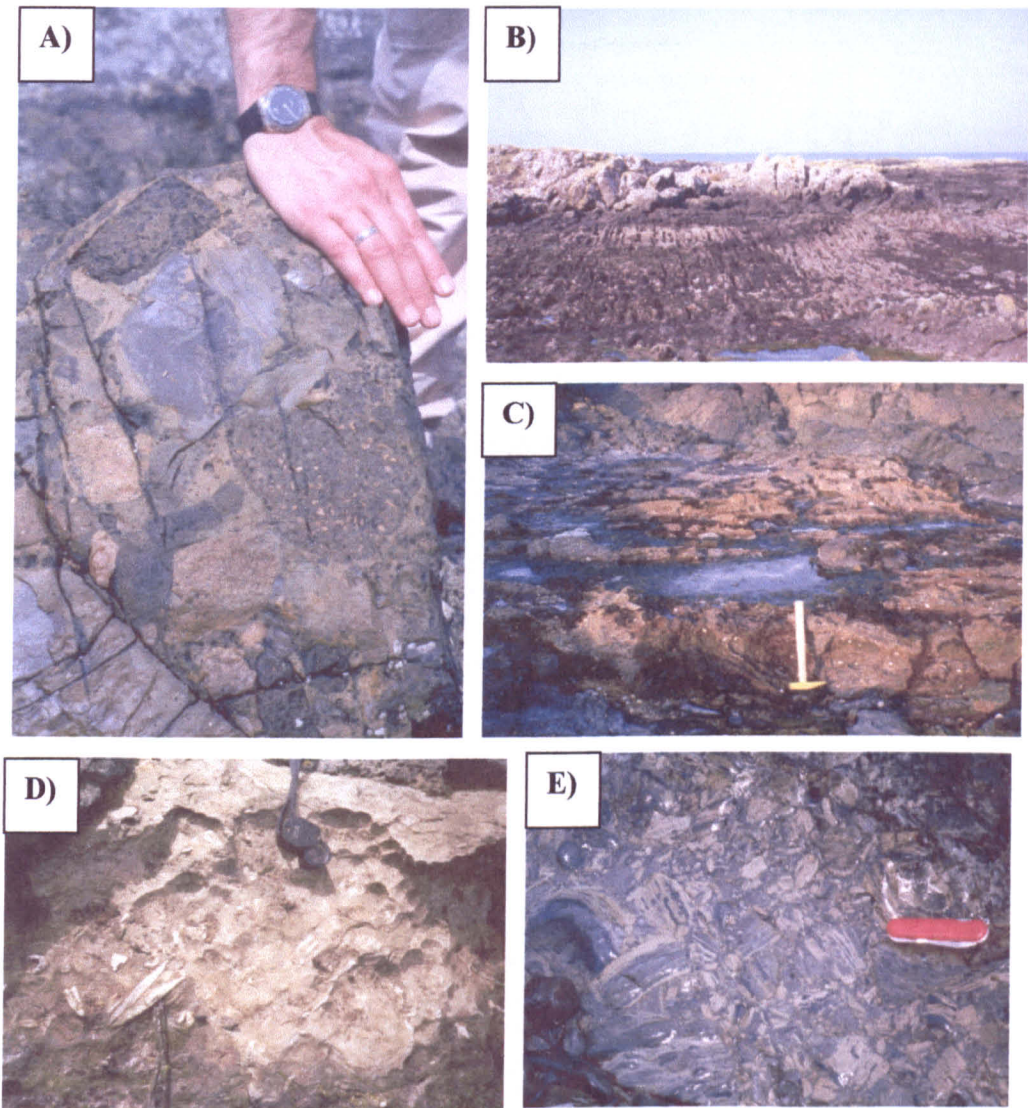


**Figure 5.21 – Clast lithologies in the Northern Conglomerate Formation. a)** Conglomerate at Fascaidale Bay rich in felsic clasts. Pale pink clasts are microgranite (NM49717097). **b)** Block of pseudo-bedded calcareous sandstone at Rubha na h-Acairseid measuring 30m by 25m (NM52067085). **c)** Typical examples of calcareous sandstone within the conglomerate (NM52067087). **d)** Block of Lower Jurassic limestone (Broadford Beds) displaying belemnites and *Ostrea* (NM51907055). **e)** Chaotic distribution of clast supported baked shale within conglomerate at Rubha na h-Acairseid (NM52157088).

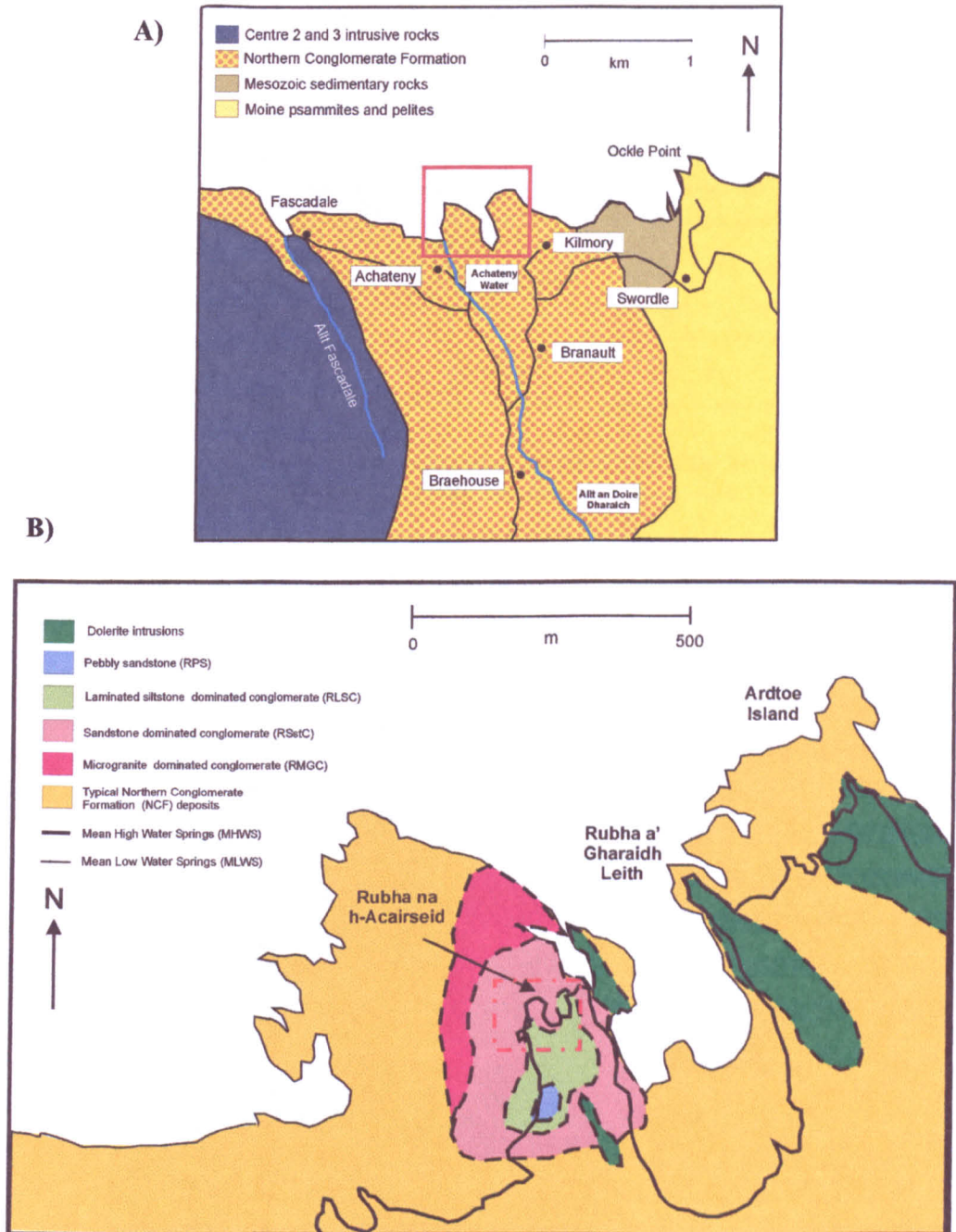


**Figure 5.22 – Location map and lithoclast dominated flow units in the Northern Conglomerate Formation (NCF). A) Simplified geological map of the NCF showing place names and location of Fig. 5.22b. (after Edinburgh Geological Society 1976) B) Map of clast dominated flow units in the NCF at Rubha na h-Acairseid. Location of Fig. 5.23 is indicated.**

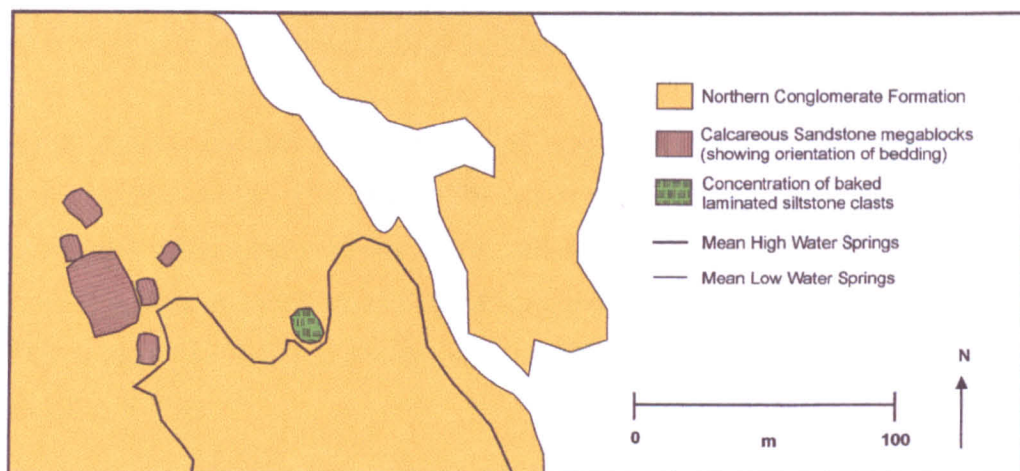


**Figure 5.23 – Distribution of calcareous sandstone megablocks in the Northern Conglomerate Formation (NM521708). See Fig. 5.22 for location.**

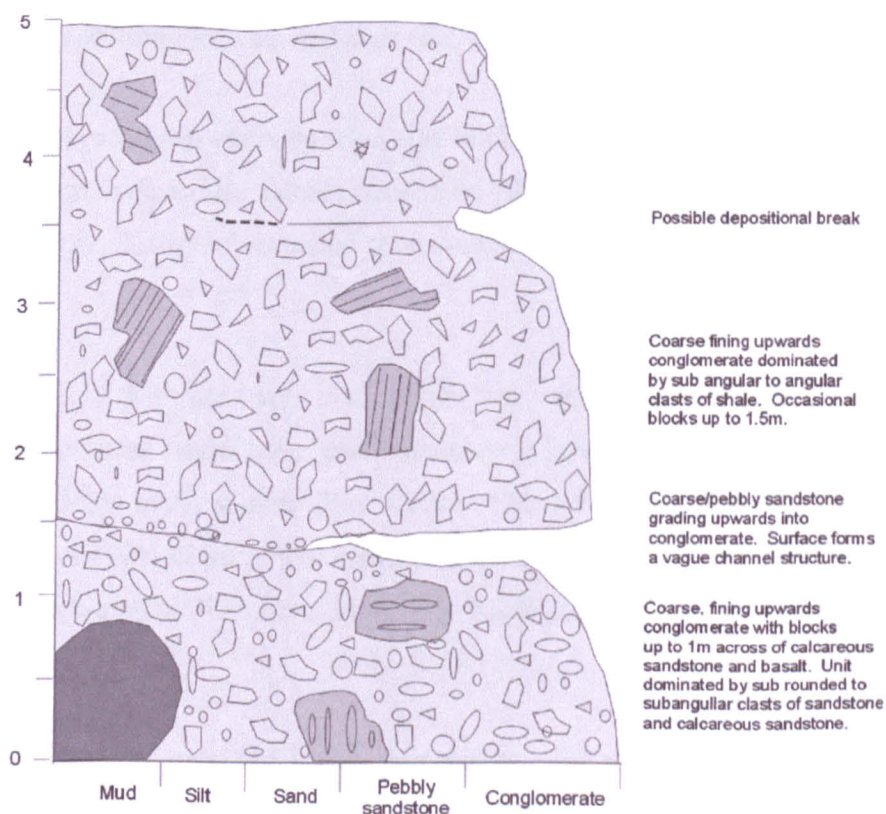


**Figure 5.24 – Vertical log of the Rubha na h-Acairseid sandstone and laminated siltstone dominated conglomerate flow units (NM52297075). Vertical scale in metres.**

The boundary between the RSstC and the RLSC is defined by several undulating channel-like surfaces, with up to *ca.* 1m relief, indicating a break in sedimentation. In addition, the RSstC contains many somewhat smaller (typically 10 to 20cm depth), channels, their cross-cutting inter-relationships indicating multiple depositional events.

A gently dipping channel within the RSstC, approximately 2m wide and 30cm deep is shown in Figure 5.25a. The channel fill is finer-grained than that in the channel below. The irregular surface between the RSstC and RLSC units is illustrated in Figure 5.25b. Figure 5.25c is an enlarged view, illustrating the different lithoclasts in the RSstC and the RLSC. Broad, low-relief channels are identified by small variations in dip within the RSstC (Fig. 5.25d).

Outweathered conglomeratic 'dykes' typically 1m long and *ca.* 10cm wide are identified on a bedding surface of the RSstC (Fig. 5.26a). These linear features apparently fill cracks on the surface of the RSstC and are composed of clast supported pebbly sandstone or fine conglomerate, comprising rounded clasts *ca.* 1-2cm across (Fig. 5.26b).

The RLSC is locally overlain by a *ca.* 1m thick unit of reddish-brown pebbly sandstone. The Rubha na h-Acairseid pebbly sandstone (RPS) is matrix supported and comprises small (typically <2cm) sub-rounded to sub-angular pebbles of sandstone and basalt (Fig. 5.26c).

At Kilmory Bay there are two *ca.* 15m high 'sea stacks' composed of conglomerate. The successions in these stacks have gently undulating layers, from 2 to 5m thick, which may represent bedding or flow units (Fig. 5.27a). These dark brown to black clast-supported conglomerates (70% clasts; 30% matrix) contain large (2-40cm; rarely up to 1m), sub-rounded to sub-angular lithoclasts of aphyric basalt, and less commonly scoriaceous basalt (Fig. 5.27b).

Numerous other exposures at Kilmory Bay might be interpreted as basaltic lava flows, with pitted, rubbly tops, but the presence of rare rounded clasts of microgranite and basalt, most obvious on prepared, slabbed surfaces, confirms their sedimentary nature (Fig. 5.27c). A *ca.* 50cm thick reddened, lateritic horizon is recognised between two units indicating the sub-aerial character of these deposits (Fig. 5.27d).

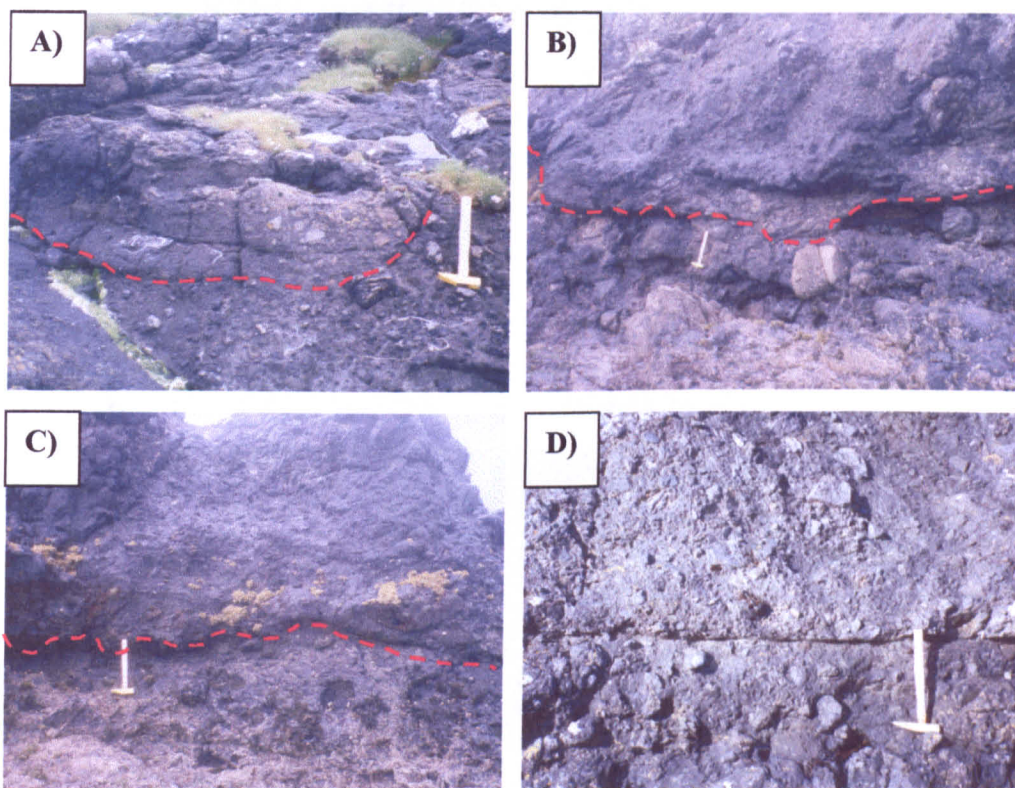


**Figure 5.25 – Channel structures in the Rubha na h-Acairseid area (NM52297075). a) Small channel feature within the RSstC (NM52007080). b) Undulating contact between the RSstC and the RLSC. c) Relationship between RSstC and RLSC deposits showing contrasting lithologies (pitted calcareous sandstone clasts in the underlying RSstC) and channels between flows. d) Bedding plane in RSstC deposit.**

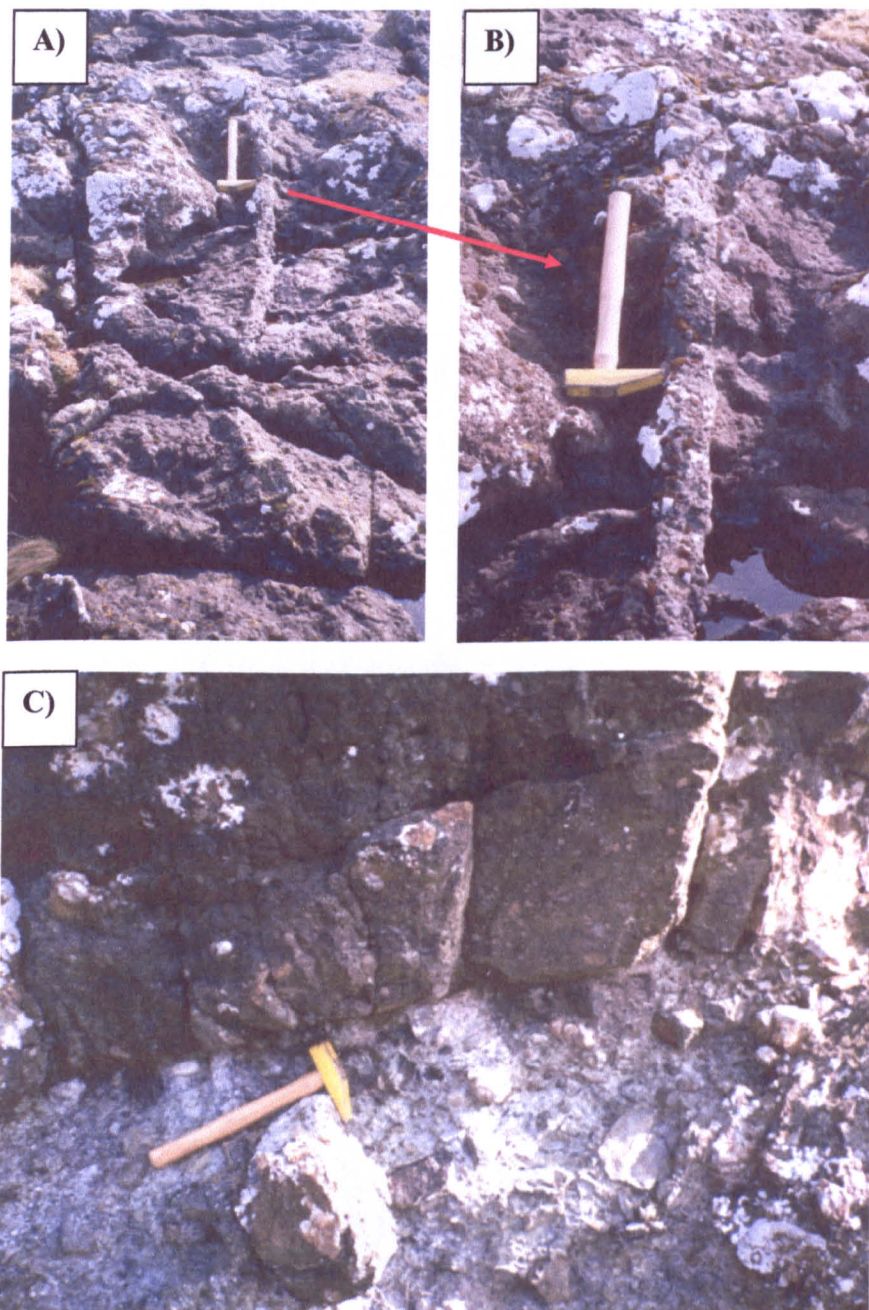


**Figure 5.26 – Conglomeratic dykes and stratification in the Rubha na h-Acairseid area. A) 1m long and 10cm wide conglomeratic ‘dyke’ on surface of RSstC (NM52007080). B) Enlarged view of ‘dyke,’ comprising clast supported pebbly sandstone. C) Stratification within the NCF, showing RLSC overlain by 1m thick reddish-brown matrix supported pebbly sandstone/fine conglomerate (RPS) (NM52117080).**

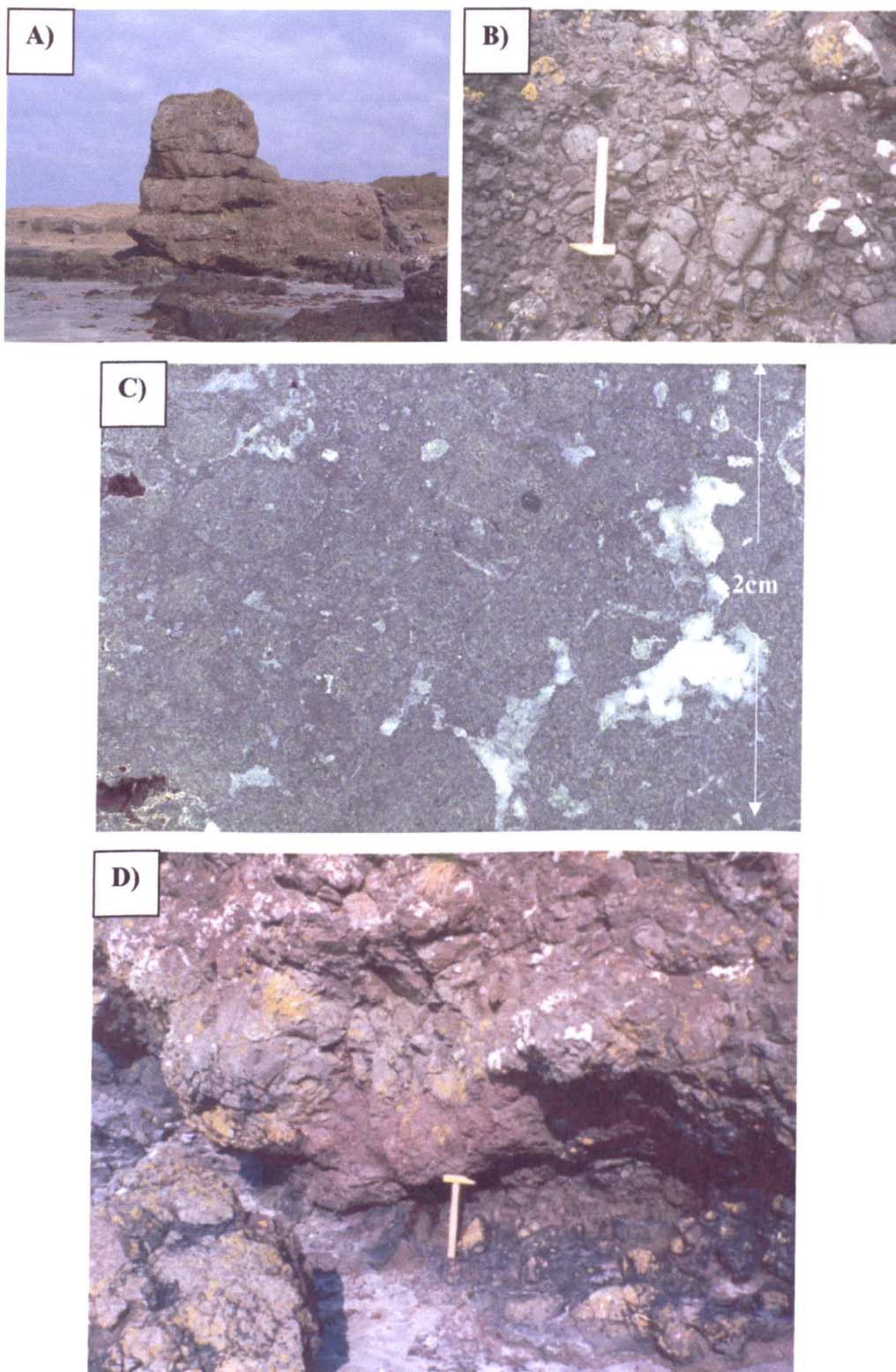


**Figure 5.27** – Kilmory Bay stacks displaying flow units and lateritic horizon (NM52477057). a) Kilmory Bay stack displaying pseudo-beds or flows of *ca.* 2m thickness b) Sub-rounded to sub-angular clasts of basalt within the Kilmory stacks c) Polished surface of apparent rubbly top lava, revealing sub-rounded clasts of basalt in conglomerate. D) 0.5m thick reddened, lateritic horizon between flows in the Kilmory stacks.

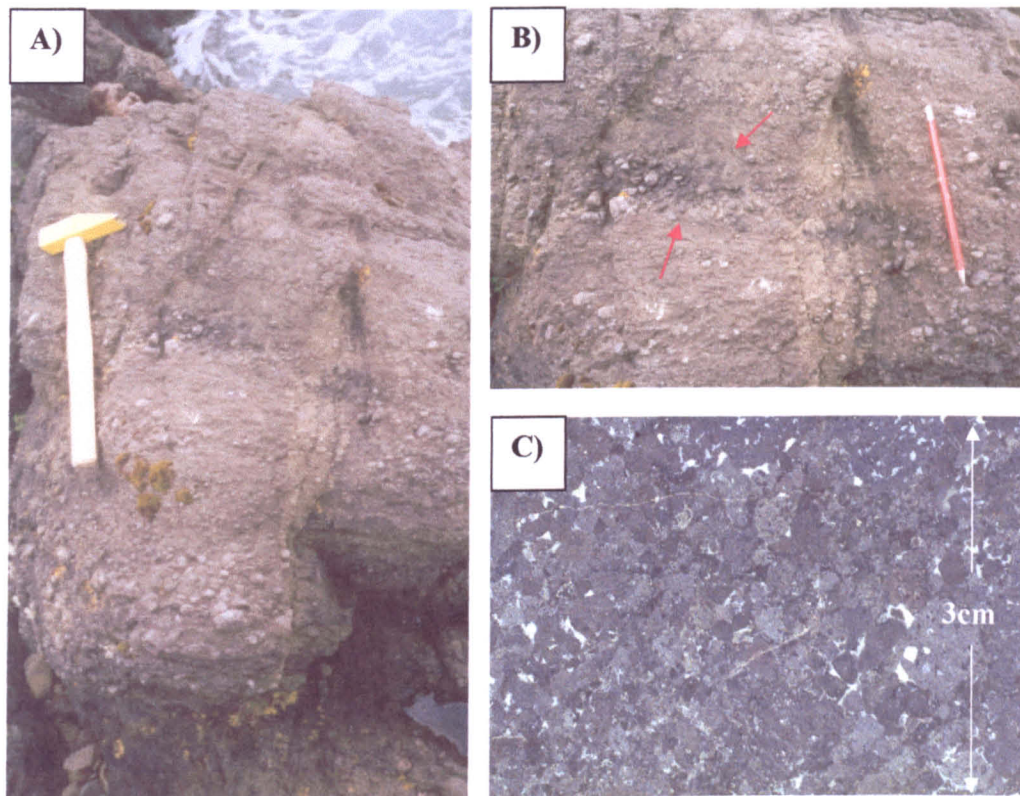


Figure 5.28 – Sedimentary features from Rubha a' Gharaidh Leith (NM52417099). a) Fining up sequence of fine conglomerates/pebbly sandstone showing distinct bedding. b) Coarse, clast supported 5cm thick layers within the pebbly sandstone c) Polished slab of pebbly sandstone showing rounded, closely packed grains.

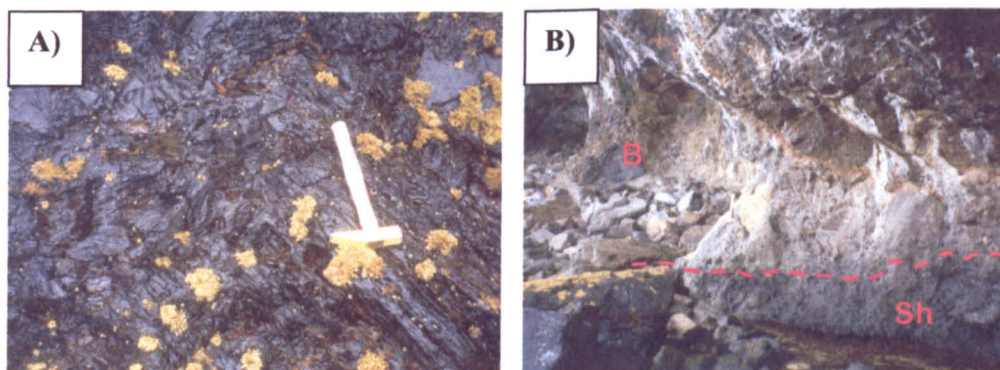


Figure 5.29 – Chaotically arranged shale clasts and layers in conglomerate from Swordle Cave (NM53237083). a) Concentration of chaotically arranged broken shale clasts at Swordle Cave. b) Shale layer (Sh) overlain by deposits containing sandstone and basalt megablocks (B).

North of Kilmory Bay, at Rubha a' Gharaidh Leith, another local conglomerate variation is identified. Here, normally-graded, matrix-supported beds of light to dark brown conglomerate and pebbly sandstone form a *ca.* 5m thick sequence (Fig. 5.28a), interbedded with *ca.* 5cm thick, pebble-rich layers (Fig. 5.28b). The clasts throughout this sequence are sub-rounded and range from 2 to 5cm across. Clast lithologies include: aphyric basalt, plagioclase megacrystic basalt, amygdaloidal basalt, scoriaceous basalt, and rarer sandstone.

Near Ardtoe Island two exposures, each *ca.* 10m across, of shattered and fractured massive basalt occur inland at NM52817084, and are typical of basalt megablocks recognised in the Northern Conglomerate Formation.

The conglomerates at Swordle Cave are locally dominated by angular lithoclasts of Mesozoic shale, typically 5-10cm across (Fig. 5.29a), forming a 1m thick layer. Unlike the shale clasts elsewhere in the NCF, the material here does not appear to be thermally altered. Immediately overlying these shale-rich deposits are conglomerates, *ca.* 10 - 15m thick, dominated by sub-rounded megablocks up to 1m across of sandstone, aphyric basalt and rare limestone, (Fig. 5.29b).

A wide range of lithologies and structures are present in the NCF deposits between Fasadale Bay and Swordle Cave on the north coast of the peninsula. The dominant depositional characteristics of these bedded deposits are normal grading and channels. Blocks of Mesozoic sedimentary rock are present throughout, with localised concentrations of other lithologies, including microgranite and scoriaceous basalt, neither of which are found *in situ* in this area. The wider implications of their presence only as lithoclasts in the conglomerates is discussed in Section 5.7.

#### **5.4.4 Rubha Carrach**

The conglomerates of Rubha Carrach, at the head of the Glendrian valley, are separated from the main NCF outcrops by the major gabbroic intrusions of Centres 2 and 3, and a large dolerite Centre 1 cone sheet. Rubha Carrach forms a prominent and spectacular 60m high cliff, 500m in length, tapering to a point at its seaward end (Fig. 5.30a). The conglomerates are cut by multiple minor intrusions, including a 5m wide dyke trending north-south along the base of the cliff, which weathers to a series of spaced 'ribs' 10cm

across. Another 5m wide dyke intrudes the cliff section, again trending north-south. A series of jet black, basaltic cone sheets trending east-west, also cut the cliff section, but at high angles. They range in thickness from a few centimetres to 2m and typically have non-planar geometries, as seen in the cliff section (Fig. 5.30b). The intrusions are cross-cutting and 'xenoliths' of conglomerate are often preserved within the intrusions (Fig. 5.30c).

The conglomerate deposits of Rubha Carrach typically weather grey to yellow-brown, much paler than the conglomerates of the NCF and the BHCF. These conglomerates are clast supported with approximately equal proportions of sub-rounded and sub-angular lithoclasts, ranging from 2 to 30cm across, with rarer blocks up to 60cm. Clast lithologies include: aphyric basalt, porphyritic tholeiitic andesite, quartzite, sandstone, calcareous sandstone, limestone, microgranite, ignimbrite and rhyolite. Sub-angular quartzite and sub-rounded massive basalt lithoclasts typically dominate the unit (approximately 70% of total clasts). The matrix is of quartz-rich sandstone, and highly resistant to weathering. Thus, the lithoclasts and the matrix are differentially weathered, with the lithoclasts being in-weathered relative to the matrix.

Three lithological units can be identified at Rubha Carrach and are outlined in a vertical log (Fig. 5.32a). The lowest unit is a *ca.* 15m thick, clast-supported conglomerate containing lithoclasts ranging in size from 10 to 20cm across, with rarer blocks of quartzite and porphyritic tholeiitic andesite up to 50cm (Fig. 5.31a). Overlying this is a 70cm thick unit of grey, carbonate-cemented, quartz-rich sandstone. This extends laterally for only 15m, before tapering out. The carbonate-cemented sandstone is bedded with alternating fine and pebble-rich coarse layers of 2cm thickness (Fig. 5.31a). Rare lithoclasts, 5 to 10cm across, of porphyritic andesite and ignimbrite are present within the sandstone (Fig. 5.31b) and in places, the sedimentary material forms small scale drapes over clasts in the underlying conglomerate (Fig. 5.31c). Lithoclasts from the overlying conglomerate project into the top of the sandstone, as a result of loading, indicating that the sandstone was not completely lithified when the conglomerate was deposited. Micro-scale, normal and reverse syn-sedimentary faults, with displacements of a few mm to 2cm, are also identified within the sandstone unit (Fig. 5.31d).

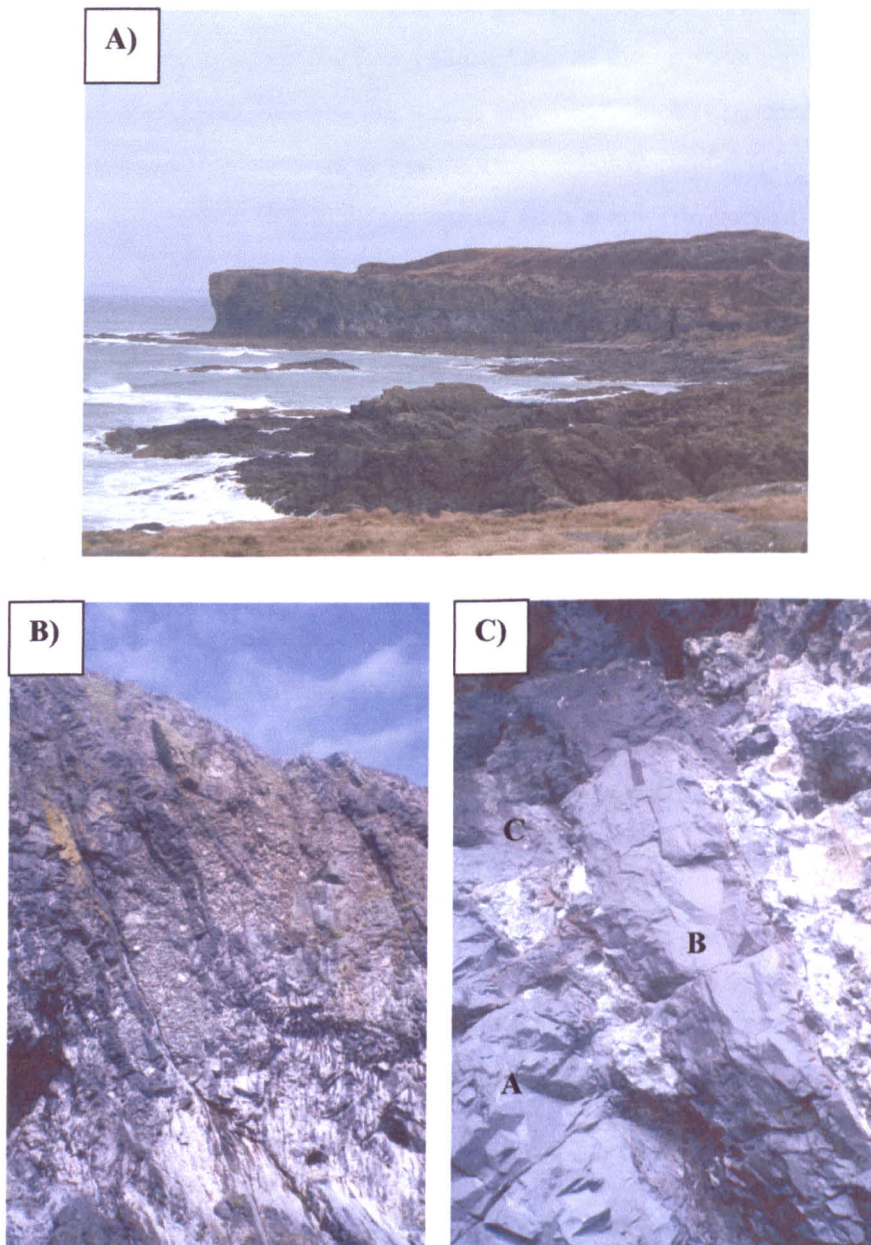


**Figure 5.30 – Topography and intrusions of the Rubha Carrach area (NM46137074). a) Topography of the Rubha Carrach cliff section. Conglomerate forms the cliff face below the plateau in the midground. b) Numerous basaltic intrusions cutting the section at variable angles. c) Cross-cutting intrusions in the conglomerate. Vertical intrusions A and B cut the conglomerate. They are then cut by intrusion C.**

Approximately 45m of conglomerate overlie the sandstone. This contains a higher proportion of aphyric basalt clasts than the lower unit but is also more matrix supported. The clasts are sub-rounded to sub-angular, and generally 10 to 25 cm across, but scattered blocks up to 1m are also common. Towards the base of the upper conglomerate unit there are lenses of sandstone, *ca.* 70cm to 1m across and 40cm thick (Fig. 5.31e). These lenses are composed of sandstone identical to that in the unit below, and display micro-scale syn-sedimentary normal faults. Rare macro-faults, with displacements of 10 to 50cm, are present between sandstone lenses. Typically these are reverse faults, which tentatively link the lenses, suggesting the unit was originally more laterally extensive, and has been subsequently 'thickened'. Therefore, the current thickness of the unit may be somewhat exaggerated. Fault positions are shown schematically in Figure 5.32b.

Although the Rubha Carrach conglomerates have distinctive features, such as the presence of porphyritic andesite and rhyolite lithoclasts, a quartz-rich matrix, and evidence of syn-depositional faulting, they also share features typical of the NCF and BHCF deposits. The Rubha Carrach conglomerates are typically clast supported, with sub-rounded, coarse and relatively large lithoclasts. They also form a stratified sequence, indicating hiatuses in sedimentation, and finer grained lithologies can also be identified. Thus, notwithstanding the differences, the overall characteristics of these deposits suggest a mode of deposition similar to that of the NCF and BHCF elsewhere on the peninsula.

## **5.5 Clast Count Analysis**

### **5.5.1 Introduction**

The coarse-grained conglomerates of the Ardnamurchan Peninsula have in the past been interpreted as explosive vent agglomerates. In an effort to understand their true nature and identify any distribution trends, a series of clast counts were carried out. The purpose of these counts was to describe the deposits and interpret them where possible. These data, together with more general field observations, enable the characteristics of the deposits to be compared with those of deposits reflecting a variety of modes of deposition. Simple statistics will be used to test conclusions.

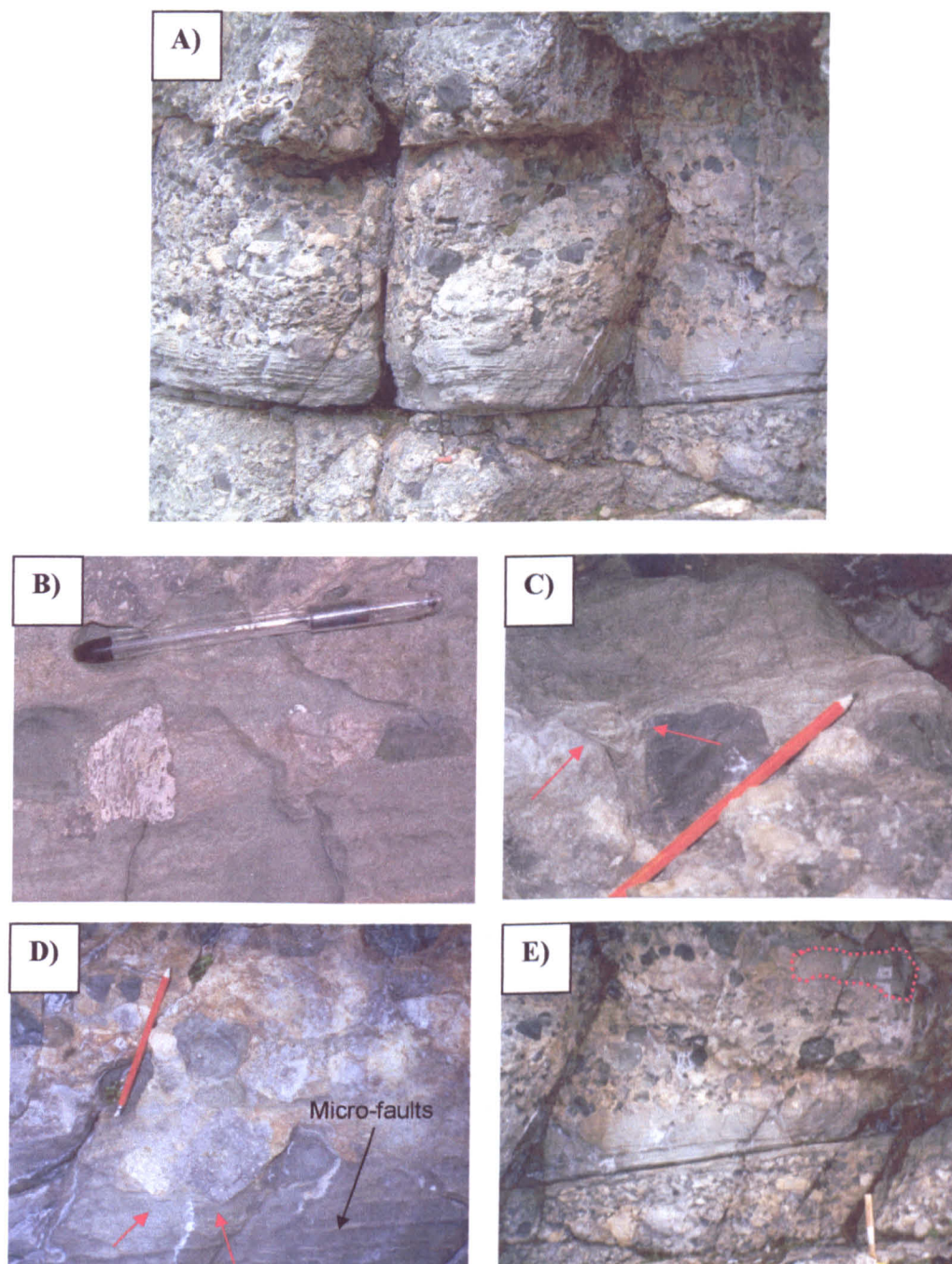
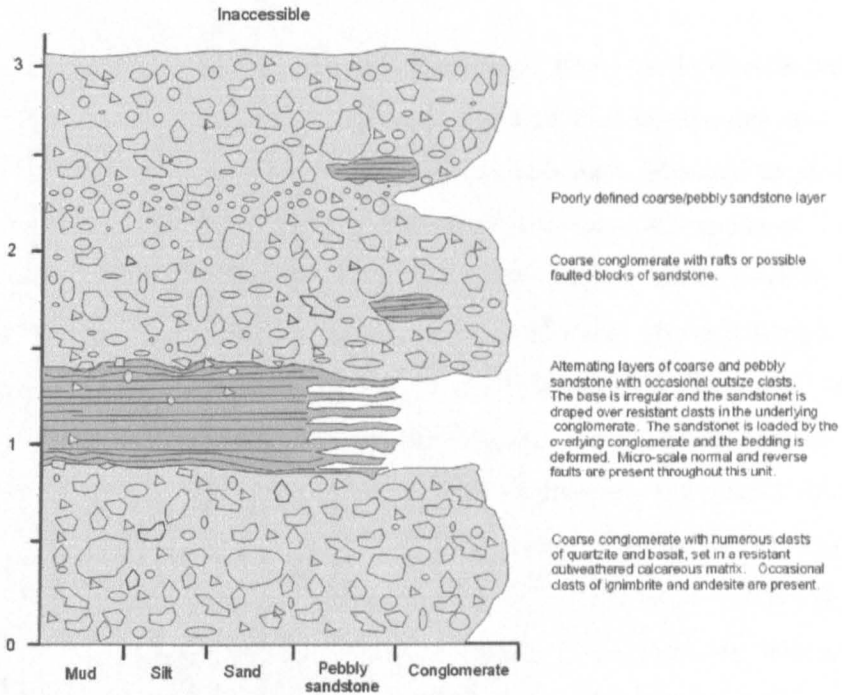


**Figure 5.31 – Sedimentary structures from the Rubha Carrach area (NM46177053). a) Lower finer more matrix supported unit overlain by thin, bedded fine and coarse sandstone unit. This is overlain by a coarse clast supported unit. b) Clasts of porphyritic tholeiitic andesite and ignimbrite within the sandstone. c) Small scale drape structures (indicated by arrows) in sandstone overlying conglomerate. d) Clasts impacting into underlying sandstone (indicated by red arrows), causing loading and deformation structures. Below this, micro-scale normal and reverse faults within the sandstone unit are recognised. e) Lenses of sandstone within the upper conglomerate unit.**

A)



B)

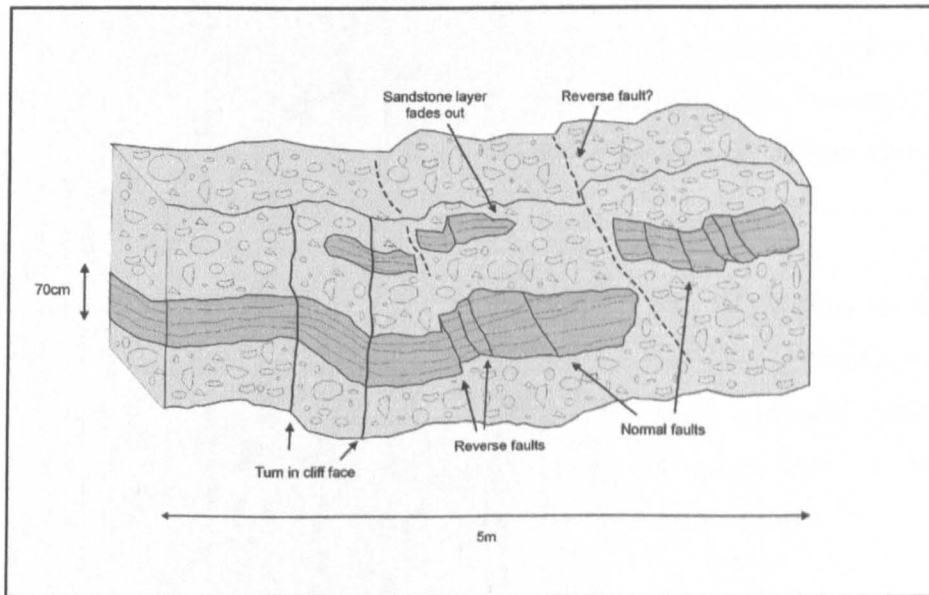


**Figure 5.32 – Vertical log and reconstruction of faulting in the Rubha Carrach area (NM46177053). a) Vertical log of the lowest 3m of the Rubha Carrach cliff section. b) Schematic reconstruction of faulting in the lower portion of the Rubha Carrach conglomerates.**

## 5.5.2 Methods

A series of traverses across the coarse-grained deposits of the Peninsula were selected in order to provide a network of data. These comprised four north-south and two east-west traverses of varying length. One vertical section was also subjected to analysis. Counts were undertaken at points along traverses wherever suitable exposures were available. However, the nature and quality of the exposures limited these traverses, and regular sampling was only possible on coastal and high relief areas. At each sample point a linear transect of 10m was measured out and clast lithology and degree of rounding were recorded at 10cm intervals along this. For this purpose a clast was defined as >2cm (Fisher 1960) and roundness was described as rounded, sub-rounded, sub-angular or angular. If no clast was present at the sample point, the gap was recorded as matrix. Over a 10m transect 100 data points were recorded, giving detailed information on clast lithology, the amount of rounding and the proportion of clasts to matrix. At 25cm intervals, clast size was measured in order to provide an idea of mean clast size at that locality. If the 25cm intervals coincided with matrix, then the 'clast size' was recorded as 2cm. In total, forty clast counts were conducted and are included in the traverses described. However, this method is limited as clast counts were only performed where exposure is suitable, and the stratigraphic positions of the conglomerates cannot be certain. For example, a series of traverses along the base of the topography formed by the conglomerate units may not represent the same stratigraphical interval.

Data were compiled in a series of graphs, plotting clast composition, clast roundness and mean clast size against distance. This allows variation within the deposits to be visually assessed. For mean clast size data a simple linear regression can be performed to assess the relationship between size and distance. The best-fit line through the data points provides a formula relating the variables, together with confidence limits.

## 5.5.3 The Traverses

The traverses are indicated in Figure 5.33 by black lines, with each sample point indicated by a letter or number. The traverse from MacLean's Nose to Swordle Cave provides data from the north to the south coasts, but is analysed as two separate traverses from MacLean's Nose to East Ben Hiant Gully and from Tom na

Gainmheich to Swordle Cave. Other north-south traverses were conducted from Camphouse to Portban, Allt an Doire Dharraich to Ardtoe Island, and at Rubha Carrach. East-west traverses were possible from Rubha Carrach to Swordle Cave and from Allt na Mi Chomhdhail to Tom na Gainmheich. All values are rounded to the nearest percent.

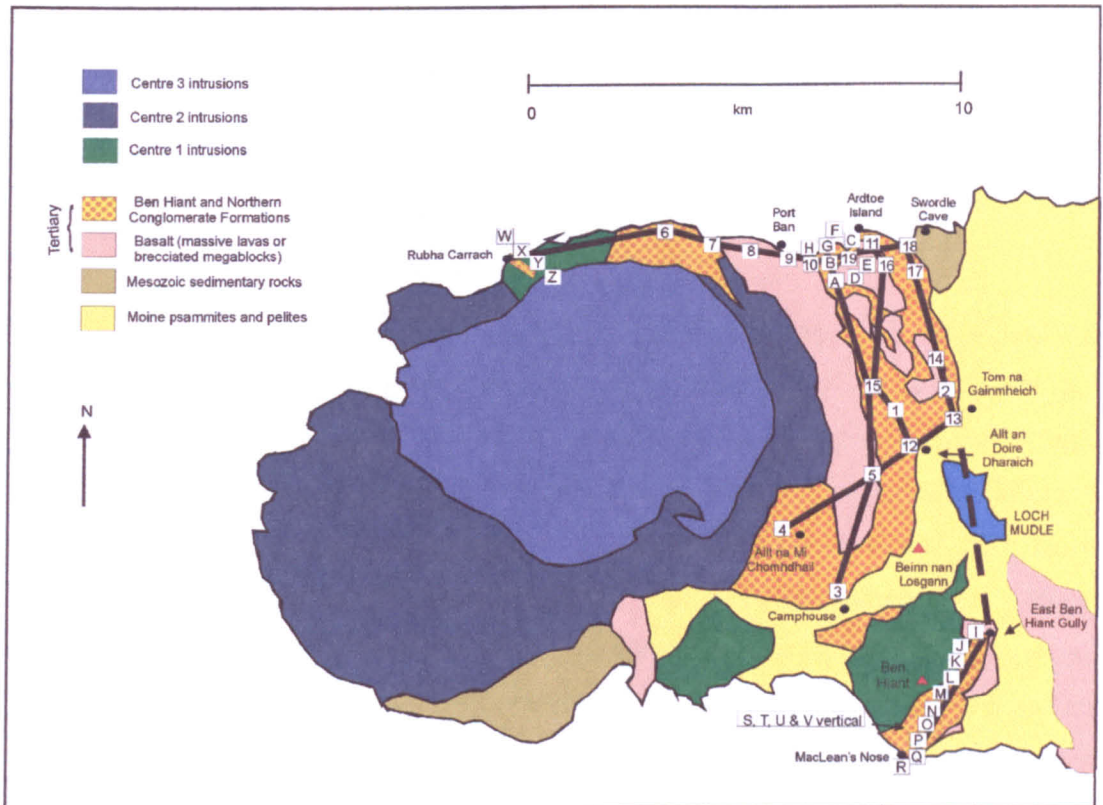


Figure 5.33 – Map of traverses and sample sites on the Ardnamurchan Peninsula

#### 5.5.4 Allt an Doire Dharraich to Ardtoe Island

This traverse (Fig. 5.33) reveals a number of trends that are reflected throughout the study. At Allt an Doire Dharraich clast composition is quite limited with only aphyric basalt, Moine psammite and quartzite present. To the south there are only minor additions of sandstone and porphyritic basalt and localised variations in the proportions of quartzite and Moine psammite, until sample point 16 at 3.5km is reached. North of this the clast assemblage becomes more heterogeneous. Sandstone becomes the dominant clast type (41%). There is a dramatic fall in the proportions of Moine psammite, massive basalt and porphyritic basalt clasts, and a corresponding increase in lithologies including calcareous

sandstone, dolerite, gabbro, microgranite and shale (Fig. 5.34a). The clasts are matrix-supported but the proportion of matrix does not vary greatly, ranging from 44% to a peak of 55%, decreasing towards the north before rising to 50% at Ardtoe Island (Fig. 5.34b). Rounding of clasts increases to the north. At Allt an Doire Dharaich, 83% of the clasts are sub-angular, progressively decreasing to 13%, as sub-rounded clasts increase from 29 to 79%. (Fig. 5.34c). The mean size of clasts shows a parallel trend, increasing to the north from 4 to 16 cm, although there is a slight decrease at sample point 15 (Fig. 5.34d). Linear regression reveals a strong underlying trend in these variables with confidence values above 65% (Fig. 5.34e).

### 5.5.5 Camphouse to Portban

There is again a trend of increasing heterogeneity, roundness and mean size of clasts from south to north. Towards the southern end of the traverse (Fig. 5.33) at Camphouse, the range of clast compositions is limited, and aphyric basalt and Moine psammite dominate, with smaller proportions of sandstone and shale (laminated siltstone). There is a significant rise in the proportion of aphyric basalt immediately to the north (forming 95% of the deposit) with a corresponding decrease in quartzite and Moine psammite. Following this, however, aphyric basalt clasts steadily decrease in number and, at 4km, quartzite forms 48% of the clasts. The northern section of the traverse is characterised by a continued reduction in the proportion of aphyric basalt and a large increase in clasts of shale and sandstone (up to 65%), with smaller numbers of calcareous sandstone, microgranite and scoriaceous basalt (Fig. 5.35a). Observations from Portban at 5.75km, 6km and 6.25km reveal local variations. At point A (5.75km) there is a large proportion of shale (47%) and sandstone (35%) with little aphyric basalt. At point B (6km), the shale content falls to 5%, and sandstone forms 66% of the deposit with calcareous sandstone comprising a further 23%. Finally, at point G (6.25km), shale is absent, and sandstone has fallen to 16%, but 35% of clasts are microgranite with 19% of scoriaceous basalt (Fig. 5.35b). These variations are interpreted as reflecting differing sources for a series of localised flow units within the deposit, which are reviewed in Section 5.4.

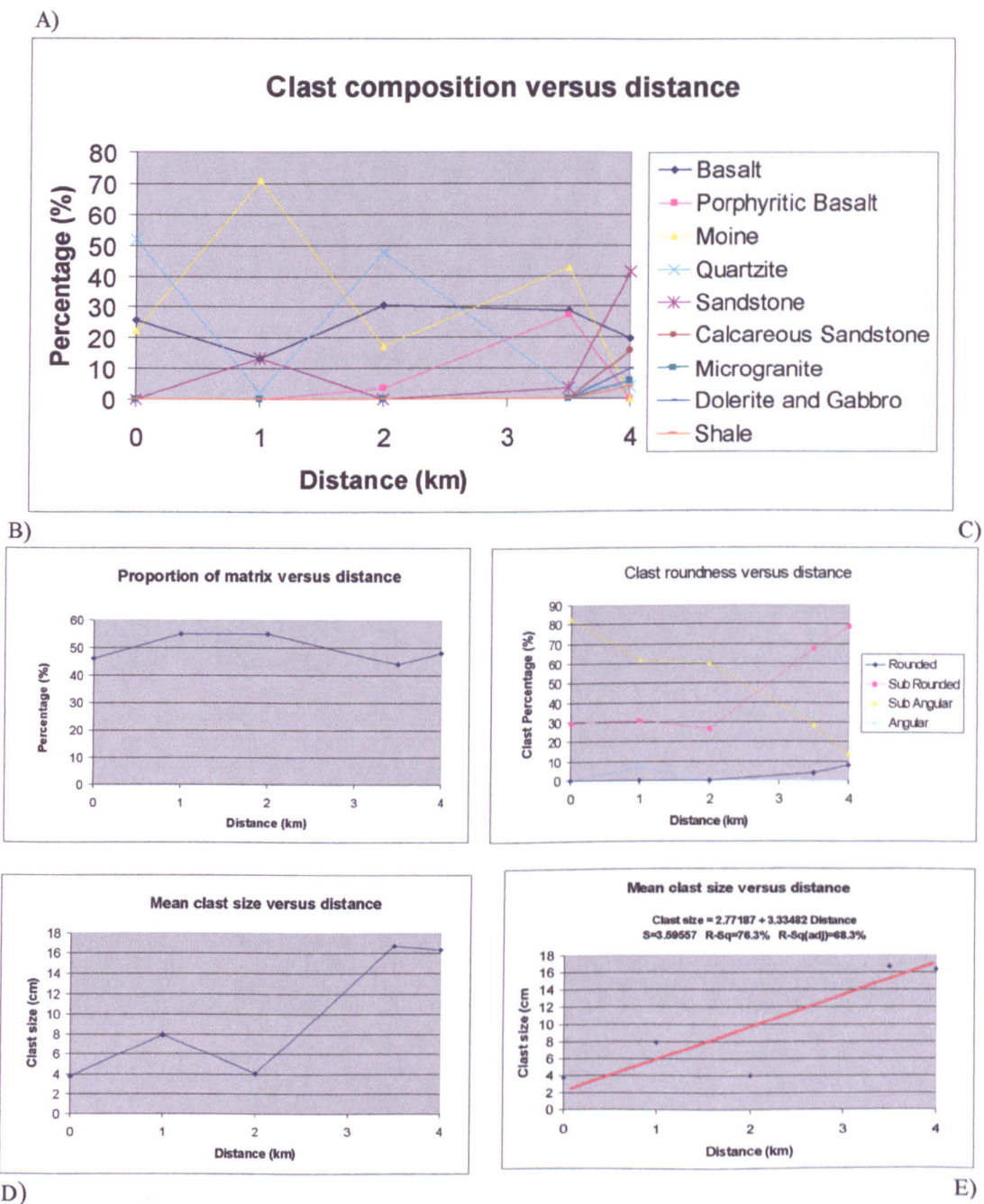


Figure 5.34 – Allt an Doire Dharaich to Ardtoe Island Clast Count Analysis: a) Clast composition versus distance; b) Proportion of matrix versus distance; c) Clast roundness versus distance; d) Mean clast size versus distance; e) Best-fit regression line of mean clast size versus distance.

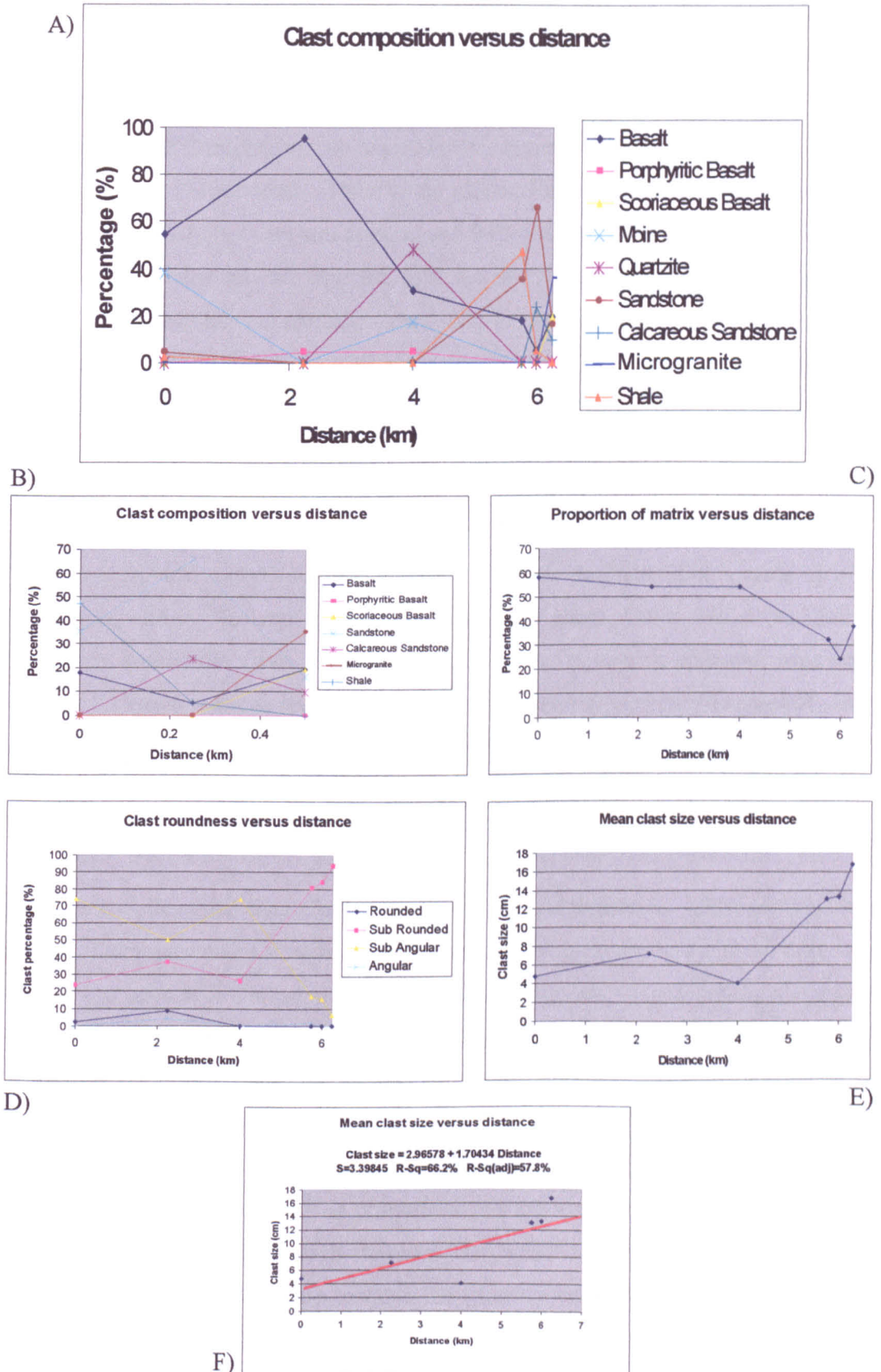


Figure 5.35 - Camphouse to Portban Clast Count Analysis: a) Clast composition versus distance; b) Portban - clast composition versus distance; c) Proportion of matrix versus distance; d) Clast roundness versus distance; e) Mean clast size versus distance; f) Best-fit regression line of mean clast size versus distance.

The deposits between Camphouse and Portban show a transition from matrix to clast support. The matrix represents 54% of the deposit at Camphouse, decreasing to around 24% at Portban (Fig. 5.35c). There is a parallel trend of increasing clast roundness from south to north. At Camphouse, sub-angular clasts comprise 74% of the deposit, with 24% sub-rounded and 2% rounded. There is an almost linear change in proportions and, at Portban, only 7% of clasts are sub-angular and 94% sub-rounded (Fig. 5.35d). The mean size of clasts increases towards Portban, from 4.5 to >16cm, with a slight decrease at point 15 (4km). This parallels the increase recorded in the traverse from Allt an Doire Dharaich to Ardtoe Island (Fig. 5.35e). Linear regression indicates the strong relationship between these variables, with confidence levels up to 66% (Fig. 5.35f).

### **5.5.6 MacLean's Nose to Swordle Cave**

This section provides a north-south traverse of the whole peninsula, but is made up of two sub-traverses, from MacLean's Nose to East Ben Hiant Gully and from Tom na Gainmheich to Swordle Cave. The area between these is densely forested, with limited exposure. The two sections reveal contrasting trends, and are described separately before examining the overall character of the traverse.

#### **5.5.6.1 MacLean's Nose to East Ben Hiant Gully**

This traverse follows the unconformable base of the conglomerate. Clast composition is relatively heterogeneous throughout, but many lithologies are present in only small amounts. Sandstone is the dominant lithology at MacLean's Nose, where it comprises approximately 39% of clasts; aphyric basalt forms 26%, and amygdaloidal basalt 18%. There are smaller proportions of porphyritic basalt, plagioclase megacrystic basalt and siltstone. There are numerous local fluctuations in subsidiary lithologies, with scattered clasts of scoriaceous basalt, Moine quartzite, microgranite, trachyte, ignimbrite and shale. Towards East Ben Hiant Gully, the proportion of sandstone falls steadily to *ca.* 6%, and amygdaloidal and porphyritic basalt are reduced to isolated pebbles. Generally, ignimbrite and shale become more abundant towards the southern portion of the traverse. Aphyric basalt rises to 54% at East Ben Hiant Gully where it is the dominant lithology. Porphyritic feldspar and scoriaceous basalt also increase towards East Ben Hiant Gully. (Fig. 5.36a).

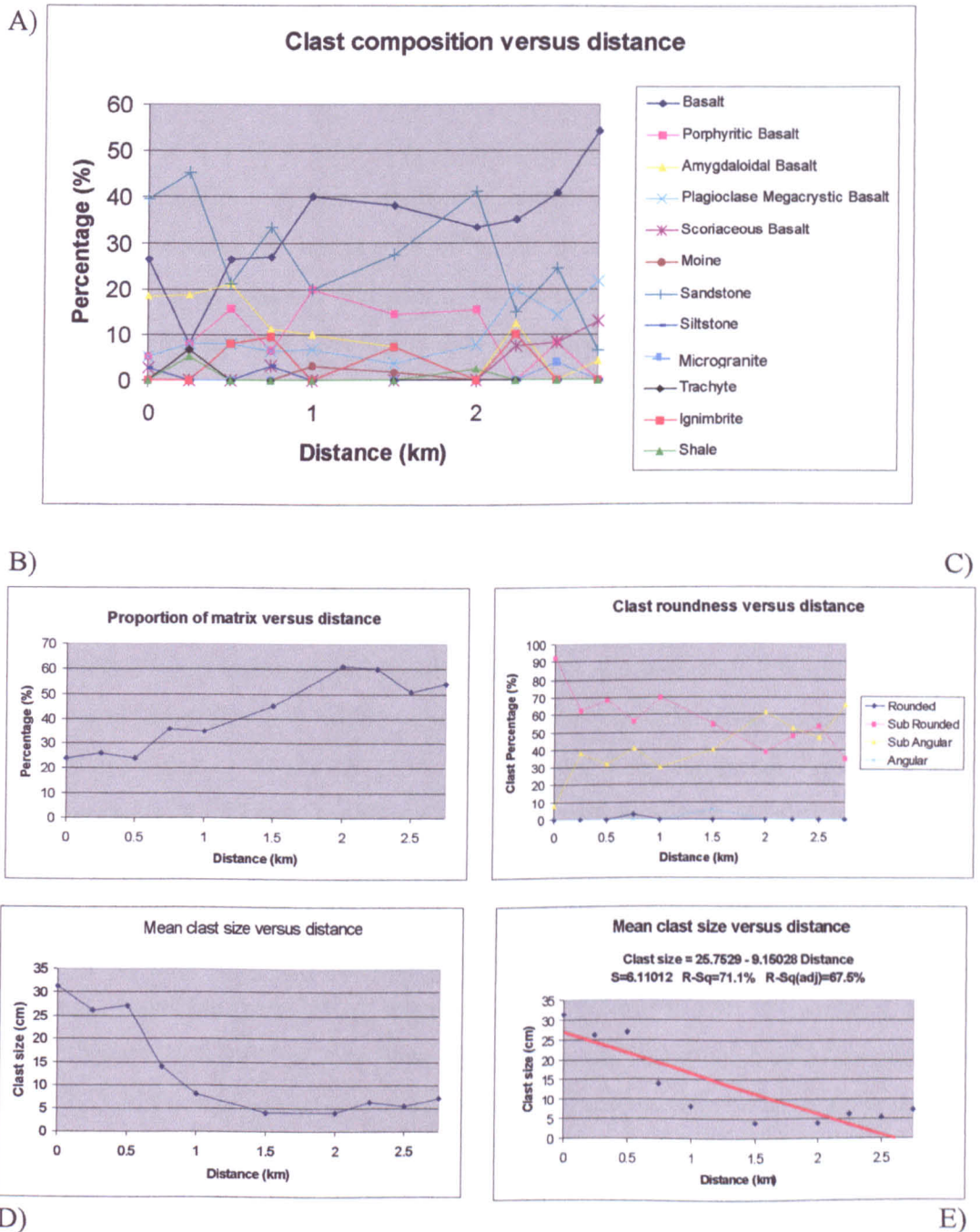


Figure 5.36 – MacLean’s Nose to East Ben Hiant Gully Clast Count Analysis: a) Clast composition versus distance; b) Proportion of matrix versus distance; c) Clast roundness versus distance; d) Mean clast size versus distance; e) Best-fit regression line of mean clast size versus distance.

Overall, heterogeneity increases towards the south. The proportion of matrix also increases, from 24% at MacLean's Nose to 54% at East Ben Hiant Gully, and locally is as high as 60% (Fig. 5.36b). There is a significant decrease in roundness to the north, with the proportion of sub-rounded clasts falling from 92% at MacLean's Nose to 35% at East Ben Hiant Gully. The proportion of sub-angular material increases from 8% at MacLean's Nose to 65% at East Ben Hiant Gully (Fig. 5.36c). Mean clast size decreases from over 30cm at MacLean's Nose to below 10cm 1km to the north, but becomes relatively uniform thereafter (Fig. 5.36d). A linear regression shows a strong relationship between these variables, with confidence levels over 68%. It reveals a negative correlation, in which compositional, morphological and mean size all increase towards the south, contrasting with the northward increase seen in previous examples (Fig. 5.36e).

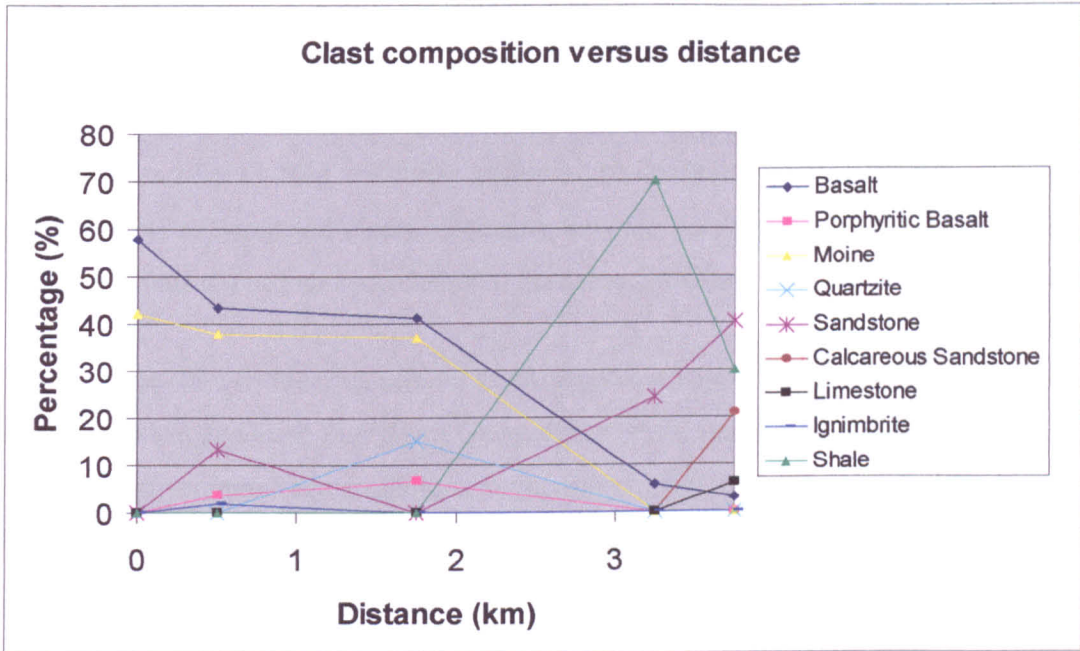
### **5.5.6.2 Tom na Gainmheich to Swordle Cave**

At Tom na Gainmheich clasts are only of aphyric basalt and Moine psammite. The proportion of aphyric basalt decreases to the north from 58% to less than 3%. The Moine psammite follows a similar trend, falling from 42% to zero. These changes are complemented by an influx of new lithologies and an increase in clast heterogeneity to the north, towards Swordle Cave, where pebbles of sandstone, calcareous sandstone, shale and limestone are present. At sample point 17 (3.25km), shale comprises 70% of the clasts, whereas at point 18 (3.75km) sandstone is the dominant lithology (40%) (Fig. 5.37a). The proportion of matrix steadily declines from 50% to 35% and the unit becomes more clast supported to the north (Fig. 5.37b). The degree of roundness also increases to the north. At Tom na Gainmheich, 28% of clasts are sub-rounded, rising to 82% at Swordle Cave. Sub-angular clasts fall from 85% at sample point 2 (7.75km) to 18% at Swordle Cave (Fig. 5.37c). Mean clast size increases from 7cm at Tom na Gainmheich to 25cm at Swordle Cave (Fig. 5.37d). A linear regression shows a strong relationship between these variables, with confidence values up to 71% (Fig. 5.37e). This traverse again reveals trends of increasing clast heterogeneity, clast support, roundness and mean clast size to the north.

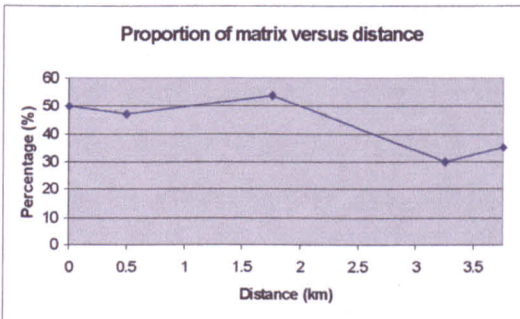
### **5.5.6.3 Analysis of both traverses**

Combining the data from the two traverses from MacLean's Nose to East Ben Hiant Gully and from Tom na Gainmheich to Swordle Cave, a larger picture can be built up (Fig. 5.38a).

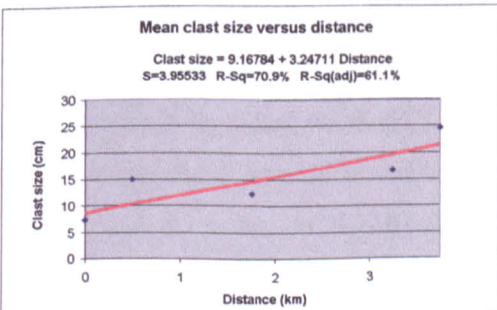
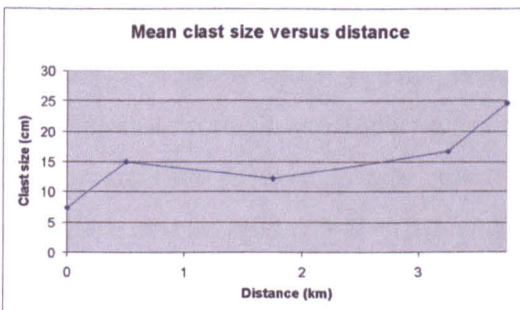
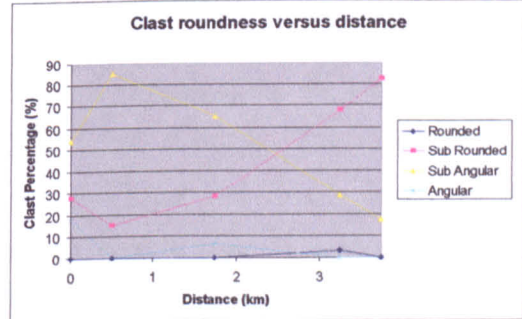
A)



B)



C)



D)

E)

Figure 5.37 – Tom na Gainmheich to Swordle Cave Clast Count Analysis: a) Clast composition versus distance; b) Proportion of matrix versus distance; c) Clast roundness versus distance; d) Mean clast size versus distance; e) Best-fit regression line of mean clast size versus distance.

Clast heterogeneity is low in the central area and increases in opposing directions. Only aphyric basalt, small numbers of Moine quartzite clasts and rare sandstone are present in the centre whereas to the north and south, sandstone clasts are dominant with large numbers of calcareous sandstone, shale and some limestone and minor amounts of Palaeogene igneous rocks. The reasons for this gradation will be discussed in Section 5.7, below. The proportions of matrix decrease as clast support increases towards the ends of the traverses (Fig. 5.38b). Similar patterns are observed in clast roundness, with the proportion of sub-rounded clasts increasing towards the outer ends of the traverses (Fig. 5.38c), with mean clast size increasing in the same directions (Fig. 5.38d).

This suggests that in the area around Loch Mudle and Beinn nan Losgann, between Tom na Gainmheich and East Ben Hiant Gully, there was a 'sediment parting' or 'watershed,' with similar sediment accumulations reflecting similar methods of deposition on either flank. This may indicate an area of high relief in the palaeo-topography from which these deposits were derived. This will be reviewed in detail in Sections 5.7 and 5.10, below.

### **5.5.7 Rubha Carrach**

The final north-south traverse was only 0.75km in length, along the outcrop at Rubha Carrach, with the objective of identifying small-scale changes. The data reveal little variation in clast characteristics against distance. There are locally higher or lower proportions of Moine quartzite, and at the last sample point (Z) small amounts of ignimbrite (Fig. 5.39a). There is no significant change in the proportion of matrix (Fig. 5.39b). Clast roundness shows no overall trend, only recording covariation in the proportions of sub-rounded and sub-angular clasts (Fig. 5.39c). Mean clast size shows a slight increase from 12.5 to 14cm, suggesting this is not a significant trend (Fig. 5.39d). A linear regression reveals a poor relationship between these variables with maximum confidence percentages of only 23% (Fig. 5.39e). Thus, there are no significant trends at Rubha Carrach.

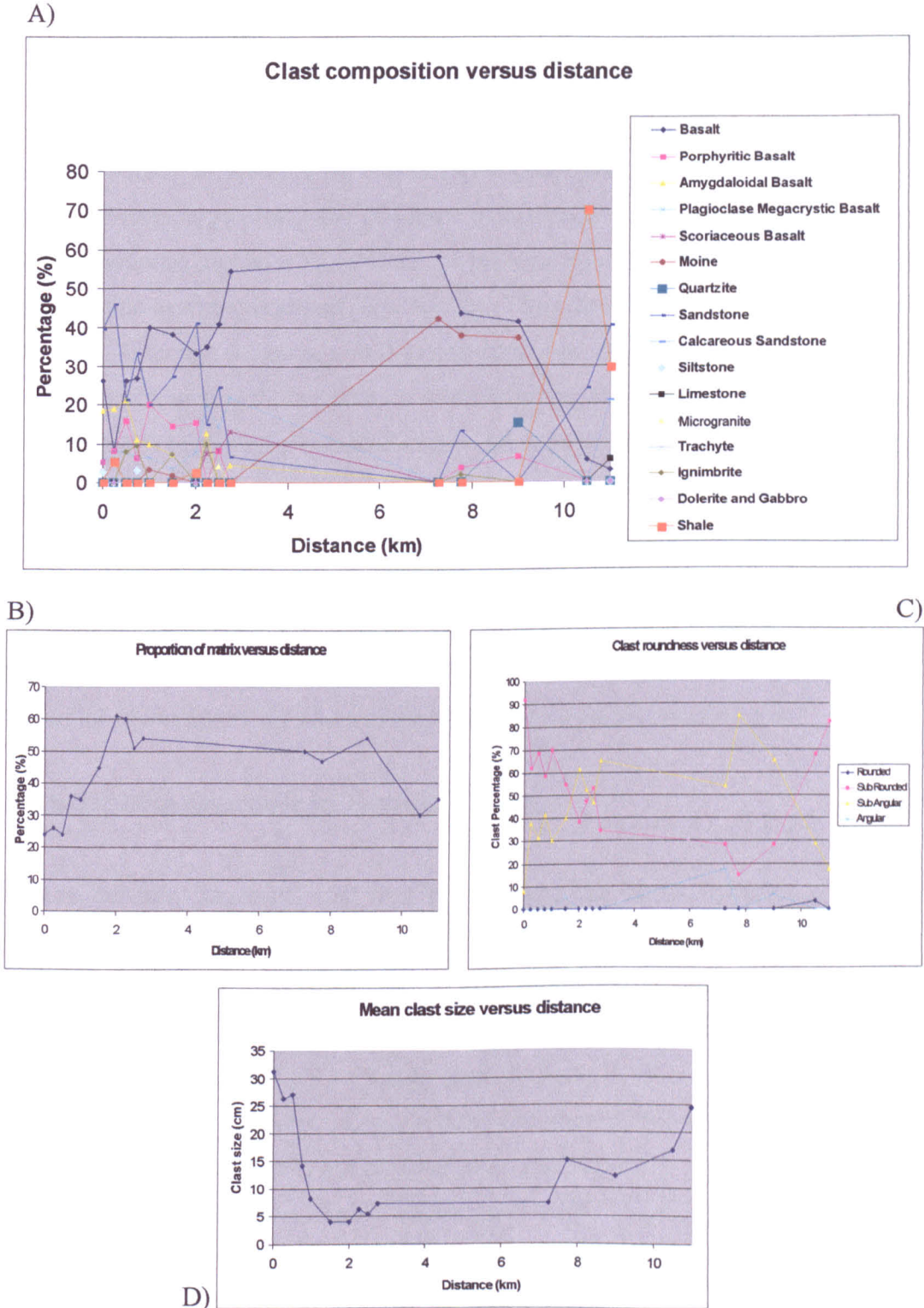


Figure 5.38 – MacLean’s Nose to Swordle Cave Clast Count Analysis: a) Clast composition versus distance; b) Proportion of matrix versus distance; c) Clast roundness versus distance; d) Mean clast size versus distance.

### 5.5.8 Allt na Mi Chomhdhail to Tom na Gainmheich

This east-west traverse is characterised by low clast heterogeneity. At Allt na Mi Chomhdhail in the west, the unit is dominated by aphyric basalt clasts (72.5%) with only minor amounts of porphyritic basalt, Moine psammite and sandstone. There is an increase in the proportion of basalt to the east (95%) although this falls to 26% at sample point 12 (3km), where a large proportion of Moine quartzite (52%) is present. The proportion of Moine psammite increases from scattered pebbles to over 40% at Tom na Gainmheich, where Moine quartzite is absent (Fig. 5.40a). The proportion of matrix falls steadily from 60 to 50%, although the entire unit is matrix-supported (Fig. 5.40b). There are no trends in the degree of rounding of the clasts. Variations in the proportions of sub-rounded and sub-angular clasts are generally balanced at any particular sample point (Fig. 5.40c). However, a large increase in sub-angular clasts at sample point 12 (3km), most likely reflects the concentration of Moine quartzite clasts. Mean clast size fluctuates from 3 to 7cm, but with no consistent trend. Typically, the deposits are relatively fine-grained (Fig. 5.40d). Linear regression indicates no significant relationship between clast size and distance, with confidence values of no more than 30% (Fig. 5.40e). With the exception of the increasing content of Moine psammite clasts to the east, there are no systematic trends.

### 5.5.9 Rubha Carrach to Swordle Cave

This is the most extensive east-west traverse and the coastal location provides good exposure. There are few simple linear trends, although a number of more small-scale (local) variations may be significant. Throughout this traverse there is high clast heterogeneity. Certain lithologies are concentrated in specific areas and are absent elsewhere. It is only at Rubha Carrach (sample point W) that any Moine quartzite and porphyritic andesite are present, suggesting that these lithologies were only available locally. Several broad trends are observed across this traverse. Sandstone increases from only minor amounts between Rubha Carrach and sample point 10 (6km), to the dominant clast type (46%) at Swordle Cave. Shale and calcareous sandstone do not appear until east of sample point 9 (5.5km), where they locally comprise 30% and 40% of clasts. Some limestone is also present here (5%). Similar accumulations of Mesozoic sedimentary clasts were recorded in north-south traverses. Between sample points 6 (3km) and 7 (3.75km) scoriaceous basalt and microgranite are the dominant lithologies forming 41% and 31%

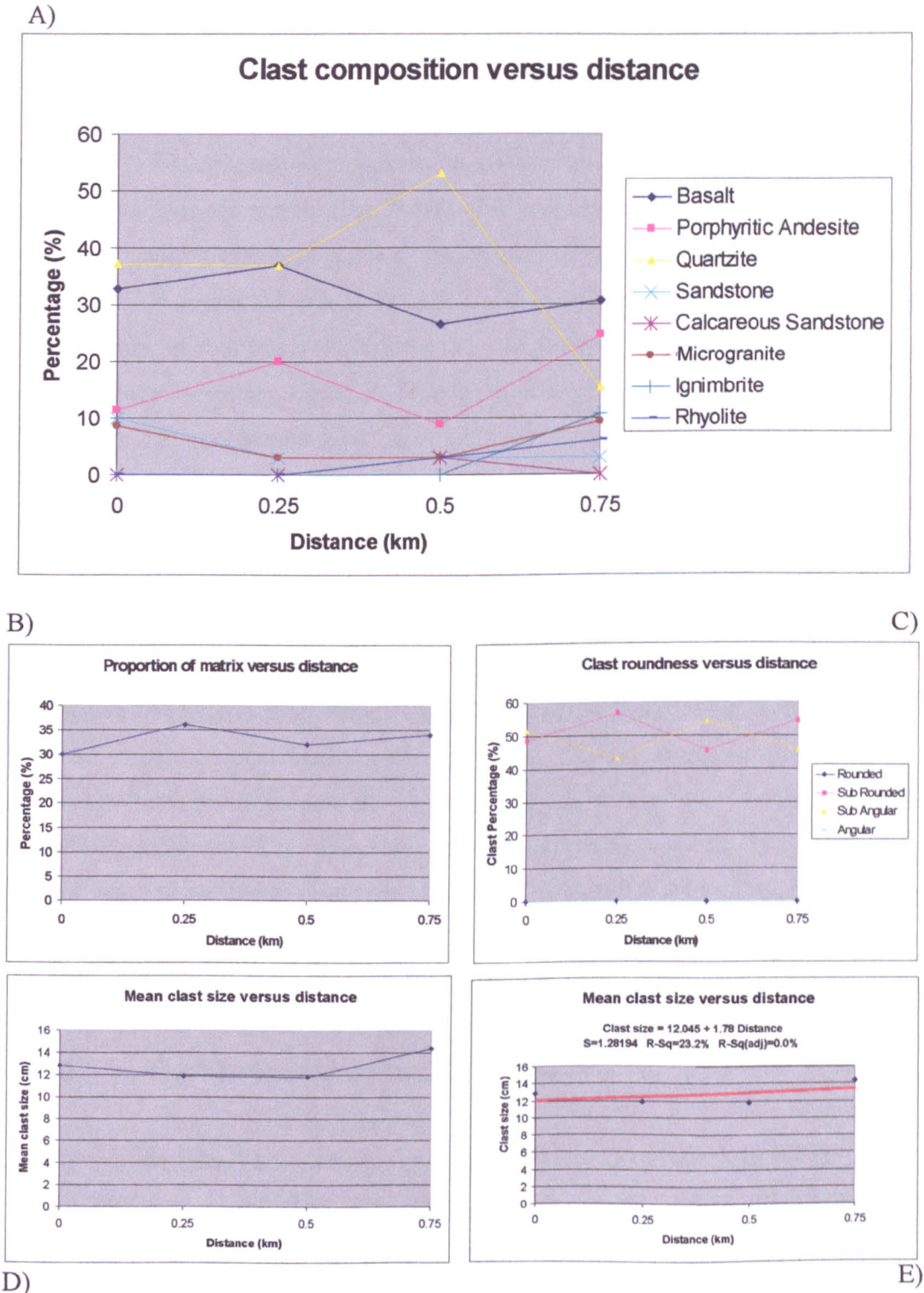


Figure 5.39 – Rubha Carrach Clast Count Analysis: a) Clast composition versus distance; b) Proportion of matrix versus distance; c) Clast roundness versus distance; d) Mean clast size versus distance; e) Best-fit regression line of mean clast size versus distance.

respectively of clasts. They form only minor proportions of clasts in deposits at Portban (points 8 and 9) and towards Swordle Cave. These concentrations suggest local source areas. Aphyric basalt forms 37% of clasts at Rubha Carrach, but decreases in the Fascadale area where microgranite and scoriaceous basalt are concentrated. Further east, the proportion of aphyric basalt clasts steadily decreases towards Swordle Cave. There are no general trends in clast heterogeneity along this traverse, but local concentrations of specific lithologies are present (Fig. 5.41a). The proportion of matrix increases from 35 to 45%, from Rubha Carrach to point 8, and to over 50% at Portban, before decreasing to 35% in the clast supported area of Swordle Cave, indicating more clast supported deposits at the margins of this traverse (Fig. 5.41b). At Rubha Carrach, the proportion of sub-rounded and sub-angular clasts is broadly similar, but in the Fascadale area where microgranite and scoriaceous basalt are dominant, there is a significant increase in clast roundness, with up to 100% clasts sub-rounded. At sample points 8 (4.75km), 9 (5.5km), 10 (6km) and 19 (6.25km) the proportion of sub-rounded material decreases sharply from nearly 100% to approximately 54%, with sub-angular clasts increasing to 30%. Rounded clasts are also present forming up to 17% of the conglomerate. Finally, sub-rounded clasts increase up to 82% in the Ardtoe Island and Swordle Cave areas (Fig. 5.41c). Mean clast size appears to increase from Rubha Carrach (12cm) to Swordle Cave (25cm), although there are numerous local variations (Fig. 5.41d). Linear regression indicates a poor relationship between these variables, with confidence values of only 37% (Fig. 5.41e). Mean clast size, however, is relatively high, especially in the Swordle Cave area, and these variations may be related to clast type. There are no significant trends along this traverse, but instead local areas are characterised by concentrations of certain lithologies, clast roundness and mean clast size.

### **5.5.10 Ben Hiant – Vertical Section**

The relief of the Ben Hiant cliff section enables a vertical section to be constructed from 110m to 240m above sea level. The section was close to MacLean's Nose and therefore there is high clast heterogeneity (Section 5.5.6.1). Many lithologies show only minor variations up section. There is a steady upwards increase in amygdaloidal basalt from 21 to 41% to 190m, before decreasing again to 33% at the top of the section. Aphyric basalt and sandstone show similar trends, increasing from 170-220m before decreasing at the top

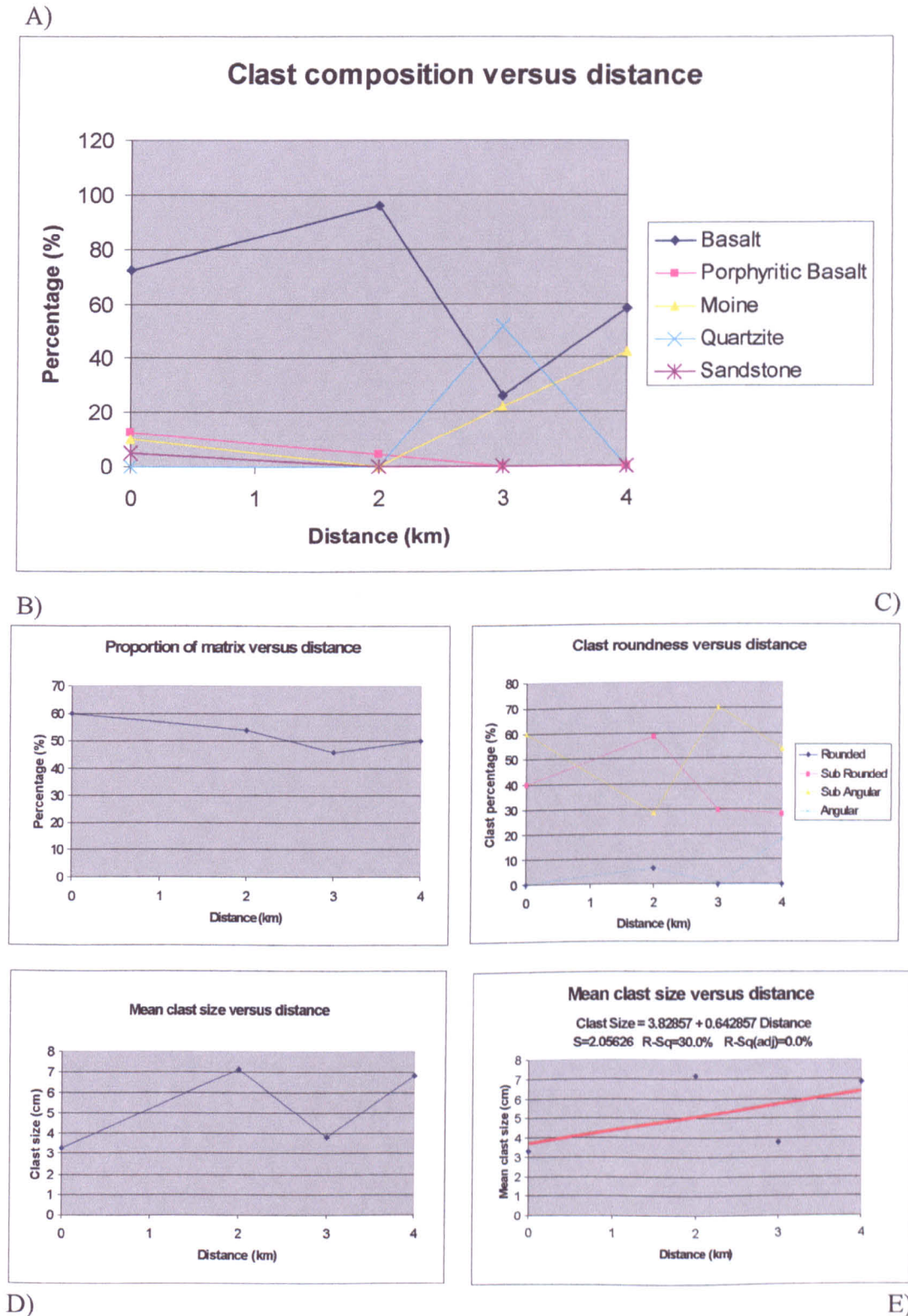
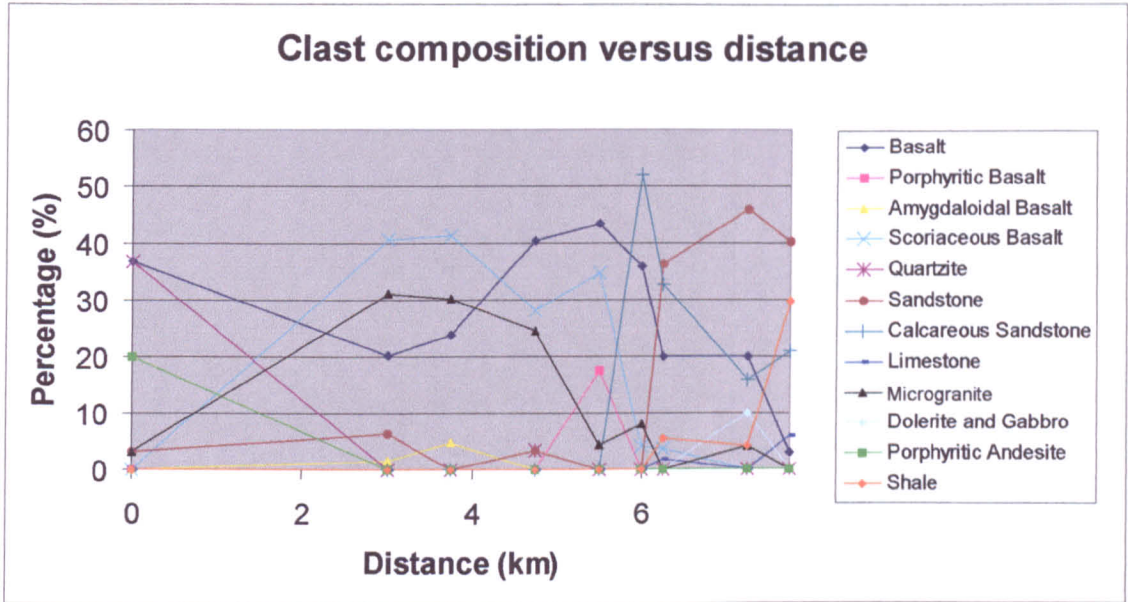
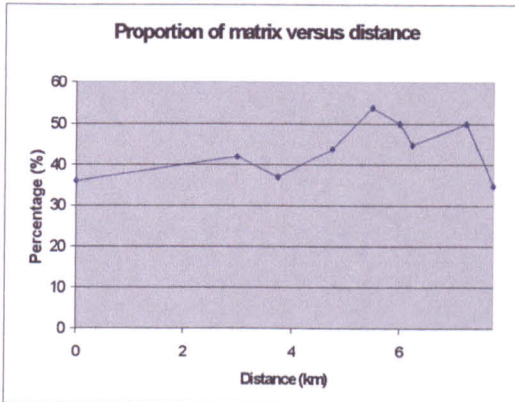


Figure 5.40 – Allt na Mi Chomhdhail to Tom na Gainmheich Clast Count Analysis: a) Clast composition versus distance; b) Proportion of matrix versus distance; c) Clast roundness versus distance. N.B. The rounded and angular clasts share the same data series with the exception of the sample point at 4km; d) Mean clast size versus distance; e) Best-fit regression line of mean clast size versus distance.

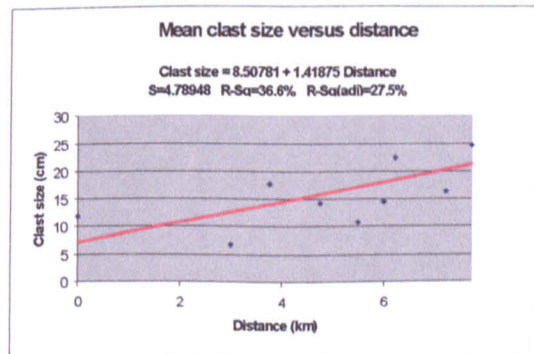
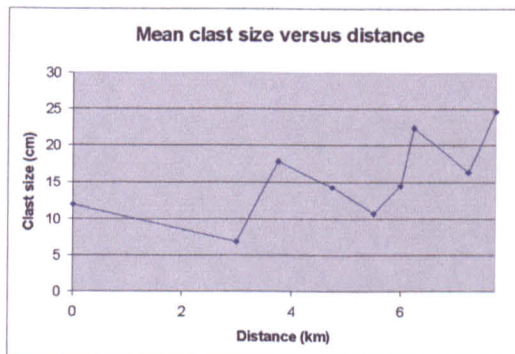
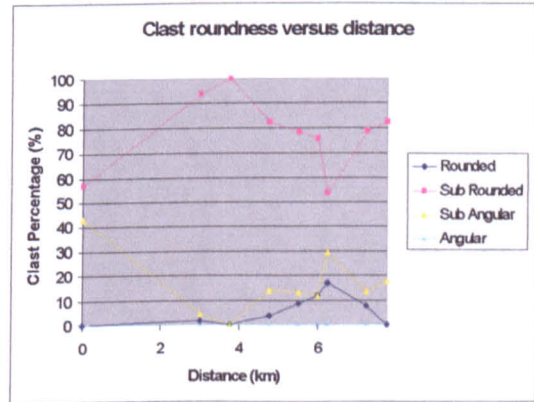
A)



B)



C)

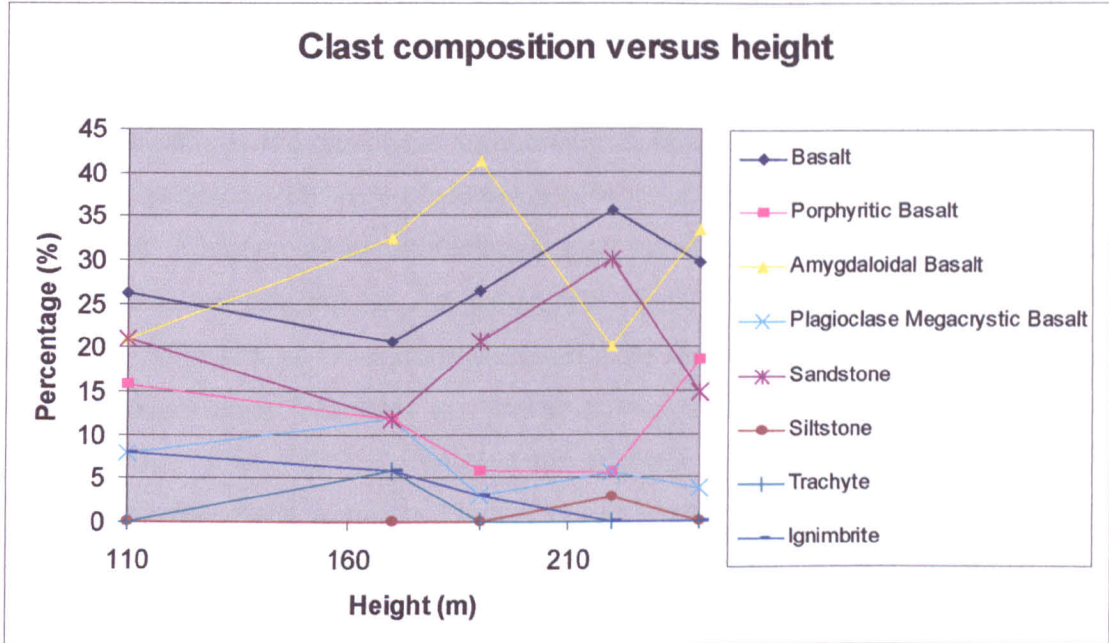


D)

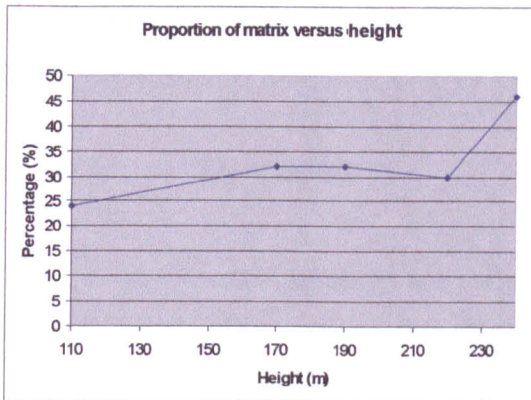
E)

**Figure 5.41 – Rubha Carrach to Swordle Cave Clast Count Analysis: a) Clast composition versus distance; b) Proportion of matrix versus distance; c) Clast roundness versus distance; d) Mean clast size versus distance; e) Best-fit regression line of mean clast size versus distance.**

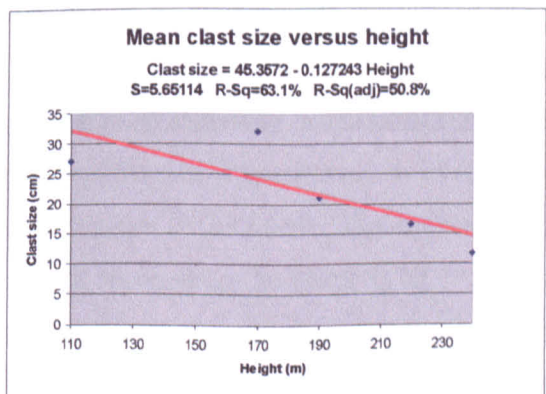
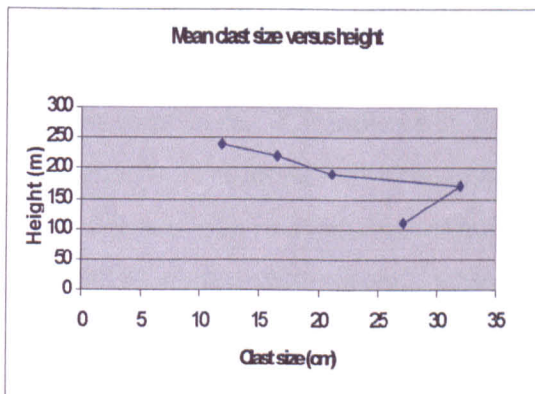
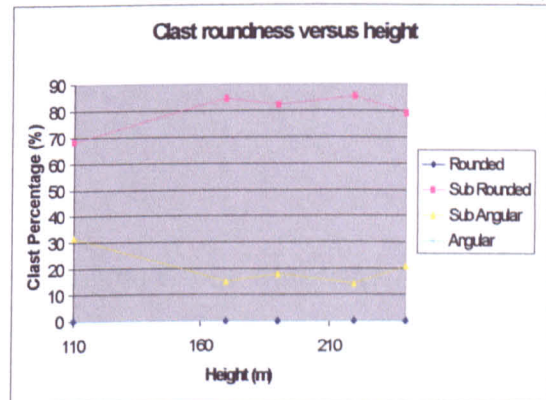
A)



B)



C)



D)

E)

**Figure 5.42 – Ben Hiant-Vertical Section Clast Count Analysis: a) Clast composition versus height; b) Proportion of matrix versus height; c) Clast roundness versus height; d) Mean clast size versus height; e) Best-fit regression line of mean clast size versus height.**

of the section. Ignimbrite decreases towards the top of the section and other lithologies are present only in minor amounts (Fig. 5.42a). There seem to be no significant trends relating clast composition to height in the section. By contrast, the proportion of matrix rises steadily from 24% at 110m (at the base of the section) to 30% at 220m, before a sharp increase to 46% at the top of the section (Fig. 5.42b). This correlates with the matrix supported Stallachan Dubha Conglomerate Formation (SDCF), as described in Section 5.3.9 above. There are no trends relating to clast roundness, with only minor variations in the proportions of sub-rounded and sub-angular clasts. Sub-angular clasts decrease from 32% at 110m to 15% at 170m from which point the series stabilises. There is an increase in sub-rounded clasts from 68% at 110m to 85% at 170m, from which point the series again stabilises (Fig. 5.42c). Mean clast size coarsens upwards, increasing from 27cm at 110m at the base of the section to 32cm at 170m. Above this there is a steady decrease to 12cm at the top of the unit (Fig. 5.42d), reflecting a general upward fining. Linear regression demonstrates a relatively strong relationship between these variables with confidence values of 63% (Fig. 5.42e). The vertical section reveals no trends in clast composition and roundness, but the unit becomes more matrix supported and finer grained towards the top.

### 5.5.11 Synthesis

These data indicate that there are compositional correlations within the Ardnamurchan conglomerates. The north-south and east-west traverses and the vertical section studied reveal trends in clast heterogeneity, degree of roundness, the level of matrix support and changes in mean clast size. The following results were obtained:

- Traverses in the NCF indicate an increase in clast heterogeneity to the north, showing a transition from domination by aphyric basalt and Moine psammite clasts in the south, to deposits rich in Mesozoic sedimentary rocks clasts to the north. The degree of clast support, clast roundness and mean clast size all increase to the north in NCF deposits. At their southern end, NCF deposits are typically homogeneous and matrix-supported, with relatively angular, small clasts (2-20cm across), whereas to the north they are heterogenous and clast supported, with large rounded clasts (2cm-3m across).

- A mirror image of these trends is seen in the traverse from MacLean's Nose to East Ben Hiant Gully in the BHCF. This indicates an increase in clast heterogeneity to the south, revealing a transition from typically aphyric basalt clasts to the north, to deposits rich in Mesozoic sedimentary rocks to the south. The degree of clast support, clast roundness and mean clast size all increase to the south. At their northern end, BHCF deposits are typically homogeneous and matrix-supported, with relatively angular, small clasts (2-20cm across), whereas at their southern end they are typically heterogeneous and clast supported, with large rounded clasts (2cm-3m across).
- The BHCF and NCF deposits display lobate geometries, sourced from an area around Beinn nan Losgann and Loch Mudle (Fig. 5.33), where they are at their minimum thicknesses. This may represent an area of relatively high relief forming a 'sedimentary watershed' from which the conglomerates were derived and spread out in both northerly and southerly directions, producing the compositional correlations described above. The NCF was transported in a northerly direction, displaying increasing clast heterogeneity, roundness, size and increasing clast support to the north, whereas the BHCF was transported to the south, but shows a similar increasing clast heterogeneity, roundness, size and support. This sediment parting forms the 'Beinn nan Losgann-Loch Mudle sedimentary watershed' outlined in Figure 5.54.
- The east-west traverses reveal no particular trends through the conglomerates. They record localised concentrations of blocks of microgranite and scoriaceous basalt, that may indicate localised sources for these rock types. The heterogeneity implies that they sample a series of discrete transport systems rather than longitudinal variation within a single system
- A vertical traverse at Ben Hiant reveals an increase in the percentage of matrix and a decrease in mean clast size in younger deposits. However, the limited vertical exposure means that this observation cannot be generally applied.

These traverses, with other observations, provide evidence for deposition by epiclastic mass flow processes, which are reviewed in Section 5.7, below.

## **5.6 Photo-statistical analysis of preferred clast orientation in the Ben Hiant Conglomerate Formation and Northern Conglomerate Formation**

### **5.6.1 Introduction**

Statistical methods of photo-analysis have been developed to quantify the strength of clast orientation, or directional clast fabric, in various types of volcanoclastic mass flow deposits (Karatson *et al.* 2002). This fabric strength ( $R$ ) is defined as ‘the resultant vector length of clast alignment computed from clast angles visible on a vertical outcrop face.’  $R$  can be obtained from image analysis and statistical assessment of photographs of outcrops, with regard to clast number and palaeoflow. This method is independent of subjective clast selection. It uses a minimum of one hundred and fifty measured clasts per sample to obtain reliable  $R$ -values and is applicable to any deposit that displays a preferred fabric. Karatson *et al.* (2002) studied examples including near-vent breccias, block-and-ash flow deposits and cohesive volcanoclastic debris flow deposits from selected exposures. Following this study, near-vent breccias show a relatively weak fabric ( $R=28\%$  on average), whereas volcanoclastic mass flow deposits display a stronger fabric ( $R=46\%$  on average) between 0.5 and 1km from source.

The method was applied to deposits of the Ben Hiant Conglomerate Formation (BHCF) and the Northern Conglomerate Formation (NCF), to determine the strength of their clast fabric, and whether the  $R$ -values suggested by Karatson *et al.* (2002) for mass flow deposits are applicable to the BHCF and the NCF. Further analysis in the form of rose diagrams was also produced for these deposits.

### **5.6.2 Associated problems of clast orientation data**

In both pyroclastic and debris flows the high concentration of clasts and significant shear stress between particles, typically results in a parallel-to-flow orientation of the longest axes ( $a$  axes) of clasts (Davies & Walker 1974; Smith 1986). In contrast, if clasts are supported by traction and rolled on the depositional surface, for example in pyroclastic surge or fluvial deposits, then long axes may be transverse to flow (Davies & Walker 1974; Smith 1986). Bimodal fabrics may develop where both flow mechanisms occur, for

example in hyperconcentrated flows (Smith 1986) or in front of debris flows (Major and Voight 1986). Evidence of preferentially oriented parallel-to-flow clasts in mass flow deposits is found in both non-volcanic (Bertran *et al.* 1997) and volcanoclastic deposits (Smith 1986; Major & Voight 1986; Cappaccioni & Sarrochi 1996.).

Many problems however are associated with the collection of clast orientation data in the field, irrespective of the type of deposit. Many data sets are collected by manual measurement, on either a selected portion of the deposit, or on specific clasts (typically the largest ones). As a result, this leads to bias in sampling and may not give a true reflection of clast orientation. Furthermore, field sample sizes rarely exceed 20-50 clasts. This can reveal whether clasts are oriented but cannot sufficiently quantify the strength of orientation (Karatson *et al.* 2002). To address this problem, Cappaccioni & Sarrochi (1996) collected decimetre-size cubes of ignimbrite and, using a computer-assisted image analysis, measured 1500-2000 particles in each sample. This approach, however, is only applicable to fine-grained deposits. The anisotropy of magnetic susceptibility (AMS), which detects the alignment of magnetic minerals in the matrix of volcanoclastic mass flow deposits that were emplaced hot, such as ignimbrites, has also been applied (Fisher *et al.* 1993). This approach, however, is not applicable to coarse-grained debris flow deposits that were emplaced cold. Finally, measuring clast sizes or axis ratios in the field is time consuming, and if the rocks are heavily cemented individual dimensions may be hard to obtain. Therefore, due to these difficulties Karatson *et al.* (2002) suggested the need for a quantitative method suitable for statistical comparison of clast fabric in coarse-grained deposits. The values obtained could then be used to determine the strength of clast orientation and to discriminate between types of deposit and hence their emplacement.

### **5.6.3 Methodology**

#### **5.6.3.1 Preparing and measuring an image for analysis**

The first step in preparation is to take a photograph of a vertical face of an exposure containing a number of clasts (Fig. 5.43). This face should ideally be a vertical view, parallel to the assumed palaeoflow. Where the exposure face differs from the assumed palaeoflow direction, a correction factor must be applied. This will be discussed in Section 5.6.3.2. The plane of the lens should be parallel to the plane of the outcrop to minimise distortion. The distance between the object and lens should be as consistent as

possible. Some volcanoclastic mass flows close to source may be deposited on moderately steep slopes that will influence the apparent dip of elongate clast axes (Major & Voight 1986). Where bed thickness far exceeds outcrop height it may be difficult to determine whether dip has resulted from imbrication or depositional slope. Therefore, Karatson *et al.* (2002) suggested that the term clast alignment should only be applied to side view clast orientation resulting from both imbricated and bed-parallel clasts.

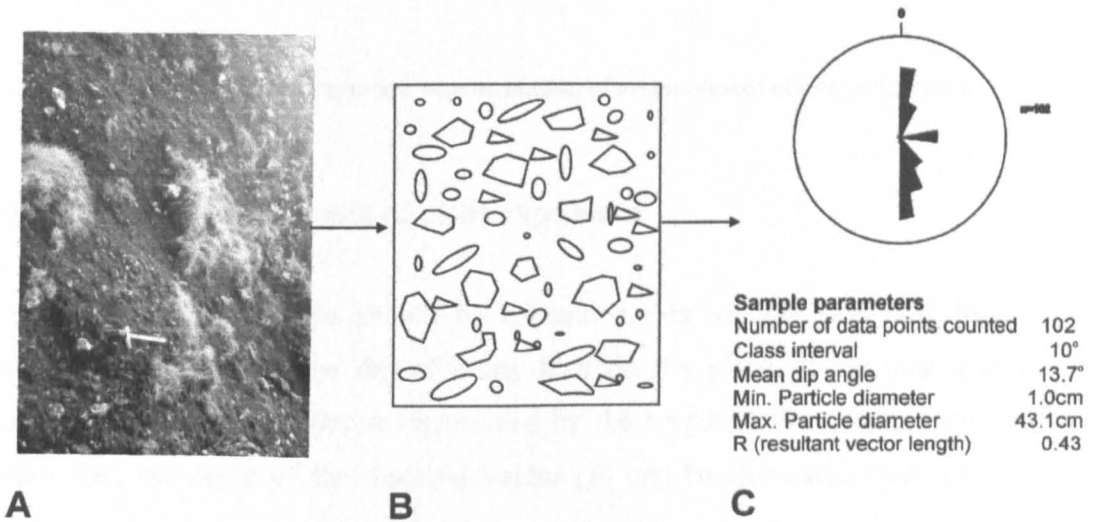


**Figure 5.43** – Calculation of clast alignment statistics of mass-flow deposits: a scaled photo of a vertical cut of an exposure (A) is followed by drawing the clast contours (B), and the result is treated by a computer-aided procedure (C) (after Karatson *et al.* 2002).

The photograph is scanned or transferred directly from the digital camera. The outlines of identified clasts are drawn (preferably manually to differentiate clasts from alteration and vegetation), and the digitised image improved (Fig. 5.43). Photo-statistical software can be applied to calibrate image dimensions and required variables. Karatson *et al.* (2002), use UTHSCSA Image Tool 2.00 and clast orientations can be measured using this programme, but they can also be determined manually if this software is not available. Clast orientation is measured as the angle of the longest axis of the clast relative to a horizontal plane (Fig. 5.44). This information is entered into a database for further statistical analysis and the production of Rose diagrams.

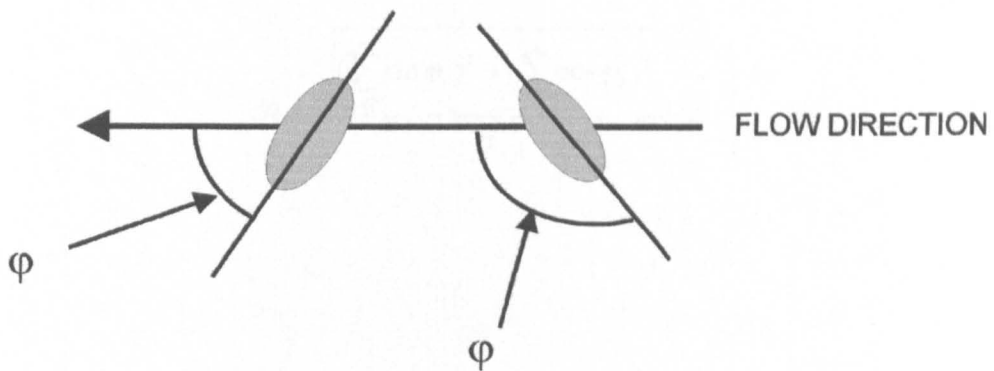


Figure 5.44– Diagrammatic representation of measurement of clast orientation

### 5.6.3.2 Statistical analysis of clast alignment

First the mean clast angle should be calculated. In vertical side-view images, this corresponds to the average dip of clasts seen on the plane of the photograph. The dominant direction of angles is represented by the length of the resultant vector (Davis 1986), i.e., the angle of the resultant vector ( $\beta$ ) can be calculated from the following formula:

$$\beta = \text{arc tan} \frac{\sum_{i=1}^n \sin \varphi_i}{\sum_{i=1}^n \cos \varphi_i}$$

(1)

where  $\varphi$  represents individual directional data. The resultant vector also provides information on the degree of clast alignment in a deposit. Where a sample is well aligned, fewer clasts will be perpendicular to the dip angle. Therefore the spread of vector directions will be smaller and the resultant vector length will be longer. As the resultant vector length ( $R$ ) is controlled by the number of clasts ( $n$ ), Davis (1986) suggested that  $R$  should be standardised:

$$R = \frac{\sqrt{\left(\sum_{i=1}^n \sin \varphi_i\right)^2 + \left(\sum_{i=1}^n \cos \varphi_i\right)^2}}{n}$$

(2)

$R$  will be between 0 and 1, meaning that a preferred clast fabric will produce an  $R$ -value closer to 1, whereas widely dispersed clasts will tend towards a value of 0. Values of  $R$  can then be expressed as a percentage and this can be referred to as the 'strength' of directional fabric. Following other publications (e.g. Bertran *et al.* 1997),  $R$ -values above 40% are considered high. Only non-spheroidal clasts can show a preferred fabric, and to identify such clasts an axis ratio (e.g. 3:2 or 5:2) can be applied (Allen 1984). This is restrictive however, due to the problems outlined in Section 5.6.2. To take into account all clasts, a modified resultant vector length ( $R_e$ ) can be calculated by weighting clast orientation with elongation value ( $e_i = \text{Length/Width}$ ):

$$R_e = \frac{\sqrt{\left(\sum_{i=1}^n e_i \sin \varphi_i\right)^2 + \left(\sum_{i=1}^n e_i \cos \varphi_i\right)^2}}{\sum_{i=1}^n e_i}$$

(3)

$R_e$  is typically greater than  $R$ .

A number of statistical tests (Rayleigh, Tukey  $\chi^2$ , Goodness-of-fit tests, Von Mises distribution) can be carried out to determine whether a circular distribution is uniform or not. For more detailed information on these tests consult Davis (1986) and Karatson *et al.* (2002).

Karatson *et al.* (2002) recommended measuring 150 clasts per sample, following the work of Bertran *et al.* (1997) who discovered that if only 30-50 clasts per sample were measured, values of  $R$  were too wide ranging. Finally, the problem of three-dimensional assessment of exposure face to palaeoflow direction must also be considered. Figure 5.45 represents a three-dimensional section of a volcanoclastic mass flow. Karatson *et al.* (2002) typically dealt with vertical side views, which are parallel to palaeoflow, allowing fabric strength characteristics to be analysed. Flow markers such as sole marks, cross-bedding and clast imbrication can also determine palaeoflow. If the exposure face differs from the palaeoflow, a numerical transformation can be performed to correct  $R$ . The approximate angle ( $\epsilon$ ) between the strike of exposure face and flow direction, can be applied in the formula:

$$\tan \varphi = \tan \varphi' \cos \epsilon$$

(4)

where  $\varphi$  is the real angle of the clast long axis with respect to the horizontal, and  $\varphi'$  is the apparent (measured) angle with respect to the horizontal. Therefore the original  $\varphi$  values can be computed and a corrected  $R$  can be determined. This correction is not applicable if the angle between the palaeoflow direction and the strike of the exposure face is greater than  $45^\circ$ .

## 5.6.4 Results of photo-statistical analysis

### 5.6.4.1 Ben Hiant Conglomerate Formation

At Ben Hiant a traverse was carried out from MacLean's Nose to East Ben Hiant Gully. At six selected points a photograph of a vertical side view of an exposure was taken, and a photo-statistical analysis undertaken. Figure 5.46 is a map of the sample points and Figure 5.47 shows the selected exposure faces. A correction factor was not needed on these analyses, as all the exposure faces are considered to be parallel to palaeoflow. In all cases, assumed palaeoflow is from right to left (NNE to SSW).

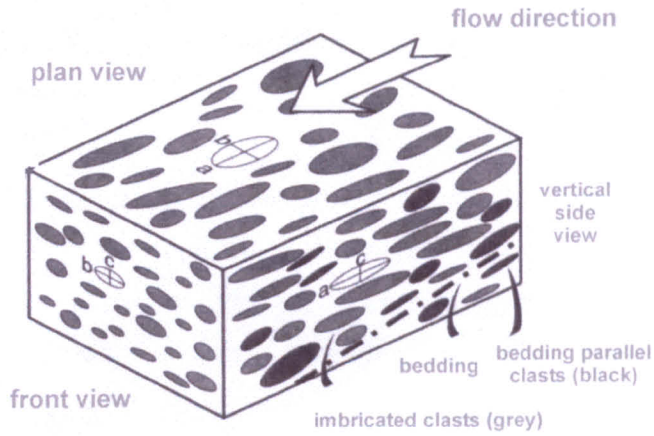


Figure 5.45 – Three-dimensional view of an idealised block of a mass flow unit (from Davies & Walker 1974)

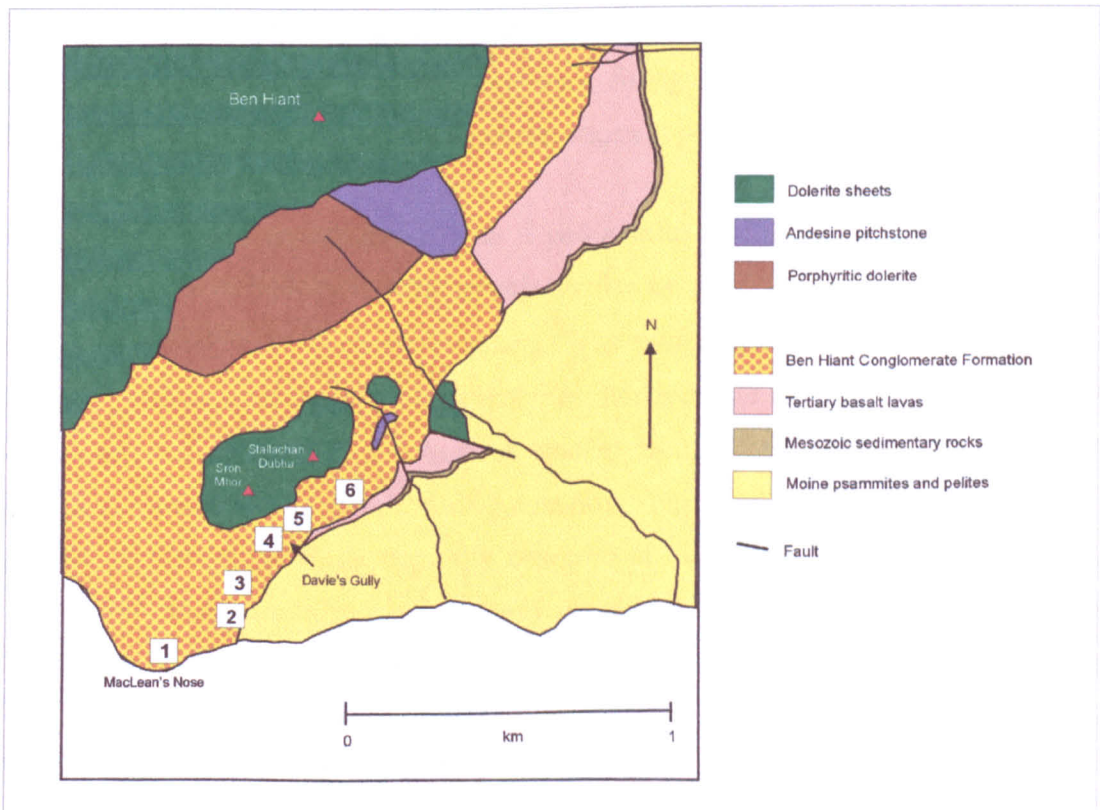
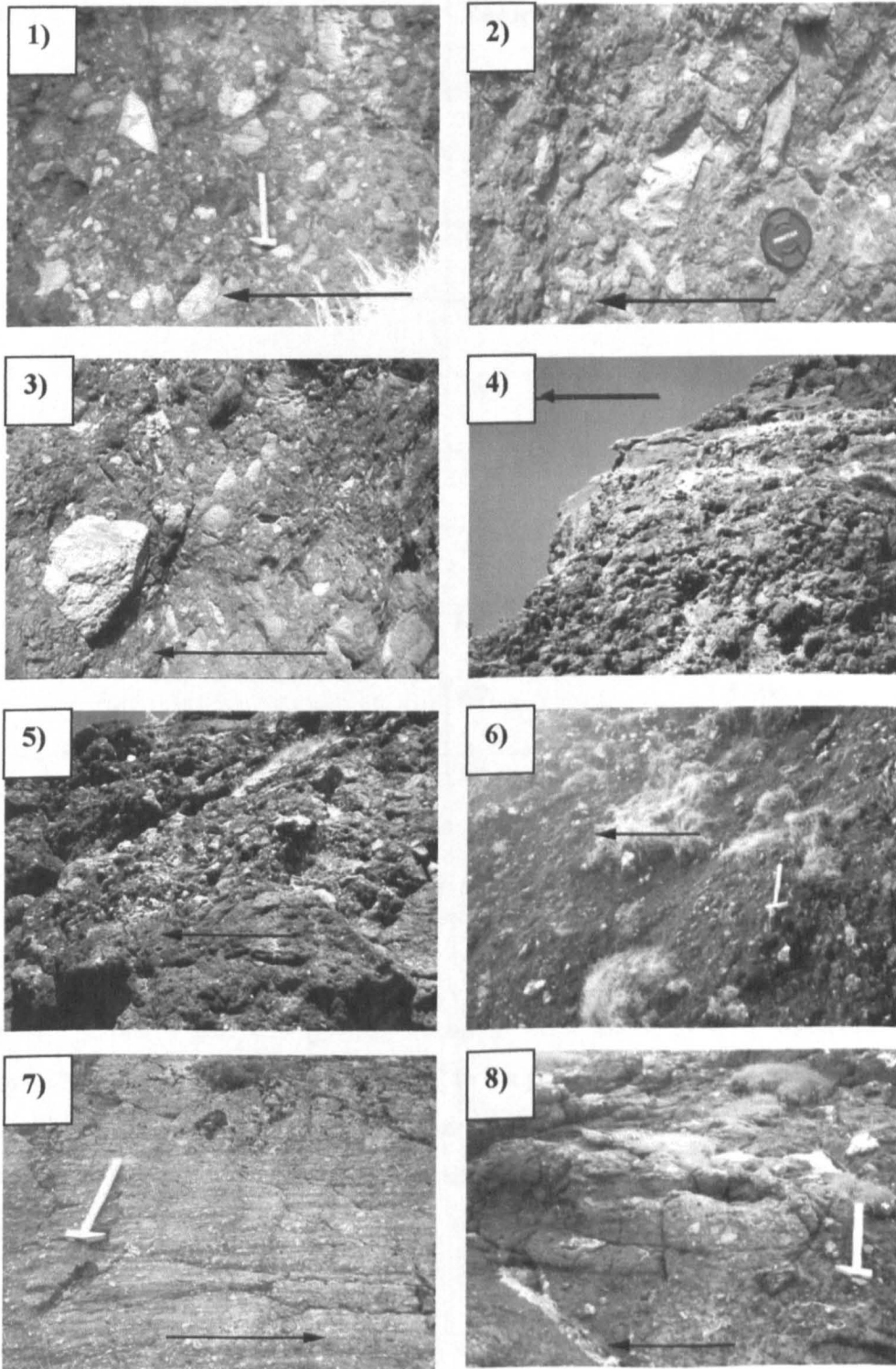


Figure 5.46 – Ben Hiant: Simplified geological map showing photo-statistical sample points in the Ben Hiant Conglomerate Formation (after Edinburgh Geological Society 1976).

Table 5.1 is a simplified database of the studied exposures containing information on site number, distance from source, number of analysed clasts ( $n$ ) and  $R$ -values. All deposits in this study give  $R$ -values greater than 40%, and so can be characterised as having a strong preferred fabric (Bertran *et al.* 1997). Karatson *et al.* (2002) recorded lag and vent breccias (emplaced near to source) as having  $R$ -values with an average of 28%, reflecting their disorganised unsorted nature, whereas coarse-grained pyroclastic flow deposits and debris flow deposits have  $R$ -values on average of 44.9 and 46.9% respectively.  $R$ -values from Ben Hiant range between 44% to 64%, and are on average 56.2%. These values strongly correspond to pyroclastic flow and debris flow deposits and, in conjunction with the evidence presented in Section 5.7 below, suggest a debris flow mode of emplacement for these deposits. The  $R$ -values appear to increase in a southerly direction, indicating a stronger preferred orientation, and correspond to the interpreted direction of palaeoflow. There are, however, inconsistent results at sample points 2 and 6. Point 2 has an  $R$ -value of 44.68% and although still considered high, it is lower than others. This may be because  $n < 150$  in this sample, and therefore less reliable. Points 1 to 5 are all recorded at the base of the BHCF and therefore are at the same stratigraphic level. Point 6 however is taken from a much higher stratigraphical level in a fine-grained matrix supported unit and, therefore, cannot be expected to follow observations at points 1 to 5.

Figure 5.48 includes rose diagrams with  $R$  and  $n$  values for points 1 to 6. In each case, clast orientation is indicated, with respect to the assumed palaeoflow direction. This direction is depicted as  $0^\circ$  on the diagrams. The sample points all produce similar rose diagrams, with an abundance of clasts with near horizontal orientation, parallel to bedding and the assumed palaeoflow direction. A smaller group of imbricated clasts can also be identified, stacked in the direction of palaeoflow (Fig. 5.48). Together these reflect a bimodal distribution of clasts, typically observed at the front of debris flows (Major & Voight 1986) and caused by the commonly developed imbrication and/or remobilisation and mixing of deposits (Huguet *et al.* 2001). This bimodal distribution is represented diagrammatically in Figure 5.49. Karatson *et al.* (2002) observed that the directional fabric strength improves from the bottom to the top of the deposit. This is attributed to the fact that clast imbrication tends to decrease towards the top of mass flow deposits (Major & Voight 1986) and is caused by the decrease of shear stress and inter-particle forces between clasts during deposition. Clasts deposited higher in a mass flow are therefore, typically more bedding-parallel (Fig. 5.49) (Branney & Kokelaar 1992).



**Figure 5.47 – Photographs of vertical side view exposure faces. Palaeoflow direction is depicted by an arrow. Sample sites (1-6 for the Ben Hiant Conglomerate Formation and 7-8 for the Northern Conglomerate Formation) are indicated.**

Site No.	Distance from 'source' (km)	Recorded value ( <i>n</i> )	<i>R</i> value
<b>Ben Hiant Conglomerate Formation (BHCF)</b>			
1	4	215	63.26
2	3.75	102	44.68
3	3.6	137	58.09
4	3.25	165	58.38
5	3.15	155	50.81
6	3	160	61.81
<b>Northern Conglomerate Formation (NCF)</b>			
7	2	67	47.06
8	5	66	59.12

**Table 5.1- Fabric data of Ben Hiant Conglomerate Formation and Northern Conglomerate Formation mass flow deposits**

In sample points 1 and 6 a greater spread of clast orientations is observed, with a concentration of clasts at approximately 90° to the palaeoflow, so that they appear to stand vertically (Fig. 5.48). The appearance of 'vertically stacked' clasts suggests that they were supported within a flow, which was deposited *en masse*, and were not rolling on the surface.

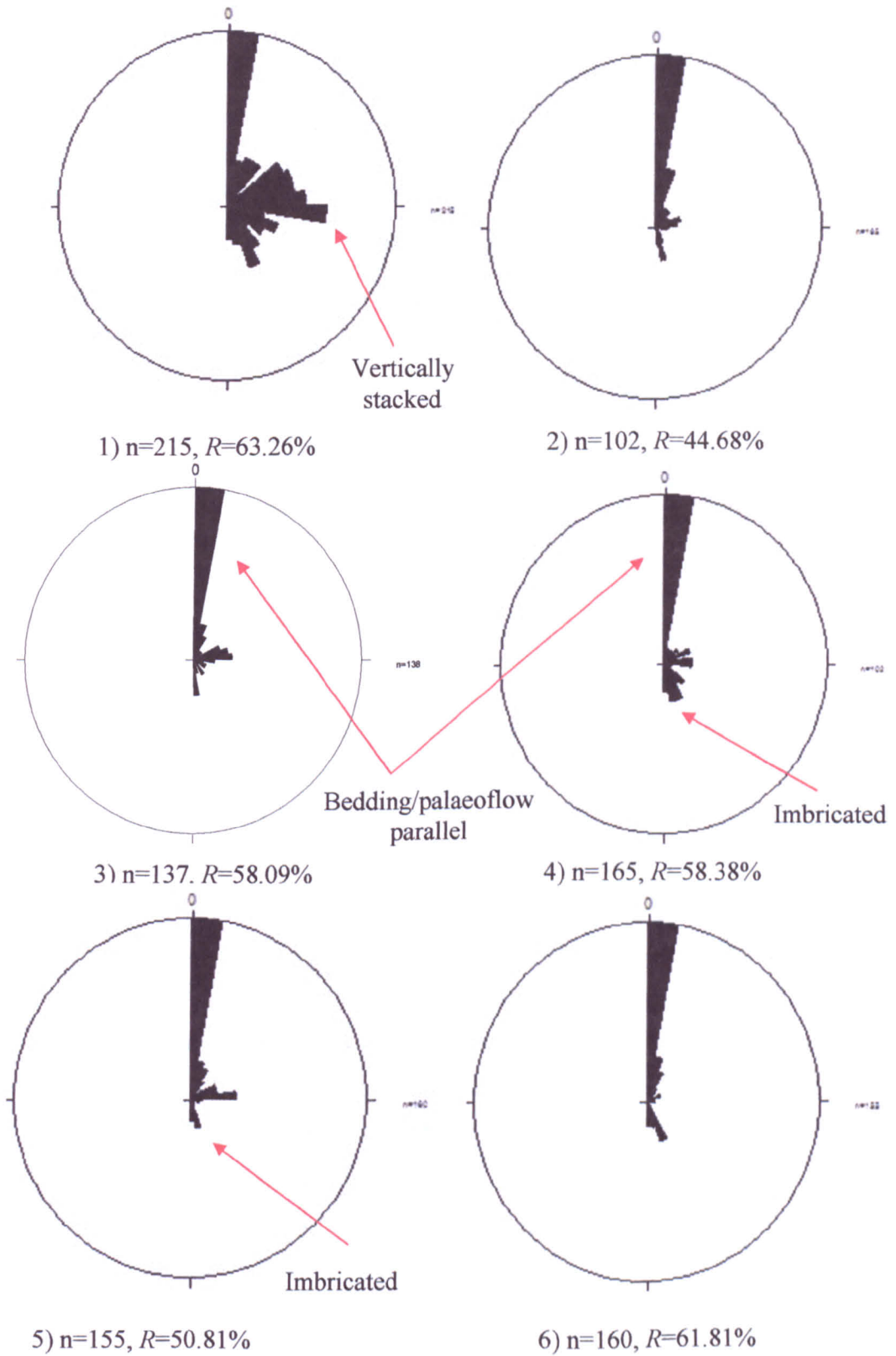


Figure 5.48 - Rose diagrams of Ben Hiant Conglomerate Formation exposures displaying clast alignment and directional fabric strength values ( $R$ ). Clast orientation is measured with respect to palaeoflow direction (i.e.  $0^\circ$ ). Examples of 'imbricated,' 'vertically stacked' and 'bedding/palaeoflow parallel' populations are labelled.

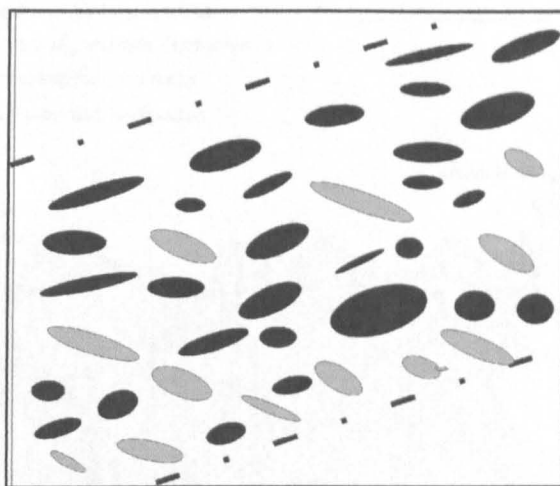


Figure 5.49 - Upwards decrease in angle of imbrication, common in volcaniclastic mass flow deposits. On lower part there are numerous imbricated clasts (grey) and bed-parallel clasts (black) towards the top (from Karatson *et al.* 2002)

#### 5.6.4.2 Northern Conglomerate Formation

The NCF is neither as vertically extensive nor as well exposed as the BHCF, and so suitable photographs, particularly of vertical side view exposures, were difficult to obtain. Photo-statistical analyses were successfully carried out at proximal and distal localities within the NCF (Fig. 5.50). The proximal locality (sample point 7) has an  $R$ -value of 47.06%, whereas the distal locality (sample point 8) has an  $R$ -value of 59.12%. These values are again typical of directional fabric strength for debris flows, although are based on  $n$  values of  $<150$ , and are not entirely reliable. Rose diagrams reveal bimodal distributions similar to those recorded in the Ben Hiatt analyses, suggesting similar modes of deposition (Fig. 5.51). The majority of exposures in the NCF provide front views of the flow and, therefore, show little variation in clast orientation (Figs. 5.45 and 5.52). This corresponds with information provided in Section 5.5, where no trends of sorting, roundness or grain size could be identified in east-west traverses (across the fronts of the flows) through the conglomerates.

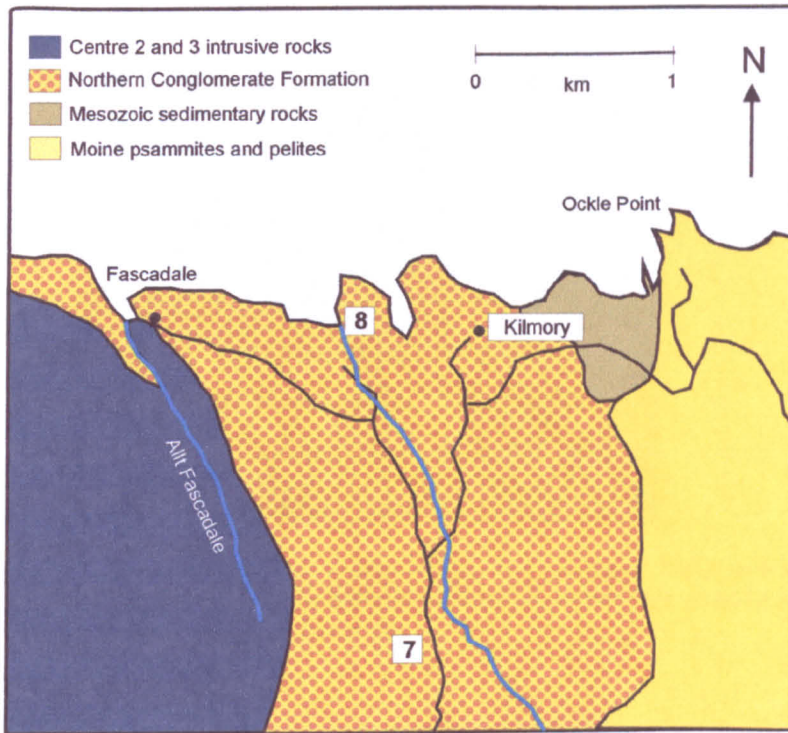


Figure 5.50 – Simplified geological map showing sample points in the Northern Conglomerate Formation (after Edinburgh Geological Society 1976).

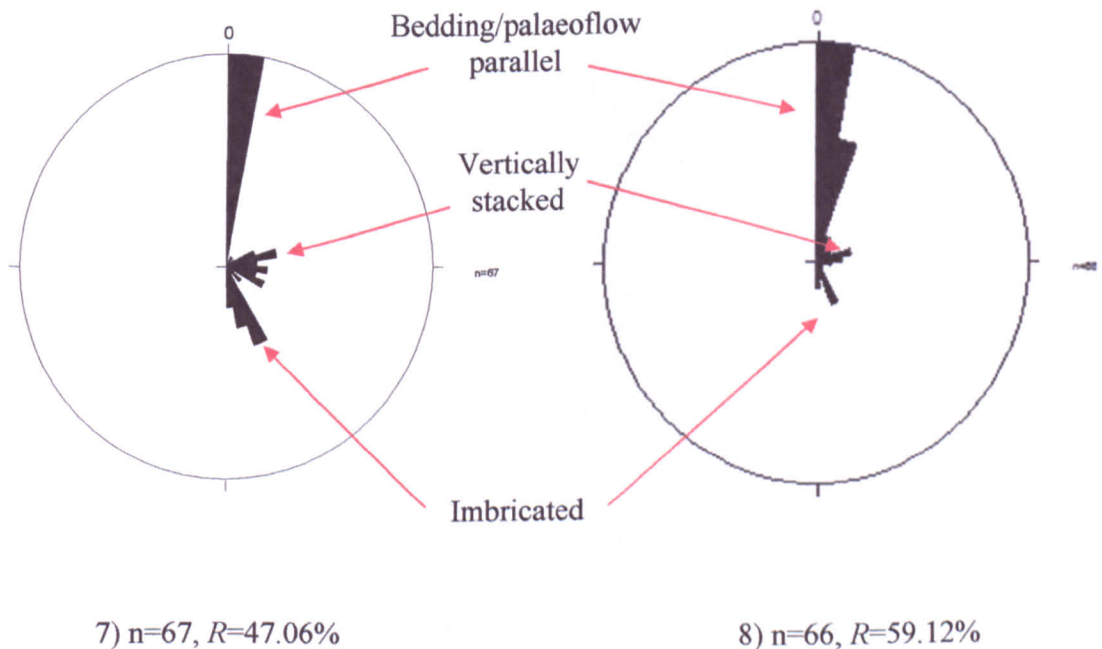


Figure 5.51 - Rose diagrams of Northern Conglomerate Formation exposures displaying clast alignment and directional fabric strength values ( $R$ ). Clast orientation is measured with respect to palaeoflow direction (i.e.  $0^\circ$ ). Examples of 'imbricated,' 'vertically stacked' and 'bedding/palaeoflow parallel' populations are labelled.



**Figure 5.52** – Typical front view of deposit within the Northern Conglomerate Formation (NM53147092). Orientation of clasts is difficult to measure, as they are typically aligned in flow direction. Cross sectional views are preferred.

### 5.6.5 Summary

The photo-statistical analysis outlined by Karatson *et al.* (2002) provides a method for quantifying the strength of directional clast fabric within mass flow deposits. Fabric strength ( $R$ ) can be computed by measuring clast orientations from photographs of vertical side view (parallel to palaeoflow) exposures of mass flow deposits. Strong directional fabrics are said to be over 40% and in debris flows are on average 46.9%. This method can be applied to deposits of the BHCF and the NCF and gives average  $R$ -values of 56.2% and 53.1%, respectively. Rose diagrams of these deposits reveal bimodal distributions of clast orientations, with dominant orientation of bedding/flow parallel clasts and a second mode of imbricated clasts. A decrease in imbrication is observed towards the top of units. These features are all typical of deposition within debris flows.

## 5.7 Modes of deposition

As described in Section 5.5, a number of compositional, size and morphological trends are identified within the BHCF and NCF. North-south traverses from Tom na Gainmheich to Swordle Cave, Allt an Doire Dharaich to Ardtoe Island and Camphouse to Portban all display increasing lithoclast heterogeneity, clast roundness, extent of clast support and mean clast size towards the north. In contrast, the traverse from East Ben Hiant Gully to

MacLean's Nose displays the same variation in characteristics, but towards the south. Between these traverses a sedimentary 'watershed' can therefore be inferred in the Beinn nan Losgann-Loch Mudle area, with material apparently being transported in opposite directions from this inferred 'source'. Within the various deposits, certain sedimentary features can be identified, including normal grading and channels. As outlined in Section 5.3, a number of fine-grained sedimentary units, displaying bedding features and cross laminae, are recognised within the stratified BHCF. Analysis of contacts indicates that the conglomerate lies unconformably on a variety of different country rocks, typically at low angles, with only local vertical contacts. Together, this evidence suggests a sedimentary (or epiclastic) mode of deposition for these rocks. East-west traverses from Allt na Mi Chomhdhail to Tom na Gainmheich, and Rubha Carrach to Swordle Cave, exhibit no lateral trends, but reveal localised assemblages of lithologies. These clast assemblages may have been sourced from nearby *in situ* deposits that are no longer preserved. The compositional, size and morphological trends may be linked with those of epiclastic mass flow processes, as outlined in Chapter 4, to suggest a mode of deposition for the Ardnamurchan conglomerates.

Richey & Thomas (1930) identified the Ardnamurchan conglomerates as 'vent agglomerates.' Evidence for this origin included the predominantly volcanic nature of the material 'filling' the vent and a suggested vertical, vent wall contact, apparently visible at Richey's Gully (Fig. 5.53). The stratified deposits of the 'Ben Hiant Vent' were interpreted as a series of rhythmic eruptions from a Ben Hiant volcano, with intervening air-fall ash deposits (Richey 1938). Richey's model (1938) suggested that Moine and Mesozoic materials were relatively rare and were blown out of the vent, followed by collapse of the overlying basaltic plateau into the 'crater.' The composition of the clasts within these deposits is variable, and, as indicated in Section 5.5, strongly reflects/correlates with the bedrock geology. Contacts between the BHCF, the NCF and the land surface beneath are typically at low angles, and basalt lava, Mesozoic shale and Moine psammities and pelites, are all overlain unconformably by conglomerate. Contacts between the conglomerates and the land surface beneath are rarely vertical and those identified are small-scale, localised features, that most likely represent original topography. The apparent contact at the top of the main waterfall below Richey's Gully (Fig. 5.5) is heavily weathered and complicated by multiple minor intrusions. Thus, the identification of a 'vent wall' is doubtful.



**Figure 5.53– Inferred vertical vent wall contact at Richey’s Gully (NM54086221) (Richey & Thomas 1930, Richey 1938). The near vertical feature is a basaltic dyke.**

The fine-grained deposits are not of air-fall ‘ash’, but are of lacustrine origin due to the presence of cross-bedded muddy laminae, sand-grade layers and palynological evidence (Sections 5.3.4, 5.3.5, 5.3.6, 5.3.8 and 5.10).

Megablocks of aphyric basalt and calcareous sandstone up to 30m across are present in the NCF. Although the basalt blocks appear shattered, the calcareous sandstone blocks are intact, and it is unlikely that blocks of such considerable size and mass were deposited by an explosive, air-fall mechanism. They are more likely to indicate sliding in a mass flow deposit. These features, together with other sedimentary structures, such as normal grading and cross-cutting channels, indicate that the term vent agglomerate is inappropriate for these deposits.

There is no direct evidence of an eruptive, primary pyroclastic mode of deposition in the BHCF and NCF deposits. No gas streaming or volcanic bombs are identified, and although ignimbrite and scoriaceous basalt are present (typical primary pyroclastic material), it is only as lithoclasts within the breccia and not as *in situ* deposits. Application of the term ‘agglomerate’ is incorrect, as this is now clearly defined as referring to ‘a coarse, pyroclastic deposit composed of a large proportion of rounded, fluidally shaped volcanic bombs greater than 64mm in size’ (Cas & Wright 1987). It is essential that evidence of true volcanic bombs displaying, for example, spindle, breadcrust or cow-pat textures, or bomb sags is present. Agglomerates are fall deposits, indicating proximity to a vent, and the term is best applied to scoria deposits that form Strombolian cones. The absence of these features requires that the term ‘agglomerate’ should not be applied to the

Ardnamurchan deposits, as it is confusing and implies a direct link with a volcanic vent, which may not be the case.

As the compositional trends described in Section 5.5 revealed, clast heterogeneity, roundness, mean size and degree of support increase in opposing directions from a broadly defined 'source' area. This source, in the Beinn nan Losgann and Loch Mudle area, represents a possible watershed from which debris was eroded and deposited to form the BHCF and NCF deposits (Fig. 5.54). Evidence for mode of deposition from this watershed by debris flow/avalanche processes has been identified and will be reviewed below.

Debris flows and avalanches share the characteristics that are reviewed in Chapter 4. Both sets of deposits contain coarse, relatively unsorted clasts set in a fine-grained matrix, but may also include larger blocks. Coarser material dominates the head of the flow in both types of deposit, due to dispersive shear pressures acting on the debris and forcing it to the front. Both debris flows and avalanches are transported and deposited as semi-rigid plugs or masses. Debris flows are typically smaller scale deposits, commonly less than 5m thick and can form a series of cross-cutting channels or lobes. Normal and reverse grading are common and clast imbrication is often preserved. The maximum clast size is typically 10m and intense fracturing is rare. Clasts may be rounded, angular or mixtures and they are often matrix-supported, although this is variable. Debris flows may be initiated by breaching of crater lakes, by heavy rain acting on loose debris or from direct eruptive activity.

Debris avalanches display sheet-like geometries and can extend as much as 15km laterally. They are typically non-graded, although some reverse grading may occur due to comminution at their base. Blocks are commonly sub-angular to angular and deposits are clast-supported. Intensely fractured blocks up to 100m in size are found, whilst the surface of debris avalanche deposits is typically hummocky. Sector collapse or direct eruptive activity initiates debris avalanches, and the role of water is negligible.

Debris flows and avalanches can be very difficult to differentiate and flow transformations may blur the distinction between them. Transformations are caused by the addition of fluid (dilution) or sediment (bulking). Debris flows are commonly found downslope of, or adjacent to debris avalanches where these become diluted as more water is incorporated (Palmer *et al.* 1991; Smith & Lowe 1991).

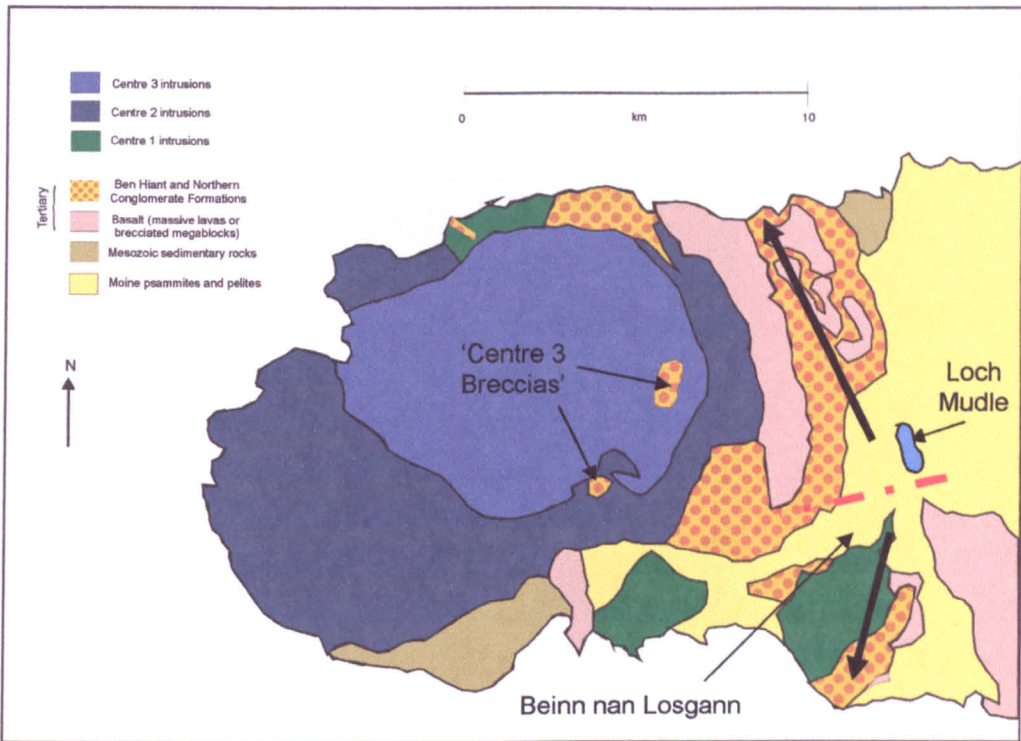


**Figure 5.54 – Sedimentary watershed in the area around Beinn nan Losgann-Loch Mudle, Ardnamurchan. Northern Conglomerate Formation deposits spread out to the north, whilst Ben Hiant Conglomerate Formation deposits flowed to the south. Location of ‘Centre 3 Breccias’ is indicated (see Section 5.9).**

To the north of the Beinn nan Losgann-Loch Mudle watershed, the conglomerates are composed primarily of angular and sub-angular aphyric basalt and Moine psammite and pelite lithoclasts. In this area, megablocks of basalt up to 30m in length are recognised, forming a hummocky present-day topography. The megablocks are heavily fractured, and both overlie and are locally overlain by the conglomerate. These relationships suggest that they may have been transported within a semi-rigid mass of debris, where large blocks are delimited due to faulting and begin to slide, with shear pressures fragmenting the moving mass. This mass then transforms to a semi-rigid flow with brecciated and fractured upper and middle zones (Reubi & Hernandez 2000).

Debris avalanches typically have a basal friction layer, composed of homogeneous, cataclastic, comminuted material formed by grinding and abrasion of the ‘overriding’ megablocks and clasts (Schneider & Fisher 1998). No such cataclastic layer is identified in the NCF. A pebbly sandstone occurs locally beneath the megablocks, but this is composed of sub-rounded pebbles and coarse sand, not angular, cataclastically derived

material. The 'jigsaw fit' or crackle textures commonly recognised within debris avalanche deposits, (Fig. 5.55) (Smith & Lowe 1991) have not been identified in the Ardnamurchan deposits.



**Figure 5.55 – Highly brecciated megaclast or crackle breccia from Mount England, New Zealand (from Smith & Lowe 1991).**

Debris avalanche deposits are also typically highly clast supported, but proximal to the watershed 'source,' at Braehouse and Tom na Gainmheich, the conglomerates are matrix-supported (matrix forming approximately 50% of the rock). The conglomerates show significant clast heterogeneity with large rounded blocks of locally derived country rock material. A degree of mixing may occur within debris avalanches when the basal layer develops a turbulent behaviour and picks up clasts from the source edifice (Reubi & Hernandez 2000). This characteristic is uncommon, however, and certainly not developed to the degree observed in the Ardnamurchan conglomerates. Finally, towards the north coast, normally graded units and cross-cutting channels are observed, which are not recognised in debris avalanches.

In summary, the NCF deposits share some characteristics with debris avalanche deposits, such as shattered megablocks and hummocky topography. The presence, however, of numerous rounded locally-derived clasts, the absence of jigsaw textures or a basal cataclastic layer, and their common matrix-support, suggests that the NCF represents debris flows rather than debris avalanche deposits. The shattered megablocks may, however, indicate the influence of catastrophic slides at some stage in their formation.

There is no evidence of debris avalanche deposits south of the watershed, at Ben Hiant. Megablocks are typically 1-2m, and no more than 5m in size, and are not always shattered. Neither jigsaw textures nor basal cataclastic layers are present and rounded locally derived clasts are abundant. The BHCF section preserves a stratified sequence, in which various members or 'flow units' are identified. These vary from 5m to 25m in thickness. The coarse units display normal grading, but between these are various siltstones and sandstones, where bedding and other minor sedimentary structures are recognised. This sequence indicates a series of cyclic, high and low energy flows with changing environments and styles of deposition that are not recognised in debris avalanche deposits.

Debris flow deposits are typically more matrix-supported than debris avalanche deposits and are usually formed from loose surface material, following initiation by heavy rain, lake collapse, eruptive activity or rock collapses. They are typically water-rich, transported *en masse* and can be diluted to produce stream-flow style deposits, or bulked up with loose debris to become coarser-grained and more clast-supported. Transitions from coarse breccia or conglomerate deposits to finer grained fluvial deposits and vice versa have been described in debris flows as a result of flow transformations by dilution or bulking (Smith & Lowe 1991). Where hillslope material is saturated *in situ* and affected by heavy rainfall and/or overland flow, it can fail and 'bulk up' with loose sediment downslope, explaining the abundance of rounded and compositionally heterogeneous lithoclasts downslope. Such trends are common in Ardnamurchan, for example in the north-south traverse from Tom na Gainmheich to Swordle Cave. Close to the watershed, only aphyric basalt, abundant *in situ*, and Moine clasts, on which the conglomerate is locally unconformable, are present. Where conglomerate overlies Moine rocks, it is dominated by Moine psammite and pelite clasts, suggesting these were entrained from the surface beneath. This trend continues to the north, where increasingly rounded and compositionally heterogeneous clasts are present. Where the contacts are with Mesozoic shale, clasts from this form the dominant lithology within the conglomerate. Clasts of limestone and sandstone only appear in the conglomerate on the northern coastline, within a few hundred metres of exposures of these lithologies. Sandstone, calcareous sandstone and limestone typically form sub-rounded clasts, indicating previous weathering and transport. They would therefore have been available as surface deposits to be incorporated within the conglomerate. Shale clasts remain sub-angular, reflecting their structure.

Debris flows may display clast imbrication in places and this is identified in the MacLean's Nose Conglomerate Member (Fig. 5.10; Section 5.3.2) and from photo-statistical clast analysis, reviewed in Section 5.6 above (Figs. 5.48; 5.51). Debris flows are typically restricted to channels and also tend to break into localised finger-like overlapping lobes (Yarnold 1993). Small-scale channels and depositional surfaces, present in the NCF (Fig. 5.25) may have formed by such methods. Blair & McPherson (1998) described the stacking of debris flows to produce a vertical profile of debris flow deposits with intervening fine-grained sediments at Owens Valley, California. The deposits are commonly discontinuous, eroding and filling small gullies and channels. The debris flows occur infrequently and fine-grained fluvial sedimentation occurs in the hiatuses between flows. In these periods, water washing of debris flow deposits and recycling may take place. Features reflecting these processes are identified in the BHCF, as outlined in Section 5.3, where channelised units such as the Ben Hiant Upper Siltstone Member (BHUSM), and bedded siltstone and sandstone units are recognised. Blair & McPherson (1998) also recognised lobes of poorly sorted, clast to matrix supported, pebbly gravel beds and lobes in Owens Valley and similar features are present in the MacLean's Nose Conglomerate Member of Ben Hiant.

Flow transformations are responsible for a variety of fine-grained beds within debris flow settings. Hyperconcentrated flows are defined as intermediate between dilute, normal streamflow and viscous non-turbulent debris flows (Smith & Lowe 1991). They typically form sand and granule size deposits and exhibit crude horizontal stratification, commonly better developed in their upper finer-grained margins. Cross-bedding and ripples are rare, but outsize blocks are common. These features cannot be applied to all fine-grained deposits of the BHCF. The Ben Hiant Upper Siltstone Member and the Ben Hiant Lower Siltstone Member, are of silt to fine sand-grade, and both contain cross-bedding and muddy laminae. Possible examples of hyperconcentrated flow deposits may be recognised in the MacLean's Nose Conglomerate Member (Fig. 5.10) and in the layered fine-grained deposits at Rubha a' Gharaidh Leith (Fig. 5.28; Section 5.4.3). These deposits are of coarse sand to gravel grade, with a well-defined stratification and similar to deposits described by Smith & Lowe (1991) (Fig. 5.56).

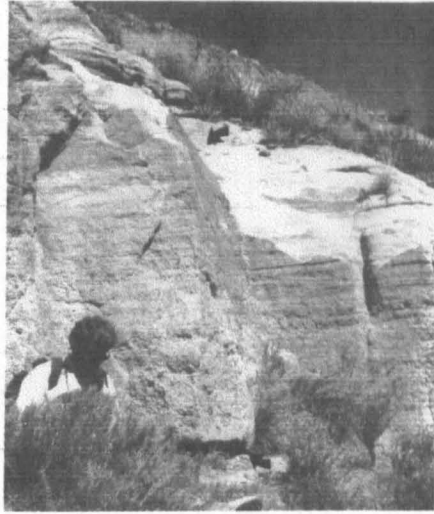


**Figure 5.56 – Graded-stratified hyperconcentrated flow deposits from the Ellensburg Formation, Washington, USA (from Smith & Lowe 1991).**

This evidence suggests that the BHCF and NCF deposits were formed primarily by debris flow mechanisms. Typical debris flow features are identified in the two units and pyroclastic and other origins can be eliminated. However, some distinctive features can be recognised. In the NCF, shattered megablocks preserve a hummocky topography. This suggests the influence of sliding or debris avalanches to the north. A series of massive basalt blocks were involved in an avalanche by gravitational collapse or mass wasting, and began to slide downslope. Towards the northern coast the deposits increasingly resemble debris flow deposits. Kessler & Bedard (2000) suggest how this could occur. Shattered blocks move downslope with little to no matrix. Sliding and granular flow produce a ‘proto-debris’ flow with isolated, angular and sub-rounded boulders and cobbles set in a matrix of small cobbles and granules, by a combination of clast grinding and dilution by water. Further grinding and sieving continues, producing typical unsorted, coarse deposits with a sand grade matrix (Fig. 5.57). A similar process may explain the textural and compositional trends in the NCF, where clast type strongly correlates with rocks of the pre depositional land surface. Channels (or lobes) and bedding planes are typically found at the heads of debris flows (Yarnold 1993). At Rubha na Acairseid, three such flow units are identified, Microgranite-dominated, Sandstone-dominated and Laminated Siltstone-dominated. Stratified pebbly sandstones at Rubha a’ Gharaidh Leith, may reflect localised flow transformations from debris flow to hyperconcentrated flow deposits, due to dilution by water.

The BHCF incorporates numerous fine-grained inter-flow sedimentary units, indicating deposition over a substantial period. This suggests that the material separated at the 'source' may have undergone slightly different modes of transport. The NCF was formed by one major event with possible flow transformations, whereas the BHCF comprises a series of multiple flow units interrupted by periods of quiescence and fluvial sedimentation. At the base of the formation, the normally graded MacLean's Nose Conglomerate Member, is composed of pebbly sandstone or gravel-grade material with occasional imbrication of outsize clasts. These are features of hyperconcentrated flows (Smith 1986) and in this sequence may represent the initial stage of debris flows draining south from the 'source' in the Loch Mudle area. The following four conglomerates are of debris flow origin: (the Sron Mhor Lower, Middle and Upper Conglomerate Members and the Stallachan Dubha Conglomerate Member), and are separated by fine-grained units (the Ben Hiant Lower and Upper Siltstone Members and the Stallachan Dubha Sandstone Member) representing the hiatuses between debris flows. These fluvial units include channels, which cut into the surfaces of the debris flow deposits. The sandy layers and cross-bedded muddy laminae within the Ben Hiant Upper Siltstone Member indicate inputs of different sediment and demonstrate weak current activity. *Nyssa* pollen grains (see Section 5.10) suggest nearby lacustrine conditions. Clasts at the top of the Ben Hiant Upper Siltstone Member and load structures indicate that the unit was not lithified before deposition of the next debris flow. Discontinuous lobes or sheets, in the Stallachan Dubha Sandstone Member, may represent localised gully erosion and deposition.

In summary, the BHCF was deposited by south draining debris flows. The short-lived events responsible were interspersed with periods of relative quiescence, when fluvial sediments were deposited in a series of channels. Increasing clast heterogeneity, roundness and size to the south, indicate progressive bulking by loose surface debris. Similar processes are identified at Rubha Carrach.

As outlined in Section 5.5, clasts include local concentrations of ignimbrite, scoriaceous basalt and microgranite. Ignimbrite are of pyroclastic origin, and scoriaceous basalt may be formed by explosive spatter, but these materials have not been recognised *in situ* on the peninsula. Their presence indicates earlier (pre-conglomerate) pyroclastic activity and their sub-rounded morphology suggests that they formed loose debris on the contemporary land surface. The conglomerates moved only short distances and thus the ignimbrite and scoriaceous basalt must have been sourced locally.

## STAGES IN DEBRIS FLOW DEVELOPMENT

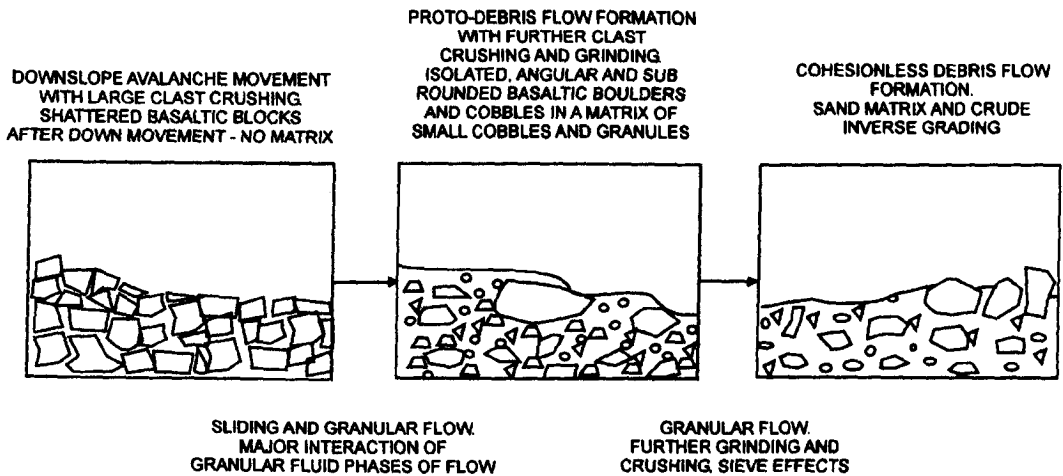


Figure 5.57 – Transition from debris avalanche to proto-debris flow to debris flow (from Kessler & Bedard 2000)

The clasts of microgranite may reflect the unroofing of earlier silicic intrusions. The Ardnamurchan area was tectonically active throughout the volcanic and intrusive activity. Although Centre 1 cone sheets cut the conglomerates the related uplift may have been earlier. Doming due to upwelling magma (silicic diapirs) and the formation of localised vents is widely recognised in central complexes (Walker, G. P. L. 1975), and the microgranite, ignimbrite and scoriaceous basalt may be remnants of such processes. Opposing directions on the north and south coasts of the peninsula imply doming. This may explain the initiation of the debris flows and avalanches of the BHCF and NCF, with local volcano-tectonic activity expressed in faulting and/or collapse events in the basaltic plateau from which these deposits originated. Heavy rainfall associated with volcanic activity may have aided debris flow formation (Caine 1980; Innes 1983).

## 5.8 Loch Mudle

Near Loch Mudle, at NM55106481, a 50m wide and 10m deep channel is present at the top of a lava flow (Fig. 5.58a). The channel fill is a matrix-supported breccia, comprising angular to rounded clasts, 2 to 15cm across set in a dark brown, silt grade matrix. Pale brown equant to oblate clasts of highly weathered aphyric basalt display irregular curved margins that vary from crenulate, through rounded to curvilinear. 'Jigsaw fit' textures are common, in which adjacent clasts have parallel margins, apparently separated by fractures filled by sediment (Fig. 5.58b). Elongate and bulbous projections, from clast surfaces appear to have worked their way into the host sediment, in places isolating rafts of sediment. The clasts display 'fluidal' shapes and appear to double back on themselves, with the sediment filling the voids between the clasts. The matrix is a dark basaltic silt. The unit is light grey towards its base and appears bleached. A 1m thick lenticular body of bedded, fine-grained, light grey siltstone is identified towards the base of the unit (Fig. 5.58c). At the base of the unit a number of discontinuous lenticular bodies of black shale are recognised. Forming layers of approximately 10cm thickness and up to 2m in length, these are highly disrupted and in places show complex interaction with the igneous clasts, as outlined above (Fig. 5.58d).

These relationships reflect the interaction of hot igneous material with sediment. The fractured, rounded and crenulate clast margins indicate that the sediment into which the igneous material was emplaced was water-saturated, causing it to quench and fracture, producing jigsaw fit textures. The hot lava worked its way through the sediment, forming irregular shapes, but at the same time heating and fluidising/mobilising the sediment. The mobilised sediment filled fractures and voids between clasts (Kokelaar 1982). These rocks are 'peperites', defined as 'formed essentially *in situ* by disintegration of magma intruding and mingling with unconsolidated or poorly consolidated, typically wet sediments' (White *et al.* 2000). More examples of peperites are reviewed in Chapter 6. This example suggests that lava was emplaced into a small lake or pond containing silt and mud. This provides further evidence of lacustrine environments on the Ardnamurchan peninsula at this time.

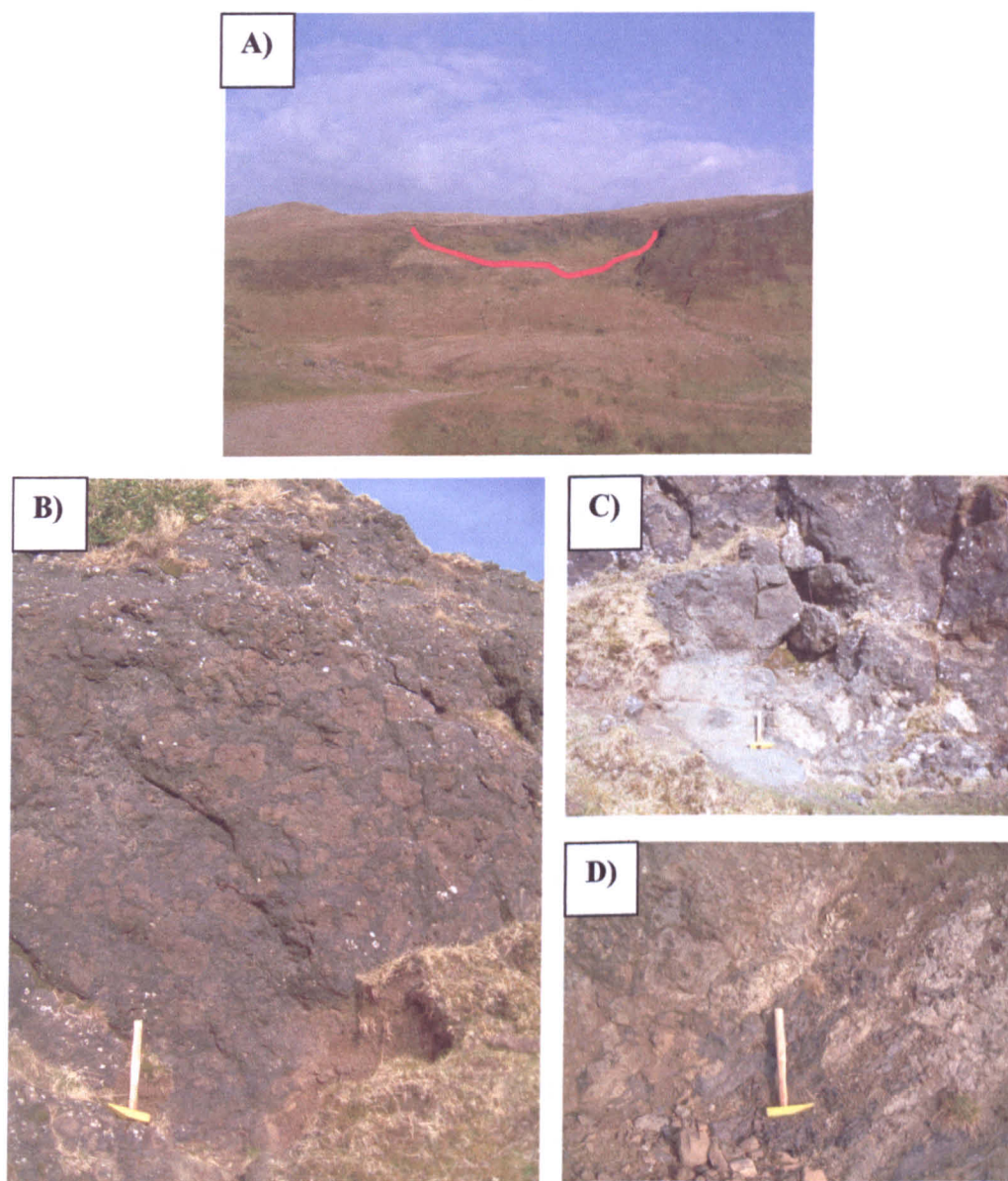


**Figure 5.58 – Peperite lithologies from the Loch Mudle area, Ardnamurchan (NM55106481). a) Loch Mudle lava field displaying a 50m wide channel structure between lava flows. View looking east from the road b) Pale brown basalt clasts with irregular, curvilinear margins, set within a dark brown silty matrix. c) Bleached base of the unit, displaying lenticular bodies of light grey siltstone. d) Discontinuous lenticular bodies of black shale showing complex interaction with igneous clasts.**

## 5.9 Centre 3 'Breccias'

Evidence has been provided for deposition of the Ben Hiant Conglomerate Formation and Northern Conglomerate Formation by debris flows. However, the Geological Survey map of Ardnamurchan, indicates that breccias interpreted as vent agglomerates (Richey & Thomas (1930) are preserved near Meall nan Con and Meall an Tarmaichan in the middle of the Centre 3 intrusive complex (Fig. 5.54).

However, if the debris flow model developed here is applied throughout the peninsula, their presence within Centre 3 is anomalous. Centre 3 was intruded after the Ben Hiant and Northern conglomerates were deposited, and therefore breccias within it could not have been contemporaneous. They are approximately 400-450m above sea level and are considerably higher topographically than the BHCF and NCF deposits. BHCF and NCF deposits are thought to have formed prior to Centre 1, indicating that the Centre 3 breccias were not formed as part of the early conglomerate-forming event(s), and that a vent agglomerate or later debris flow origin may be possible.

Analysis of the Centre 3 breccias, however, reveals that neither hypothesis is correct. This material is not a breccia or a conglomerate. The exposures represent intrusions of light brown to light grey porphyritic dolerite with net veining of granitic material. Where the veining is intense the rock takes on a brecciated appearance. The dolerite consists of 1-2mm grains of plagioclase and pyroxene with minor olivine, together with plagioclase phenocrysts no more than 5mm in size, with rare chlorite alteration. The veins range from 2mm to 10cm across, and are composed predominantly of plagioclase crystals 1-2mm across. Two distinct vein morphologies are present: simple planar veins 2-3cm wide (Fig. 5.59a), and cross-cutting networks. Dense networks form a texture in which angular 'clasts' of dolerite are separated in a granitic 'matrix' (Fig. 5.59b). Wider patches of granitic vein material, up to 10cm across, surround small areas of dolerite again giving a false brecciated texture (Fig. 5.59c). These textures suggest the rock formed by the intrusion of the dolerite as part of the Centre 3 intrusive complex and, after cooling, was broken by net-veining in which a later silicic magma was emplaced. These rocks are not breccias and are unrelated to the BHCF and NCF deposits.



**Figure 5.59 – Net veining textures in the ‘Centre 3 breccias.’ (NM50396807) a) Linear veins within porphyritic dolerite of Meall nan Con b) Cross-cutting network structure of veins intruding porphyritic dolerite c) Thicker patches of silicic veins producing ‘false’ brecciated texture.**

## 5.10 Palaeotopography and environments

Clast-matrix relationships and the distributions of specific lithologies indicate that the Ardnamurchan conglomerates were deposited by debris flows draining to both north and south and divided by a watershed. This lay between Beinn nan Losgann and the Loch Mudle area and represents a high point in a topography seemingly paralleled by the current land surface. This 'high' is close to the Loch Mudle lava pile and the thin lava pile at Ben Hiant, locally overlain by the conglomerates. These lavas, related to the Mull lava field (Bailey *et al.* 1924), were originally thicker and more extensive (Walker, G. P. L. 1971). Proximal conglomerate deposits are dominated by angular to sub-angular clasts of aphyric basalt with less common surface-derived materials including Moine rocks. The lava pile was therefore the most likely original source for the debris flows that later entrained other materials.

The NCF currently fills the Achateny valley as far as the northern coastline, covering an area of approximately 10km<sup>2</sup>, dipping gently at 5-10° to the north. Once initiated, debris avalanches can run out over large areas without steep slopes (Glicken 1986). The unconformable contacts of the NCF with Moine and Mesozoic rocks indicate transport over these areas. The conglomerate is confined within the present day Achateny valley where it rests on Moine rocks approximately 110m above sea level. To the east an irregular landscape of Moine hills rises to 350m, suggesting that the present valley broadly exhumes the early Tertiary (Palaeogene) palaeotopography of this area. Unfortunately, west of the valley relationships are obscured by Centre 2 and 3 intrusions.

At Ben Hiant, conglomerates up to 5m thick are preserved close to source. The most northerly exposure, in the East Ben Hiant Gully area, crops out at 250m and over a distance of 2.5km descends in a series of oversteps to the sea. This is a significant slope, with a gradient of approximately 1 in 10. Debris including scree easily gathers on such slopes and would thus be available for incorporation into debris flows. Rivers would drain areas of such relief, and water will collect in hollows in valley floors to form small lakes. These conditions would therefore be suitable for the formation of the fluvial and lacustrine deposits identified in the BHCF. Lacustrine deposits of the BHCF are localised and found only in distal parts of flows, away from the Beinn nan Losgann-Loch Mudle watershed. This suggests that debris flows were initiated in areas of high relief and steep slopes, before spreading out into gently sloping valley floors in lowland areas.

The Tertiary climate was relatively warm and wet. The hilly landscape was characterised by impounded lakes; fossil trees and plant remains within inter-lava sedimentary units provide evidence of lush vegetation (Bailey *et al.* 1924; Lyle 2000; Bell & Williamson 2002). In the area represented by the Ardnamurchan Peninsula volcanism interrupted periods of sedimentation. At Ben Hiant this is recognised with a series of lowland lacustrine deposits and upland Pine and Taxodiaceae trees, as outlined in Sections 5.3.4, 5.3.5, 5.3.6 and 5.3.7. The presence of peperites at Loch Mudle (Section 5.8) provides further evidence for impounded lakes in the early Tertiary lava field. A 50m wide channel is identified, indicating that lava was emplaced into a small lake or pond containing silt and mud.

## 5.11 Synthesis

Analysis of the BHCF and NCF outcrops indicates that they were not formed by explosive, pyroclastic processes but by epiclastic modes of deposition. No fluidally shaped, breadcrust or spindle bombs can be identified and no primary pyroclastic material is present. The ‘vent agglomerates’ or ‘breccias’ are typically conglomerates with clasts ranging from rounded to (less commonly) sub-angular, and from 2cm up to 3m in size. Together, the BHCF and NCF deposits form a stratified sequence containing numerous channels and bedding planes. Sandy layers, muddy laminae and cross-bedding are present within fine-grained fluvio-lacustrine units. Analysis of these features, clast - matrix relationships and the distribution of particular lithologies, provides evidence for debris flow/avalanche deposition with increasing clast size, heterogeneity and clast roundness away from ‘source.’ The developing heterogeneity of the deposits strongly correlates with the bedrock geology of the original land surface beneath. The Beinn nan Losgann-Loch Mudle area formed a sedimentary watershed.

To the north of the watershed, shattered megablocks of basalt are present in the NCF, indicating large-scale collapse and the initiation of debris avalanche processes. As flows were diluted with water, the megablocks broke down and flows entrained loose basaltic and Moine lithoclasts. Downslope, large rounded to sub-rounded lithoclasts, typically of Mesozoic sedimentary rocks were also incorporated into the debris flows. The head of the flow consists of overlapping, lobes and channels. Similar debris flows are identified in the Ben Hiant area. Interbedded fluvio-lacustrine units of siltstone and sandstone represent periods of quiescence between flows. The high concentration of angular basaltic clasts

indicates that these processes were most likely initiated, and the material sourced from the lava field around Loch Mudle.

Localised accumulations of ignimbrite, scoriaceous basalt and microgranite clasts suggest minor pyroclastic activity and possibly silicic doming and unroofing had occurred before deposition of the debris flows. The instability and uplift that these represent may reflect the early stages of the intrusion of Centre 1, and have been responsible for the initiation of debris flows and avalanches. Outcrops suggest that the present Achateny valley broadly exhumes the Palaeogene topography of this area. This was a volcanically active area with heavy rainfall, crossed by rivers and sheltering small lakes. These features are summarised in Figure 5.60, and in Chapter 8, Figure 8.1. The 'breccias' identified within Centre 3 are net-veined dolerite intrusions and bear no relationship to the debris flow conglomerates of the BHCF and NCF.

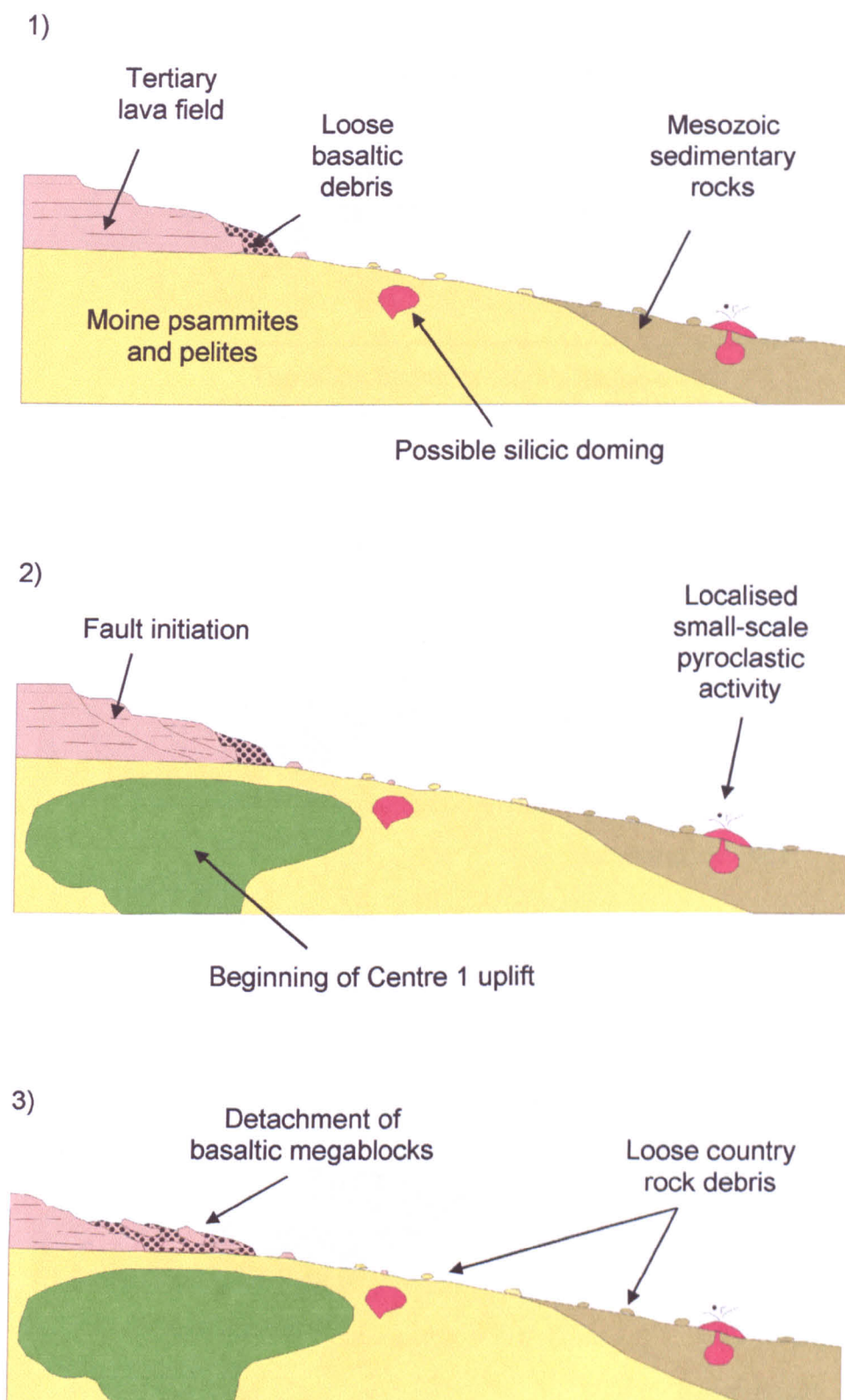


**Figure 5.60 – Schematic reconstruction of modes of formation of Ben Hiant Conglomerate Formation and Northern Conglomerate Formation deposits in Ardnamurchan (continued over).**

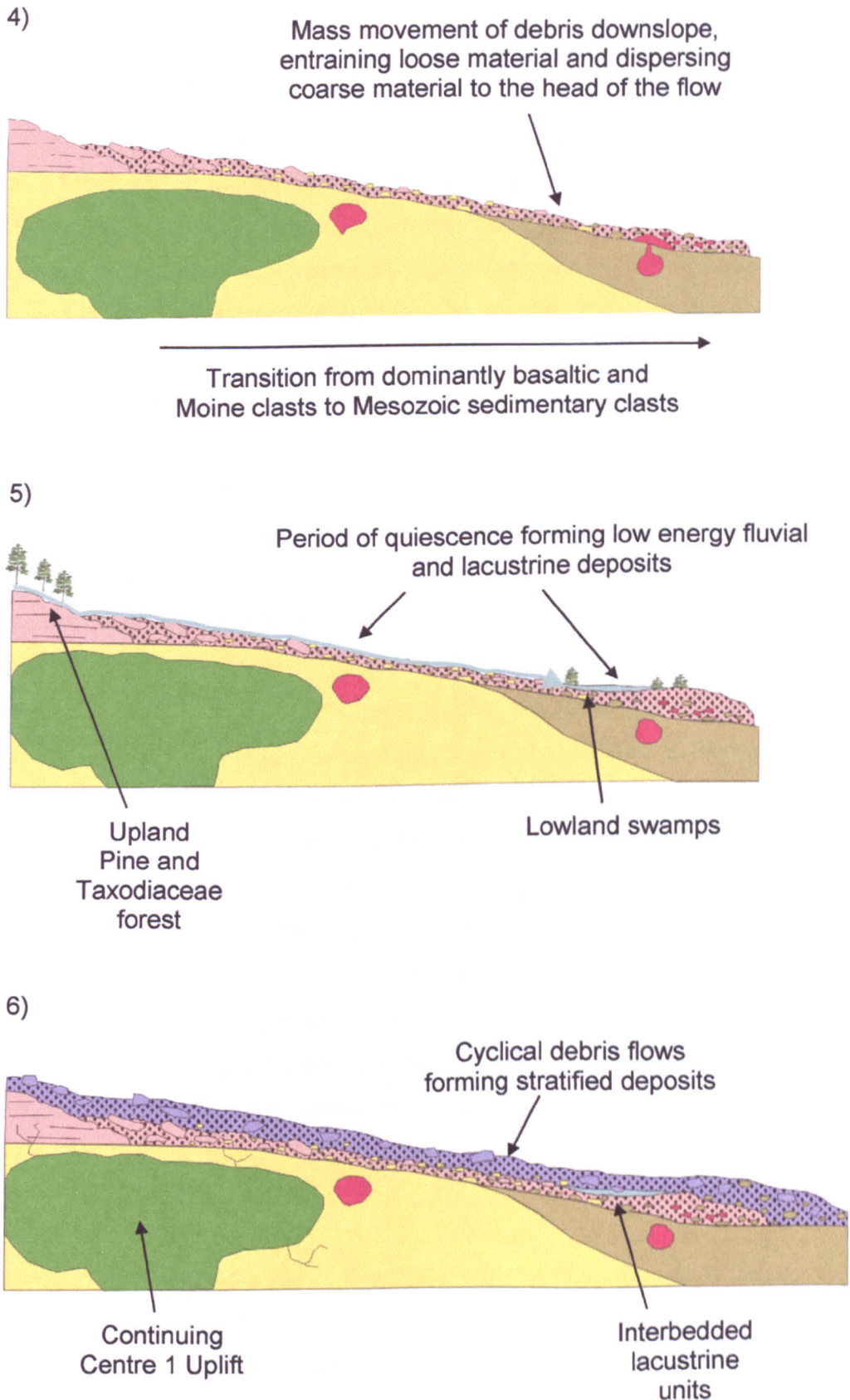


Figure 5.60 cont. – Schematic reconstruction of modes of formation of Ben Hiant Conglomerate Formation and Northern Conglomerate Formation deposits in Ardnamurchan.

## 6 Mull

### 6.1 Carraig Mhor

At Carraig Mhor, east of Carsaig Bay on the south coast of Brolass, Isle of Mull, breccias 20m thick show a complex interaction between pale igneous clasts with a variety of morphologies, and a dark, finely laminated, sedimentary matrix. The igneous clasts were originally of glassy basic material, now thoroughly altered. Some clasts are angular and display quench textures, suggesting rapid fragmentation by autoclastic processes, involving the explosive expansion of water vapour released from the associated sediments. Fluidised sediment filled fractures and was deformed around the igneous clasts. Other clasts comprise bulbous and finger-like projections, indicating the injection of melt into surrounding sediment. The upper 10m of the breccia displays grading in vertical section, with large flame-like clasts, aligned at the base of the unit, in equal proportion to the sediment. These grade upwards, with a progressive reduction in sediment content to form an angular 'network' breccia at the top of the unit, indicating turbulent flow between basaltic magma and argillaceous sediment, and a transition from ductile to brittle deformation. Gravitational settling mechanisms may also contribute to the grading. The lava is interpreted as having 'bulldozed' its way through the sediment and was cooled rapidly, forming glassy clasts, whilst the water-saturated sediment was flash heated, producing steam. The explosive expansion of the steam resulted in the formation of fractures, which were then filled by fluidised, deformed sediment. Evidence suggests that the breccia formed as a result of a lava flowing into a shallow lagoon floored by water-saturated silts and muds. An ignimbrite towards the base of the Carraig Mhor sequence, beneath the breccias, indicates silicic pyroclastic activity very early in the lava field construction (the base of the sequence cannot be recognised here).

#### 6.1.1 Introduction

This section is concerned with highly distinctive breccias that crop out at Carraig Mhor within the Mull lava pile on the south coast of Brolass, Ross of Mull, SW Mull (Fig. 6.1). The breccias comprise clasts of an altered pale brown to green-brown igneous material, in a dark brown matrix of silt to mud grade sedimentary material. Clasts vary from highly angular, through to rounded and crenulate forms, suggesting a spectrum of processes during breccia formation. The clasts range in size from <1mm, up to several tens of

centimetres across, and are of virtually all aspect ratios, from near spherical, through to highly tabular. Four principal clast types can be identified: (i) elongate finger-like structures; (ii) large fluid in appearance/flame-like clasts; (iii) sub-rounded clasts; and (iv) small angular clasts. This section describes the various textures and grading observed within this unit and discusses possible mechanisms for their formation. The significance of an ignimbrite towards the base of this sequence will also be addressed.

### **6.1.2 Geological Setting**

The Brolass area on the Ross of Mull peninsula, SW Mull forms part of the Palaeogene Mull Lava Field. The lavas overlie Moine basement rocks, typically with an intervening section of Triassic, Jurassic and Cretaceous strata. In Carsaig Bay where the base of the lava field is exposed, the lowermost Staffa Lava Group overlies a thick sedimentary sequence comprising Lower Jurassic Pabay Shales and Scalpay Sandstones, and Upper Cretaceous Morvern Greensands (Table 6.1). The Staffa Lava Group comprises a thick sequence of flows of predominantly basaltic composition. This sequence contains a substantial number of flows that exhibit well-developed columnar jointing. The presence of columnar jointing within these flows, their overall lensoid geometries, the presence of pillowed facies and the nature of interbedded sedimentary rocks, indicate that they were erupted into lakes impounded within broad valleys (e.g. Bell & Williamson 2002). Substantial swamps developed within these valleys, resulting in sedimentary units including coal beds, over which the lavas flowed, entraining trees and other surface materials (Fig. 6.2). The breccias described here crop out at the base of these flows.

### **6.1.3 Field Relationships of the Breccias**

The breccias crop out on the foreshore between Carraig Mhor and An Dunan, *ca.* 1.7km ESE of Carsaig, between the Low and High Water Lines, and in a 20m high vertical cliff section above the beach. Figure 6.3 illustrates the main lithologies, comprising the Carraig Mhor section, indicating their general appearance and spatial relationships. Figure 6.4 is a more extensive and detailed schematic diagram of the section, which accurately documents these various field relationships. The lowest exposed rocks are highly altered amygdaloidal basalt sills that form a low tide platform. These intrusions are overlain by

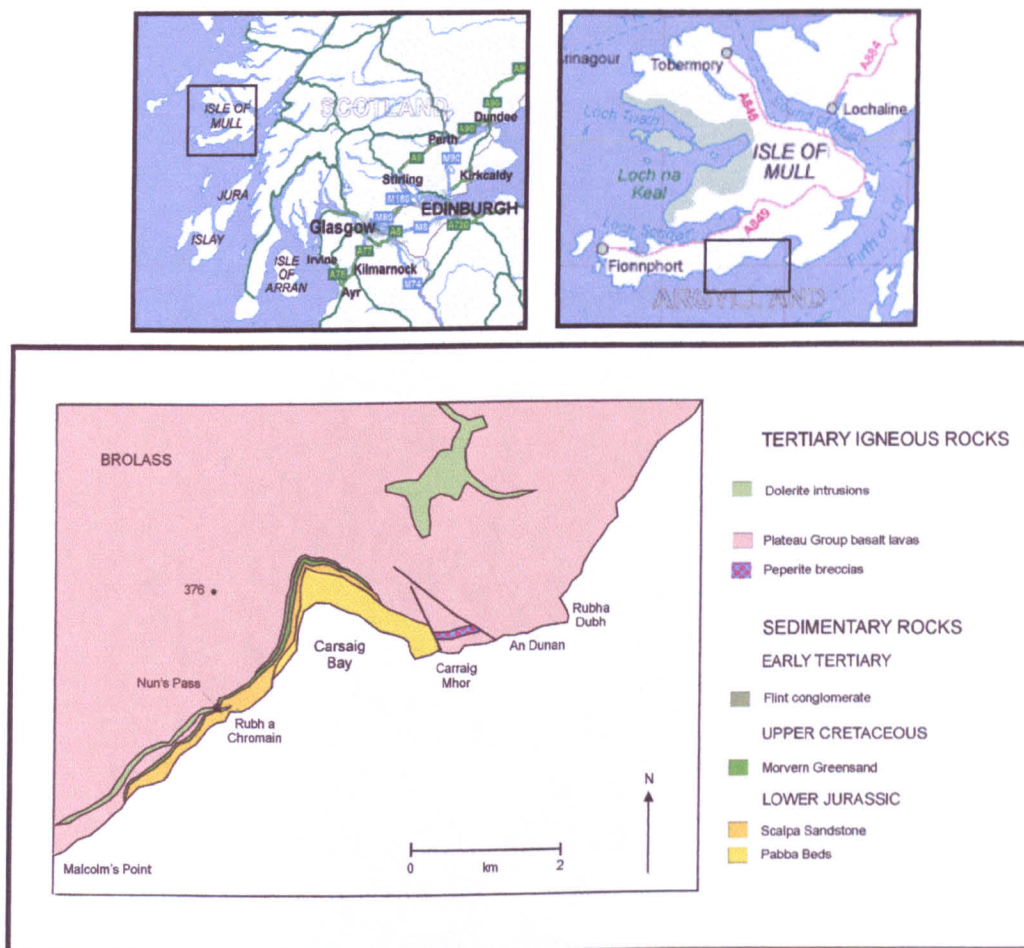
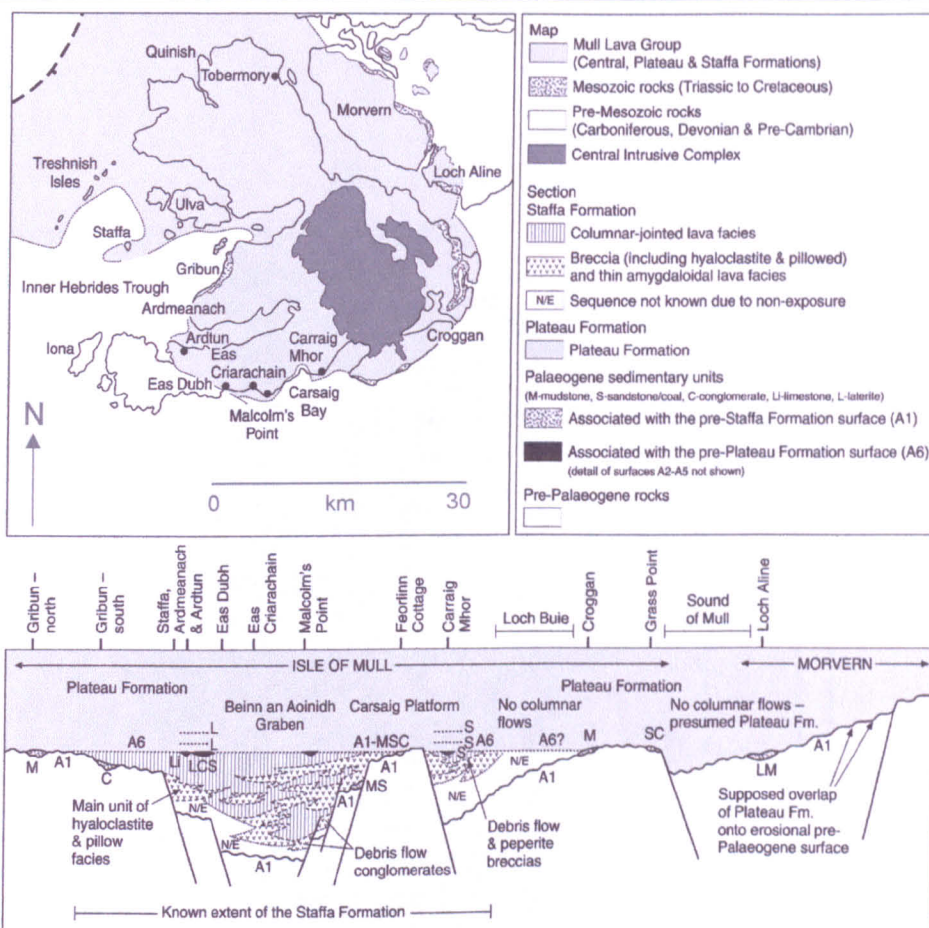


Figure 6.1 – Location map and geological map of Carsaig Bay, south coast of Broilass, Ross of Mull, NW Scotland.

Lava Field	Sector	Formation	Members
Mull <sup>1</sup>	Mull	Mull Central Lava	Undivided tholeiitic basalts
		Mull Plateau Lava	Pale, Main, Quinish Lava <sup>2</sup> , Geochemical subdivisions <sup>3</sup>
	Mull & Morvern	Staffa Lava <sup>2</sup>	Ardtun Conglomerate and equivalents Macculloch's Tree/ Fingal's Cave/Carraig Mhor Flow Undivided sequence in Ross of Mull Malcolm's Point Conglomerate Gribun Mudstone/Croggan Flint Conglomerate and equivalents
	Ardnamurchan	Mull Plateau Lava <sup>4</sup>	Undivided

Table 6.1 – Lithostratigraphical subdivisions of the Mull Lava Field Sequence (<sup>1</sup>Bailey *et al.* 1924; <sup>2</sup>Williamson *et al.* (in prep); <sup>3</sup>Kerr 1995; <sup>4</sup>Richey & Thomas 1930)



**Figure 6.2 – Geological map and cross section through Morvern and the Isle of Mull, including Carsaig Bay, outlining lithologies and spatial relationships observed. Columnar lava flows, breccias and sedimentary units are indicators of palaeoenvironment (from Bell & Williamson 2002)**

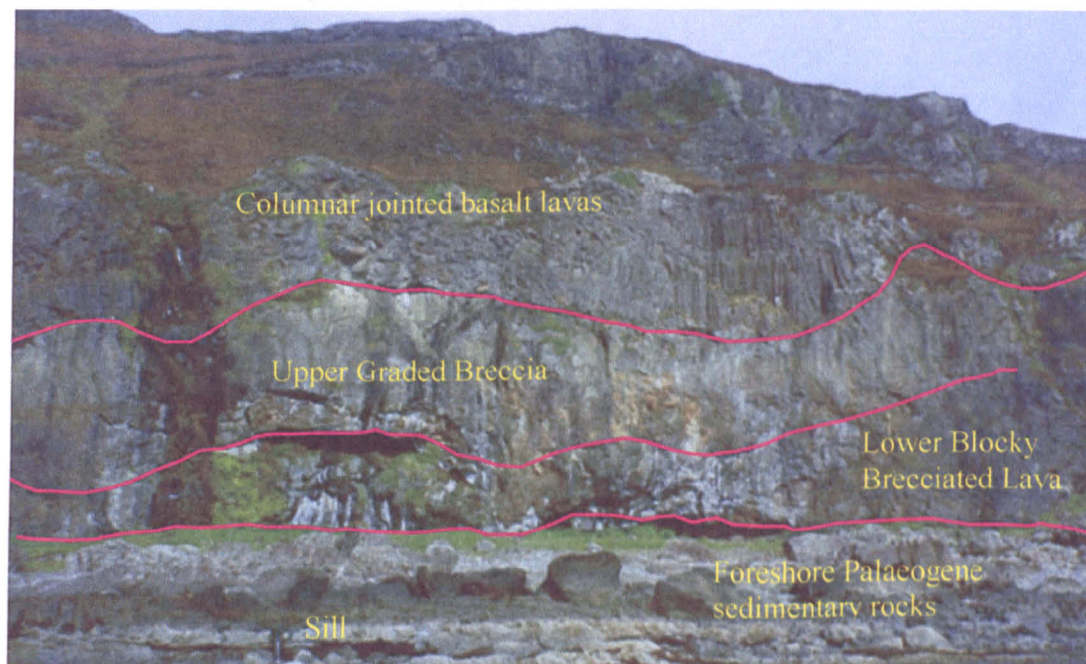


**Figure 6.3 – View of Carrraig Mhor coastal section showing relationships between sedimentary rocks, lavas, breccias and intrusions (NM55532105). Foreshore sequence of Palaeogene mudstones, shales and sandstones, cut by composite sill. Overlain in a 30m high cliff section by the Lower Blocky Brecciated Lava (LBBL) unit and Upper Graded Breccia (UGB) unit, whose bases form a series of channel-like structures, apparently filling topographic depressions. These are overlain by columnar jointed basalt lavas.**

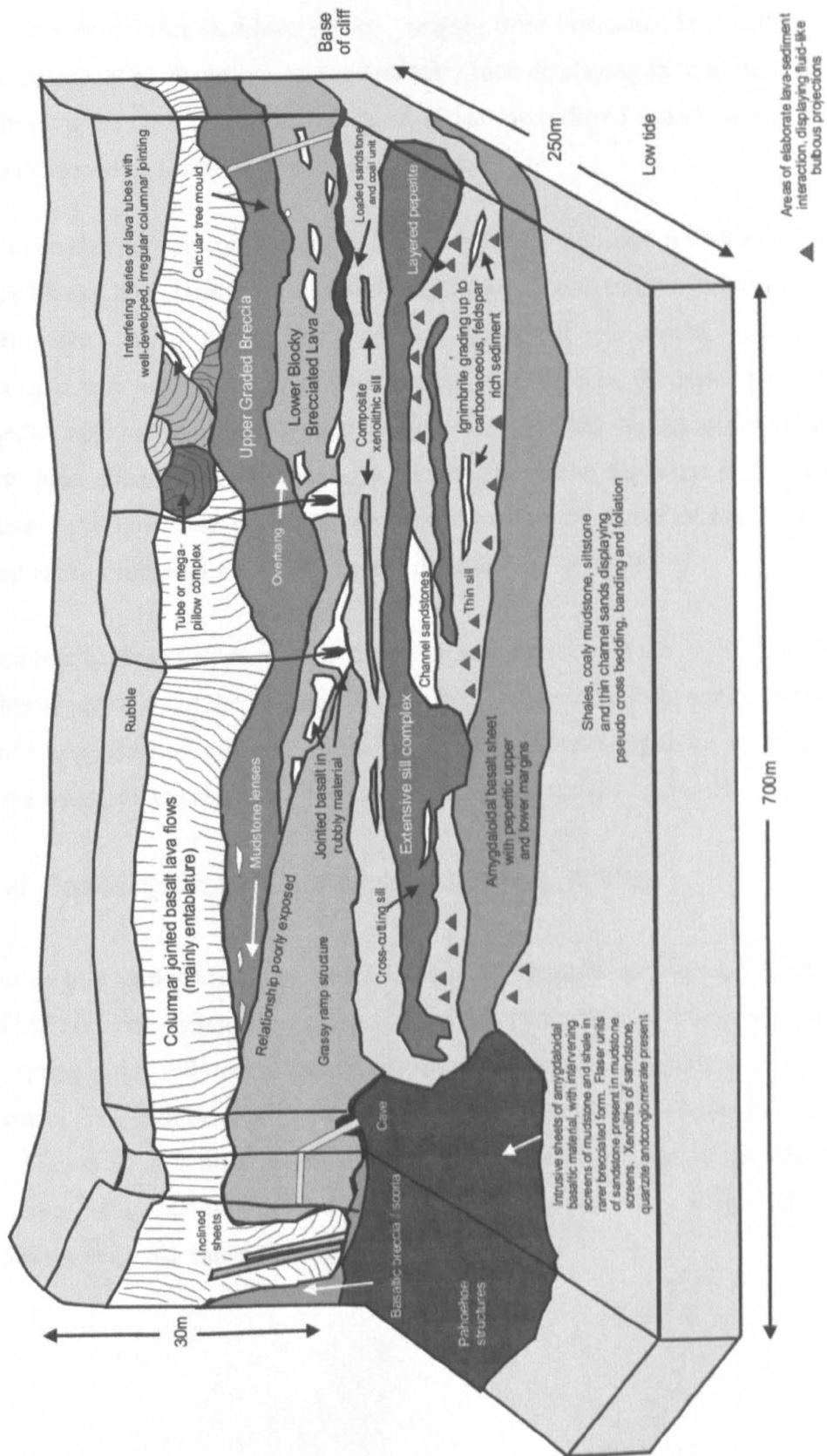


Figure 6.4 Schematic diagram of Carsaig Bay cliff section, illustrating field structures and spatial relationships.

a sequence of sandstones, shales and mudstones, in places invaded by an extensive sill or sheet complex. A thin ignimbrite is present locally. A number of relationships may be identified within this foreshore section, ranging from brecciated lava within sedimentary rock, to injections of magma into sedimentary rock displaying little to no brecciation. At the base of the cliff, above the foreshore, a thin inweathered sandstone and coal unit has been deformed by loading of the overlying rocks.

The main cliff section consists of two main lithologies, outlined in Figures 6.3 and 6.4. A lower blocky brecciated lava, has been highly weathered and its features are difficult to differentiate. At its top surface there is a horizontal tree mould. The lower blocky brecciated lava is overlain by a spectacular graded breccia, the base of which is highly irregular, apparently filling topographic depressions in the surface of the blocky breccia. At its base abundant sub-horizontally aligned flame-like clasts up to 50cm in size are present. The unit fines over an interval of 10m into a network of small, angular clasts. These various lithologies are described in detail in Section 6.1.5.

Autointrusive basaltic lavas with tube-like geometries and distinctive, well-developed columnar jointing cap the breccias. Their irregular lower surface, again, forms a series of channels, suggesting filling of a palaeotopography. Overlying these are tabular flows of olivine basalt, giving rise to the typical trap topography of the lava field.

#### **6.1.4 Basal ignimbrites and sedimentary rocks**

A series of sedimentary rocks and a localised ignimbrite are exposed on the foreshore platform at Carraig Mhor. These deposits are only accessible for a maximum of 3 hours, in low spring tide, full moon conditions during Equinox. Numerous sills intrude this sequence. The relationships on this foreshore platform are summarised in Figures 6.5 and 6.6. Figure 6.5 is a schematic diagram of the foreshore sequence showing the various lithologies, their relationships and structural levels. Figure 6.6 is a detailed log that subdivides the sequence into a series of units labelled A-R.

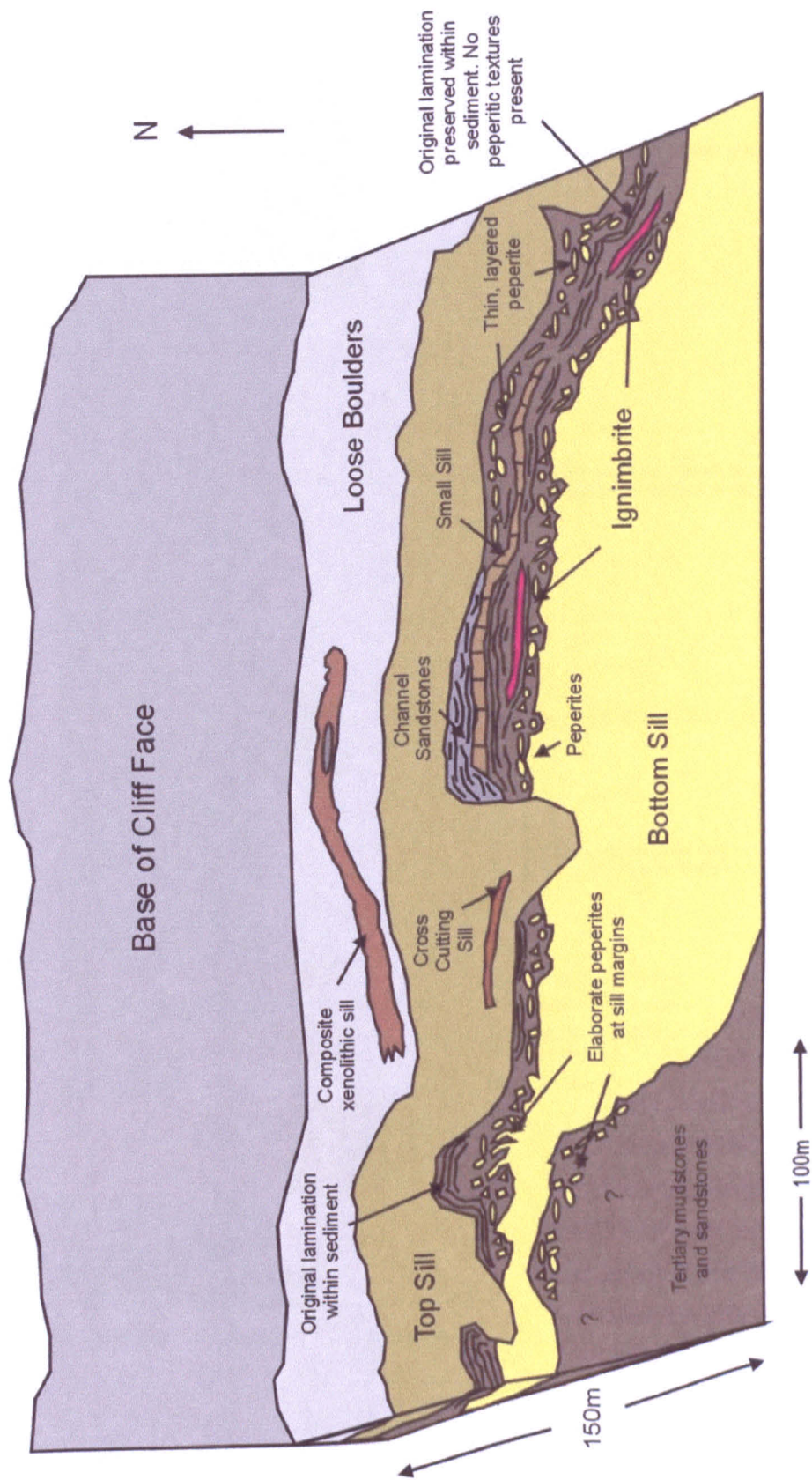


Figure 6.5 Detailed schematic diagram of Carraig Mhor foreshore platform

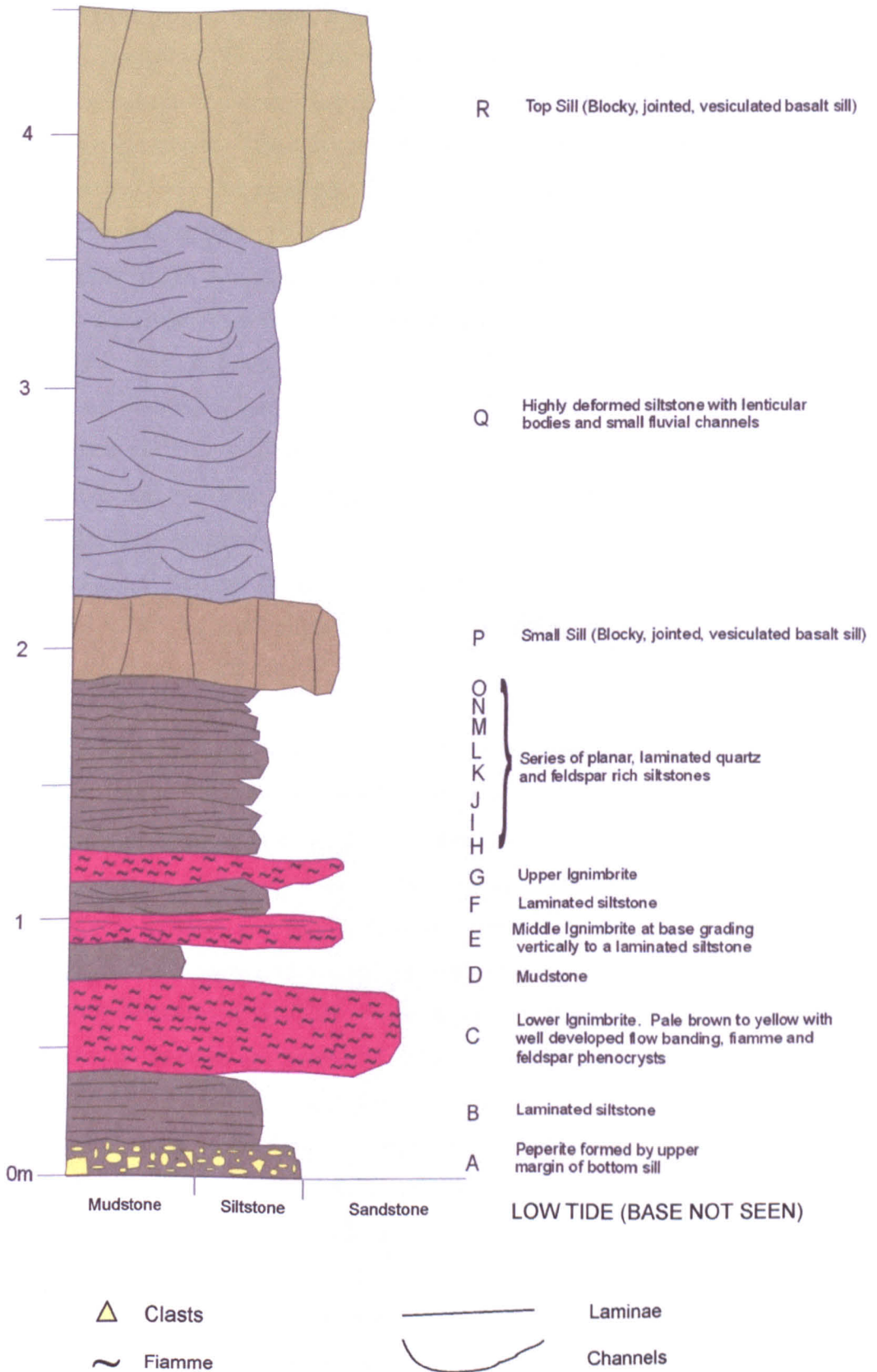


Figure 6.6 – Detailed log of the Carraig Mhor foreshore platform (NM55642110).

At the base of the sequence is an amygdaloidal basalt sill (A). Weathered pale yellow to green its upper margin is highly irregular and brecciated. This margin forms bulbous and finger-like projections (*ca.* 5-20cm in length) into the surrounding sedimentary rock, and small, sub-rounded to sub-angular clasts of basalt are present in surrounding sedimentary rock at the sill margins. These deposits are peperites, and are described in detail in Section 6.1.5 below. Above the peperites is a 30cm thick laminated siltstone (B) typical of the sedimentary rocks exposed in the foreshore sequence. It is dark grey to brown, with 2mm thick wavy laminae. Rounded to sub-rounded grains of quartz, with occasional feldspar and mica dominate the macroscopic components. The sediment is compacted and all primary pore space is filled with mud (Fig. 6.7a). A 40cm thick ignimbrite unit overlies the siltstone, forming a lenticular body 15m wide before pinching out laterally (C) (Fig. 6.7b). This, the Lower Ignimbrite is pale brown to yellow with well-developed flow banding, fiamme and feldspar phenocrysts. The flow banding is <2mm thick, and the fiamme display a eutaxitic texture. Phenocrysts (<1mm across) are composed of highly altered orthoclase feldspar. Fragments of basalt, glass and zircon crystals are also present (Fig. 6.7c). The ignimbrite has a silicic composition and reflects an early period of explosive, pyroclastic activity.

Overlying the ignimbrite is a 10cm thick, dark brown massive mudstone (D). This is then overlain in turn by a 10cm thick ignimbrite (E) with similar features and composition to the Lower Ignimbrite (C), but comprises distinct layers that grade vertically to laminated siltstone (Fig. 6.7d). This Middle Ignimbrite is slightly coarser than the Lower with less well-developed fiamme, and forms the lower 5cm of unit E. At this point, ignimbritic textures begin to disappear and the unit fines upwards into a laminated siltstone, indicating a return to sedimentary deposition. At the top of the siltstone several black streaks (*ca.* 1mm thick) are present, and when the rock is cleaved, these reveal carbonised organic matter (Fig. 6.7e). These abundant plant and wood remains range in size from 0.5cm to 3cm in length and up to 1cm wide. The siltstone is dominated by quartz and the laminae vary from 0.25mm to 1mm thick. A 10cm thick laminated siltstone (F) and another graded ignimbrite (G) overlie unit E. This Upper Ignimbrite is reverse graded, coarsening from a fine-grained, flow banded variety, with well developed fiamme at the base, to a coarser ignimbrite over the next 6cm and then into a quartz-rich laminated siltstone at the top. Carbonaceous organic matter in the form of small woody plant fragments (*ca.* 1mm thick) is present at the top of the sequence.

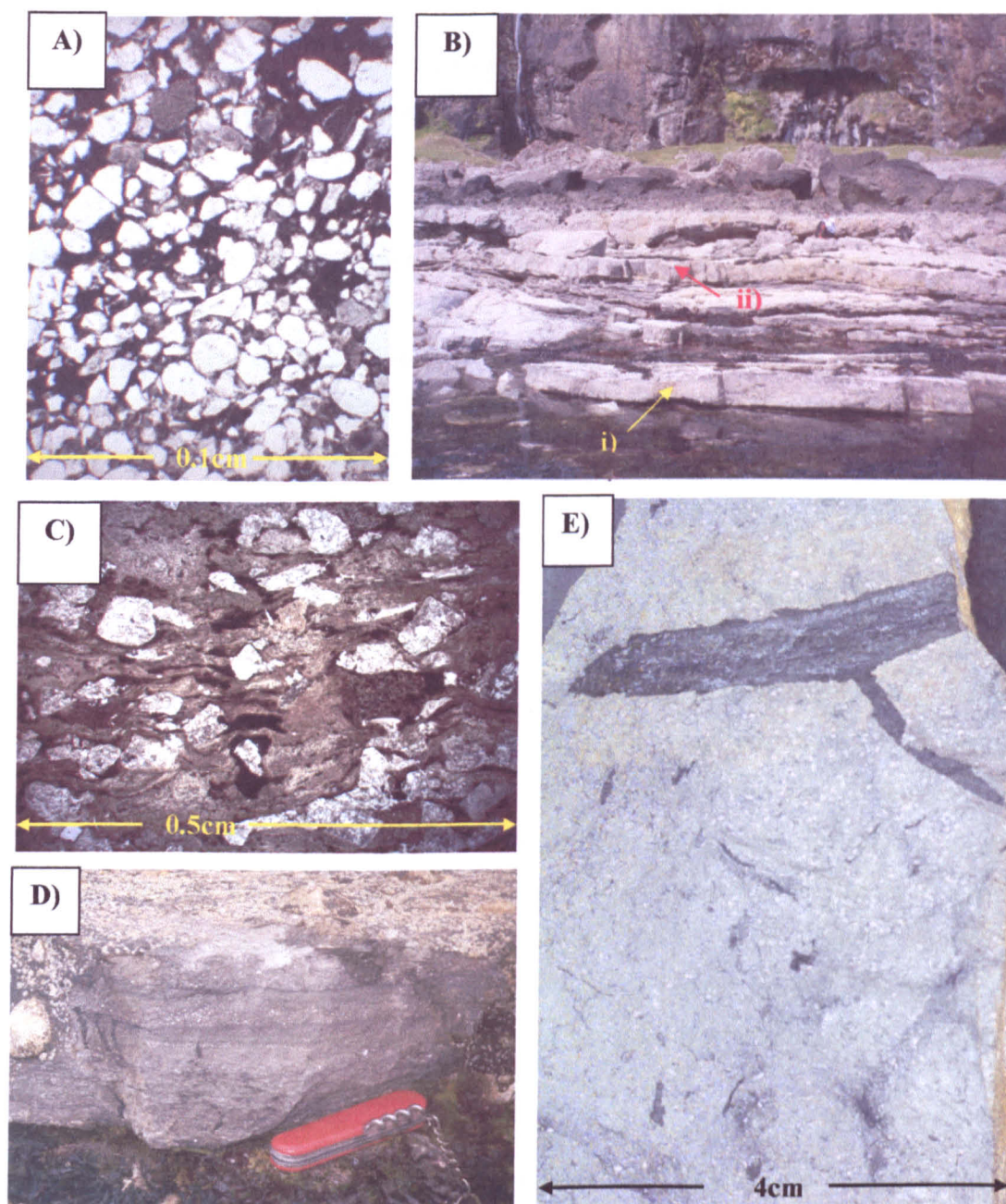


Figure 6.7 – Ignimbrite and sedimentary rock units from the Carraig Mhor foreshore platform (NM55642110). A) Laminated siltstone (Unit B) from the foreshore sequence. This argillaceous sedimentary rock is dominated by compacted quartz grains. B) i) Exposure of 40cm thick ignimbrite (Unit C). Ignimbrite tapers out to the east. ii) Thin basaltic sill. C) Photomicrograph of ignimbrite displaying feldspar phenocrysts, flow banding and fiamme. D) Unit E ignimbrite grading into a laminated siltstone. E) Fossilised plant material from the top of Unit E.

A series of thin, planar laminated siltstones (H to O) overlie the Upper Ignimbrite. These range from 5cm to 10cm thick and the lithology is similar to that of unit B (Fig. 6.7a). They are dark grey to brown, with 2mm thick wavy, laminae. Rounded to sub-rounded grains of quartz, with occasional feldspars and micas dominate the siltstone. The rock is well compacted and all primary pores are filled with mud. A 30cm thick basaltic sill (P), labelled 'Small Sill' on Figure 6.5, intrudes the sequence here and is blocky, jointed and highly vesiculated. A 1.5m thick unit of highly deformed siltstone/fine sandstone (Q) is above the small sill. This unit contains a series of small cross-cutting, fluvial channels (*ca.* 20cm across, 5cm depth) which fill a larger channel (*ca.* 5m across, 1.5m depth) that tapers out to the east, and is cut by a sill to the west. Finally, a blocky, jointed, vesiculated basalt sill (R, the 'Top Sill' on Figure 6.5.) cuts these channelised sandstones. The sill is up to 2m thick, and the base is locally brecciated, although no interaction with sediment is observed.

An ignimbrite is defined as a rock or deposit formed from pumiceous pyroclastic flows, irrespective of the degree of welding or volume (Sparks *et al.* 1973). However the term causes some confusion as it is used in a lithological sense to mean welded tuff, and in a genetic sense to mean the rock or deposit formed from pyroclastic flows. Such deposits are typically poorly sorted, ranging from ash to blocks more than 1m in diameter. The welding of pumice fragments, lapilli and glass shards forms welded ignimbrites or tuffs. Hot gases and the weight of overlying material stretch and flatten pumice fragments producing fiamme and eutaxitic textures (Cas & Wright 1987). In summary, ignimbrites often represent silicic pyroclastic deposits, and their presence towards the base of the Carraig Mhor sequence, indicates the occurrence of explosive, silicic, pyroclastic activity at the time of deposition.

The Unit C ignimbrite and the two graded transitional ignimbrites (Units E and G) described above form lenticular bodies no more than 15m across, and were deposited on the tops of laminated siltstone units. Another small ignimbrite at the same structural level (Fig. 6.5) is also recognised 50m east of the described deposits. This sedimentary sequence is located towards the base of the Tertiary, and formed before the eruption of the majority of the lava field. The presence of multiple ignimbrites indicates a series of small silicic pyroclastic eruptions at this time. These must have originated from vents that are not recognised on the present day surface. The early stages of development of the lava field predominantly involved basaltic magma, yet these deposits indicate that silicic

magma was also present when eruptions began. This may represent the products of fractional crystallisation in a magma chamber, or small-scale crustal melts. The Unit C ignimbrite erupted onto a palaeosurface, but the eruption was followed by a return to sedimentation and the deposition of mudstone (D). Further eruptions resulted in the deposition of the Unit E and G ignimbrites, but in each case there was a relatively rapid return to clastic sedimentation, as each grades up into laminated siltstone. At the tops of Units E and G, carbonaceous, plant remains suggest that the lava field environment included a substantial vegetation.

### **6.1.5 Breccia Lithologies**

The various components of the breccia units, as outlined in Section 6.1.3, are described in detail below in (approximate) stratigraphic order.

#### **6.1.5.1 Foreshore Intrusions**

A complex of sills and thin igneous sheets cuts the foreshore exposures of mudstone, siltstone and ignimbrite. Ranging in size from a few centimetres to 1m thick they are typically cross cutting and highly irregular. There is a wide range of contact relationships, some are planar, whereas others have crenulate, irregular margins, forming bulbous projections into the sedimentary host. Some have brecciated contacts at their bases. Figure 6.8a illustrates the brecciated base of a sill. Clasts are typically small (<5cm across), highly angular and indicate no interaction with the host strata. Other foreshore sheets are typically highly amygdaloidal and ropy textures are locally identified on their upper surfaces (Figure 6.8b), suggesting that they represent lava flows that are locally invasive, or intrusions formed at very shallow levels.

On the foreshore, fine-grained, dark grey to black shales and mudstones and pale yellow sandstones, are interbedded with sheets of fine-grained, pale brown to green-brown, altered igneous material ranging from 2cm to 10cm thick. The igneous layers are discontinuous and form lenticular bodies no more than 2m in length. The sedimentary rocks are never coarser than fine sand and display a closely-spaced lamination.

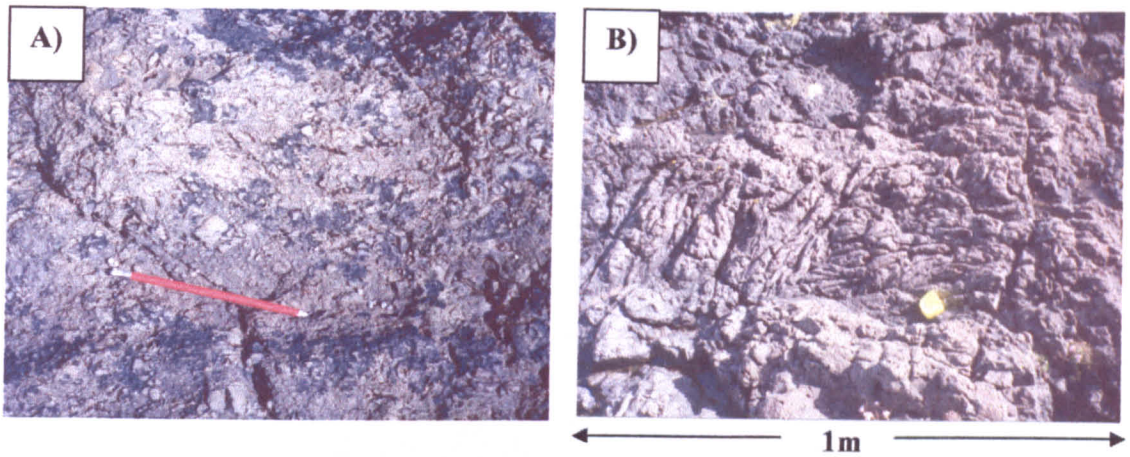


**Figure 6.8 – Shallow intrusion features from Carraig Mhor foreshore platform. A) Sill with brecciated base (NM55512108). B) Ropy texture, pahoehoe style flow on the upper surface of a thin lava flow/shallow level intrusion (NM55442109).**

The contact relationships between the pale igneous layers and the sedimentary rocks show a range of features. Figure 6.9 highlights two such examples:

- 1) Irregular discordant contacts, and locally lobe-like, at i) in Figure 6.9a.
- 2) Simple planar contacts, in Figure 6.9b.

Further examples are observed on the foreshore, where layers of igneous material, apparently interbedded with the sedimentary rock, have been considerably brecciated and their clasts are surrounded by sedimentary rock. These layers contain clasts with a range of morphologies, ranging from sub-angular to sub-rounded to highly irregular and crenulate, typically 1 to 2cm in size (Fig. 6.9c, Fig. 6.18), and locally with jigsaw fit textures. The term ‘jigsaw fit’ texture suggests the originally intact nature of the clasts and their subsequent fracturing as the igneous material is broken apart or fragmented (Kokelaar 1982) (Fig. 6.9d). The layered breccias are typically no more than 1m thick, and the clasts form a well-aligned horizontal fabric. The spectacular morphologies present in these intrusive units on the foreshore, suggests a complex origin, to be reviewed in Sections 6.1.8 and 6.1.9.

Higher in the sequence, a complex composite sill is characterised by basic globules of paler igneous material up to 5cm in length, with crenulate to angular margins, preserved

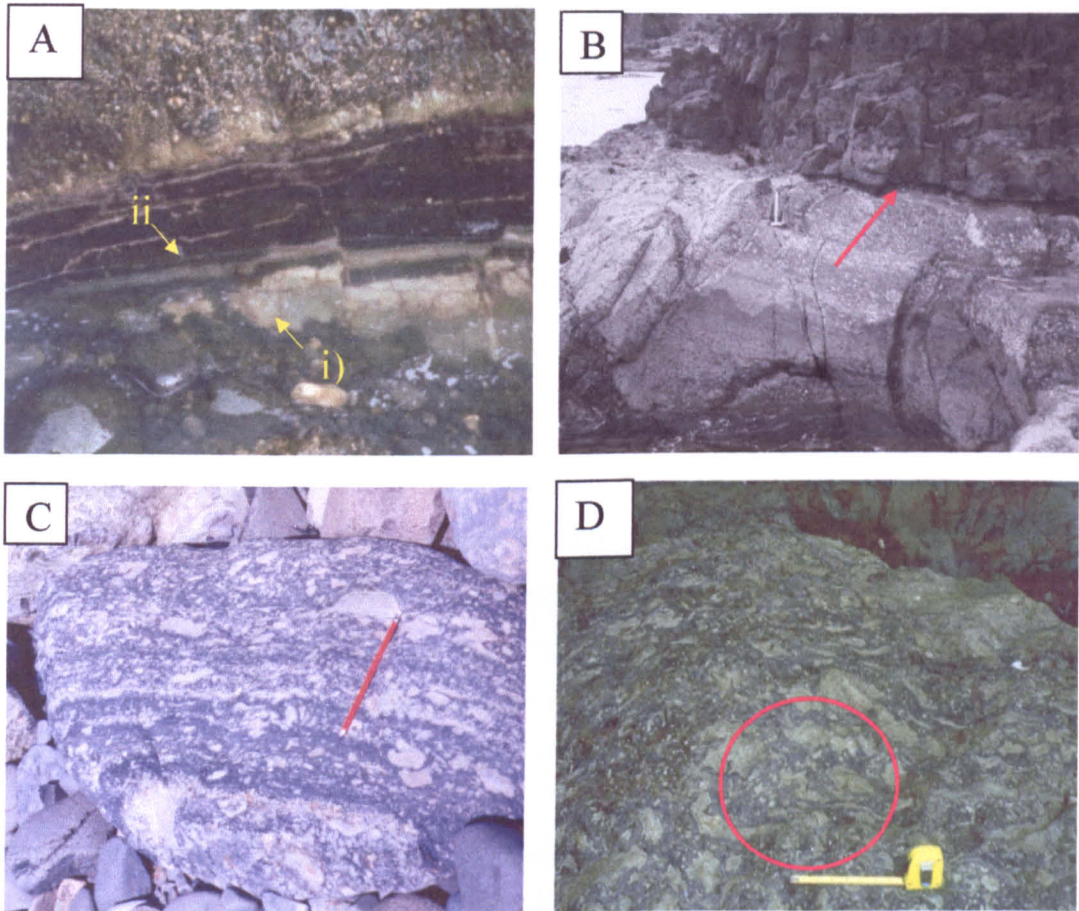


**Figure 6.9 – Variations in intrusive contacts and jigsaw fit textures from Carraig Mhor (NM55532105). A) i) Irregular discordant contact zone 15cm in thickness, displaying two distinct lobes with disrupted margins ii) 5cm thick sandstone layer. Both i) and ii) display faulting with a 5cm displacement. B) Base of a sill showing simple planar contact with sediment. Arrow indicates base of sill (NM55692110). C) Layered block showing complex injections of magma into sediment. Clasts range from sub-rounded through sub-angular (Type iii and iv) to crenulate finger like projections (Type ii). The clasts display a sub horizontal alignment of layers *ca.* 2cm thick. D) Complex block exhibiting clasts (Type ii) with elaborate crenulate and curvilinear margins. The irregular facing edges of the clasts exhibit a geometrically interlocking pattern, whereby the clast margins appear to parallel each other. This is referred to as a ‘jigsaw fit’ of clasts, suggesting the originally intact nature of the clasts and their subsequent fracturing. Tape rule 20cm.**

within the body of the intrusion (Fig. 6.10a). Xenoliths of supposed Triassic conglomerate up to 1m across are also present (Fig. 6.10b).

As outlined above and in Figure 6.9, magma injections appear to have been involved in a complex sequence of interactions with sediment. Where the intrusions have crenulate margins and bulbous projections, or are layered (Fig. 6.11, Fig. 6.18), the original lamination in the sediment is disturbed and wraps around the clasts. Where intrusions simply cut the sediment with planar contacts, the original sedimentary lamination is preserved, and no breccia (peperite, see Section 6.1.8 and 6.1.9) is developed.

### **6.1.5.2 Bulbous projections of igneous material on the foreshore**

Higher in the sequence there are spectacular examples of more complex interactions between the now altered igneous material and sediment. Large quantities of pale igneous material are contained within the sediment and display an elaborate and irregular array of rounded, angular and crenulate margins. Clasts of the igneous material range from 2cm across to 'sheets' 1m in length. These clasts comprise elongate and bulbous projections that appear to have worked their way into the sediment, in places forming isolated sediment rafts. Clast shapes are irregular and deformed, doubling back on themselves, with the sediment filling the voids between (Fig. 6.11).

Further examples in fallen blocks on the foreshore, reveal a spectrum of clast shapes. Clast morphologies are highly variable and can occur as a multitude of clast components arranged with complex geometrical associations, or as domains of predominantly one clast component. Four principal clast types can be identified: (i) elongate finger-like structures; (ii) large fluid flame-like clasts; (iii) sub-rounded clasts; and (iv) small angular clasts (Fig. 6.12).

The elongate finger-like structures (i) are typical of those illustrated and described in Figs. 6.9c and 6.11 but are consistently longer, ranging from 10-20cm in length. The fingers taper and disperse from larger lobes of the igneous material and the embayments formed are filled by small amounts of sediment. Typically, they display a jigsaw fit texture with adjacent clasts.

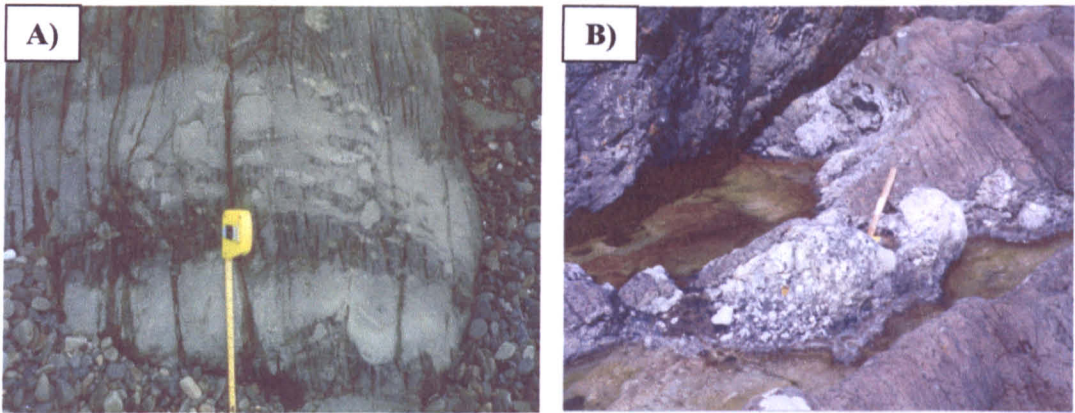


**Figure 6.10 – Composite sill features from the Carraig Mhor foreshore platform (NM55602101). a) Composite sill high on the foreshore formed by multiple injections of magma. b) Triassic quartzite conglomerate xenolith (*ca.* 1m across) within composite sill.**



**Figure 6.11 - Bulbous projections of igneous material (Type i) displaying irregular margins and complex relationships with sediment host (NM55532105). Clasts of the igneous material range in size from 2cm across up to larger 'sheets,' in places up to 1m in length. These clasts comprise elongate and bulbous projections, which appear to have worked their way into the sediment, in places leading to isolated rafts of sediment within the igneous material. The clasts have irregular, deformed shapes and in places appear to double back on themselves, with the sediment repeatedly filling the voids between the clasts.**

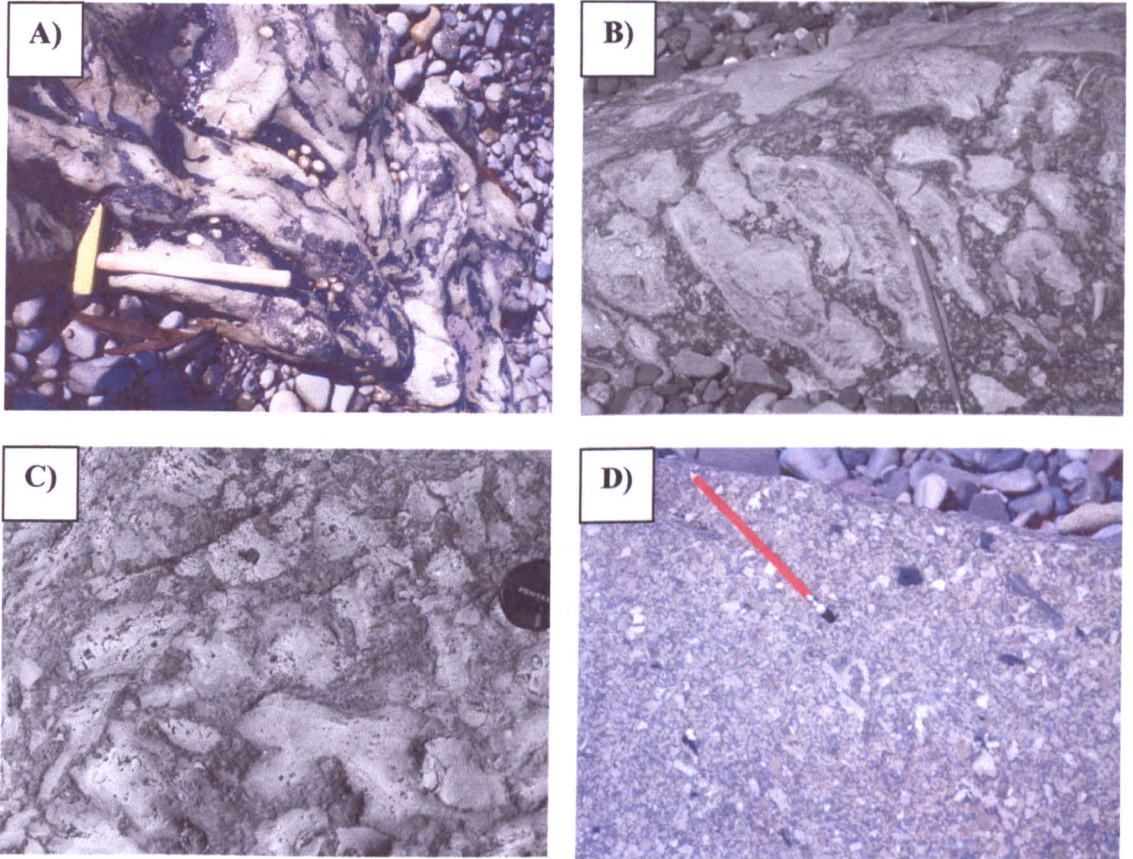


Figure 6.12 – Clast types in the Carraig Mhor breccias (NM55532105). A) Type i. Elongate, finger-like structures (*ca.* 20cm in length) dispersed from larger lobes of igneous material, which display irregular, crenulate margins. B) Type ii. Rag or flame-like clasts (*ca.* 10-50cm across) with spectacular, crenulate margins, which exhibit a jigsaw fit texture. Note quench texture rims on certain clasts. C) Type iii. Sub-rounded to sub-angular clasts (*ca.* 0.5 to 10cm) displaying equant to oblate shapes and curvilinear margins. D) Type iv. Small angular to sub-angular clasts (*ca.* 0.5 to 5cm across), typically with sharp terminations.

The large fluid, flame-like clasts (ii) range in size from 10 to 50cm and display a spectacular array of morphologies. They are generally elongate and their margins are highly irregular with a 'rag' or 'flame-like' appearance. They retain a fluidal shape with rounded and crenulate contacts between the clasts and the sediment host. These clasts also display jigsaw fit textures, and in places are aligned sub-horizontally.

The sub-rounded clasts (iii) also exhibit a range of morphologies and sizes. They vary from 0.5 to 10 cm and may be sub-rounded to sub-angular in shape and from equant to oblate. Their margins vary from crenulate, through rounded to curvilinear, and jigsaw fit textures are again common.

The small angular clasts (iv) range in size from 0.5 to 5cm, typically < 2cm and can be very angular with sharp terminations.

The irregular facing edges of clasts exhibit a geometrically interlocking pattern, whereby the clast margins commonly parallel each other. This is referred to here as 'jigsaw fit' clasts, following Kokelaar (1982) and indicating that the original igneous material was fragmented (Fig. 6.5d). Certain igneous clasts display pale yellow-green quench texture rims typically no more than 2mm in width and parallel to their margins. These rims are generally present on larger, angular clasts (>2cm), but overall are observable on less than 5 vol. % of all clasts (Fig. 6.12b).

### **6.1.5.3 The Lower Blocky Brecciated Lava (LBBL)**

The overlying sequence at the foot of the cliff begins with an approximate 8m thick unit referred to as the Lower Blocky Brecciated Lava (LBBL). This is heavily vegetated and weathered to a reddish-brown to yellow-brown colour and is cut by numerous minor basaltic intrusions (Fig 6.4), but shows some of the features outlined. Typically, it comprises angular clasts of moderately altered basalt ranging in size from 0.5 to 20cm, although a few larger clasts up to 1m across are present. A few unaltered basalt clasts range in size from 2 to 20cm. Large parts of this unit are not brecciated, and are simply composed of fractured basalt. Brecciated areas are predominantly clast supported, with a matrix of dark fine-grained sediment comprising at most 10 vol.% of the unit. The clast morphologies are less elaborate than those described in Section 6.1.5.2. The unit is heavily fractured and in conjunction with the high percentage of angular clasts, gives the LBBL its

'blocky' appearance. Interaction with sediment is rare and only present towards the top of the unit. The upper surface is poorly defined and it is difficult to identify the contact with the overlying unit. In places there is no clear boundary and the two units appear to merge into each other. A horizontal tree mould, 10cm in diameter is preserved on the upper surface of the unit.

#### **6.1.5.4 The Upper Graded Breccia (UGB)**

The Upper Graded Breccia (UGB) comprises a number of transitional variants over its 10m thickness (Fig. 6.13a) but shows a general upwards grading from sub-rounded fluid-like clasts to angular clasts.

The base of the UGB, where it is in contact with the LBBL, is irregular with 2-3m relief filling topographic depressions. Three distinct 'channels' are present in the exposed section. Towards the base of the UGB, abundant 'flame' or 'rag-like' clasts (Types i and ii) are observed, ranging in size from 30 to 50cm. These clasts are elongate and fluidally shaped, with crenulate and rounded margins, and jigsaw fit textures. The clasts are sub-horizontally aligned and dip at approximately 10° to the west in the exposed section (Fig. 6.13c). At the base the clasts are in equal proportion to the sediment, whereas at higher levels the percentage of sediment appears to reduce. Rare loose blocks on the foreshore contain angular lithoclasts of black shale ranging in size from 5 to 10cm. These are finely laminated and appear unaffected by interaction between the pale igneous clasts and sediment (Fig. 6.13b).

Towards the middle of the unit the clast size reduces to, on average, 2-5cm with rarer examples 10cm across. Shapes are sub-angular to sub-rounded (Type iii), with margins ranging from crenulate, through rounded to curvilinear, and there are no examples of the flame-like geometries, seen lower in the unit. Furthermore, the sub-horizontal alignment of the clasts has also been lost, although a 'jigsaw fit' fracture pattern is maintained. The unit is considerably more clast-supported at this level, and sediment matrix comprises only approximately 33 vol. % of the rock (Fig. 6.13d).

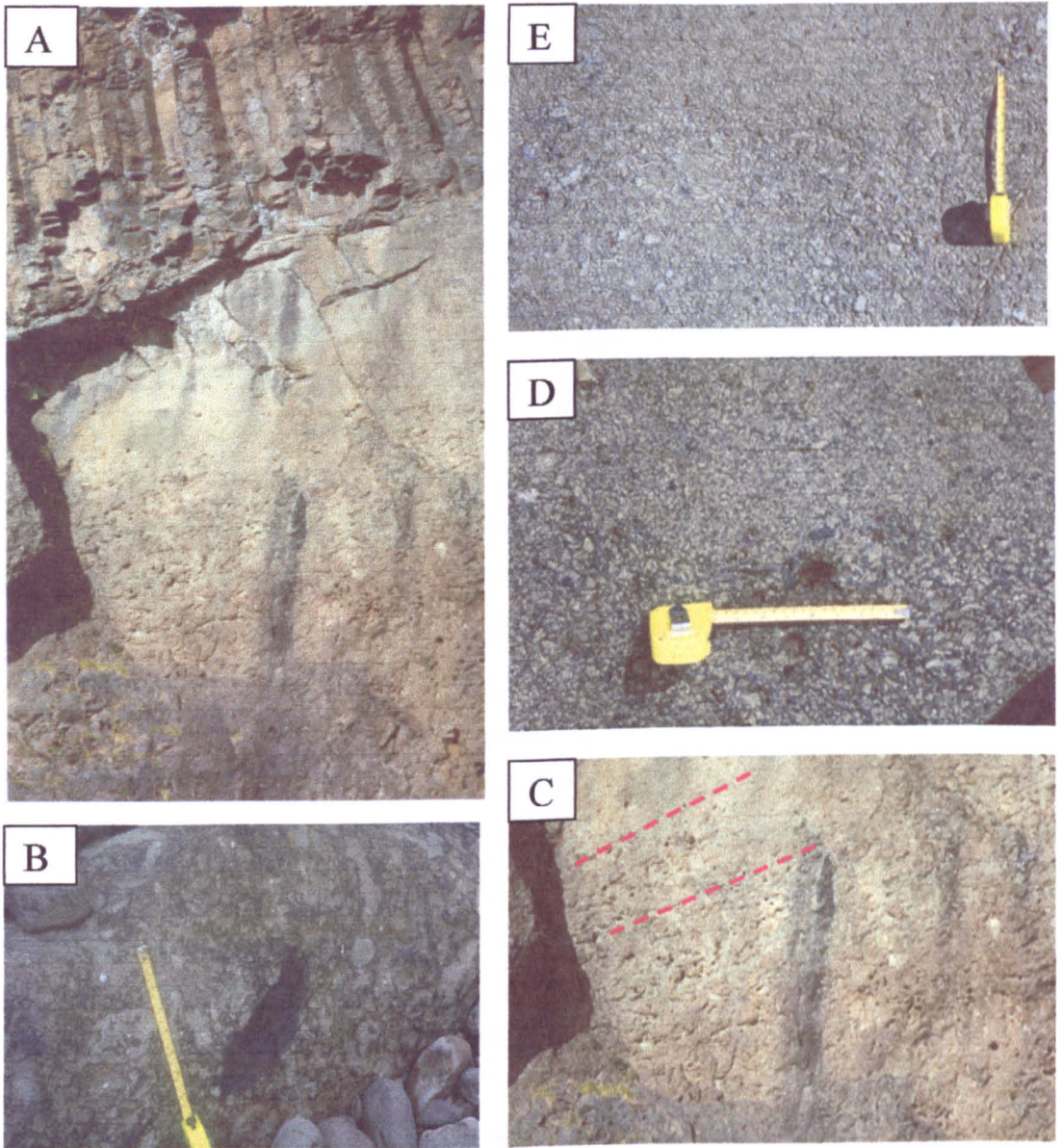


**Figure 6.13 – The Upper Graded Breccia Unit (UGB) (NM55652118):** A) Vertical section (10m) of the UGB, displaying grading from large, ‘flame-like’ clasts to an angular network of clasts. Overlain by columnar jointed basalt lavas. B) Rare loose block on the foreshore exhibiting an angular lithoclast of laminated black shale. This clast is apparently unaffected by interaction between the igneous clasts and the sediment. Tape rule 20cm. C) Sub-horizontally aligned, plastically deformed, ‘flame-like’ clasts (Type ii) of igneous material, dipping at approximately 10° to the west in the exposed section, at the base of the UGB. Ranging in size from 30-50cm these elongate clasts exhibit elaborate, crenulate margins. Clasts are in equal proportion to the sediment. D) Towards the middle of the UGB, flame-like geometries and sub-horizontal alignments of clasts are no longer observable. Clast size has reduced to on average 2-5cm, with rarer clasts of *ca.* 10cm. The clasts are sub-rounded to sub-angular (Type iii) displaying a jigsaw fit fracture pattern. Sediment comprises approximately one third of the rock. E) ‘Network’ structure breccia at the top of the UGB, containing small angular clasts (Type iv) of igneous material ranging in size from 0.5 to 2cm separated only by ‘stems’ of sediment, comprising 5-10 vol. % of the rock. Fluid style clasts are absent and jigsaw fit textures rare.

The top of the UGB unit is virtually completely clast supported, forming a 'network' structure, with the sediment comprising only 5-10 vol. % of the rock (Fig. 6.13e). The clasts are separated by small 'stems' or 'branches' of the sediment, in places only *ca.* 1-2mm wide. The igneous clasts range in size from 0.5-2cm and are angular to sub-angular (Type iv). There are no fluid style clasts and there appears to have been little or no interaction with the sediment, compared with examples lower in the unit, which exhibit flame-like clasts (Fig. 6.13c), and there is no evidence of the bulbous and finger-like projections observed at sheet margins on the foreshore (Fig. 6.11).

#### **6.1.5.5 Columnar Basalt Lavas**

The base of the columnar basalt lavas, overlying the UGB, appears to fill a series of topographic depressions, producing a number of channel-like features. Where the lavas overlie the breccias (they are more laterally extensive than the breccia exposure) the channels broadly follow the channels observed at the base of the UGB. These autointrusive basalt lavas locally form, a series of four poorly developed, approximately circular interfering tube-like structures, approximately 5-10m wide, displaying irregular columnar jointing. Typically, the lavas are characterised by well-developed entablature (flat, irregular) and colonnade (vertical, well-defined) jointing, forming columns 15-20cm wide (Figs. 6.3, 6.4 & 6.13a). Thereafter there appears to be a return to near continuous effusion of subaerial facies basaltic lavas in the overlying sequence, with few, typically minor, hiatuses in the volcanism, represented by inter-lava sedimentary deposits.

#### **6.1.6 Petrography of the Breccias**

Selected examples are illustrated and described in detail in Figure 6.14.

The pale igneous clasts display a variety of sub-angular, through sub-rounded, to 'fluid-like' morphologies. Certain clasts are highly fractured, with irregular margins/edges, commonly displaying a jigsaw fit of clasts, and 'bulbous' and 'finger-like' projections. Most clasts are composed of highly altered semi-hyaline igneous material, although small patches of fine-grained crystalline material are also present. The glassy clasts have been hydrothermally altered, resulting in a light brown-green colour. Alteration has led to considerable variation in the appearance of the clasts, with some displaying a vein like texture, others a honeycombed appearance, and still others exhibiting a zoned texture,

although the majority are relatively undifferentiated. Some glass clasts are grey, and contrast with the more typical light brown-green colours. All include abundant small (0.5mm) white laths of plagioclase feldspar.

Heavily altered crystals of olivine can also be tentatively identified, indicating the original magma was of basic composition. A small proportion of the clasts have quench textures at their rims

The clasts are surrounded by a dark brown sedimentary matrix of silt and mud, although there are also isolated patches of coarser sediment (1-2mm). Throughout the matrix there is a very fine lamination, which is typically highly deformed and closely parallels clast margins, filling late-stage fractures and propagating cracks within the clasts. Rounded vesicles are filled by sediment with lamination that follows the vesicle margins. A number of quartz and calcite-filled vesicles, ranging from 1 to 5mm are present within the rock, both in the glassy clasts and within the sediment. Furthermore, quartz veins and lenses are present within the matrix.

### **6.1.7 Environment of Deposition**

It is apparent from the dominance of semi-hyaline clasts and the development of quench textures within this breccia that the igneous material was rapidly cooled in order to produce the fracture textures described in Section 6.1.5. Such rapid cooling can be produced by the quenching and granulation of magma in water (e.g. Pichler 1965; Walker & Blake 1966; Fisher & Schmincke 1984); however, it appears in the example described here that some additional influence of the intimately associated sediment can be inferred. In general terms, the environment of deposition must have allowed for a magma-water-sediment interaction to occur.

Columnar jointed lava flows displaying pillowed facies and interbedded sediments, indicate lavas erupted into drainage systems or depressions containing standing water (e.g. Skelhorn 1969; Saemundsson 1970; Long & Wood 1986; Lyle & Preston 1998; Lyle 2000). A series of channel structures are recognised at the base of the Carraig Mhor

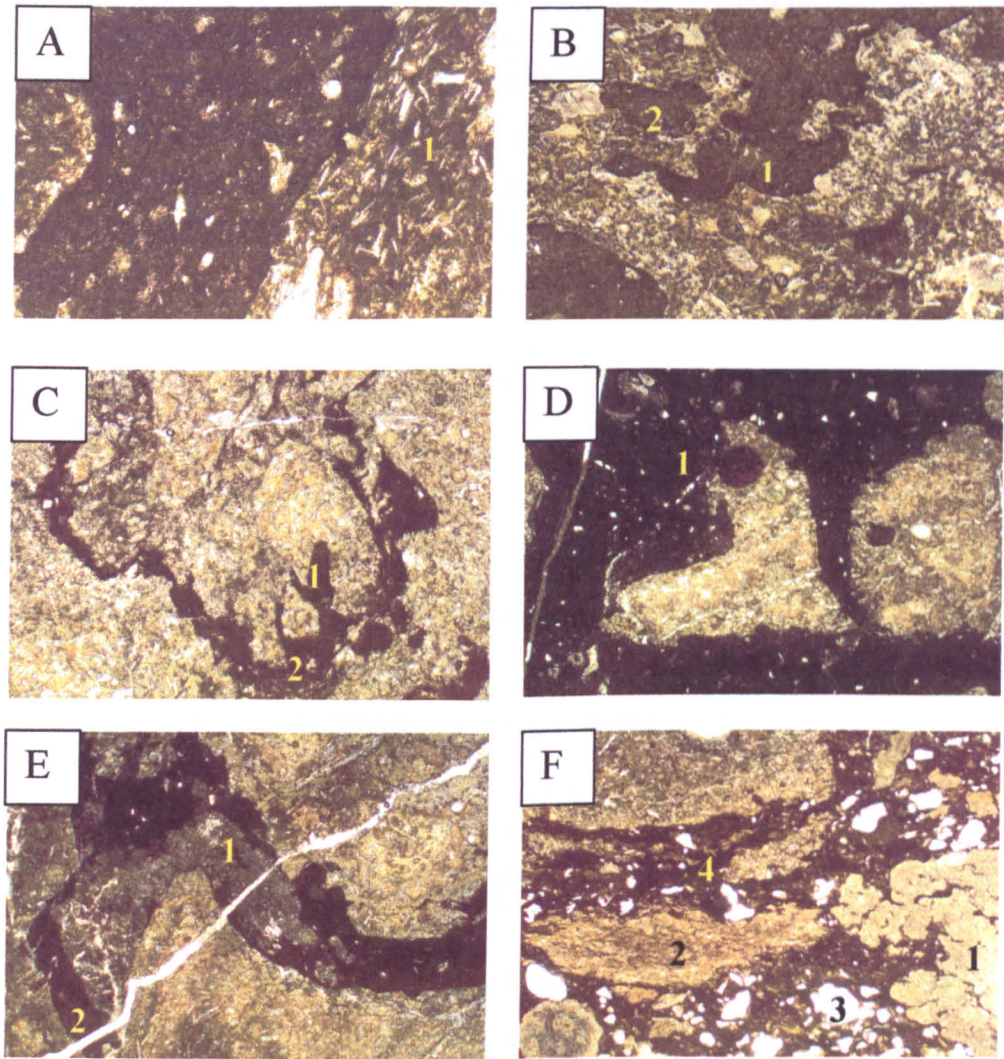


**Figure 6.14** – Photomicrographs of Carrraig Mhor breccias displaying fracture and clast textures. All views are plane-polarized light, 3mm across. **A)** Clast-sediment boundaries involving two igneous clasts. The paler igneous clasts contain small, white laths of plagioclase feldspar and small glassy shards are also present within the sediment. In this example the semi-crystalline clast (1) is relatively unaffected by alteration. The dark, fine-grained sediment displays a very fine lamination, which parallels the margin of the clasts. **B)** Clast of igneous material with irregular, crenulate margins. The clast appears to have fragmented as it quenched. At 1 the fractured clast is filled by a finger of sediment wrapping in and around the clast margin: its lamination precisely parallels the clast boundary. At 2 an isolated patch of sediment is contained within an igneous clast. **C)** The margins of this clast are highly irregular and fractured, with elaborate fingers and bulbous projections at 1. The clast is highly disrupted by a narrow band of the host sediment, producing a loop structure (2). The clast margins are geometrically interlocking, indicative of a jigsaw fit of clasts. **D)** Two sub-angular to angular clasts of igneous material display a jigsaw fit texture. At 1 a vesicle has been filled by fluidised sediment. **E)** Sub-rounded clasts displaying crenulate and curvilinear margins and jigsaw fit textures. A grey, crystalline clast is present at 1, in contrast to the other semi-hyaline clasts. A thin vein of quartz cuts the photomicrograph (2). **F)** Complex clast morphologies. 1) Hyaline clast displaying jigsaw fit textures, bulbous projections and fluidal shapes. 2) Sub-rounded clast with small finger-like projections and curvilinear margins. 3) The sediment is filled with quartz fragments and quartz filled vesicles. 4) The sediment fills fractures and its lamination is deformed around clasts.

breccia units, suggesting small depressions where water and muddy sediments could accumulate. Within these depressions surface vegetation could develop, or plant material could be washed into the system. Lavas subsequently flowed into these depressions, both interacting with the water and wet sediment, and entraining trees or other surface materials. Thus, we can reconstruct an environment whereby magma, water and sediment could interact (e.g. Jones 1969; Kokelaar 1982). The presence of a tree mould and fossil plant material in the Carraig Mhor sequence is consistent with this interpretation.

When a lava flows into water, pillows can typically be expected to form (e.g. Williams & McBirney 1979). At this particular locality, however, no pillow structures are observed. Their absence may be explained by Walker's (1993a) suggestion that pillows only form on underwater slopes of 20° or more. This suggests that the slopes of the channels at Carraig Mhor may have been less than 20° and therefore the magma responded in a different manner, forming the lithologies outlined. Furthermore, the presence of water saturated sediments, would enable the process of magma-water-sediment interaction to occur (Kokelaar 1982).

### **6.1.8 Mechanisms of Breccia Formation**

From the lithological descriptions and environmental interpretations outlined above, it is apparent that a complex interaction has occurred between basic magma, water and sediment. This section sets out to examine briefly previously suggested models of breccia formation and compare them with the morphologies observed at Carraig Mhor.

The commonly fractured and irregular clast margins, their jig-saw fit, and associated quench textures observed within the Carraig Mhor breccias are all indicative of an autoclastic process as a simplified fragmentation mechanism (e.g. Pichler 1965; Walker & Blake 1966; Fisher & Schmincke 1984). One such mechanism, hyaloclastization, a magma-water interaction process, produces textures similar to those of the Carraig Mhor breccias.

The term hyaloclastite was first introduced to describe rocks fractured by the quenching and granulation of magma in water (Rittmann 1962; Fisher & Schmincke 1984; Kokelaar, 1986). The process involves the rapid cooling initiated by emplacing magma in water and accounts for its transformation into glass. Hyaloclastization, however, does not explain the apparent interaction with sediment as observed in the Carraig Mhor breccias.

The concept of the fluidisation of wet sediments during the emplacement and cooling of igneous bodies (Kokelaar 1982) appears to be a more realistic and viable process. This mechanism assumes poorly consolidated and water saturated (or nearly so) sediment. As magma is emplaced into this water-sediment mixture and cools, the sediment is fluidised as its pore water is flash heated to boiling point, and pressure release occurs during the opening of fractures. As the magma and sediment interact, the magma appears to tear itself apart due to explosively expanding steam, as a result of the boiling of pore water within the sediment. This process, termed bulk interaction steam explosivity by Kokelaar (1986), explains the presence of vesicles both within the clasts and the sediment of the breccias. The fracturing of the chilled magma and fluidisation of the sediment are synchronous, causing the fluidised sediment to fill cracks and fractures and deform around the newly formed clast material, destroying original sedimentary structures. Lamination may be preserved but is now highly irregular. As outlined in Sections 6.1.5 and 6.1.6, numerous examples of sediment deformation and vesicles are present within the Carraig Mhor breccias. Examples of this process have been observed in Lower Old Red Sandstone (Devonian) rocks of Scotland (Kokelaar 1982). At Turnberry, in the SW of the Midland Valley of Scotland, a sequence of andesite sheets show features reflecting the interaction of magma with fine- to medium-grained sandstones. Interaction between magma and sediment may produce fluidal igneous clasts due to the ductile fragmentation of magma (Kokelaar 1982). Preservation of these clasts requires insulation of the magma from direct contact with pore water in the sediment, by the formation of stable vapour films at the magma-host sediment interface (Kokelaar 1982). These vapour films are generated and maintained providing a certain critical temperature is exceeded and there is ample pore water. With time the magma will cool until film boiling no longer occurs and the magma is not insulated (Mills 1984). Fracture textures and sediment deformation structures are similar to those observed in the Carraig Mhor breccias (Fig. 6.15).

Walker & Francis (1987) proposed a similar mechanism to explain the emplacement of an olivine dolerite sill into a series of Carboniferous sediments, including a coal formation, near Cardenden in Fife. This model supports the ideas of Kokelaar (1982, 1986), highlighting how magma may follow irregular paths through an unstable fluidised host. They noted, however, that the process was enhanced when the sill intruded the coal seams (Fig. 6.16). This was explained by the high water content (up to 75%) and low tensile strength of the coal, indicating the key role of water in the interaction.

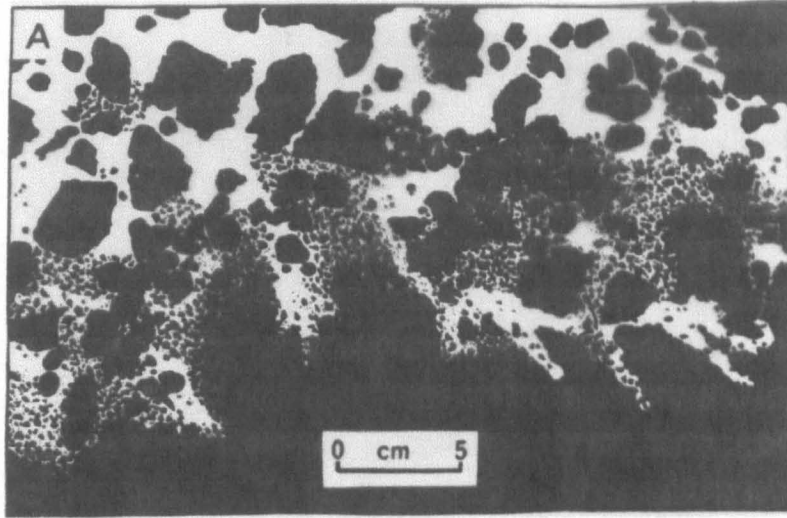


**Figure 6.15** - Diagrammatic representation of andesite-sandstone interaction at Turnberry, Scotland (from Kokelaar, 1982), illustrating the resulting fracture textures. The black shading represents the andesite, which was emplaced into the white shaded sandstone. The andesite fractured into clasts with crenulate and sub-rounded to sub-angular margins, many of which exhibit a jigsaw fit texture, indicating where they were ripped apart. Bulbous and finger-like projections are also observed.

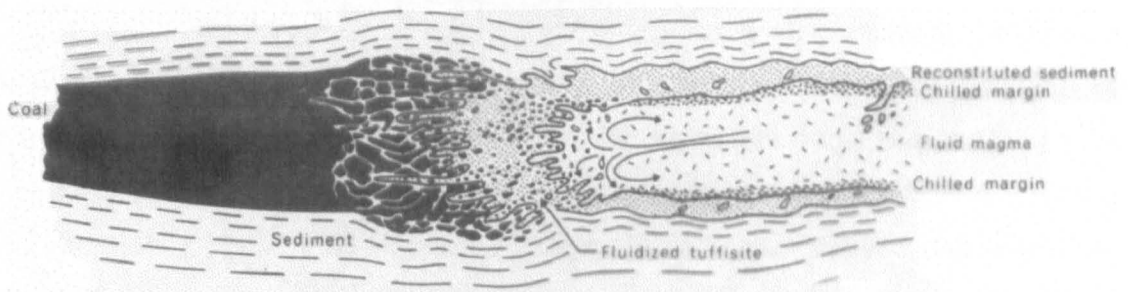


**Figure 6.16** - Diagrammatic representation of coal-magma interaction (from Walker and Francis, 1987). An olivine dolerite sill was emplaced into a series of Carboniferous sediments, including a coal formation, near Cardenden in Fife, Scotland. Fluidised structures are observed where the magma interacted with unconsolidated sediments, and this was enhanced when the sill intruded the coal seam, due to its high water content (75%). The fluidised sediment filled fractures within the coal and was deformed around the fragmented coal clasts.

The term peperite has been widely used for a number of years and is typically applied in a genetic sense, attributing textures to the simultaneous quench-fragmentation of magma and the fluidisation and mingling of water saturated sediments. Peperites have been the subject of much debate in respect to their formation, textures and definition. Scrope (1858) originally introduced the term as a descriptive one based on spotty, basaltic breccias with a carbonate clastic matrix. He interpreted these rocks as resulting from explosive eruption and air-fall deposition of basaltic pyroclasts into a lake in which carbonate sedimentation was occurring, a view supported from the type locality of Gergovia volcano in the Auvergne, France (Jones 1969). Following this, further terms of a genetic origin were introduced. Michel-Levy (1890) and Michel (1948) suggested an intrusive origin, whereby basalt intruded carbonate sediment, accompanied by quenching and/or explosive activity, and mixing and/or redeposition. This theme was followed by Fisher (1960) who classified them as resulting from the shallow intrusion of fluid magma into unconsolidated or poorly consolidated sediments. Schmincke (1967) interpreted peperites from the Ellensburg Formation in Washington as resulting from the flow of basaltic lavas over water-saturated lake sediments, and described the partial intrusion of the base of the lava into the sediments. This resulted in quench fragmentation, local steam explosions, and mixing of the basalt and sediment to produce the peperite texture.

Recently, other authors have suggested a return to a descriptive use due to difficulties in establishing the origin of these magma-sediment mixtures (Cas & Wright 1987; Cas *et al.* 1988). However, White *et al.* (2000) defined peperite as 'a genetic term applied to a rock formed essentially in situ by disintegration of magma intruding and mingling with unconsolidated, or poorly consolidated, typically wet sediments.' They argued that the genetic use of the term 'peperite' recognises a specific set of processes, which no other term can be applied to. 'Magma' is used to include any molten material, either intruded or effused as lava, or as hot pyroclasts. Mingling coincides with fragmentation and is a consequence of magma and/or sediment movement. White *et al.* (2000) identified a number of characteristic features in peperites. These include: the close spatial association with unmixed coherent intrusions of lavas of the same composition; disruption or destruction of sedimentary structures in the sediment component; and partial or complete chilling of the igneous component in contact with the sediment, features all observable within the Carraig Mhor breccias. Other peperite textures are identified. Busby-Spera & White (1987) identified two textural types of peperite. A 'blocky' peperite will have clasts of blocky shape and show jigsaw fit textures, whereas in a 'globular' peperite, juvenile

clasts are bulbous. In peperites with tightly packed fabrics, the sedimentary component also fills joints and fractures (e.g. Watanabe & Katsui 1976; Brooks *et al.* 1982; and Yamagishi 1991). These various textures are summarised by Doyle (2000). Squire & McPhie (2002) describe peperites in which fluidal and blocky clasts co-exist and suggest successive ductile and brittle fragmentation of magma in a sediment host. They suggest the change from fluidal to blocky peperite may have resulted from the progressive cooling of the magma during intrusion, and from the breakdown of fluidisation when the supply of sediment was exhausted.

Recent work on peperites in Namibia has suggested that the processes responsible are diverse and may not always require water (Jerram & Stollhofen 2002). However, the observed textures typically involve lava or magma/sediment interaction, demonstrating the features outlined earlier.

The textures in the Carraig Mhor breccias can be compared with those described in the studies of Kokelaar (1982, 1986), Walker & Francis (1987) and Squire & McPhie (2002), and the extensive literature on peperites (e.g. White *et al.* 2000 and Doyle 2000). It appears that the processes described in these can be used to explain the fracturing mechanism required to produce the Carraig Mhor breccias and this has been summarised in diagrammatic form (Fig. 6.17).

The genetic use of the term peperite suggested by White *et al.* (2000) appears appropriate for the Carraig Mhor breccias, due to features such as quench fragmentation, jigsaw fit of clasts and fluidisation of sediment. However, peperites do not typically display stratification or grading or an apparent transition from fluid, ductile, sub-rounded clasts to angular, brittle clasts within one unit (White *et al.* 2000). These features are characteristic of the Carraig Mhor breccias and, as such, a multi-stage mechanism for their formation is tentatively proposed.

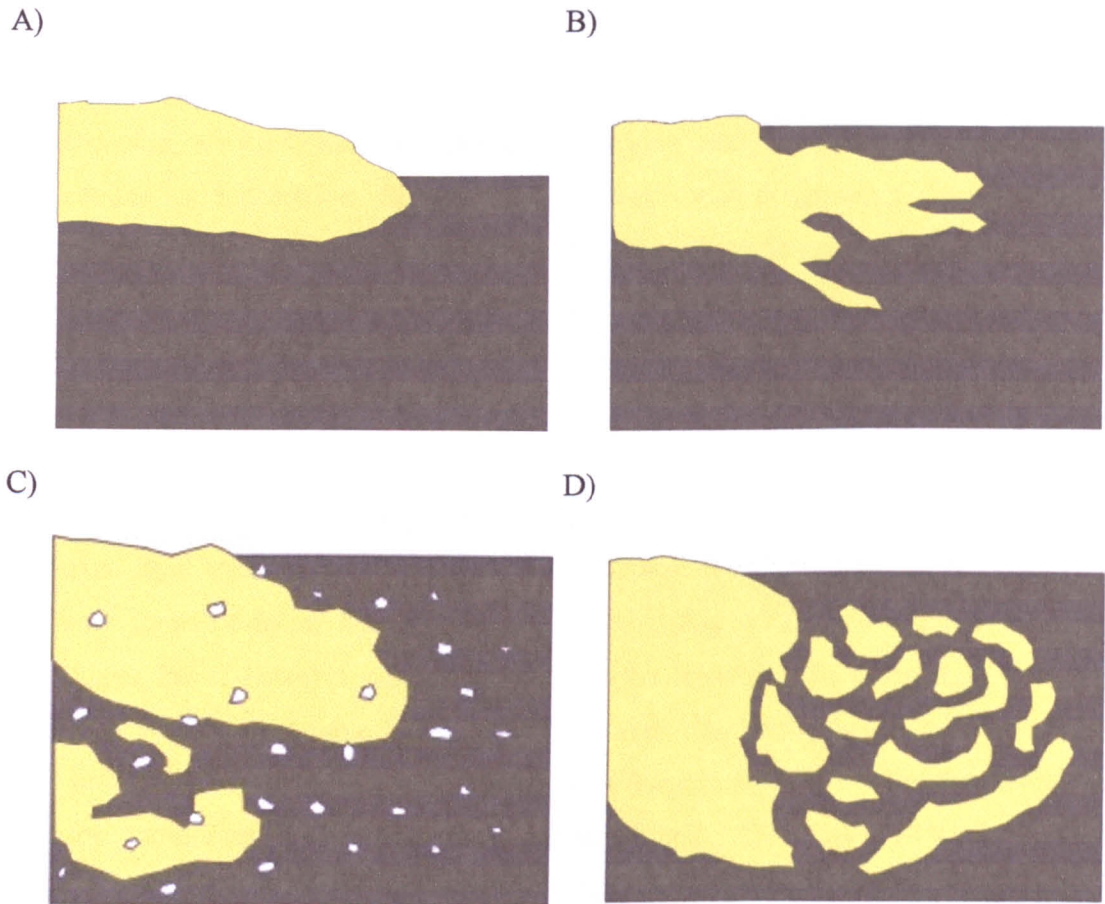


**Figure 6.17 – Diagrammatic representation of peperite formation. A) Eruption of lava, bulldozing its way down into unconsolidated, water-saturated sediments. B) Invasive magma follows irregular flow paths into the sediment and begins to heat and fluidise it. C) Turbulent mixing occurs between the lava and the sediment. Water within the sediment is flash-heated to steam, causing Bulk Interaction Steam Explosivity (Kokelaar, 1986). Explosive expansion of the steam fractures the lava and forms a glassy material. D) The lava is fractured although a jigsaw fit of clasts with interlocking margins is maintained. The fluidised sediment fills these fractures and is highly deformed around the clasts.**

## **6.1.9 Mechanisms of Formation of the Carraig Mhor breccias**

### **6.1.9.1 Variation in Foreshore Magma Injections**

Figures 6.9a and 6.9b illustrate injections of magma into sediment within the foreshore sequence at Carraig Mhor, where clast-sediment contacts display contrasting relationships. Some examples retained margins, which are not disrupted and parallel the lamination of the sediment, whereas others have disrupted margins, with the development of finger-like projections and brecciation. Figure 6.18 depicts two such occurrences. The upper of the two layers is the base of a sill, showing no disruption along its margins, whereas the lower is a thin sill which is highly fractured and displays jigsaw fit of clasts and bulbous and finger-like projections. These contrasting appearances suggest variations in the response of the magma to different sediment pore water contents, or the degree of lithification. It seems unlikely that if both layers, which are only 10cm apart, were injected at similar times into the same sedimentary unit, that they would behave so differently. The lower, disrupted layer appears to have been injected into water rich, unconsolidated sediment and has been fractured in the fashion described by Kokelaar (1982) and White *et al.* (2000). The upper layer, however, appears to have been injected into lithified or fluid poor sediment, restricting magma water interaction and brecciation therefore did not occur. This implies that the upper layer may have been injected some time after the lower layer, therefore permitting the sediment to dry out and lithify. This suggests that the complex, brecciated peperite morphologies on the foreshore were formed at an early stage, when the sediment was still water-saturated and unconsolidated. Following this there was the injection of a shallow sill complex, which intruded a consolidated, lithified sediment pile forming sheets with typical planar contacts.

### **6.1.9.2 The origin of the Lower Blocky Brecciated Lava**

It is difficult to differentiate between the Lower Blocky Brecciated Lava (LBBL) and the Upper Graded Breccia (UGB), and in places no obvious contact is observed, and the two units merge into each other. The LBBL is highly fractured and blocky, but is relatively massive, and brecciated only at its upper margin, with fluidally shaped clasts implying magma-sediment interaction. This suggests that the LBBL is the core of a lava flow that formed the UGB and was emplaced into water saturated, unconsolidated sediment and formed the breccia morphologies recognised in the UGB at its margins. Although

morphologically quite different and distinguishable from each other, the LBBL and UGB appear to have been derived from the same lava flow.

### 6.1.9.3 Grading and Transition in Clast Morphology

Gravitational settling provides a possible means of producing the grading observed in the UGB in the Carraig Mhor sequence. This involves a lava bulldozing its way into a wet sediment and interacting with it as outlined in Section 6.1.8 (e.g. Schmincke 1967; Kokelaar 1982,1986) fracturing into large and small clasts. As a result, the larger clasts sink to the bottom of the UGB and hence the unit becomes graded. The deformation of the lamination observed within the sediment could be attributed to the sinking of the clasts through the water-saturated sediment. This is comparable to sag structures as the clasts distort the unlithified sediment. An element of loading may also be attributable to such structures. This method suggests hot sediment (essentially boiling mud) then infiltrating the pile of clasts. The deformation observed is very complex however, wrapping around and encircling clasts and occurring within late-stage fractures and vesicles, suggesting a very 'mobile' fabric and therefore the significant role of fluidisation of sediment (e.g. Schmincke 1967; Kokelaar 1982; Walker & Francis 1987). Furthermore, a gravitational settling mechanism does not adequately explain the transition in clast morphology within the graded sequence.

An adjunct to the model is proposed here to address these problems and this is summarised in diagrammatic form in Figure 6.19. This entails a relatively fluid system whose heat loss and subsequent reduction in magma-sediment interaction are responsible for the development of the above textures.

As previously noted, a number of small, shallow topographical depressions filled with water-saturated, unconsolidated sediments were present prior to the introduction of the magma. Lava was 'emplaced' into these depressions and, due to the soft, unconsolidated nature of the sediments, began to bulldoze its way down into them, in an invasive fashion (Schmincke 1967) following irregular paths at its leading edge. At this initial stage, the magma continued to react in a fluid manner, resulting in plastically deformed rag and flame-like clasts as it was torn apart (Busby-Spera & White 1987; Squire & McPhie 2002). The resulting clasts display a sub-horizontal fabric reflecting the initial movement of the magma. The magma continued to flow through the sediment, but as heat dissipated from its leading edge, the interaction became restricted and reduced. Where the magma

had been effectively insulated and behaved in a ductile fashion, it now simply chilled and quenched, undergoing brittle fracture into smaller, angular clasts (Squire & McPhie 2002). These processes (possibly in conjunction with gravitational settling) reflect the ‘grading’ in the unit, as there is progressively less ductile behaviour of the magma due to accelerated heat loss. Gradually less sediment is incorporated higher in the unit, and ultimately brittle fracturing leads to a ‘network’ of small, quenched, angular clasts. Overall, this reflects the decreasing influence of fluidisation of sediment. Squire & McPhie (2002) describe similar processes. Where the system allows slow heat loss, the magma fragments remain plastic and ductile.



**Figure 6.18 - Diverse injections of magma into sediment host from Carraig Mhor foreshore (NM55672110). A) Simple, planar contact of sill, showing no disruption along its margins. B) Highly irregular and fractured layer displaying jigsaw fit textures and bulbous and finger like projections. These two layers are injected into the same sedimentary unit, but have highly contrasting appearances. B appears to have been injected into water rich, unconsolidated sediment, and fractured as outlined in Figure 6.17, whereas A appears to have been intruded into a coherent sediment, eliminating magma-water interaction, and therefore brecciation. This suggests different relative ages of intrusion. Tape rule 20cm.**

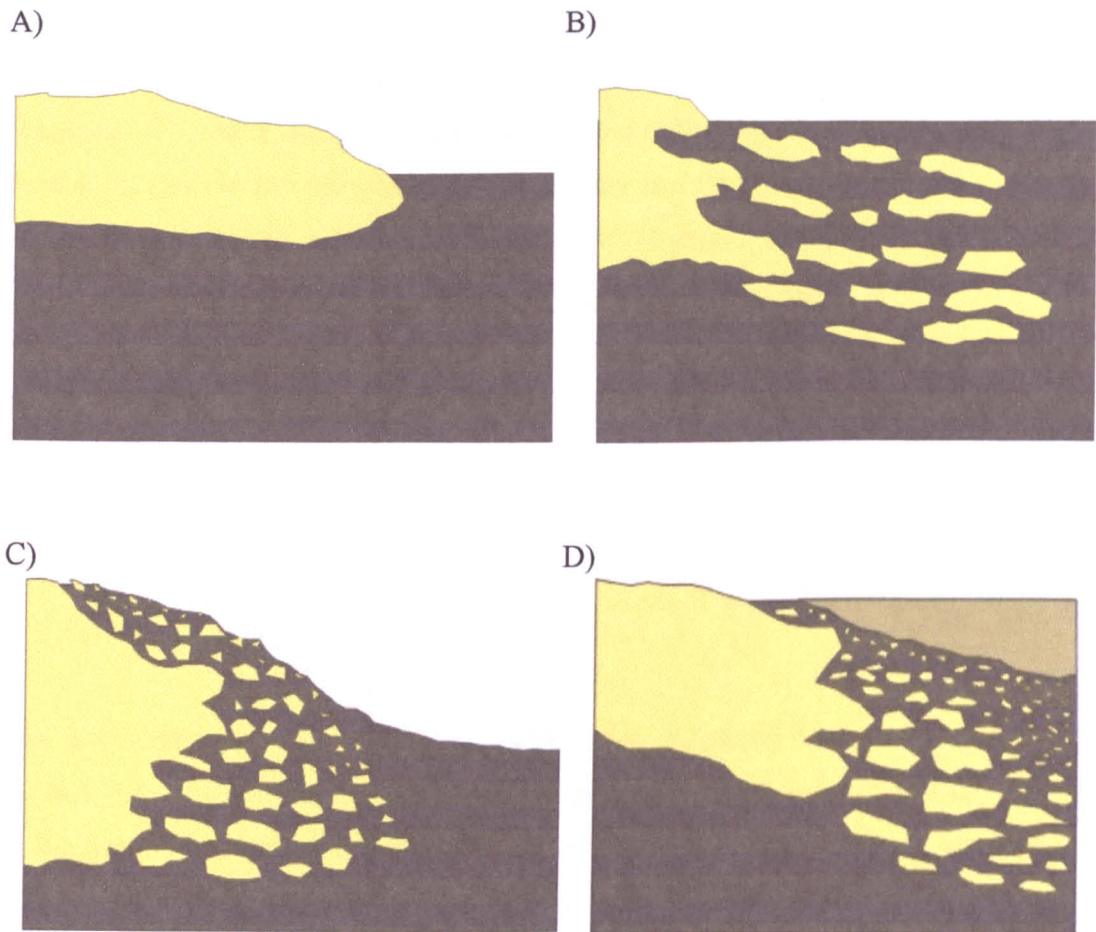


**Figure 6.19 – Diagrammatic representation of mode of formation of Carraig Mhor breccias.** A) Lava flows into water-saturated sediments and bulldozes downwards. B) Mixing of magma and wet sediment results in plastically deformed, flame-like clasts of lava, which display a sub-horizontal fabric, as the magma follows irregular flow paths through the sediment and begins to fragment. C) As heat dissipates from the lava flow front, magma-sediment interaction is reduced, and quenched magma simply fractures into smaller and more angular clasts, indicative of a transition from ductile to brittle fracture. Coarser material then sinks to the bottom of the unit. With this heat loss the influence of fluidisation of sediment decreases, and less sediment becomes mixed within the lava. D) There follows a short hiatus in volcanism, the sediment is lithified and a palaeoslope is formed. A series of topographic depressions are filled by basalt lava flows, displaying irregular, columnar jointing.

Problems associated with this explanation concern the apparently turbulent interaction between magma and fluidised sediment, responsible for the formation of the UGB. It may be argued that bedding and sediment lamination, could not be preserved in such a fluid system. This argument favours a mechanism entirely dependent on gravitational settling of clasts through hot sediment but, as highlighted above, this does not explain the change in clast morphology or the variation in the proportions of sediment and clasts within the sequence. Therefore, the presence of grading and changing clast morphologies suggests a combined method involving a fluidised magma-sediment interaction, from which heat dissipates resulting in a transition from ductile to brittle behaviour (Squire & McPhie 2002), possibly in conjunction with the settling out of larger clasts.

These deposits filled small depressions, but preserved their own topographic surfaces. Following a short hiatus in volcanism, these new channels were filled by subsequent lava flows, which display well-developed, irregular columnar jointing.

### **6.1.10 Conclusions**

The lava-sediment breccias at Carraig Mhor, east of Carsaig Bay on the south coast of Brolass, Isle of Mull, display a number of textures and characteristics that are interpreted as the result of a complex interaction between magma and unconsolidated, water-saturated sediment. In summary, the following features are noted:

Clasts of a pale igneous material of varying morphology are set within a dark, fine-grained sedimentary matrix. The section comprises a foreshore sequence of sandstones, siltstones and mudstones, with local ignimbrites, and is cut in places by a sill complex. Other igneous sheets emplaced into this sedimentary pile, display brecciated margins and morphologies. In the cliff section above, two units, the Lower Blocky Brecciated Lava (LBBL) and the Upper Graded Breccia (UGB) fill a series of channel structures. These are overlain by columnar basalt lavas.

The pale igneous material is a highly altered glassy rock, derived from basic lava, which forms clasts of varying morphology. The clast have margins ranging from crenulate, through rounded and curvilinear, to angular, and also display elaborate bulbous and finger-like projections. In places, clast margins parallel each other, exhibiting jigsaw fit texture. Four clast types are preserved: (i) elongate finger-like structures; (ii) large fluid flame-like

clasts; (iii) sub-rounded clasts; and (iv) small angular clasts. The clasts are held within a dark brown, fine-grained sedimentary matrix, which displays a fine, highly deformed lamination.

The preferred model to explain the formation of the breccias involves the emplacement of magma into unlithified, water-saturated sediments, causing turbulent interaction between the two. The magma began to invade the sediment and as it was emplaced, the water within the sediment was flash heated to steam, causing explosive expansion but ultimately cooling, quenching and fracturing of the now vitrified magma. As the magma was ripped apart, the margins of clasts maintained a jigsaw fit. Concurrently, the sediment was fluidised by the emplacement of the magma and the escape of the super-heated steam, and wrapped around clasts and filled late-stage fractures. Lamination was deformed around clast margins. The Carraig Mhor breccias may be described as peperites.

The following sequence of events occurred producing the various lithologies described in Sections 6.1.5:

- (i) Magma was emplaced into water saturated, unlithified sediment on the Carraig Mhor foreshore sequence, forming peperites at sill margins.
- (ii) Three ignimbrites in succession were erupted on to the upper surfaces of these sedimentary deposits.
- (iii) Sedimentation resumed, with the deposition of laminated siltstones and localised channel sandstones, transporting in small amounts of plant remains.
- (iv) A thin layered peperite, with sub-horizontal alignment of clasts was emplaced into unconsolidated sediments higher in the sequence.
- (v) Further sedimentation occurred before the whole sedimentary pile was lithified.
- (vi) The Lower Blocky Brecciated Lava was emplaced onto an irregular surface topography. It is massive in places, although clasts of basalt are identified at its upper and lower margins. It may therefore represent the coherent core of a lava flow, emplaced into wet, unconsolidated sediment. The margins of the flow formed the breccias in the overlying Upper Graded Breccia (UGB).

- 
- (vii) The UGB displays vertical grading, with large, plastically deformed, flame-like clasts, sub-horizontally aligned, and in equal proportion to the sediment, at the base of the unit. This grades upwards, with a gradual reduction in sediment content, into an angular network breccia at the top of the unit. The grading may have been produced by the gravitational settling of larger clasts to the bottom of the UGB and the infiltration of boiling mud into the clast pile. This mechanism does not, however, explain the change in clast morphologies and proportions of sediment throughout the unit. In the model proposed here, as the magma was emplaced into the sediment it followed irregular flow paths, producing the sub-horizontal alignment at the base of the unit. The magma behaved in a fluid fashion and as it began to fragment, produced large, plastically deformed flame-like clasts. As heat began to dissipate from the system, the magma-sediment interaction was reduced and the magma behaved in a brittle fashion simply quenching into small, angular clasts. At this point the larger, 'plastic' clasts would have sunk to the bottom of the pile. As the magma-sediment interaction reduced, progressively less sediment was turbulently mixed throughout the unit and therefore little sediment is seen at the top of the breccia.
- (viii) Ponded columnar-jointed basaltic lavas were then erupted on to the top of the UGB.
- (ix) A sill complex was intruded at various structural levels on the foreshore, forming intrusions with simple, planar contacts. These later intrusions did not form peperites as the sediment was lithified. The timing of this event is uncertain although it does follow peperite formation.

## 6.2 Loch Ba

### 6.2.1 Introduction

The Loch Ba breccias lie within the Mull Central Complex. Three igneous centres are recognised within the Complex and the Loch Ba breccias are spatially associated with the third and last of these, the Loch Ba Centre. The Loch Ba Centre is associated with the emplacement of various silicic intrusions, including the Loch Ba Ring Dyke that was accommodated by gas brecciation and significant central subsidence. The relationship of the breccias to these and other related rocks will be described and modes of deposition suggested.

### 6.2.2 Regional geology and setting

The Mull Central Complex is relatively poorly understood, and the most detailed reviews available are by Bailey *et al.* (1924) and Skelhorn (1969). Three igneous centres are identified: 1, the Early Caldera or Glen More Centre; 2, the Beinn Chaisgidle Centre and 3, the Late Caldera or Loch Ba Centre (Skelhorn 1969) (Fig. 6.20). These reflect a gradual migration of the focus of intrusion from SE to NW, roughly corresponding with the trend of the Mull Regional Dyke Swarm. The centres, interspersed with cone sheet intrusion, are defined by ring fault fractures along which central subsidence has occurred. Folding within the country rocks appears to have developed as a result of early intrusive events and these structures include the Loch Don and Loch Spelve anticlines and the Duart Bay and Coire Mor synclines (Bailey *et al.* 1924).

#### 6.2.2.1 Centre 1 – The Glen More Centre (Early Caldera)

The present day thickness of the Mull Lava Field is *ca.* 1800m, with an estimated 900m thickness of tholeiitic basalt flows preserved as screens within the Central Complex. Hydrothermal mineral distribution patterns suggest that 1200m have been eroded from the lava pile in the Ben More area (Walker, G. P. L. 1971). The tholeiitic basalt screens within the Central Complex are hydrothermally altered, and pillow lavas were interpreted by Bailey *et al.* (1924) as having been derived from the youngest part of the Mull Lava Field (the Central Lava Formation). These lavas give a combined weighted mean Ar-Ar age of  $59.05 \pm 0.27$  Ma (Chambers & Pringle 2001). In the vicinity of the Centre 1 intrusions, the

lavas were downfaulted within the ring fracture and are preserved both inside and outside the main marginal fault. This area of Mull therefore represents the early stages of a subsiding caldera where fractures were active and the caldera was periodically filled by lakes (Bailey *et al.* 1924). These rocks were subsequently cut by early acid intrusions, the Glass Bheinn and Derrynaculen granites, whose emplacement was controlled by ring faults, causing central collapse (Bailey *et al.* 1924). Following the trace of the ring fault are breccia deposits containing sub-angular to sub-rounded clasts of chaotically arranged lithologies, including lava material, Mesozoic sedimentary rocks, Moine gneiss and coarse-grained igneous rocks. Bailey *et al.* (1924) suggested these rocks were formed by gas streaming from silicic magmas, in order to explain the presence of brecciated rhyolite as clasts within the breccia. The intrusion of more silicic magma occurred with the emplacement of the Beinn Meadhon, Torness and Creag na h' Iolaire felsites, before finally two large gabbroic bodies (Ben Buie in the SW and Beinn Bheag in the NE) were intruded (Fig. 6.20a).

#### **6.2.2.2 Centre 2 – Beinn Chaisgidle Centre**

Igneous activity on Mull migrated towards the NW (Fig. 6.20b) with the formation of a centre around Beinn Chaisgidle. This centre contains numerous, steeply dipping, outward inclined, basic and acidic ring dykes, and younger, inward inclined basalt and dolerite (Late Suite) cone sheets.

#### **6.2.2.3 Centre 3 – Loch Ba Centre (Late Caldera)**

Two large granitic intrusions, the Glen Cannel and Beinn a' Ghraig granophyres, were emplaced early in the formation of the Loch Ba Centre and were cut by the continued intrusion of Late Suite cone sheets. The Loch Ba Ring Dyke, a hybrid mixed magma intrusion was then emplaced (Bailey *et al.*, 1924; Sparks 1988). This was the last major event in the Mull Central Complex and has been dated at  $58.48 \pm 0.18$  Ma (Chambers & Pringle 2001). The Glen Cannel Granite is an oval, dome-shaped body, predominantly within the subsided block interior to the ring dyke, whereas the younger Beinn a' Ghraig Granite is located outwith the ring dyke, at its NW margin. Similar intrusions are found on the NE side of Loch Ba (Fig. 6.20c).

The Loch Ba Ring Dyke, first described by Bailey *et al.* (1924), is typically vertical, *ca.* 8km in diameter and 400m wide. It is absent in some areas, and the trace of the ring fault is

marked only by brecciation of the country rock. Walker & Skelhorn (1966) and Sparks (1988) have discussed its origin. The intrusion is dominated by silicic rock (rhyolite or felsite) with inclusions of basic and more evolved material, typically <10mm across. Glassy inclusions with irregular margins and globular morphologies are also present. Fiamme with eutaxitic texture and flow banding are present, providing evidence of a pyroclastic formation (Sparks 1988). The idea of a compositionally stratified magma chamber (basalt through dacite to rhyolite) was suggested by Sparks (1988), whereby a complete mixing occurred between rhyolitic magma and subjacent magma(s).

The hotter basic magmas released heat during this mixing, which was then absorbed by the rhyolitic magma, causing sudden, explosive vesiculation. The pyroclastic material then ascended the ring fracture and formed the ring dyke (Sparks 1988). Gas escape brecciated the surrounding country rock, before central subsidence occurred. Venting of ring dyke, mixed magma material may also have occurred, although no evidence of this is identified.

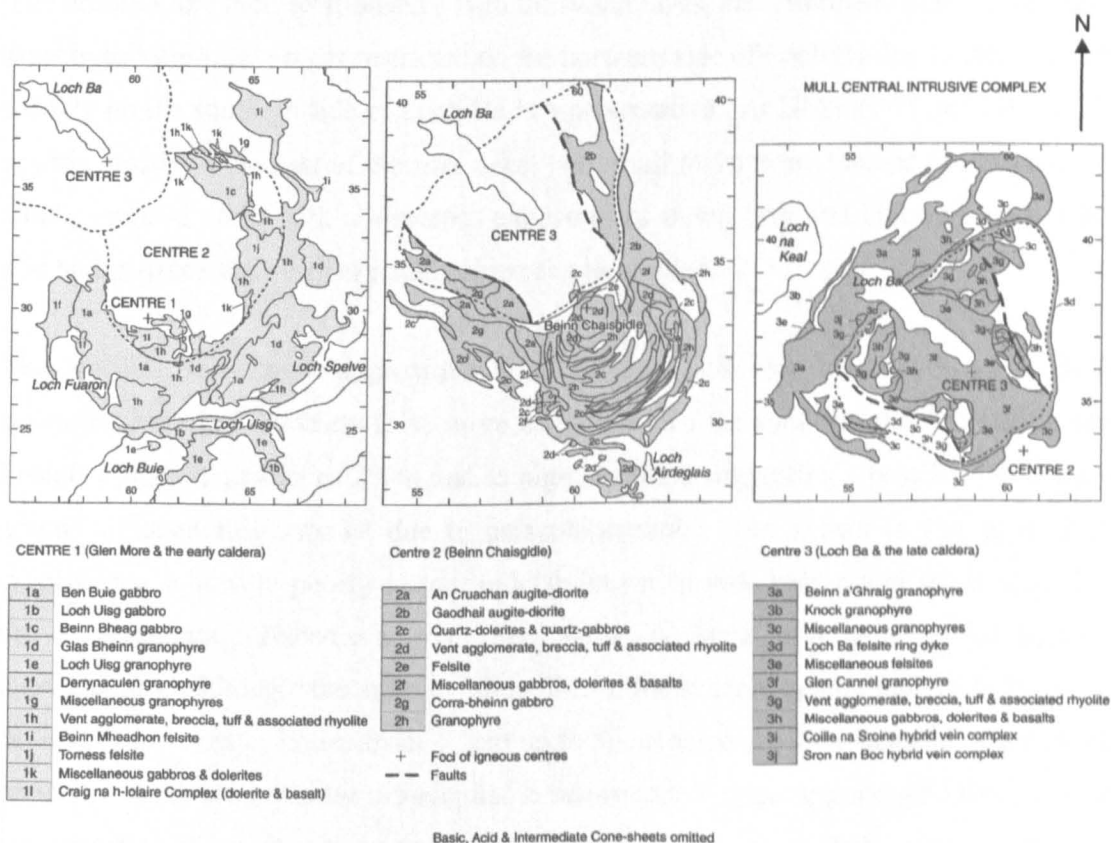


**Fig. 6.20 – Simplified geological maps of stages of the Mull Central Complex. a) Geological map of Centre 1 (Glen More), Mull Central Complex. b) Geological map of Centre 2 (Beinn Chaisgidle), Mull Central Complex. c) Geological map of Centre 3 (Loch Ba), Mull Central Complex (from Bell & Williamson 2002, after BGS 1992). Numbers at frame of map are OS grid references.**

Within the interior, subsided block of the Loch Ba Ring Dyke, a series of breccias are recognised that were interpreted as vent agglomerates (Bailey *et al.* 1924). Associated with these are rhyolites, minor dolerite intrusions and basalt screens of the Central Lava Group. The breccias will be described, and their relationship with the Central Lava Group basalts explained.

### 6.2.3 Loch Ba Breccia Formation

Preserved within the Loch Ba Centre are assemblages of chaotically arranged breccias, comprising sub-rounded to sub-angular clasts set within a fine-grained sand-grade matrix, which will be referred to as the Loch Ba Breccia Formation (Fig. 6.21). The proportion of sub-angular clasts requires that they be termed breccias and not conglomerates (Cas & Wright 1987).

The breccias and their relationships with the basalt lavas, are described below. Exposure is poor in this area and access restricted on the northern side of Loch Ba due to forestry. One locality on the southern side of Loch Ba is representative. At NM556373 and NM557371, approximately 200m east of the ring dyke, two small lochans are located to the south of a small, rounded 364m hill. Numerous exposures of basalt lava and breccia crop out here and both surface and vertical relationships can be studied.

The breccias lie between approximately 250m and 350m above sea level, although the maximum exposed thickness is no more than 50m. To the south, in the Allt Beithe area, breccia crops out as low as 250m and as high as 400m, suggesting a possible thickness of 150m, although this may be due to palaeotopography. As shown in Figure 6.22 the breccias are relatively poorly sorted, reddish-brown to grey-brown and set in a reddish-brown sand-grade tuffaceous matrix. They show considerable variation in the degree of clast support, although the matrix rarely forms more than approximately 60% of the deposit. Clasts range in size from 1-2cm up to 50cm across, with occasional larger blocks up to 1m. They are typically sub-angular to sub-rounded, with rarer rounded blocks. Clast are generally of basalt with some Moine psammities and pelites, Palaeogene granite and rhyolite and rarer blocks of Mesozoic sandstone.

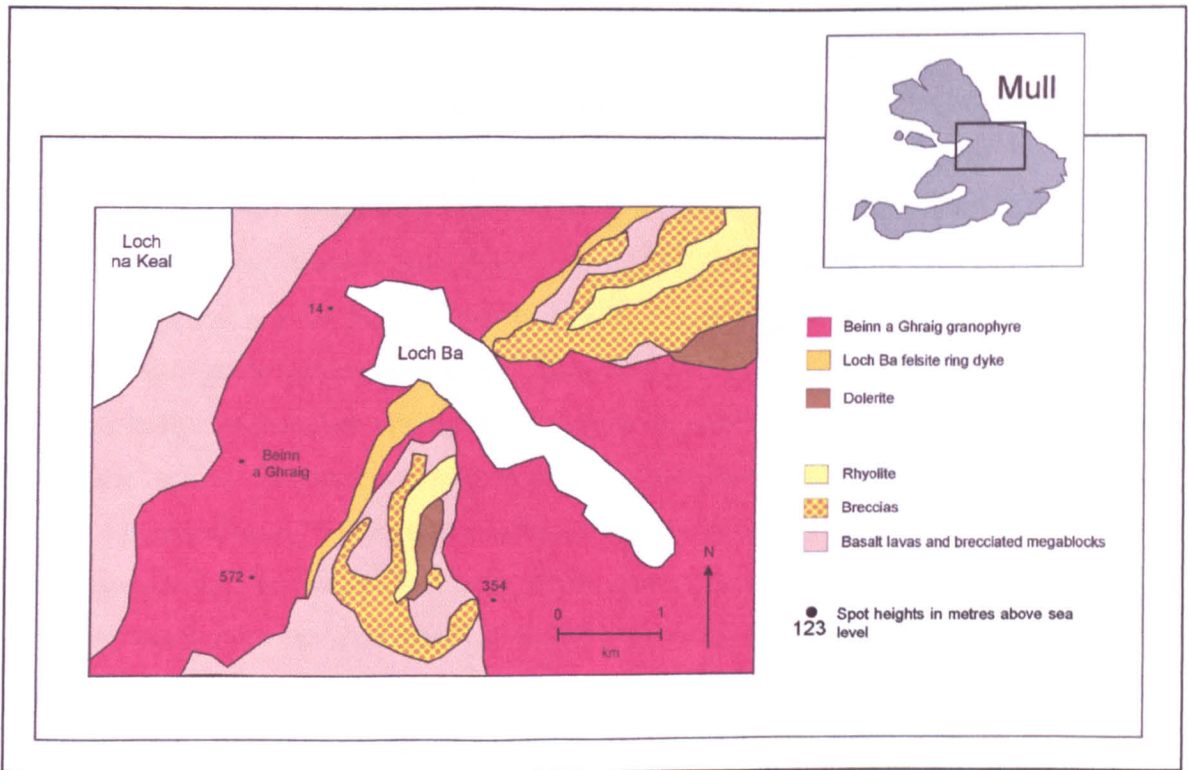


Fig. 6.21 – Simplified geological map of the area around Loch Ba, Mull (after Bailey *et al.* 1924).

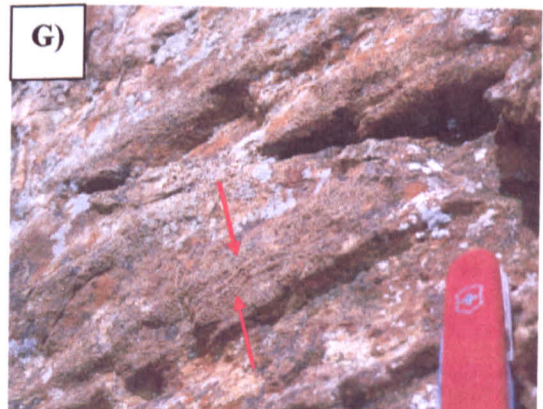
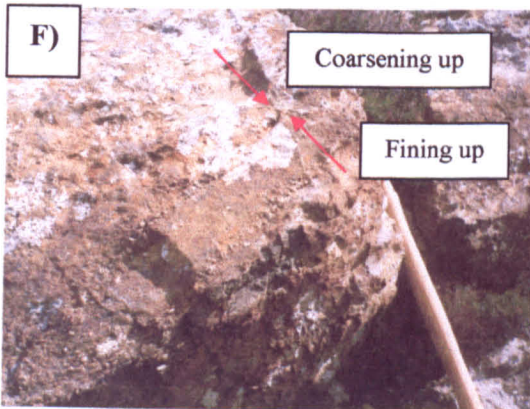
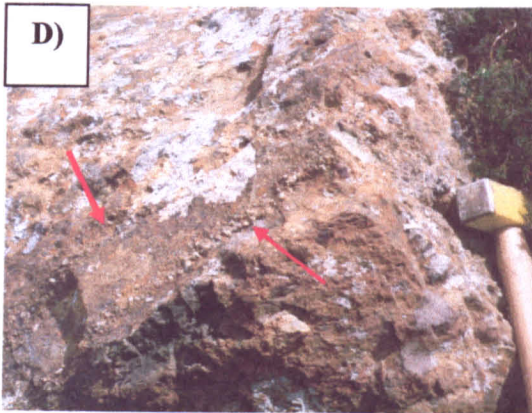
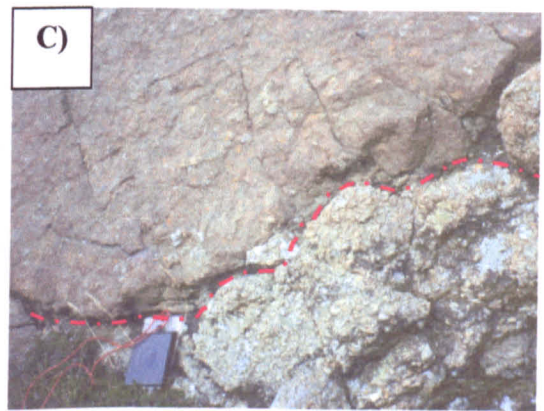
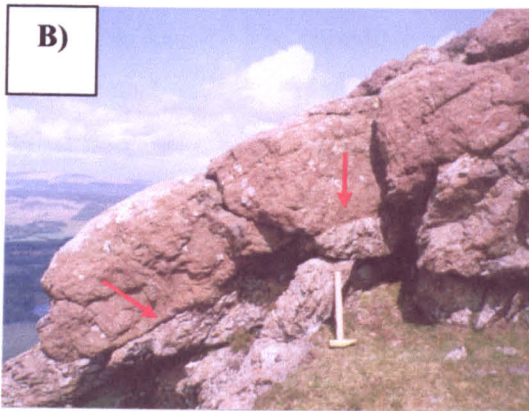


Figure 6.22 – Typical example of Loch Ba Breccia Formation deposits (NM55593724). The breccias range from clast to matrix supported, and contain clasts of sub-rounded to sub-angular basalt (*ca.* 2cm to 50cm, with rarer blocks up to 1m across).

No large-scale grading is present, but horizontal stratification is seen at NM55773732 and the 10m thick Loch Ba Breccia Formation here can be sub-divided into two distinct units.

The contact between these units is highly irregular and appears to have been folded into an anticlinal or dome structure with dips of 191/28°W and 016/35°E (Figs. 6.23a and 6.23b). The lowest unit is a 4m thick, grey-brown, coarse-grained, clast supported breccia set in a brown, sand-grade tuffaceous matrix. Clasts comprise approximately 80% of the unit, and are typically sub-rounded with rarer sub-angular examples, ranging in size from 1-2cm up to 10cm across. The unit is poorly sorted with no internal stratification. No base is seen due to poor exposure, but the upper surface is highly irregular and forms a series of troughs or channels approximately 5-10cm in depth (Fig. 6.23c). The upper unit is a 6m thick, finer-grained more matrix-supported, reddish-brown breccia (*ca.* 30 vol.% clasts), filling the small channels in the underlying breccia. The clasts are sub-angular to sub-rounded, typically 1-2cm across, with rarer blocks up to 2m across. They form a reverse grading and the unit contains numerous sedimentary structures (Fig. 6.23b). At the base of the upper unit is a 30cm thick coarse sandstone with localised pebbly sandstone layers. The pebbly sandstone layers are commonly at the base of the sandstone, though examples are identified at the top (Fig. 6.23d). These form laterally discontinuous relatively planar layers, are up to 1m in length and no more than 5cm thick. Locally, they fill small channels within the basal sandstone (Fig. 6.23e). The basal pebbly sandstone layers fine sharply upwards to brown, coarse sandstone, which then coarsens into a fine-grained matrix supported breccia (Fig. 6.23f). Fine-grained lenticular bodies of sandstone and siltstone within the breccia display wavy laminae 2-5mm in thickness (Fig. 6.23g).

At the top of this section, the upper breccia unit forms the caps of several small hills in the area. This breccia is still fine-grained and matrix supported, but numerous large sub-angular basalt clasts, typically ranging in size from 50cm to 2m across, with rarer blocks up to 10m across, are present. These blocks or megablocks, are highly fractured and shattered, whereas the matrix comprises fine-grained, comminuted basaltic material (Fig. 6.24). Locally, basalt blocks (*ca.* 90 vol.% of the deposit) dominate the breccia with only minor amounts of intervening matrix.



**Figure 6.23 – Sedimentary features from the Loch Ba Breccia Formation (NM55773732). A) Undulating nature of sub-units within the Loch Ba Breccia Formation. Bedding shows anticline or dome structure. B) Enlarged view of contact between lower and upper units in the breccia, showing relatively planar surfaces. Lower grey-brown, clast supported unit is overlain by a matrix supported, reddish brown upper unit. C) Small 5-10cm deep channels in the upper surface of the lower breccia unit. D) Localised 5cm thick, discontinuous pebbly sandstone layers in the upper breccia unit. E) Small channel structures (above knife) within pebbly sandstone at the base of the upper breccia unit. F) Normal and reverse grading within the upper breccia unit. G) 2-5cm thick, wavy laminae in lenticular body of sandstone within the upper breccia unit.**

No evidence of primary pyroclastic features, such as shaped bombs, pumice or scoriaceous basalt clasts or gas streaming is present within the breccias.

Figure 6.25 is a photomicrograph of the matrix fine-grained clast supported breccia from the lower breccia unit, comprising sub-rounded to sub-angular clasts (0.5 to 2cm across) typically of basalt. The coarser grains in the matrix (ca. 0.2mm) are closely packed and in places appear to impact into each other. Certain grain margins seem to parallel each other, so that an interlocking or jigsaw fit of clasts is maintained, suggesting pressure dissolution.

## **6.2.4 Associated rocks of the Loch Ba Breccia Formation**

### **6.2.4.1 Central Lava Group basalts**

The basaltic lavas preserved within the Loch Ba Ring Dyke are part of the Central Lava Group basalts (Bailey *et al.* 1924) but unlike those found within Centre 1 (Early Caldera) they are relatively massive, poorly vesiculated and contain no pillow structures (Bailey *et al.* 1924). No trap topography is observed in these lavas that have a very close relationship with the Loch Ba breccias, and are found together on both the northern and southern sides of the loch. Exposure is very poor, but the lavas appear to be overlain, rather than cut by, the breccia. In places the basalt is heavily fractured and shattered, and in places closely resembles, the clast supported breccia with basalt megablocks as described in Section 6.2.3 above. It can be difficult to differentiate between the basalt and breccia.

### **6.2.4.2 Rhyolites**

Small silicic (rhyolite) intrusions or domes are identified within the Loch Ba area. These poorly preserved crumbly, lithologies, represent shallow level intrusions through the breccia and basalt pile (Preston 1982). There appears to be no direct link between these and the breccias.

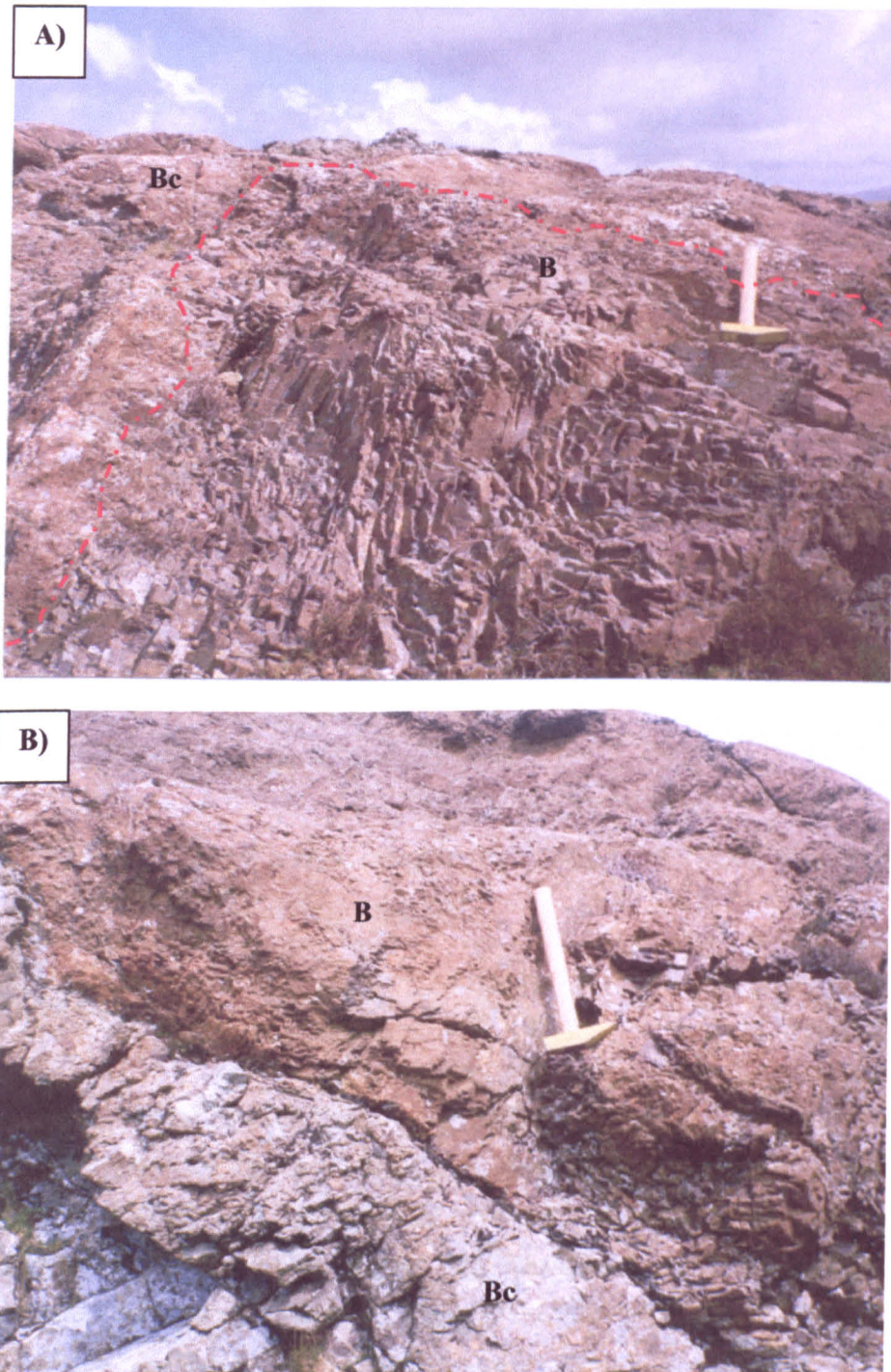


**Figure 6.24 – Fractured and shattered basalt megablocks in the Loch Ba Breccia Formation (NM55833735). A) Fractured and shattered basalt block (B), 2m across, within the upper breccia unit (Bc). B) Fractured and shattered basalt block (B), 2m across, within clast supported lower breccia unit (Bc).**

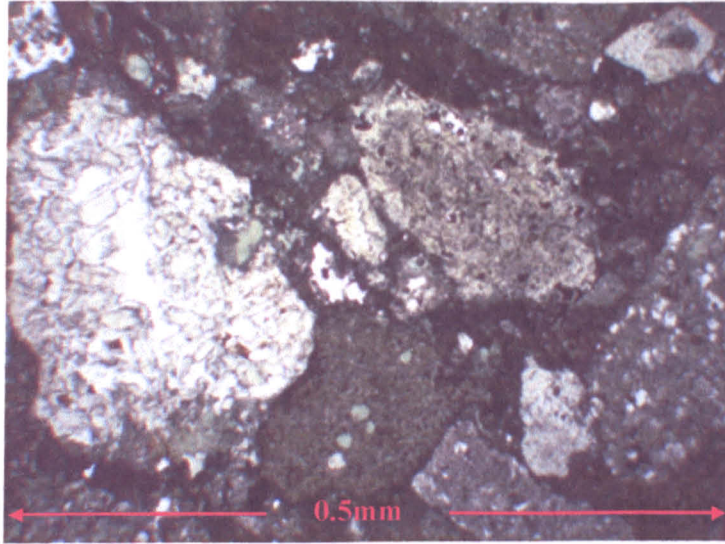


**Figure 6.25** – Photomicrograph of matrix of fine-grained clast supported breccia from the lower breccia unit of the Loch Ba Breccia Formation (NM55773732). The coarser grains (typically basalt) in the matrix (ca. 0.2mm) display an interlocking or jigsaw fit texture.

#### 6.2.4.3 Dolerites and gabbro

Small bodies of dolerite and gabbro are also found within the Loch Ba Caldera and represent late minor intrusions of basic material.

#### 6.2.5 Mode(s) of deposition

The Loch Ba Breccias are coarse-grained clastic deposits located within a fault bounded, centrally subsided block interior to the Loch Ba Ring Dyke (Centre 3) of the Mull Central Complex. These deposits were originally identified as vent agglomerates (Bailey *et al.* 1924), implying a primary pyroclastic origin. Agglomerates, however, are now defined as coarse pyroclastic deposits composed of a large proportion of rounded, fluidally shaped volcanic bombs (e.g. shaped or breadcrust types). The term implies a fall deposit indicating proximity to the vent and is best applied to the scoria deposits that build strombolian cones (Cas & Wright 1987). None of these primary pyroclastic features is present within the Loch Ba breccia, indicating that some other mode of deposition must have been involved. Clasts of rhyolite are present within the breccia but form only isolated sub-rounded clasts (<5cm) and are not traceable as single rhyolitic breccia bodies.

Rhyolite bodies are identified within the Loch Ba Centre, but appear to be shallow level intrusions into the breccia, and not directly responsible for its formation.

There is abundant evidence of epiclastic processes throughout the Loch Ba Breccia Formation (Fig. 6.23). The Formation is stratified, and distinct bedded units can be recognised, with both normal and reverse grading locally present. Within the breccia units small-scale sedimentary features such as pebbly sandstone layers, channels and slumping are identified. Small, lenticular bodies of finely laminated sandstone are present throughout the breccia units. These features all indicate transportation and deposition by sub-aerial, sedimentary processes.

Large blocks, or megablocks, of basalt up to 2m across present within the breccia are typically fractured and shattered. The blocks are supported within a fine-grained matrix, where basalt is the dominant clast type (>90%). Furthermore, the megablock dominated breccia is strongly associated with outcrops of screens of Central Lava Group basalt within the subsided block. This Central Group basalt is typically massive, and in places fractured and brecciated. Exposure is limited, but in places it appears as if large blocks of basalt are being detached from solid basalt and incorporated into the breccia (Fig. 6.24). The absence of trap topography in the Central Lava Group basalts also suggests that they are not in place and may have been subsided, as large-scale movement would destroy trap topography.

The numerous sedimentary features and the presence of basalt megablocks within the breccia suggest that these deposits were formed by mass flow processes. The presence of megablocks may indicate large landslides or collapses of material from the Central Lava Group within the subsided Loch Ba Centre. This material would have moved downslope as mass flows, shattering the basalt megablocks and providing smaller sub-rounded and sub-angular basalt clasts for incorporation within the breccia. Other lithologies sourced from the subsiding block would also be entrained and transported within these mass flows. The presence of stratification and inter-breccia sandstones indicates that there were separate, cyclical flows in both low- and high-energy environments (Leeder 1982; Yarnold 1993). Within the sandstones, discontinuous pebbly sandstone layers suggest occasional influxes of coarser material. The upper surfaces of the breccia deposits are irregular, and small channels (*ca.* 5cm deep) cut into them are filled by pebbly sandstone. These

channels provide further evidence of surface deposition. The normally graded sandstone at the base of the upper breccia unit, described in Section 6.2.3 (Fig. 6.23f), may represent the reworking of the surface of underlying breccia. Lenticular bodies of laminated sandstone and siltstone preserved within the breccias (Fig. 6.23g), suggest episodic deposition of the breccias with brief hiatuses punctuated by deposition of low-energy channel sands. The several breccias also indicate that there were multiple collapse and mass flow events.

The coarse, clast-supported breccias with intervening fine-grained deposits, display sedimentary features such as grading, bedding and channels and basalt megablocks like those of debris flow and debris avalanche deposits outlined in Chapter 4 and identified in the Ardnamurchan deposits described in Chapter 5. Such deposits are initiated by collapse of *in situ* material, typically from steep slopes such as caldera walls and valley walls. This instability can be caused by gravity, though commonly volcanic activity, uplift and/or subsidence, and heavy rainfall may be involved (Caine 1980; Smith & Lowe 1991). These blocks then moved downslope, detaching large blocks of country rock, which become fractured and brecciated. Crushing and grinding cause smaller clasts and matrix to be created, whilst loose surface material is entrained and incorporated within the mass flow (Glicken 1986; Schneider & Fisher 1998; Kessler & Bedard 2000). These flows produce coarse-grained, poorly sorted breccia deposits containing sub-rounded to sub-angular clasts and occasional megablocks. Jigsaw fit textures are common within debris avalanche breccias (Ui 1985; Yarnold 1993) and are recognised within the LBBF (Fig. 6.25). Units can be graded, overlapping channel flows may be present, and debris flows/avalanches are often associated with fine-grained deposits (Glicken 1986, 1991; Smith & Lowe 1991; Yarnold 1993; Blair & McPherson 1994; Coussot & Meunier 1996). These characteristics are all identified within the Loch Ba Breccia Formation, emphasising that they were formed by epiclastic, mass flow processes.

Mass flow processes are commonly triggered by instability in the form of volcanic activity, uplift, subsidence etc. The Loch Ba Centre (or Late Caldera) is interpreted as an active, fault-bounded caldera into which large granite bodies, felsites and rhyolites were emplaced (Bailey *et al.* 1924). These intrusions would have caused substantial uplift and instability and, as they were emplaced around the fault-controlled margins of the Centre, subsidence occurred within the ring fault preserving the outcrop of the Central Group Lavas on the caldera floor (Bailey *et al.* 1924). This subsidence and/or uplift may have led to catastrophic collapses, which would have initiated mass flows. This mechanism explains

the presence of granite, felsite and rhyolite clasts within the breccias, as these could have been sourced from earlier intrusions on the caldera floor or walls. Rhyolite also appears as small shallow intrusions piercing the breccia (see section 6.2.4.2 above, Fig. 6.21) at Loch Ba. Although this rhyolite is not directly linked to the formation of the breccia, clasts of similar material are found within the breccia, suggesting comparable rhyolite was intruded early in the Centre, and was available for incorporation in the breccia. The emplacement of the earlier rhyolite may have contributed to the instability leading to mass flows. The final event in the Loch Ba Centre was the emplacement of the Loch Ba Ring Dyke (Bailey *et al.* 1924). The breccias are clearly older than this as they contain no mixed magma ring dyke material.

The rare clasts of Moine gneiss in the Loch Ba Breccia Formation are not represented in local outcrops. The nearest exposures of Moine material are *ca.* 12km to the east in the Sgurr Dearg area, outwith the Loch Ba Centre, and on the margins of Centre 1 (Glen More Centre). This is most likely too great a distance to transport clasts in the mass flows identified in the Loch Ba Centre. However, the outcrops of Moine rocks at Sgurr Dearg are exposed at approximately 700m above sea level, considerably higher than the Loch Ba breccias (*ca.* 300m above sea level). As the Loch Ba Centre is interpreted as a caldera with central subsidence, this may tentatively suggest that Moine outcrops from a higher structural level (no longer preserved) could have collapsed into the caldera, or formed part of a subsiding block.

## 6.2.6 Conclusions

The Mull Central Complex comprises three centres of igneous activity migrating sequentially in a NW direction. The last of these centres, the Loch Ba Centre (or Late Caldera) is a fault-bounded structure with central subsidence. Within the subsided block a series of stratified breccias and associated basalt lavas and rhyolites can be identified. Clasts range in size from 1-2cm to 50cm across with rarer blocks up to 2m, and are typically sub-rounded to sub-angular with varying degrees of clast support. Clasts are typically of basalt, with some granite, felsite, rhyolite, Moine gneiss and (rare) sandstone. Shattered and fractured basaltic megablocks up to 2m across are identified. Bedded units can be recognised within the breccia and intervening fine-grained sandstones display sedimentary features including grading and fine-scale lamination, and channels and erosional surfaces are present. These characteristics indicate an epiclastic mass flow

origin. Large blocks of basalt are detached from steep slopes and move downslope in flows. The blocks become fractured and loose surface material is entrained. Such high-energy, catastrophic events are episodic, with intervening periods characterised by low-energy sedimentation and surface reworking. There is no evidence of a pyroclastic influence. The initiation of these deposits may be linked to uplift and/or (caldera) subsidence.

### 6.3 Coire Mor

To the west of Craignure (Fig. 6.26), the breccias of Coire Mor form a large outcrop within the Coire Mor Syncline, outside the margin of Centre 1 (Glen More Centre) of the Mull Central Complex. The rocks of the Coire Mor Syncline are thought to have been folded by the emplacement of the Glen More Centre (Bailey *et al.* 1924) and subsequently the Coire Mor breccias were deposited on top of the basalt lavas in this area. Bailey *et al.* (1924) interpreted these breccias as surface accumulations and again used the term 'agglomerate.'

The Coire Mor deposits are a thick succession of grey-brown, coarse, matrix-supported breccias, containing sub-angular to rounded clasts, ranging in size from 2cm to 50cm across with rarer blocks up to 3m across (Fig. 6.27). Clast lithologies include basalt, granite, flow banded rhyolite, Moine psammities and pelites and Mesozoic sedimentary rocks. The rocks are relatively unstratified, and vague bedding is seen only locally.

Relationships in the Coire Mor deposits are obscured by a profusion of basic, intermediate and silicic cone sheets. The relatively uniform nature of these deposits and their multiple intrusion by cone sheets makes an accurate assessment of their origin difficult. There is however, no evidence of primary pyroclastic material, such as fluidally shaped bombs (Cas & Wright 1987) and therefore the term agglomerate is inappropriate for these deposits. The breccias clearly rest upon basalt lavas, and this indicates a sub-aerial origin for these deposits. The emplacement of the Mull Central Complex may have initiated surface collapse processes.

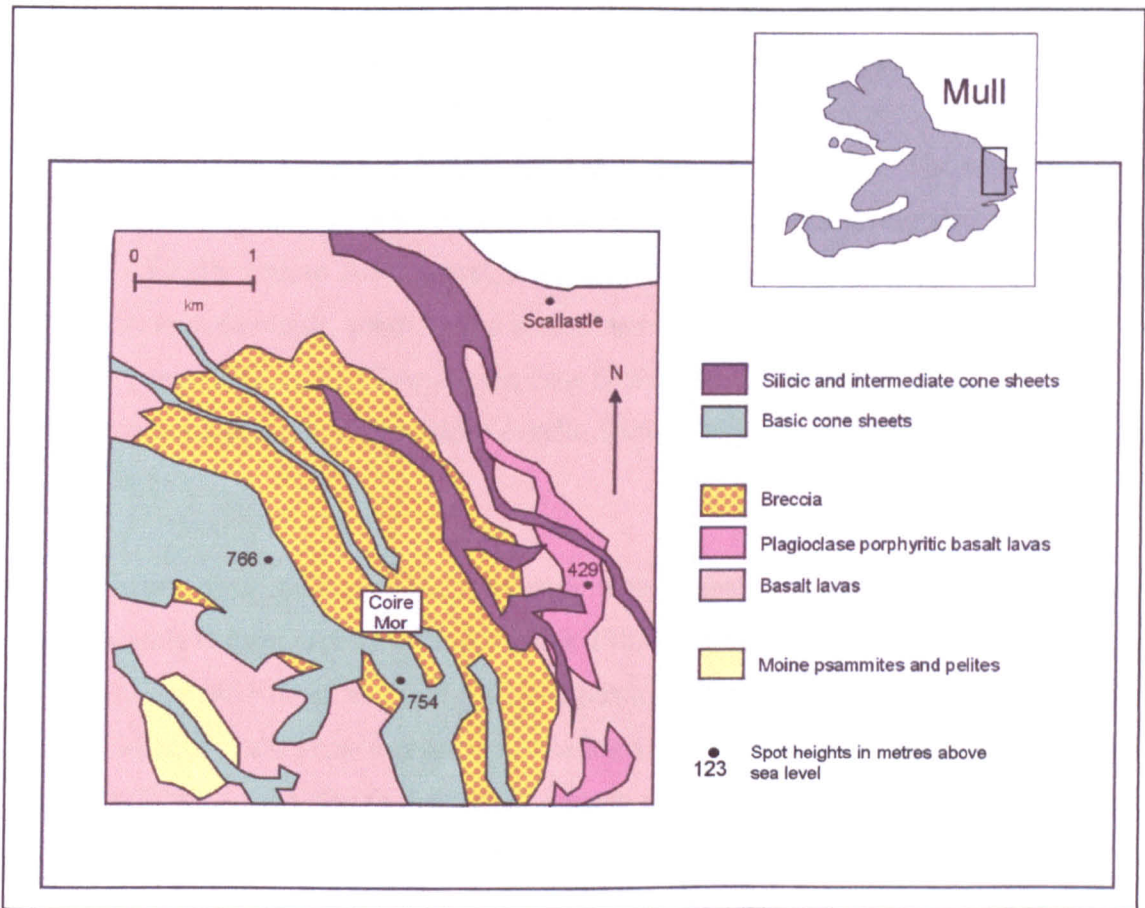


Figure 6.26 – Simplified geological map of the area around Coire Mor, Eastern Mull (after BGS 1992).

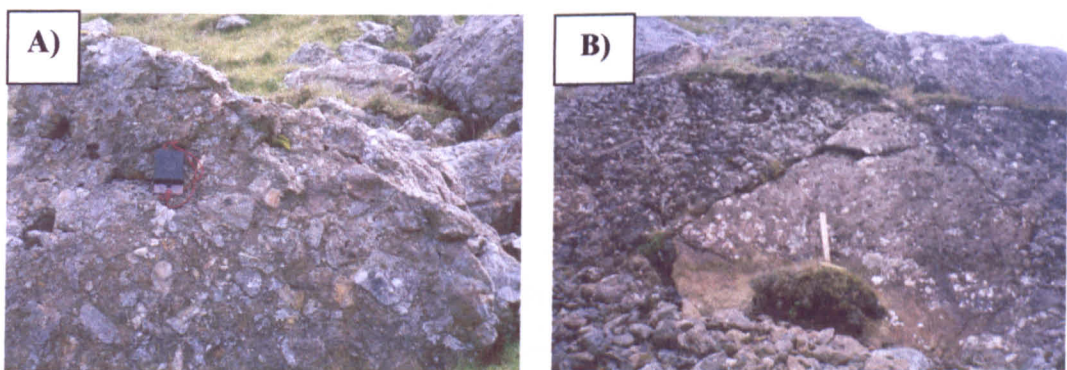


Figure 6.27 – Field photographs of textures within the Coire Mor breccias (NM695355). A) Coire Mor matrix supported breccia, comprising sub-rounded to sub-angular clasts, typically 2cm to 50cm across. B) Large rounded basalt block (*ca.* 2m across) within vaguely stratified breccia.

## 6.4 Barachandroman

At the SW end of Loch Spelve at the margin of the Glen More Centre (Centre 1) of the Mull Central Complex, the Barachandroman breccias crop out over an area of 1km<sup>2</sup> and may represent a continuation of the Coire Mor breccias (see Section 6.3 above) (Fig. 6.28). Bailey *et al.* (1924) interpreted these rocks as surface agglomerates. The breccias form an unstratified, matrix supported unit, *ca.* 10m thick, comprising sub-rounded to sub-angular clasts, typically 2cm to 20cm across, with larger blocks *ca.* 70cm across. Clast lithologies typically include basalt, quartzite and sandstone (most likely Triassic) and rarer granite and Moine gneiss (Fig. 6.29). Towards the base of the unit deformed quartzose sandstones and mudstones are present. The breccias overlie Tertiary basalt lavas on a surface sloping at an angle of 25°.

No primary pyroclastic material is present within these breccias and therefore the term agglomerate is inappropriate (Cas & Wright 1987). A brief inspection confirmed that these deposits resemble those in Coire Mor, suggesting a similar mode of origin. Bailey *et al.* (1924) describe “the lavas merging into the breccias without a sharp plane of demarcation. This, combined with the fairly certain appearance of superposition of breccia on lava, suggests that the lavas were breaking up under subaerial decay at the time of breccia gathered upon them.” This description equates with the idea of blocks of basalt being detached from a lava field by instability (possible collapse), accumulating as basaltic debris and being transported within a mass flow.

## 6.5 Salen

The Plateau Group of the Mull Lava Field crops out in the area around the village of Salen on the central eastern coast of Mull. The most common lavas in this group are basalts and picritic basalts, although rarer evolved flows are also identified. A trachytic plug and flow forms a NE trending ridge outside the village of Salen, with rocks previously interpreted as vent agglomerates cropping out at its NE edge (BGS 1992) (Fig. 6.30).

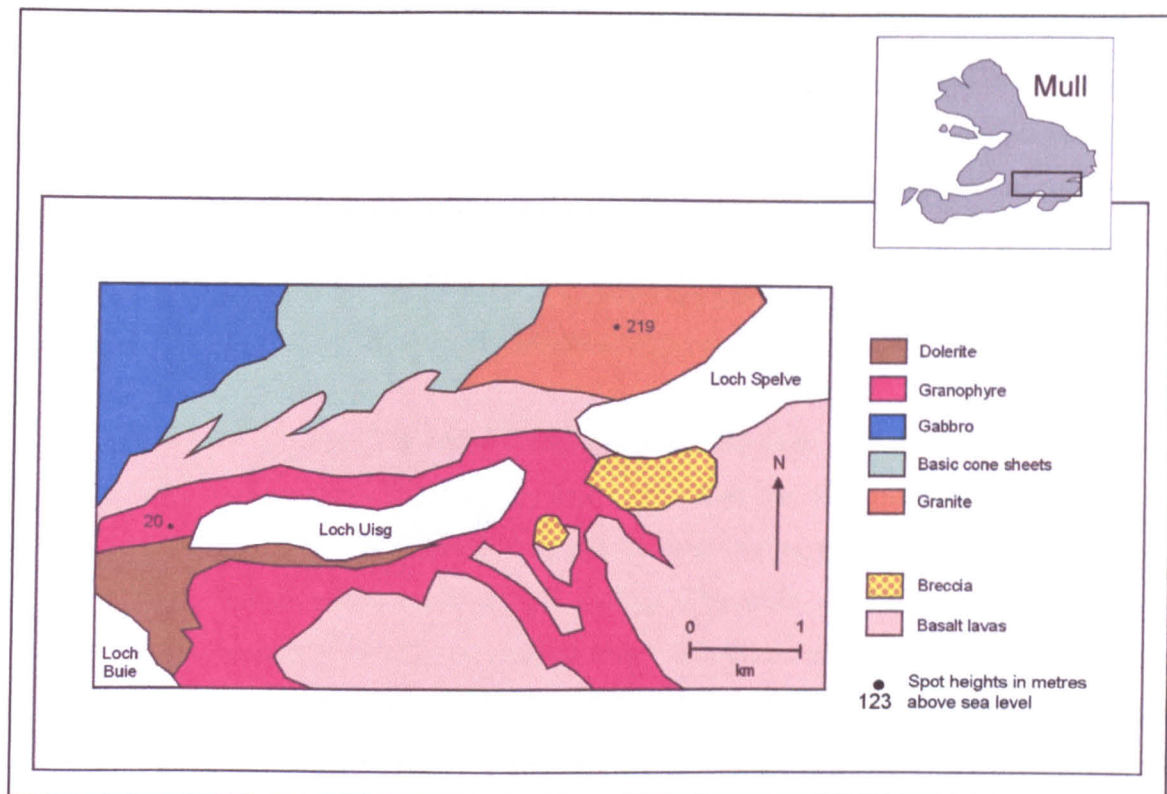


Figure 6.28 – Simplified geological map of the area around Barachandroman on the banks of Loch Spelve, South Mull (after BGS 1992).



Figure 6.29 – Field photograph of textures within the Barachandroman breccias (NM66252557). Reddish-brown, matrix supported breccia, comprising sub-rounded to sub-angular clasts, typically 2cm to 20cm across.

The trachyte is pale grey to mid-grey and well-jointed, with a faint flow banding. Small exposures of poorly stratified breccia fill a depression at the base of the leading NE edge of the flow and spread out over a short distance (*ca.* 75m). These clast-supported deposits comprise sub-angular and rarer sub-rounded clasts of trachyte and basalt in a dark grey sand-grade matrix. Clasts are commonly, 2cm to 30cm across, although numerous blocks of shattered trachyte and basalt up to 1m across are present (Fig. 6.31). There is a vague stratification and at one locality, two distinct units can be recognised.

These deposits are clearly derived from the trachyte lava flow and appear to have collapsed into a small local depression, perhaps a dry valley, at the NE end of the trachyte. The larger blocks of trachyte and basalt represent material that was detached from the lava field and accumulated as basaltic and trachytic debris. The more angular nature of the clasts in this deposit suggests the blocks travelled a very short distance. Collapse may be linked to instability due to the emplacement of the Mull Central Complex. No primary pyroclastic material is present, confirming the epiclastic origin of these breccias, and therefore the term vent agglomerate is inappropriate (Cas & Wright 1987).

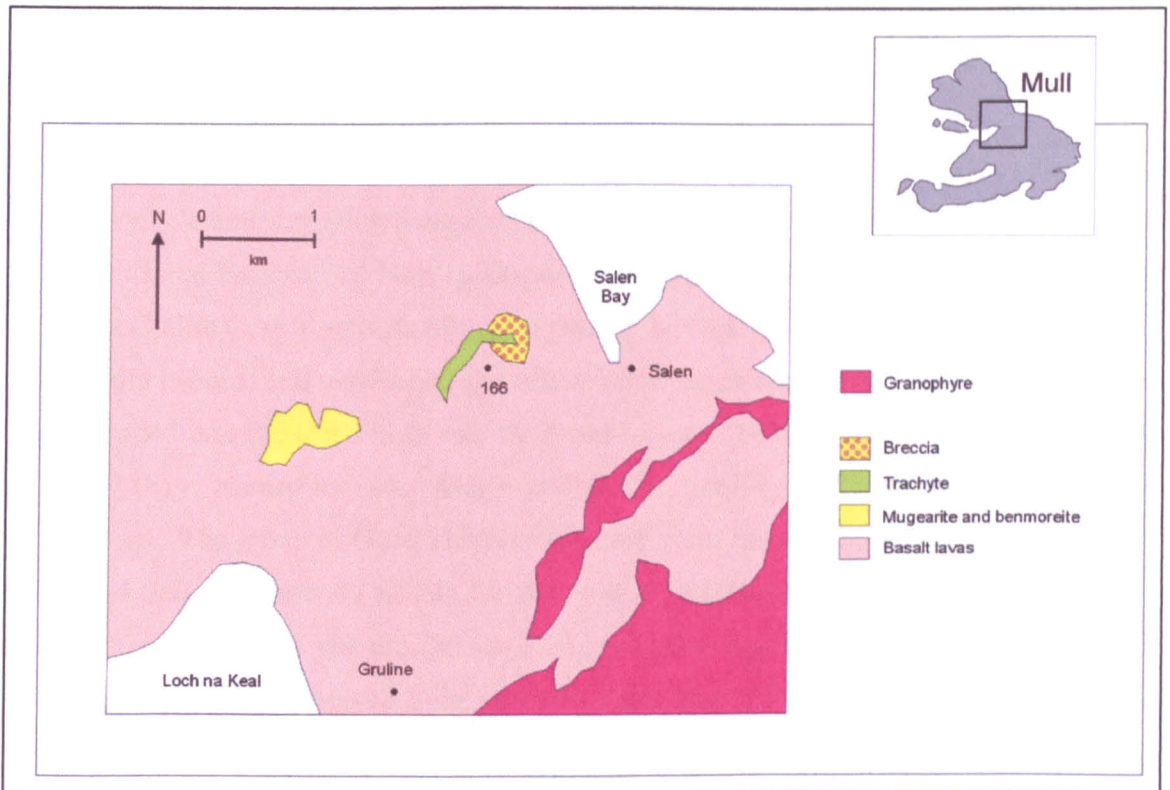


Figure 6.30 - Simplified geological map of the area around Salen, Eastern Mull (after BGS 1992).



Figure 6.31 - Field photograph of textures within the Salen breccias (NM56054340). Clast supported grey-brown breccia comprising sub-angular clasts of trachyte and basalt (ca. 2cm to 30cm across) with larger blocks up to 1m across.

## 7 Skye

### 7.1 Regional setting

The Skye Central Complex comprises the Cuillin (oldest), Srath na Creitheach, Western Red Hills and Eastern Red Hills (youngest) centres (Bell & Harris 1986) (Fig. 7.1a). The earliest Cuillin Centre consists of coarse-grained layered and unlayered intrusions of basic (typically gabbro) and ultrabasic (typically feldspathic peridotite) composition that may be sub-divided into the Outer Gabbros, the Outer Layered Suite and the Inner Layered Suite (Fig. 7.1b). Numerous cone sheets and a NW trending dyke swarm cut these ring intrusions. The group of Outer Gabbro intrusions form the main Cuillin ridge. The Outer Layered Suite comprises a xenolithic tholeiitic dolerite grading into a massive bytownite troctolite. Interior to this are the Layered Peridotites and the Outer Layered Bytownite Gabbros. The Inner Layered Suite comprises the Inner Gabbros and the Inner Bytownite Troctolites. A silicic intrusion, the Coire Uaigneich Granite crops out along the SE margin of the Centre (Fig 7.1b). Erosion of *ca.* 2km of rock from above the Cuillin Centre has removed much of the evidence as to the nature of its volcanic superstructure, although geochemical evidence indicates that the Talisker Lava Formation of west central Skye was erupted from a Cuillin Volcano (Williamson & Bell 1994).

The Srath na Creitheach Centre comprises three granite bodies: Meall Dearg, Ruadh Stac and Blaven that were intruded into the NE margin of the Cuillin Centre. The Meall Dearg Granite comprises two sheets of variable composition, and the younger Ruadh Stac Granite lies beneath these. The age relationships of the Blaven Granite cannot be determined. A large outcrop of coarse volcanoclastic breccia, defined by a ring fault lies at the southern end of the Srath na Creitheach Centre (Jassim & Gass 1970) (Fig. 7.1b). The breccias are coarse, poorly sorted, unstratified deposits, typically comprising sub-rounded to angular clasts of gabbro, basalt and dolerite. Large slabs of gabbro and laterally discontinuous sandstones are also recognised. These deposits were interpreted as vent agglomerates (Harker 1904) and Jassim & Gass (1970) described processes involving gas fluidisation and the collapse of caldera walls to explain their formation. This work will be reviewed in detail in Section 7.2.

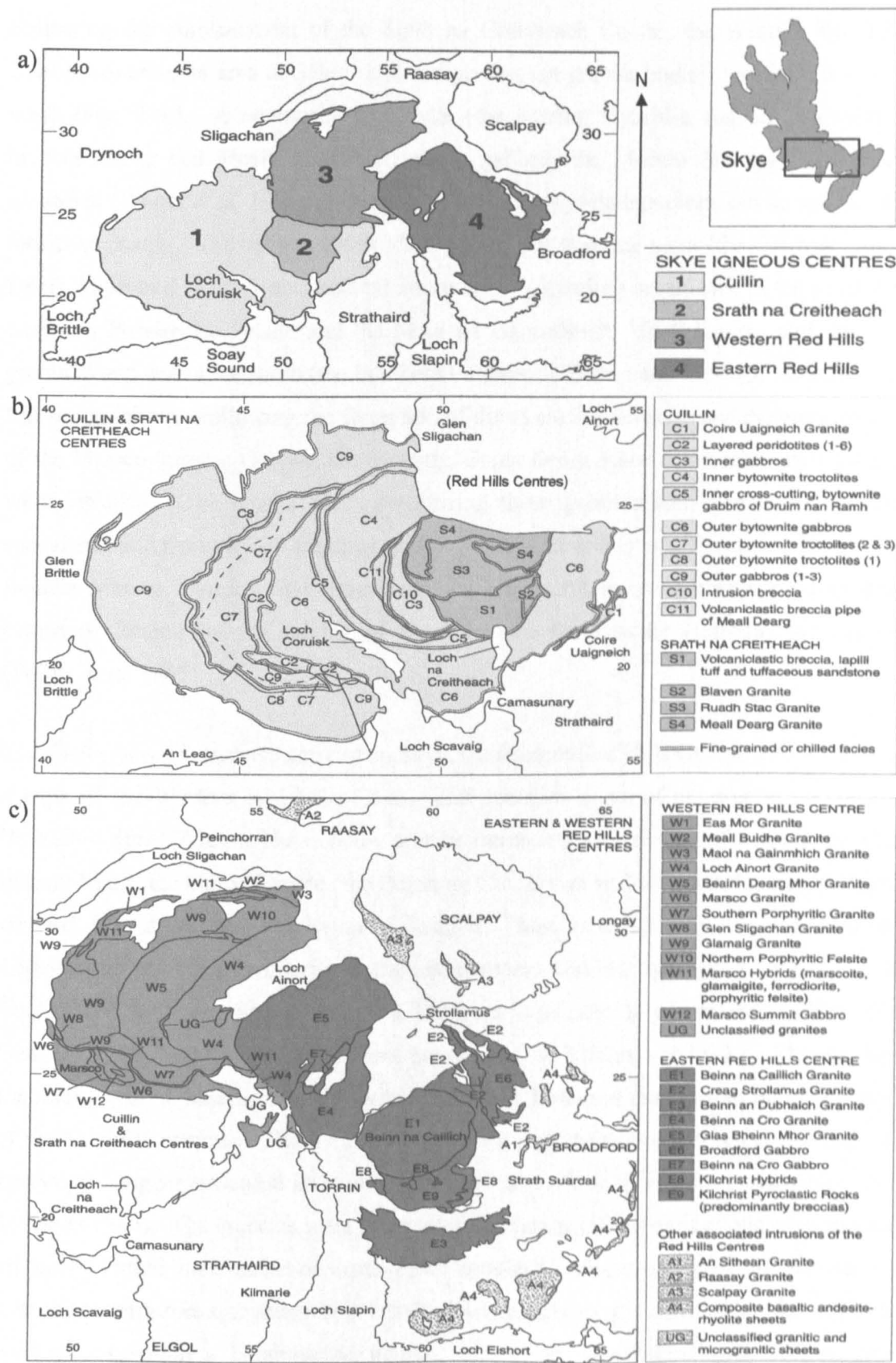


Figure 7.1 – Simplified geological map showing centres of the Skye Central Complex. Figures at frames of maps are OS grid references, with 5km increments. a) Generalised geological map of the Skye Central Complex. b) Geological map of the Cuillin and Srath na Creitheach centres. c) Geological map of the Western Red Hills and Eastern Red Hills Centres (from Bell & Williamson 2002).

Following the emplacement of the Srath na Creitheach Centre, the Western Red Hills Centre, covering an area of 35km<sup>2</sup> and comprising ten granite bodies, was intruded to the north (Fig. 7.1c). A composite ring dyke (the Marsco Hybrids), masses of explosion breccia (Belig and Meall a' Mhaoil) and a gabbro (the Marsco Summit Gabbro) are identified (Wager *et al.* 1965; Thompson 1969). The granite intrusions can be sub-divided into two groups. Thompson (1969) identified a N-S trending suite (the Glamaig, Beinn Dearg Mhor and Loch Ainort bodies) and two E-W trending suites, one in the north (the Northern Porphyritic Felsite and the Maol na Gainmheich, Meall Buidhe and Eas Mor granites) and one in the south (the Southern Porphyritic Felsite and the Glen Sligachan and Marsco granites). Following the formation of the explosion breccias and the emplacement of the Marsco Summit Gabbro, the Glamaig, Beinn Dearg Mhor and Loch Ainort granites were intruded. The crustal block comprising these granites then underwent cauldron subsidence and the two E-W trending granite suites were emplaced (Thompson 1969). The famous Marsco Hybrids first described by Harker (1904) are a composite ring dyke intrusion, formed by the mixing of rhyolitic and ferrobaltic (ferrodiorite) magmas (Wager *et al.* 1965).

The final centre of intrusive activity on Skye, the Eastern Red Hills Centre, cuts the eastern margin of the Western Red Hills Centre, and occupies much of the area to the west of Broadford (Fig. 7.1c). Three main granite intrusions are identified, comprising Glas Bheinn Mhor, the Outer Granite (the Beinn na Cro, Beinn an Dubhaich, Creag Strollamus and Allt Ferana granites) and Beinn na Caillich. These were typically emplaced into pre-Tertiary country rocks giving rise to thermal aureoles, and locally to skarn mineralisation. To the south of Beinn na Caillich, at Kilchrist, a large outcrop of breccia (Harker 1904; Bell, B. R. 1985) is cut by five hybrid intrusions (the Kilchrist Hybrids). These hybrid intrusions contain basaltic material within a granitic host, and crop out around the margin of the Kilchrist breccias. The hybrid rocks form a ring dyke, suggesting that the breccias formed at a higher structural level and underwent some form of cauldron subsidence (Bell & Harris 1986). The breccias were interpreted by Harker (1904) as vent agglomerates and are poorly sorted, unstratified deposits of sub-angular to sub-rounded clasts of various pre-Tertiary country rocks, together with basalt, dolerite, gabbro, rhyolite, ignimbrite and older breccia, set within a comminuted matrix. They are interbedded with volcanoclastic sandstones and various rhyolitic and ignimbritic bodies. Bell (1985) interpreted the breccias as forming by epiclastic processes with the eruption of various silicic pyroclastic bodies, and this hypothesis will be reviewed in Section 7.3.

## 7.2 Srath na Creitheach

### 7.2.1 Introduction

The breccias of Srath na Creitheach crop out over a *ca.* 2km<sup>2</sup> area in the valley between Blaven and Druim Hain, at the northern end of Loch na Creitheach. Jassim & Gass (1970) assigned them to the Srath na Creitheach Centre. The breccias are coarse, poorly sorted, unstratified deposits, comprising sub-rounded to angular clasts typically of gabbro, basalt and dolerite but large slabs of gabbro and laterally discontinuous sandstones are also recognised. Harker (1904) interpreted these rocks as vent agglomerates but Jassim (1970) and Jassim and Gass (1970) explained their formation in terms of processes involving gas fluidisation and the collapse of caldera walls. Following descriptions of the breccias their modes of formation will be reviewed below.

### 7.2.2 Previous Research

The breccias of Srath na Creitheach have been described in much detail. Harker (1904) defined a lenticular shaped vent (*ca.* 1.5km across and 100-150m thick) filled with angular fragments, typically of gabbro and basalt, of various size. Harker also identified an irregularly distributed fine-grained tuff with dark and light grey bands with varying dips. He suggested an explosive vent ripped through overlying rocks forming agglomerates and that the disrupted tuffs indicate further eruptions from the vent or uneven settling of material within the vent.

An excellent, detailed re-investigation of the breccias was carried out by Jassim and Gass (1970). They recognised Harker's vent agglomerates and referred to them as the Loch na Creitheach volcanic vent. This *ca.* 2km<sup>2</sup> structure has a faulted contact with the Cuillin gabbro, and the presence of gabbro megablocks of Cuillin material within the 'vent' indicated that it is younger than the Cuillin Centre. Granites of the Srath na Creitheach Centre cut the 'vent,' and a chilled margin is seen at the contact with the Ruadh Stac Granite. Jassim & Gass (1970) also identified a vertical outer contact with a zone of crushing 5m to 15m wide. They described two main rock types, pyroclastic debris ranging from coarse agglomerates to well-bedded fine-grained tuffs, and large, generally concordant slabs of gabbro 'interbedded' with the pyroclastic material.

Angular fragments in the 'agglomerate' are dominated by basalt and gabbro, with rarer peridotite, bedded tuff, and trachyte (Jassim & Gass 1970). Both non-porphyritic and a rarer olivine porphyritic basalt are present. Gabbro clasts are typically sub-rounded and *ca.* 15cm across. Sub-angular blocks of banded tuff with numerous plagioclase crystal fragments occur along with rarer poorly bedded, elongate tuff masses *ca.* 30m in length. Jassim & Gass (1970) suggested that *ca.* 15cm blocks of peridotite were sourced from xenolithic gabbro in the Cuillin Centre. Intercalated within the 'agglomerate' are two, well-bedded, typically normally graded 'tuff' horizons ranging from 30cm to 2m thick and dipping at 15 to 50° to the NW. The obvious layering within these is due to the alternation of *ca.* 2mm thick laminae of fine and coarse material. Jassim & Gass (1970) noted that some large gabbro blocks had apparently fallen into the bedded tuffs and produced 'bomb-sag' features. They suggested that the presence of graded bedding, bomb-sags and persistent bedding indicated that the bedded tuffs were pyroclastic material deposited under subaerial conditions.

Jassim & Gass (1970) identified thirteen large gabbro slabs within the agglomerate ranging in length from 40m to 900m which display brecciated or sharp contacts with the agglomerate and/or tuff (Fig. 7.2). They recognised three gabbro types (granular, ophitic and porphyritic) and identified calcic plagioclase from the granular material that is comparable to calcic phenocrysts from the bytownite gabbros of the Cuillin Centre, as described by Carr (1952) and Zinovieff (1958). Many of the gabbro slabs are brecciated, with disruption ranging from mild crystal fracturing to heavily fractured crystals set in a fragmented groundmass of gabbroic material. Jassim & Gass (1970) suggested the brecciation was caused in two ways: 1) as a result of crushing induced by the collapse of the slab and 2) by the more significant process of gas streaming (Zinovieff 1958). They argued that the interpretation of gas streaming was supported by the presence of vesicles, which are not present in non-brecciated parts of the slabs, and by the absence of juvenile pyroclastic material.

In summary, Jassim & Gass (1970) suggested that a large vent burst through the Cuillin gabbro and (presumed) overlying basalt lava. They considered that the explosive agent was gaseous rather than liquid, due to the absence of 'live pyroclastic debris.' The subsequent collapse of the vent walls filled the edifice and enlarged the vent. Further explosive activity within the caldera, produced poorly bedded tuffs and agglomerates and finely bedded tuffs. At times during this period, gabbro slabs then collapsed into the caldera.

Jassim & Gass (1970) argued that the pyroclastic deposits were either lithified before the arrival of the slabs and so were unaffected, or that the pyroclastic materials were soft and unlithified, cushioning the impacts of the slabs and preventing extensive fracturing. Due to the proposed rapid explosive history of this event, they favoured the latter explanation. They also argued that the slabs had toppled into the caldera rather than slid in by a bottom first landslide motion, although they presented no evidence to support this hypothesis. Jassim & Gass (1970) also argued that further activity took place beneath the slabs following their collapse, as in areas of active gas streaming, the unconsolidated tuffs were fluidised, and in many cases they vein the gabbro. The entire vent structure was thought to have subsided some 750-1000 metres along marginal ring fractures. Finally, as the Red Hills granites intruded the region, associated faulting tilted the pyroclastic materials.

### **7.2.3 Srath na Creitheach Breccia Formation**

Jassim & Gass (1970) provided an excellent map and description of the Srath na Creitheach deposits. Many of their arguments appear correct and they provide strong evidence for the suggested mechanism of formation of these deposits. However, new observations provide further insights into the genesis of the Srath na Creitheach Breccia Formation (SNCBF) deposits.

As previously described the breccias are dark grey, coarse, poorly sorted deposits with sub-rounded to sub-angular clasts ranging in size from 2cm to 50cm, typically of basalt, dolerite and gabbro with rarer peridotite and trachyte. The large proportion of sub-angular clasts demands that they be classified as breccias and not conglomerates (Cas & Wright 1987). The clasts are set in a matrix of fine-grained, similar, comminuted material and display both clast and matrix supported relationships (Fig. 7.3). No primary pyroclastic material, such as volcanic bombs, pumice, scoria or glassy material is recognised in the breccias. Rarer blocks of fine-grained material, both bedded and massive, are identified. Forming sub-rounded clasts (*ca.* 2cm to 5cm across) and larger elongate bodies (*ca.* 30cm length) (Fig. 7.4a), this material was identified as 'tuff' by Jassim & Gass (1970), however these are actually volcanoclastic sandstones and are not primary pyroclastic deposits (Cas & Wright 1987).

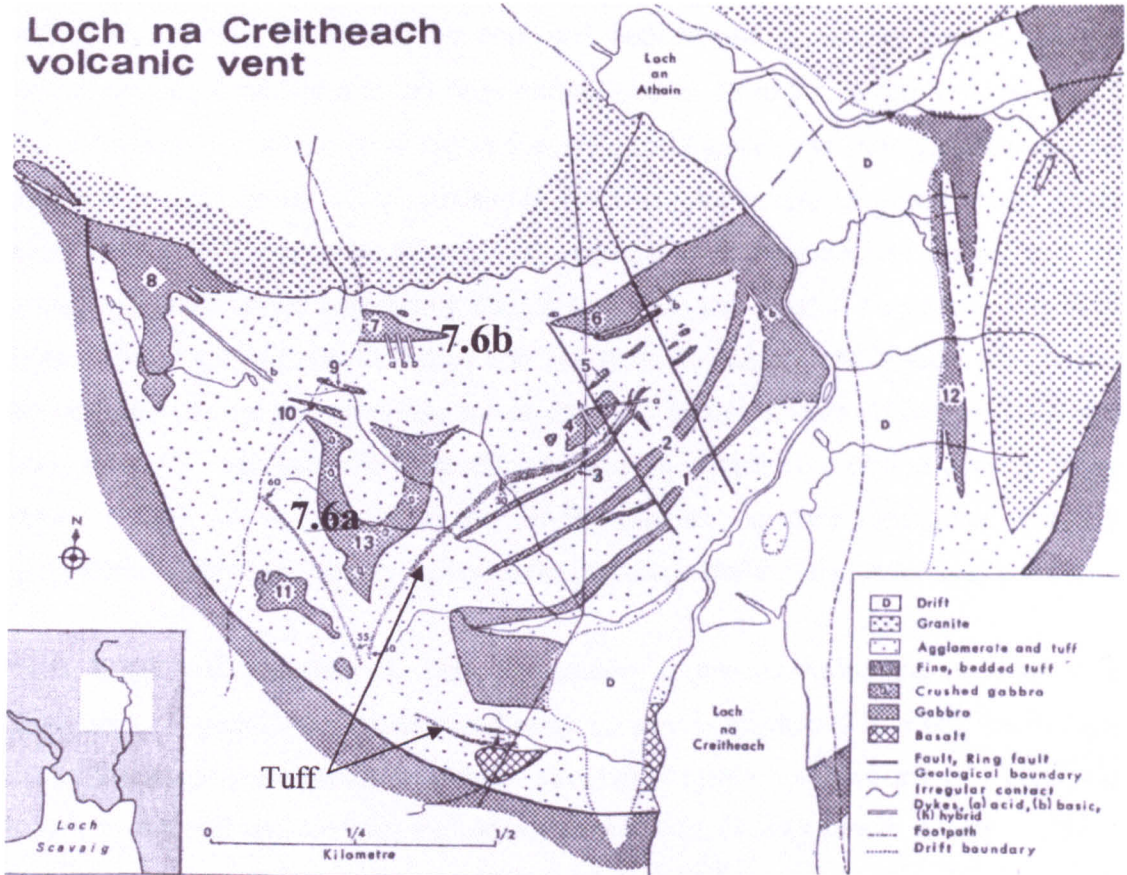


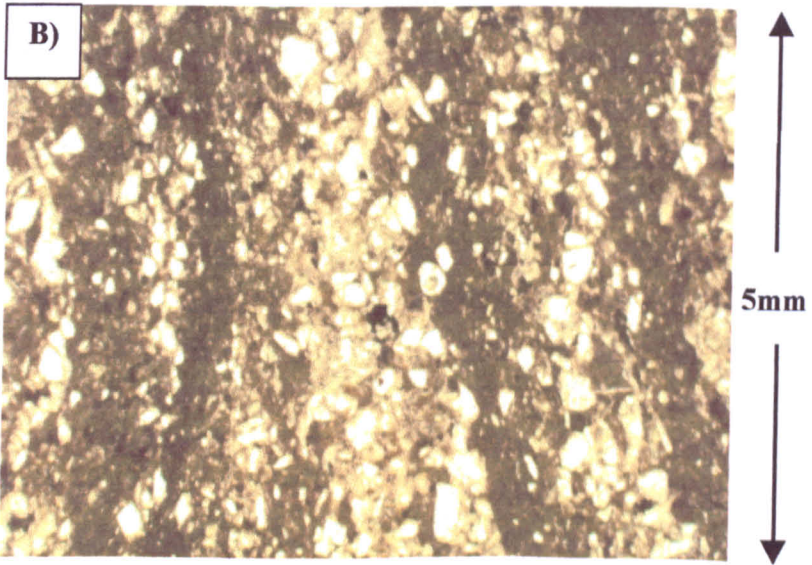
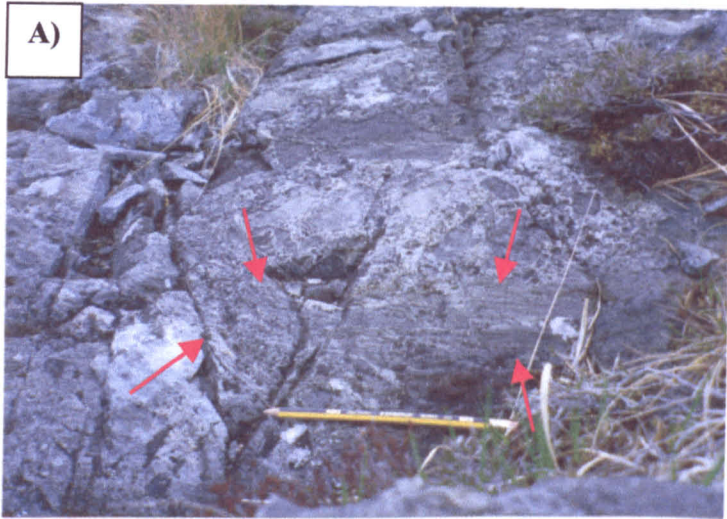
Fig. 7.2 – Map of Loch na Creitheach volcanic vent (NG5021). Small numbers indicate gabbro slabs, referred to in the text. Large numbers indicate the position of logs from Figure 7.6 (from Jassim & Gass 1970).

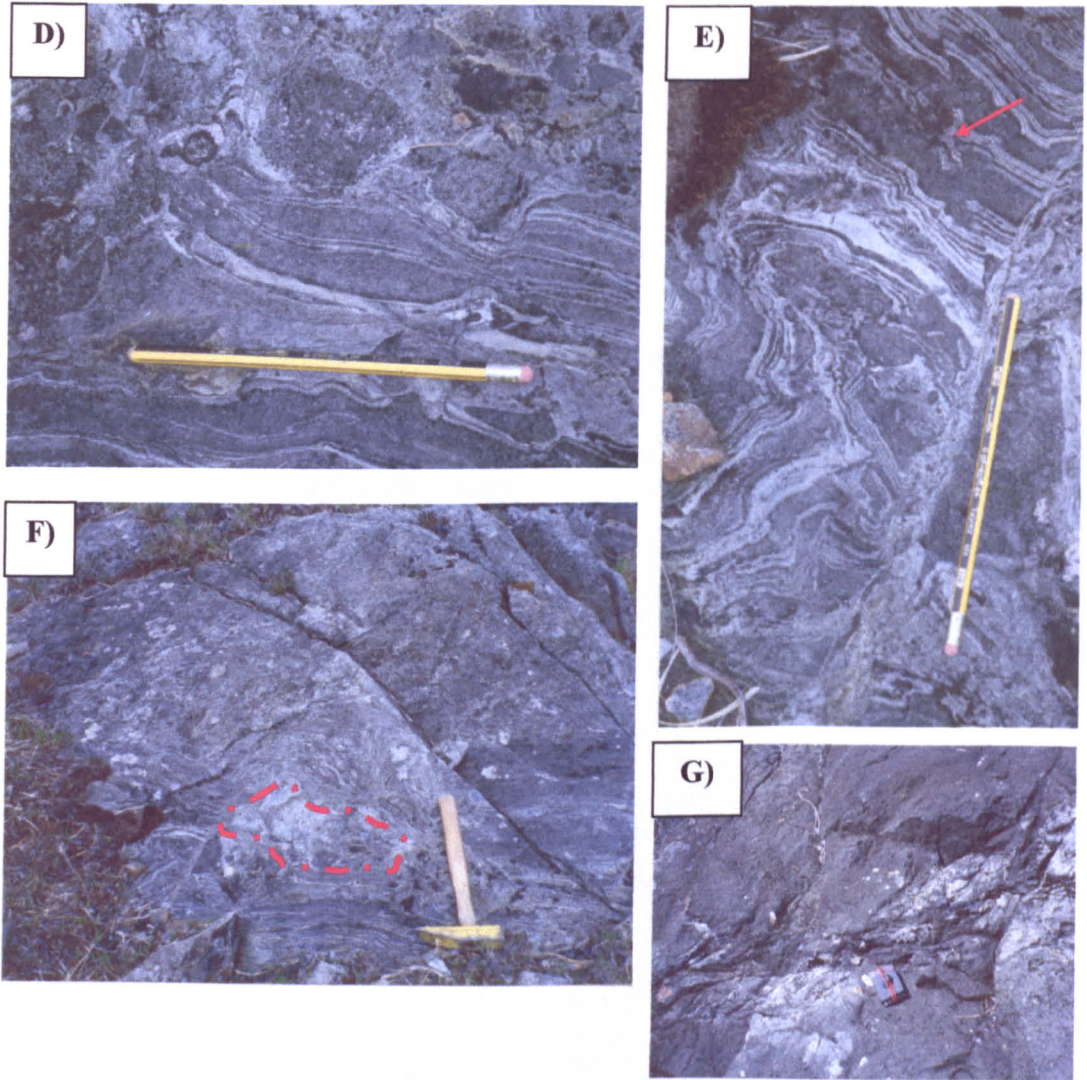


Figure 7.3 – Typical textures of the Srath na Creithaech Breccia Formation (NG50202173). Coarse-grained, poorly sorted breccia comprising sub-rounded to sub-angular clasts of gabbro and basalt set in a fine-grained comminuted matrix of similar material. Note the ca. 30cm across block of sub-rounded gabbro.

Intercalated within the breccia are two, well-bedded and commonly graded sandstone layers, ranging from 30cm to 2m thick and dipping at 15 to 50° to the NW and laterally discontinuous over distances of 2m to 5m. The bedding reflects 2mm alternation of fine and coarse 2mm bands. The sandstones (both in blocks and in *in situ* beds) display alternating pale bands (<2mm) dominated by quartz and plagioclase grains, and dark brown silt grade layers comprising mixtures of rock and mineral fragments (Fig. 7.4b). Where rock fragments are identified they are typically gabbro and basalt. No glassy or silicic fragments are present within the sandstones. Jassim & Gass (1970) described these units as 'tuffs', but here the term volcanoclastic sandstone is preferred (Cas & Wright 1987). 'Tuffs' are primary pyroclastic air-fall deposits, but these sandstones contain no pyroclastic material and simply represent the eroded products of the underlying breccias

On a larger scale considerable textural variation is present within the banding in the sandstones. Typically, the sandstones display a planar lamination (Fig. 7.4c), but in places this is disrupted by the impact of gabbro and/or basalt blocks. In these areas the lamination is highly irregular and encloses and drapes over blocks, leading Jassim & Gass (1970) to suggest they resembled 'bomb sags' (Fig. 7.4d). Locally, the lamination is substantially disrupted and elaborate patterns are developed in the sandstone. Figure 7.4e illustrates an example where lamination ranges from curvilinear to crenulate and in places doubles back on itself, forming large cusp-like structures (*ca.* 5cm across). Associated small-scale syn-sedimentary faults with *ca.* 1-2cm displacements are also recognised. Occasional blocks of breccia are observed within the sandstone and Figure 7.4f illustrates one such example where a block of breccia, 25cm across is surrounded by laminated sandstone. The underlying sandstone is distorted by the breccia block, whilst the overlying sandstone drapes over the breccia block and is apparently further distorted by the main overlying breccia mass. Contacts between the breccia and the sandstone are typically highly irregular, with the breccia filling shallow channels in the surface of the sandstone, or disrupting lamination as a result of loading (Fig. 7.4f).





**Figure 7.4 – Interbedded sandstone features in the Srath na Creitheach Breccia Formation (NG50642157). a) Elongate block (ca. 20cm across) of bedded sandstone within the Srath na Creitheach breccias (indicated by arrows). b) Photomicrograph of bedded sandstones with pale layers (<2mm) dominated by quartz and plagioclase grains, and intervening dark brown layers of typically silt grade mixtures of rock and mineral fragments. c) Planar lamination within sandstone. d) Disruption in lamination due to impact of gabbro and basalt blocks. The lamination encloses and drapes over blocks. e) Lamination within sandstone ranges from curvilinear to crenulate and doubles back on itself forming cusp-like structures (ca. 5cm across) in the centre of the photograph. Note the syn-sedimentary faulting (ca. 1-2cm displacements) to the top of the photograph (denoted by arrow). f) Block of breccia (denoted by dashed line) within sandstone. Underlying sandstone is disrupted by the breccia block whilst overlying sandstone drapes over the breccia block and is further loaded by overlying breccia. g) Elongate, narrow fingers of the sandstone (ca. 1m long) filling fractures between large blocks of gabbro.**

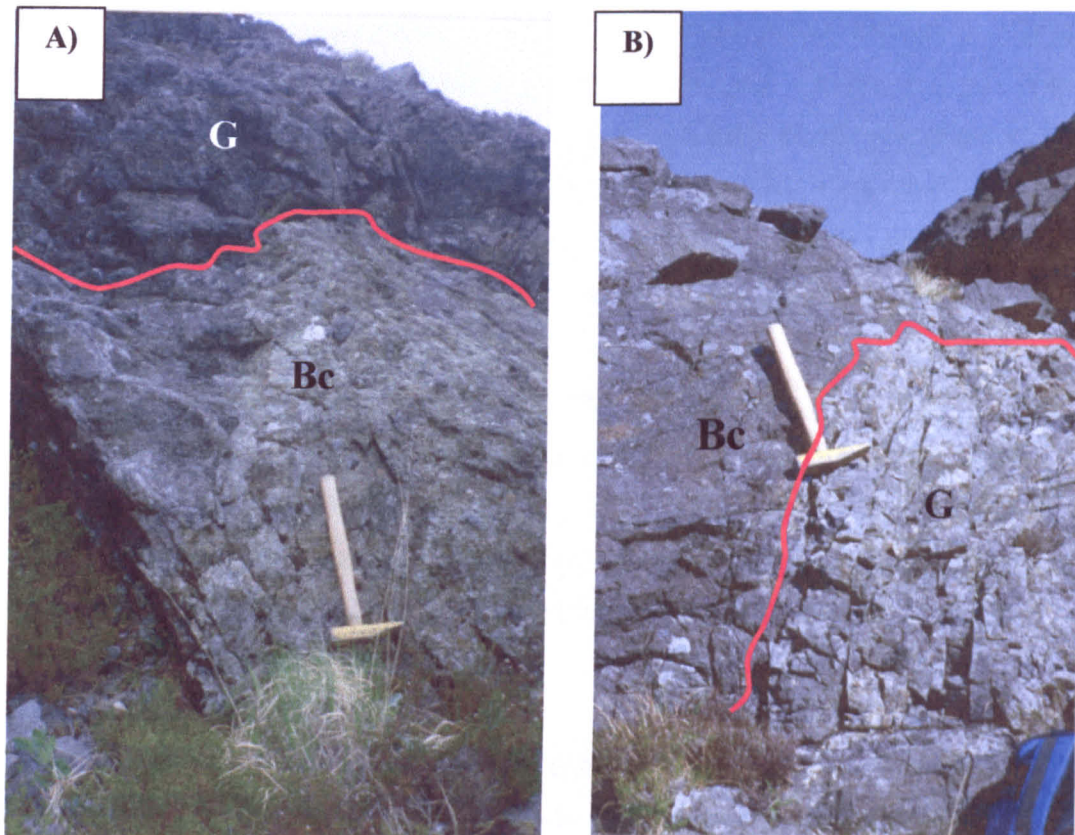


**Figure 7.5 – Gabbro-breccia relationships from the Srath na Creitheach Breccia Formation.**  
a) Brecciated base of gabbro block 7 (G) filling small channels in underlying breccia (Bc) (NG50552196). b) Vertical margin of gabbro slab 11 (G) filled by overlying breccia (Bc) (NG50332142).

Elongate, narrow fractures (*ca.* 1m long) filled with sandstone are recognised within large blocks of both gabbro (Fig. 7.4g) and breccia. Jassim & Gass (1970) suggested these were formed in areas of active gas streaming, where the unconsolidated tuffs (sandstones) beneath collapsed material were fluidised by later eruptive activity, and in many cases appeared to 'vein' the gabbro, forming near vertical structures. An alternative origin for these features will be discussed in Section 7.2.4 below.

Located within the breccia are thirteen large gabbro slabs, the largest of which is *ca.* 900m in length, although this slab is only partly exposed and may not be continuous. The gabbro slabs display a variety of contacts with the breccias and sandstones from brecciated through irregular to planar. Jassim & Gass (1970) described only two types of contact: brecciated (where numerous clasts of gabbro at the boundary are enclosed within either breccia or sandstone) and sharp (where no large blocks of gabbro are present within breccia or sandstone). Present observations suggest that brecciated contacts are dominant although planar contacts are present locally in all the slabs. However, irregular contacts between gabbro and breccia are also common. At slab 7 (Fig. 7.2) the breccia forms an uneven surface, with small troughs or channel-like structures (*ca.* 1m across and 5-20cm depth) filled by brecciated gabbro (Fig. 7.5a). A near vertical contact between gabbro and breccia is seen at slab 11 in the interior of the SNCBF (Fig. 7.2). This appears to represent the vertical boundary of a gabbro slab, which has been filled by overlying breccia (Fig. 7.5b).

Both Jassim & Gass (1970), and present investigations, have paid particular attention to the degree of brecciation of the gabbro slabs and their relationships with the breccia. Jassim & Gass (1970) noted that slabs 3, 4, 5 and 6 are only slightly fractured, whereas slabs 8 and 11 have brecciated bases. Only slab 13 is intensely brecciated (Fig. 7.2). Detailed logging during the present study, however, has revealed abundant brecciation at several new localities and additional evidence of relationships between the gabbro slabs, brecciated gabbro and typical (heterolithic) breccia. Two examples are illustrated in schematic logs (Figs. 7.6a and 7.6b) the locations of which are indicated on Figure 7.2, that are typical of breccia/gabbro slab contacts throughout the SNCBF. At the base of the sequence (Figure 7.6a), a minimum thickness of 3.5m of breccia is exposed. This is a characteristic SNCBF deposit comprising coarse, poorly sorted clasts, typically of sub-rounded to sub-angular gabbro and basalt (*ca.* 2cm to 50cm across) with rarer large sub-rounded blocks of gabbro

(ca. 1m across), set in a fine-grained matrix of comminuted material. A 50cm thick, laterally discontinuous layer of banded sandstone overlies the breccia. This consists of alternating pale and dark bands (<2mm thick) that have not been disturbed. It is overlain by a 2.5m thick unit containing abundant sub-rounded to sub-angular blocks of gabbro (ca. 10 to 20cm across), set within a matrix of angular, brecciated gabbro fragments approximately 2-5cm across. A 7m thick gabbro slab overlies this unit. The lower 5m of the slab is intensely shattered and fractured but grades up into a massive gabbro. Figure 7.6b displays similar features. At the base of this section is a minimum 4m thickness of breccia with large, rounded to sub-rounded gabbro blocks (ca 75cm across). This is overlain by a 2m thick unit of sub-rounded to sub-angular blocks of gabbro (ca. 10 to 20cm across) set within a matrix of smaller angular fragments of brecciated gabbro 2-5cm across. This is then overlain by a ca. 8m thick gabbro slab, the lower 6m of which are intensely shattered and fractured but grade up into a massive gabbro. Numerous basaltic dykes (<50cm thick) cut the whole unit. These relationships are common throughout the SNCBF and build up a picture of gabbro slabs whose bases are intensely shattered and crushed (Fractured Gabbro) (Fig. 7.7), which rest upon an intensely brecciated gabbro composed typically of sub-angular gabbro clasts set within a fine, angular matrix (Brecciated Gabbro). These overlie characteristic SNCBF deposits. These associations are illustrated in a schematic diagram (Fig. 7.8). Some gabbro slabs are fractured but not brecciated whereas others exhibit brecciation and no internal fracturing. The gabbro slabs however are rarely undisturbed, and appear to have undergone considerable physical stresses. These textures are very similar to the shattered basaltic megablocks described in Chapters 5 and 6.

Jassim & Gass (1970) suggested that the brecciation of the gabbro slabs was due partly to crushing caused by the collapse of the slab, but more significantly by gas streaming. This view was supported by the abundance of vesicles within crushed and brecciated gabbro. However, samples of uncrushed gabbro collected during the present study, display vesiculation, suggesting gas streaming may not have been the key factor in the brecciation of the gabbro slabs.

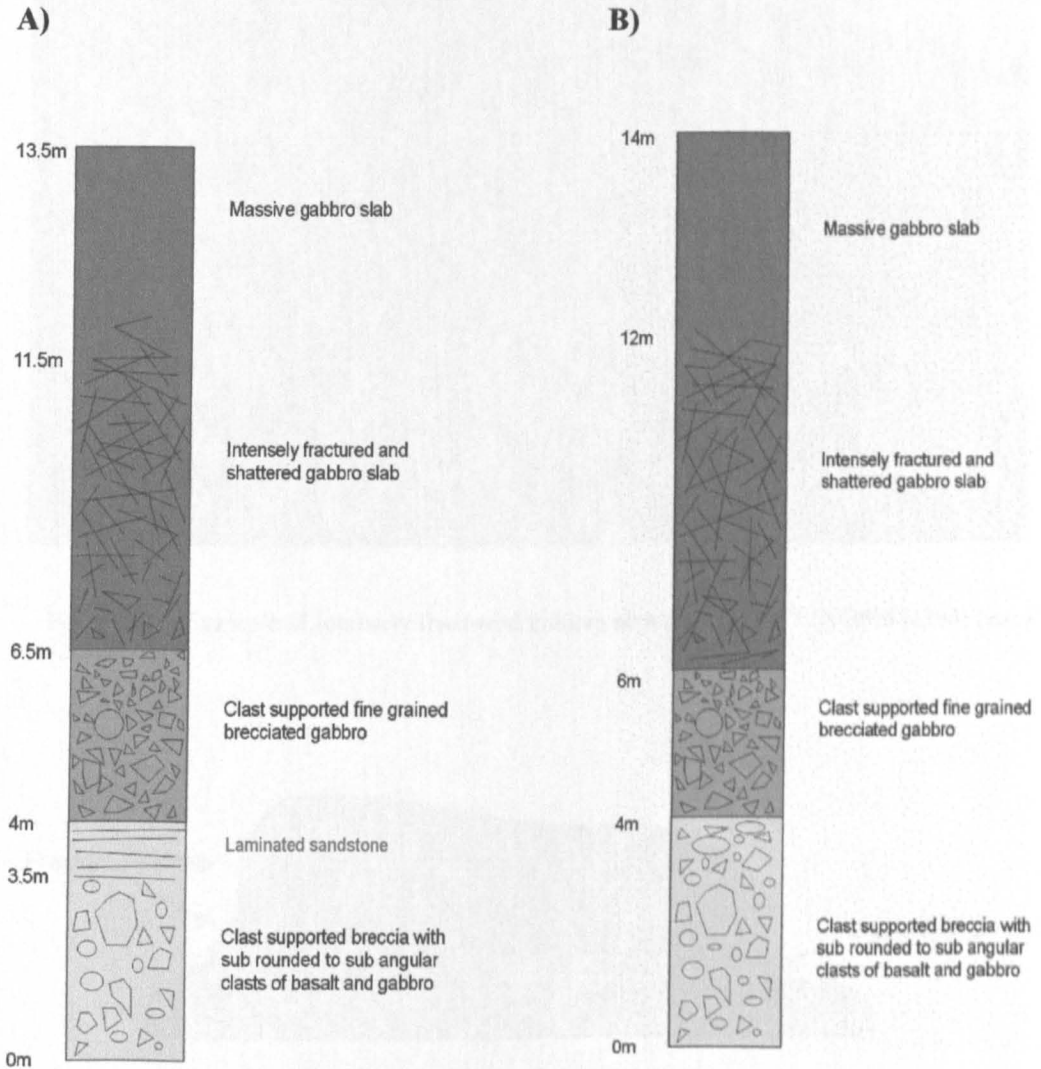


**Figure 7.6 – Schematic logs A) and B) of Srath na Creitheach Breccia Formation deposits. (A: NG50352161. B: NG50682197). See Figure 7.2 for localities.**

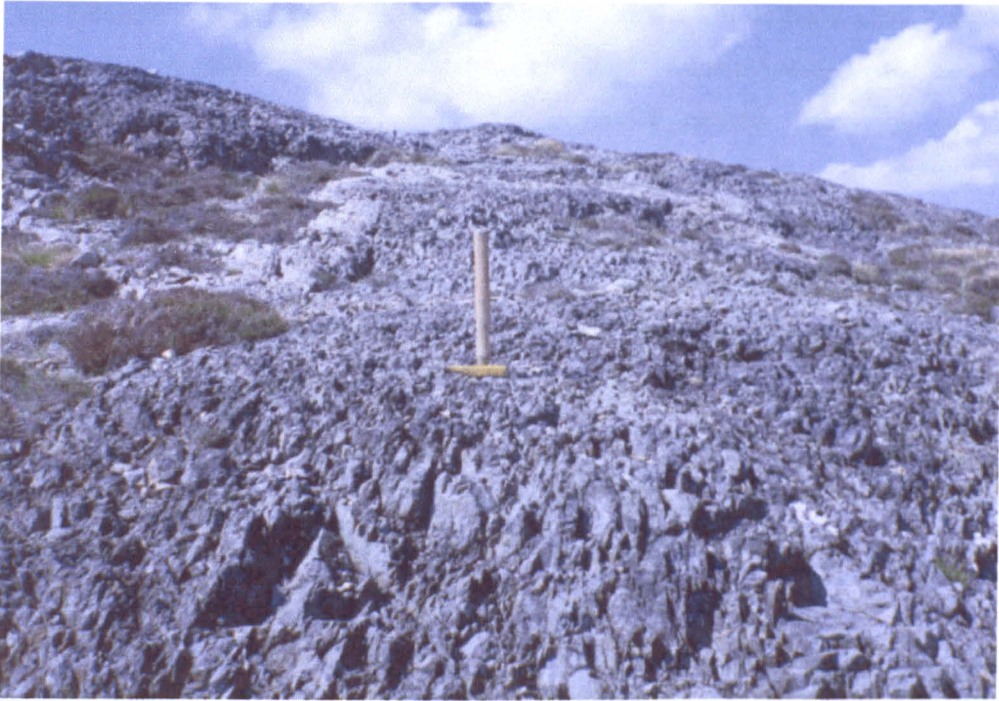


Figure 7.7 – Example of intensely fractured gabbro slab east of slab 7 (NG50682200) (see Fig. 7.2).

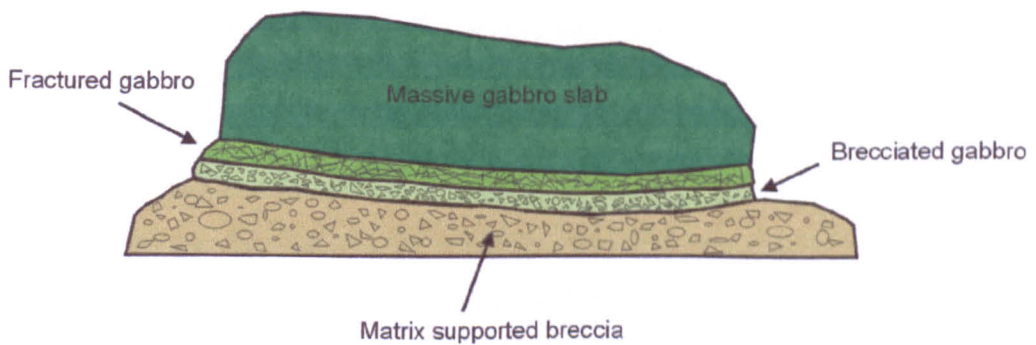


Figure 7.8 – Schematic reconstruction of gabbro slab textures in the Srath na Creitheach Breccia Formation.

## 7.2.4 Modes of deposition

Jassim & Gass (1970) believed that they had recognised a volcanic vent with a vertical contact (identified by a zone of crushed gabbro at the margin with the Cuillin Centre) that broke through overlying gabbro and basalt. This volcanic edifice was subsequently enlarged by vent wall collapse. Further explosive activity filled the caldera with pyroclastic debris including 'agglomerate and tuff,' before further subsidence occurred along marginal ring fractures. Aware of the absence of juvenile pyroclastic material, Jassim & Gass (1970) suggested that the volcanic agent responsible for the formation of the vent was gaseous rather than liquid and that the bedded tuffs within the vent indicated subaerial deposition of pyroclastic material. Finally they argued that the large gabbro blocks within the vent were detached by gas streaming from the main Cuillin mass, and that later explosive activity locally disrupted the tuffs. Recent fieldwork has indicated some problems with this argument, and these observations have suggested alternative modes of deposition for the Srath na Creitheach deposits.

Firstly the use of the term 'agglomerate' for the coarse material in the SNCBF is inappropriate as it does not contain primary pyroclastic material, such as volcanic bombs (Cas & Wright 1987). A non-genetic term such as volcanoclastic breccia is preferred. The absence of such material led Jassim & Gass (1970) to suggest that the breccia formed at a deeper level by processes involving gas escape from magma together with fluidisation. Although there is no direct evidence, gas fluidisation processes may be inferred from the brecciation and vesiculation observed in the gabbro slabs within the breccia, and from the absence of primary pyroclastic material. Jassim & Gass (1970) described subsidence along marginal ring fractures (identified by a zone of crushed gabbro at the margin with the Cuillin Centre) and the collapse of caldera walls. Williams (1941) and Smith & Bailey (1968) developed the classic model of central subsidence in an active caldera. They suggested that caldera subsidence takes place as a consequence of the release of some magma from the underlying chamber, with accompanying eruptions, and that there should be an approximate correspondence between the thickness of accumulated volcanic rocks and the extent of collapse. Caldera subsidence has been recognised in the British Tertiary Igneous Province from Mull (Bailey *et al.* 1924) and on Rum (Emeleus 1997; Troll *et al.* 2000; Donaldson *et al.* 2001). Troll *et al.* (2000) and Donaldson *et al.* (2001) noted, however, that on Rum a considerable thickness of collapse breccias accumulated before any volcanism. They argued that this evidence for an initial stage of collapse without

accompanying eruption, was an indication that the magma chamber was continuing to expand due to the addition of magma. Therefore, doming due to magma accumulation occurred, and caused both ring fracture formation and caldera collapse. They called this mechanism in which a depression develops by collapse, without magma evacuation, a 'proto caldera' (Fig. 7.9).

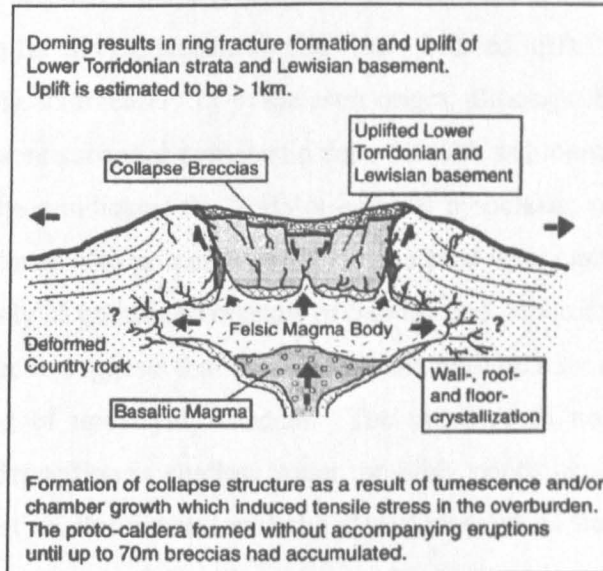


**Figure 7.9 – Evolution of the Rum Caldera.** The filling of a caldera by collapse breccias, emphasises the inflation of the chamber, causing formation of the caldera without accompanying eruptions (from Donaldson *et al.* 2001).

The SNCBF deposits appear to have undergone collapse without accompanying eruptions (absence of primary pyroclastic material) and therefore the model of Donaldson *et al.* (2001) provides a viable alternative. The role of collapse, recognised in the presence of large gabbro slabs, and local uplift and instability appears to have been underestimated. Furthermore, at the time when the breccias formed the Srath na Creitheach Centre (Fig. 7.1) had yet to cut them and may have been the source of the upwelling magma responsible for the (caldera) collapse. This seems an appropriate mechanism for the formation of the SNCBF deposits, although the idea of gas streaming and fluidisation cannot be ruled out. Local collapse may simply be caused by instability due to uplift (and/or subsidence), or associated with steep slopes rather than the extreme of caldera formation.

Jassim & Gass (1970) suggested that the 'bedded tuffs' represented material deposited under subaerial conditions, due to the presence of graded bedding and structures

resembling 'bomb sags.' This interpretation holds and suggests that the caldera or volcanic conduit was open to the surface. There is however some confusion over the details of the origin of these bedded tuffs. Jassim & Gass (1970) state that, "Structural features in the bedded tuffs are those of sedimentary rocks. The graded bedding, the bomb sags and finally the persistence of the banding, all suggest that these volcanic sediments were deposited under sub-aerial or possibly very shallow water conditions." They then however go on to state that, "Further explosive activity resulted in the production within the caldera of poorly bedded tuffs and agglomerates and finely bedded tuffs." These two statements suggest a conflicting sedimentary or pyroclastic origin, although the implication seems to be that the 'tuffs' were subaerial pyroclastic deposits with sedimentary features. Field and petrographical analysis indicates the 'tuffs' are not of pyroclastic origin but are laminated sandstone and siltstones. No primary pyroclastic material is recognised and the sandstones are composed entirely of grains and crystals of basaltic and gabbroic debris. Their laterally discontinuous character suggests that they are surface, sedimentary deposits formed locally from the reworking of underlying breccia. The presence of normal grading and fine banding indicates deposition in shallow water, possibly ponds or small lakes, with minor fluvial inputs. Together, this equates with the idea of an exposed surface conduit.

The nature and origin of disruption of banding within the sandstones must be resolved and the descriptions of Jassim & Gass (1970) are confusing. They pose the question as to how the gabbro slabs were "transported into the vent area, usually without breaking and without deforming the underlying pyroclastic debris?" This is explained by suggesting, "if these volcanic sediments were soft and un lithified, the impact of the slab would be cushioned and it would be less likely to fracture." There is strong evidence, however, to indicate that many of the gabbro slabs are highly fractured and brecciated (Figs. 7.6a, 7.6b & 7.7). It seems highly unlikely that the emplacement of a large gabbro slab (in places they measure *ca* 900m long and tens of metres thick) would not disrupt thin units of soft sediment. Furthermore, Figures 7.4d, 7.4e and 7.4f clearly demonstrate that the sandstones were disrupted as they display spectacular soft sediment deformation. Jassim & Gass (1970) also suggest that, "In certain areas where gas streaming activity was active, the unconsolidated tuffs underneath the collapsed slabs were fluidised," and, "In many cases tuffs vein the gabbro." This method of disruption of the sandstones (bedded tuffs) requires a new source of gaseous explosive activity from depth. This seems unlikely, as it would be much easier to disrupt soft sediment by surface loading than by a multi-stage fluidisation model. Further evidence of soft sediment deformation is provided by the identification of

syn-sedimentary faults with *ca.* 1-2cm displacements in the sandstone (Fig. 7.4e). Narrow fingers of sandstone (*ca.* 1m long) fill fractures between large blocks of both gabbro and breccia. Jassim & Gass (1970) described these as 'veining' the overlying blocks but they appear to represent bodies of sediment that have been loaded and disrupted by overlying material. The sediment has been squeezed and folded around blocks and in places exploits open fractures (Fig. 7.4g).

Some features of the SNCBF deposits resemble textures in debris flows and debris avalanches. Debris flow and debris avalanche deposits are generally coarse and poorly sorted with sub-rounded to sub-angular clasts set in a fine-grained comminuted matrix (Van Bemmelen 1949; Pierson & Costa 1987; Costa 1988; Coussot & Meunier 1996; Kessler & Bedard 2000). They may also display grading and stratification and features such as channels and imbrication. Fine-grained interbedded units are also common (Smith & Lowe 1991; Blair & McPherson 1994,1998). Debris avalanches in particular contain fractured and shattered megablocks (large 'boulders' *ca.* >10m across), with cataclastic layers at their bases. The megablocks typically form a hummocky topography (Siebert 1984; Ui *et al.* 1986; Glicken 1986,1991; Yarnold 1993; Schneider & Fisher 1998; Kessler & Bedard 2000). Many of these features are present within the SNCBF. The gabbro slabs are typically fractured and brecciated (Figs 7.6a, 7.6b and 7.7), and are similar to megablocks described by previous researchers. This suggests that the gabbro slabs were detached from the caldera wall at the surface and were transported by mass flow. The intensely brecciated gabbro at the bases of the slabs (Figs 7.6a, 7.6b and 7.8) may represent the basal, cataclastic layer formed in debris avalanche deposits. These are created where the megablock slides within a mass flow, undergoing intense physical stresses, and the base becomes crushed and ground down producing finer, angular debris (Schneider & Fisher 1998). A jigsaw pattern of fractures (Ui 1985) is identified in some gabbro megablocks. The gabbro blocks rest within the breccia and in places their elongate upper surfaces form a possible hummocky topography (Fig. 7.10) adding further support to the idea of a surface conduit.

Taken together, this evidence suggests a series of large-scale collapse events into a subsiding caldera forming loose basaltic and gabbroic material on the floor. Gabbro megablocks were detached from the Cuillin Centre (and possible overlying basaltic lavas) and were transported by mass flow. During transport the slabs were fractured with zones of intense brecciation at their bases. Smaller blocks were broken off the gabbro slabs and

additional surface material entrained within the flows, producing the coarse, unsorted characteristics of the SNCBF deposits. The cyclical character of collapse and debris flow activity is indicated by the presence of interbedded sandstone and siltstone. These laterally

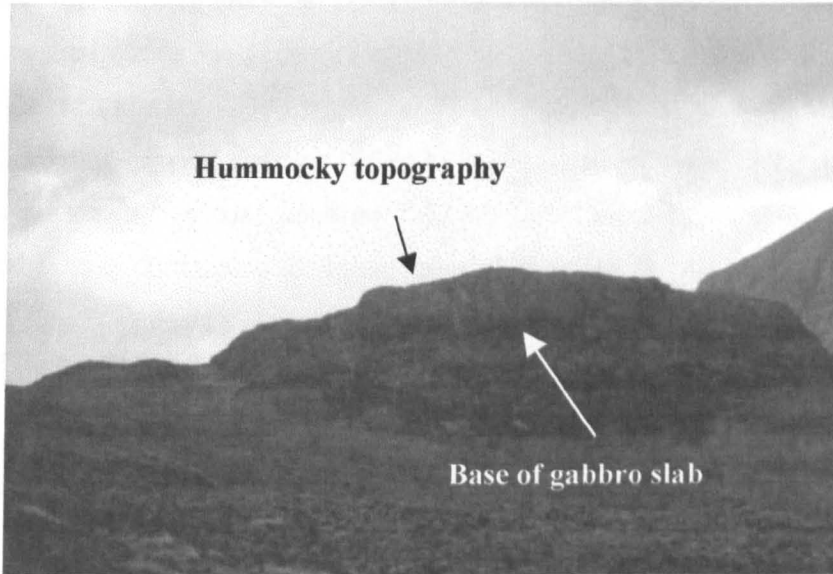


**Figure 7.10 – Possible hummocky topography of gabbro slabs in the Srath na Creitheach Breccia Formation (NG505219).**

discontinuous units represent localised, surface reworking of the breccia in relatively low-energy environments and fill channels on the breccia surface. The sandstones are then overlain by both breccia and gabbro megablocks. This indicates a return to high-energy mass flow conditions that caused loading and disruption of the underlying sandstones. Rare clasts of breccia within the sandstone suggest erosion of this material. Subsidence and collapse occurred before the intrusion of the Srath na Creitheach Centre. The SNCBF deposits therefore represent epiclastic breccias formed by multiple mass flow events, resulting from caldera subsidence. Interbedded sandstones reflect quiescent periods during which surface deposits were reworked.

## 7.2.5 Conclusion

The Srath na Creitheach Breccia Formation was deposited after the emplacement and unroofing of the Cuillin Centre and before the emplacement of the Srath na Creitheach Centre. Previous interpretations of these deposits as 'vent agglomerate,' formed by the shattering of basaltic and gabbroic material by a gaseous explosive agent and the cyclic, subaerial eruption of pyroclastic material into a subsiding caldera (Jassim & Gass 1970) were mistaken. New investigations have recognised that the coarse clastic deposits are volcanoclastic breccias. They resemble debris flow and debris avalanche deposits, and interbedded fine-grained deposits, previously identified as 'tuffs,' are sandstones formed, in shallow fluvio-lacustrine environments by the reworking of surface material. The collapse of the caldera occurred without associated explosive activity.

## 7.3 Kilchrist

### 7.3.1 Introduction

The breccias of Kilchrist crop out over an area of *ca.* 2km<sup>2</sup> south of Beinn Dearg Bheag and in a thin strip towards Creagan Dubh, NW of Beinn Dearg Mhor. Lying within the Skye Central Complex they form part of the Eastern Red Hills Centre and are cut by the Beinn na Caillich Granite (Fig. 7.11). The breccias are coarse, poorly sorted, unstratified deposits, comprising sub-angular to rounded clasts of an extremely heterogeneous range of lithologies. Intercalated within the breccias are volcanoclastic sandstones and rhyolitic ignimbrites. The margins of the breccia mass are invaded by mixed magma intrusions. These rocks were originally interpreted as vent agglomerates (Harker 1904) but were re-interpreted in detail by Bell (1985), who suggested that they formed by surface and near surface explosive volcanism and associated epiclastic processes within or marginal to a vent. The breccias are described and their modes of formation reviewed below.

### 7.3.2 Previous Research

Harker (1904) described the Kilchrist breccias as a mass of poorly sorted, unbedded debris of basaltic and country rock material, set within a matrix of basaltic composition. He believed that they were vent agglomerates formed by concussion and friction of angular

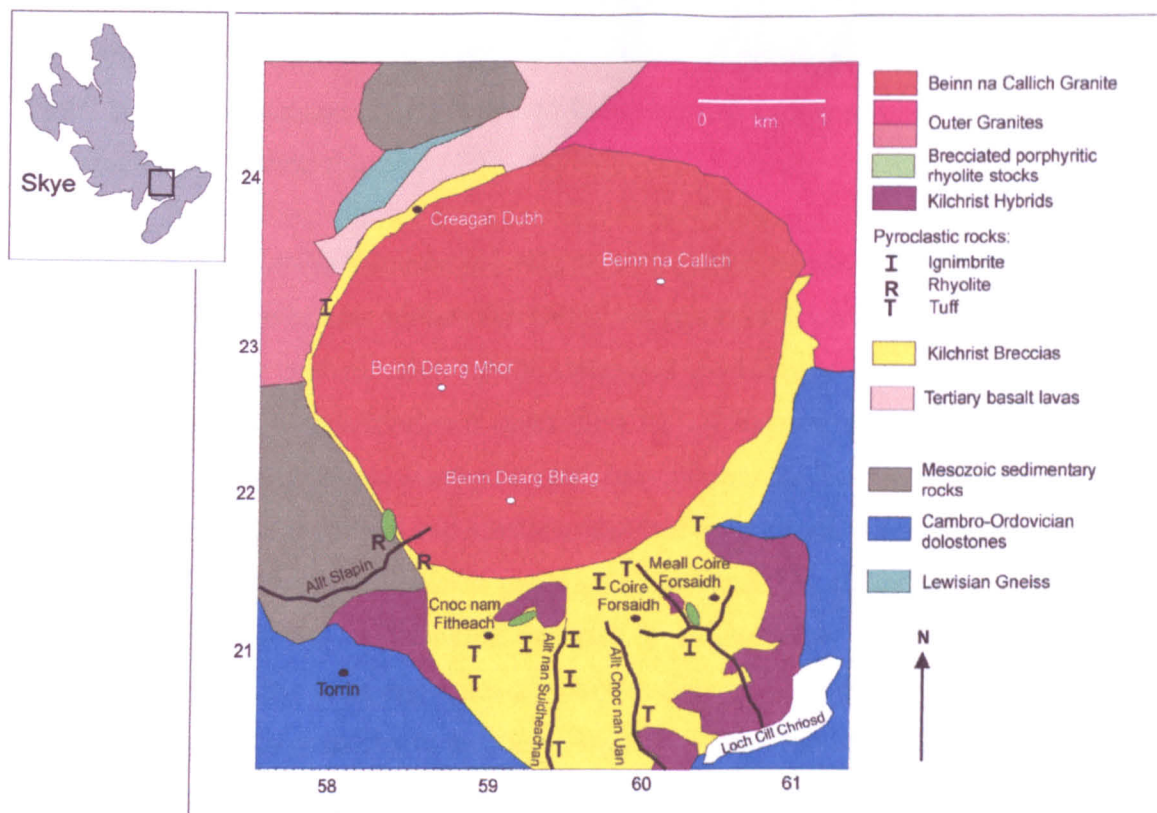


**Figure 7.11 – Geological map of the Kilchrist area, Skye (after Bell & Harris 1986). Numbers in frame of map are OS grid references.**

blocks and volcanic dust. Harker (1904) also described a thin strip of ‘bedded agglomerate’ running along the SW boundary of the Beinn na Caillich Granite, indicating the intrusive nature of the granite. He recorded a ‘granophyre intrusion with gabbro xenoliths’ at the margin of the agglomerate, suggesting the gabbro xenoliths were from a primitive magma source rather than an intruded rock body.

‘Ignimbrites’ were first recorded by Ray (1960) who described material from two localities in the Allt nan Suidheachan-Cnoc nam Fitheach area. He considered the rocks to be intrusive but Bell, B. R. (1982) re-interpreted them as of mixed magma origin. Ray (1962) first described five brecciated silicic intrusions within the Kilchrist deposits, later re-investigated by Bell (1982) and Bell & Harris (1986) who recognised only three intrusive groups (Fig. 7.11). 1) The Cnoc nam Fitheach Breccia is an oval shaped brecciated quartz-porphry, which has been severely disrupted. This intrusive mass consists of angular to rounded fragments of porphyritic felsite set in a matrix of quartz and alkali feldspars. 2) The Coire Forsaidh Brecciated Rhyolite is an elongate mass of pale, greyish-green breccia, comprising fragments of flow banded rhyolite. 3) The Allt Slapin Breccias comprise three intrusions; a vertical band of flow banded rhyolitic breccia set in a pale tuffaceous matrix of comminuted quartz and alkali feldspar; a flow banded-tuffaceous rhyolite breccia; and

a vertical sheet of flow banded tuffaceous breccia, with abundant fragments of rhyolitic tuff. Bell & Williamson (2002) described these deposits simply as small stocks of intruded brecciated porphyritic rhyolite.

A detailed study of the Kilchrist breccias by Bell (1985) concluded the breccias were the products of surface or near surface volcanism and associated epiclastic processes, in a ring-faulted, subsiding caldera. Bell (1985) described the breccias as poorly sorted, clast to matrix supported, unstratified and dominated by sub-angular to (rarer) rounded clasts. Blocks include Torridonian sandstone and shale, Cambrian limestone and quartzite and Jurassic limestone, sandstone and siltstone, together with basalt, dolerite, gabbro, rhyolite, tuff (including ignimbrite), granite, pitchstone and blocks of earlier breccia. The matrix comprises fine-grained comminuted material of similar type. Intercalated within the breccias are rhyolitic tuffs and volcanoclastic sandstones. Bell (1985) and Bell & Harris (1986) described large extrusive masses of rhyolitic ignimbrite in the Allt nan Suidheachan to Cnoc Nam Fitheach area (Fig. 7.11) that display well developed eutaxitic textures. Bell (1982) recognised that the granophyres at the margin of the breccia mass described by Harker (1904) formed part of a ring-dyke structure delimiting a central area of cauldron subsidence. Five of these intrusions (The Kilchrist Hybrids) were identified as of mixed magma origin due to the inter-relationship of silicic and basic material.

Within the breccias, Bell (1985) discovered evidence of surface weathering represented by a 0.5m thick lateritic horizon in the Allt Coire Forsaidh, north of Loch Cill Chrìosd. Vague stratification in the breccia, was also recognised in the Allt an Suidheachan. Bell (1985) concluded that these highly variable pyroclastic materials could not be grouped simply as 'agglomerate,' but are best explained as a ring-dyke intrusion with a central down-dropped block of pyroclastic rocks. Deposits accumulated on the surface and not within a vent as suggested by Harker (1904). Bell (1985) interpreted the heterogeneous breccias as resulting from a combination of surface and near surface explosive volcanism, with ignimbrites and rhyolitic tuff evidence of *in situ* extrusive material (possibly related to the brecciated rhyolite stocks). Epiclastic collapse and surface reworking are associated with this instability and explosivity, and lateritised breccias indicate prolonged surface exposure. The Kilchrist deposits are therefore a clear example of the formation of epiclastic breccias in conjunction with silicic pyroclastic material.

### 7.3.3 Further Research

Recent fieldwork has identified new evidence for epiclastic processes in the Kilchrist breccias. In addition to the lateritic horizons identified by Bell (1985), surface 'channels' and stratification are recognised. In the thin strip of breccias running north towards Creagan Dubh (Fig. 7.11), breccia fills a narrow depression or channel *ca.* 2m wide and 1m deep between two basaltic lava outcrops (Fig. 7.12a), continuing as a broadly horizontal sheet northwards for *ca.* 100m (Fig. 7.12b). The breccia is poorly sorted, clast supported and of typically heterogeneous composition with no internal stratification. This provides clear evidence of the sub-aerial nature of these deposits. The lava and breccia were later tilted to a steep angle, most likely by the emplacement of the Beinn na Caillich Granite.

In the area to the north of Cnoc nam Fitheach (Fig. 7.11) a *ca.* 5m thick stratified breccia (Fig. 7.13a) comprises six, *ca.* 75cm thick, ungraded breccia units with planar to irregular surfaces, dipping to the south at an angle of *ca.* 30°. These units may represent a series of surface flows, or alternatively, slumps within the subsiding breccia mass. Towards Creagan Dubh a 1.5m thick breccia displays a well-developed sub-horizontal fabric (Fig. 7.13b). The base of the unit (50cm) is a matrix supported breccia, typically comprising sub-rounded to sub-angular clasts (2cm to 5cm across) which display a convincing sub horizontal alignment. The breccia coarsens and grades upward into a clast supported deposit, comprising larger, sub-rounded clasts (*ca.* 50cm across) again displaying a sub-horizontal fabric. A short distance above these deposits, is a lenticular mass (*ca.* 1m across and 20cm thick) of laminated (<2mm thick) and cross-bedded tuffaceous sandstone (Fig. 7.13c). This consists of fine-grained, rounded material of similar composition to the breccia, and provided evidence of sedimentary reworking of the breccia. In thin section sub-horizontal stratification is present (Fig. 7.14a) together with 'vertically stacked' grains, indicative of re-transportation (Fig. 7.14b). These are not primary pyroclastic textures. These deposits reveal sedimentary textures with mineral grains and rock fragments showing well-aligned, commonly interlocking boundaries. These sedimentary textures provide further evidence for surface reworking.

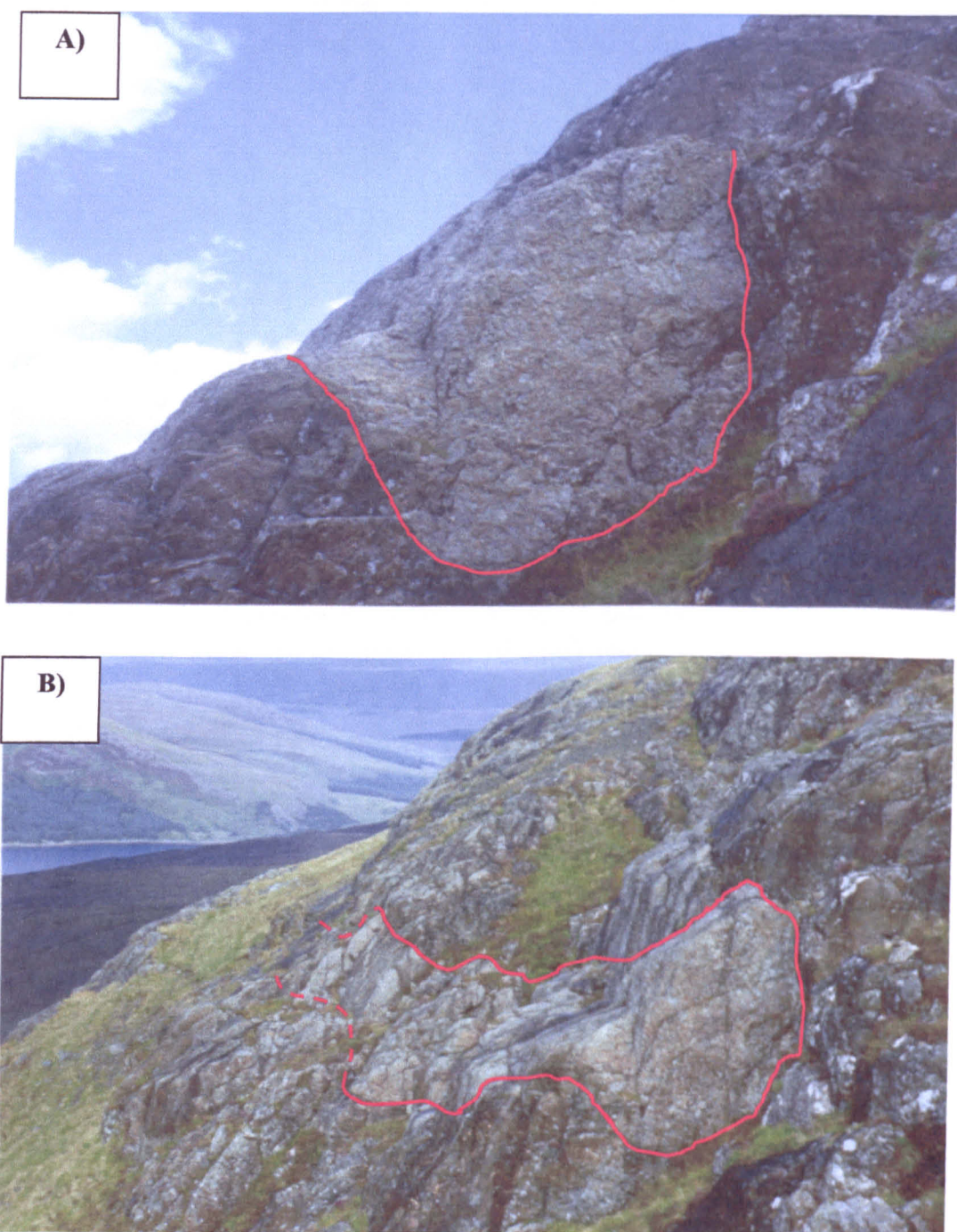


**Figure 7.12 – Channel feature in the Kilchrist breccias, SW of Creagan Dubh (NG58302371). a) A 2m wide and 1m deep ‘channel’ of breccia fills a depression or channel in basaltic lava, SW of Creagan Dubh. b) Thin, horizontal outcrop of channel filling breccia showing extent of deposit in a).**

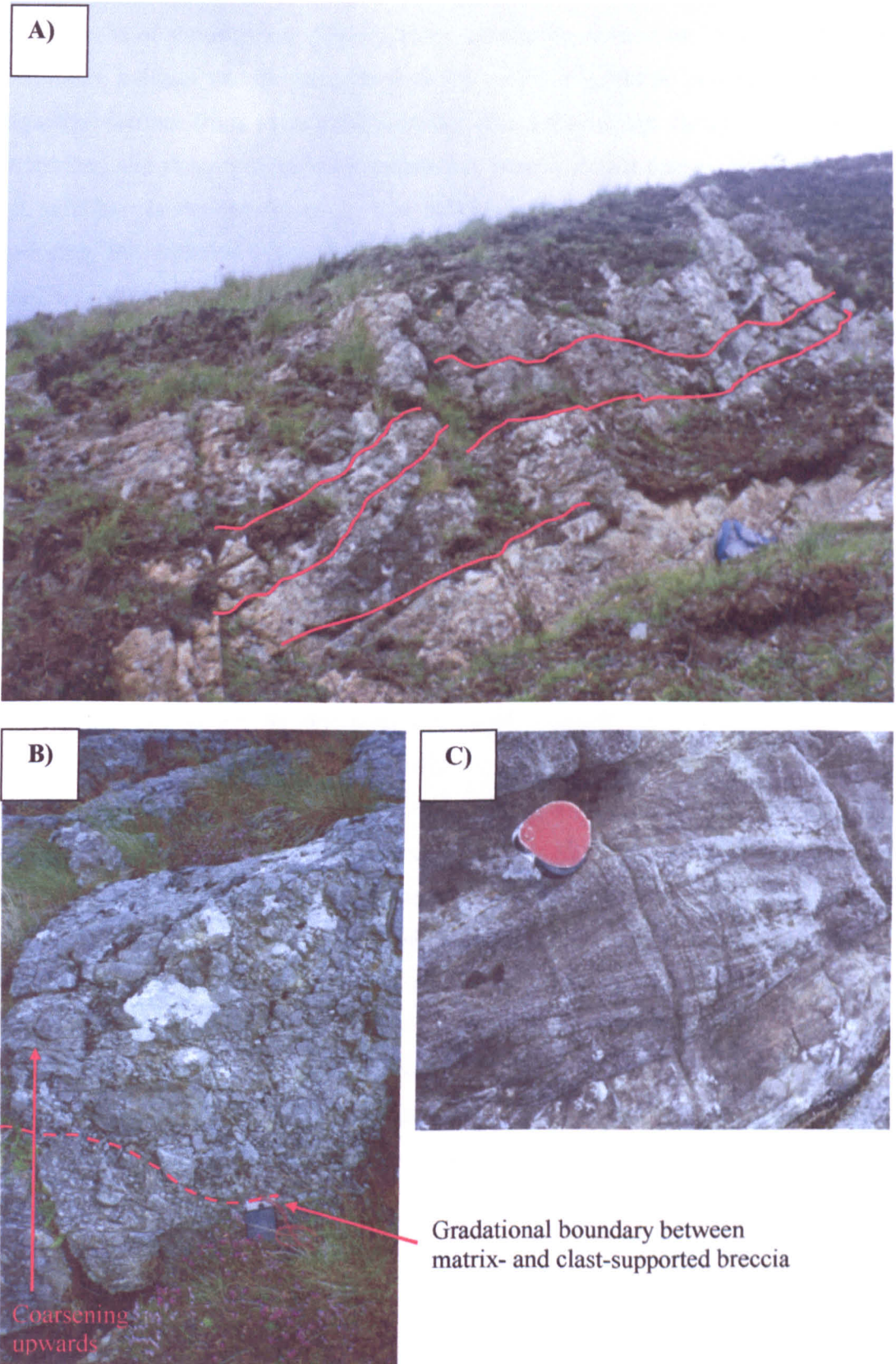


**Figure 7.13 – Sedimentary features from the Kilchrist breccias. a)** 5m thick deposit of stratified breccia, comprising six (*ca.* 75cm thick) breccia units to the north of Cnoc nam Fitheach (NG59322134) (Fig. 7.11). The units (highlighted) may represent a series of surface deposits, or alternatively, slump structures within the subsiding breccia mass. **b)** SW of Creagan Dubh a breccia mass comprising reverse graded sub horizontally aligned clasts (NG58172360). **c)** Laminated, tuffaceous sandstone intercalated within the breccia mass 5m above deposits in b). Note the fine laminae (<2mm) and *ca.* 2cm scale cross bedding (NG58172360).

The presence of stratification, grading, slump structures, erosion surfaces and intercalated sandstones, indicate that the breccias were the result of epiclastic processes. They were originally derived from pyroclastic deposits (the breccias are closely associated with ignimbrites and primary pyroclastic material is present within them). Following erosion and possible landslides/slumping, this material was subject to surface reworking, producing the features outlined above. The Kilchrist breccias should therefore be classified as epiclastic deposits (Cas & Wright 1987).

Clast analyses were undertaken in order to identify and study trends within the Kilchrist breccias. Due to limited exposure, only one E-W traverse, from Cnoc nam Fitheach to Meall Coire Forsaidh was possible (Fig. 7.11). At suitable localities a 10m traverse was undertaken. At 10cm intervals along the traverse the composition of clasts, their degree of rounding and size were noted. Sample points with no clasts were recorded as matrix. This allows the nature of the deposits to be understood and assessment of any variation with distance. The results are summarised in Figure 7.15 below.

Although some erratic results were recorded, clear trends are identified from the traverses. Figure 7.15a plots clast composition versus distance. The distribution of most clast lithologies is irregular and they display no obvious trends. Certain lithologies (e.g. quartzite) have high concentrations in localised areas that may reflect the nature of the country rock geology at the time the breccias were deposited. Limestone falls from *ca.* 40% at the west of the traverse to less than 5% in the east. Again this may reflect the absence of limestone as a country rock lithology in the area around Meall Coire Forsaidh. The most significant trend is the appearance of pebbly sandstone *ca.* 0.5km from the start of the traverse, which steadily rises to nearly 30% at the end of the traverse. This pebbly sandstone material varies from coarse sand to fine granule grade and represents clasts of material similar to the main breccia mass.

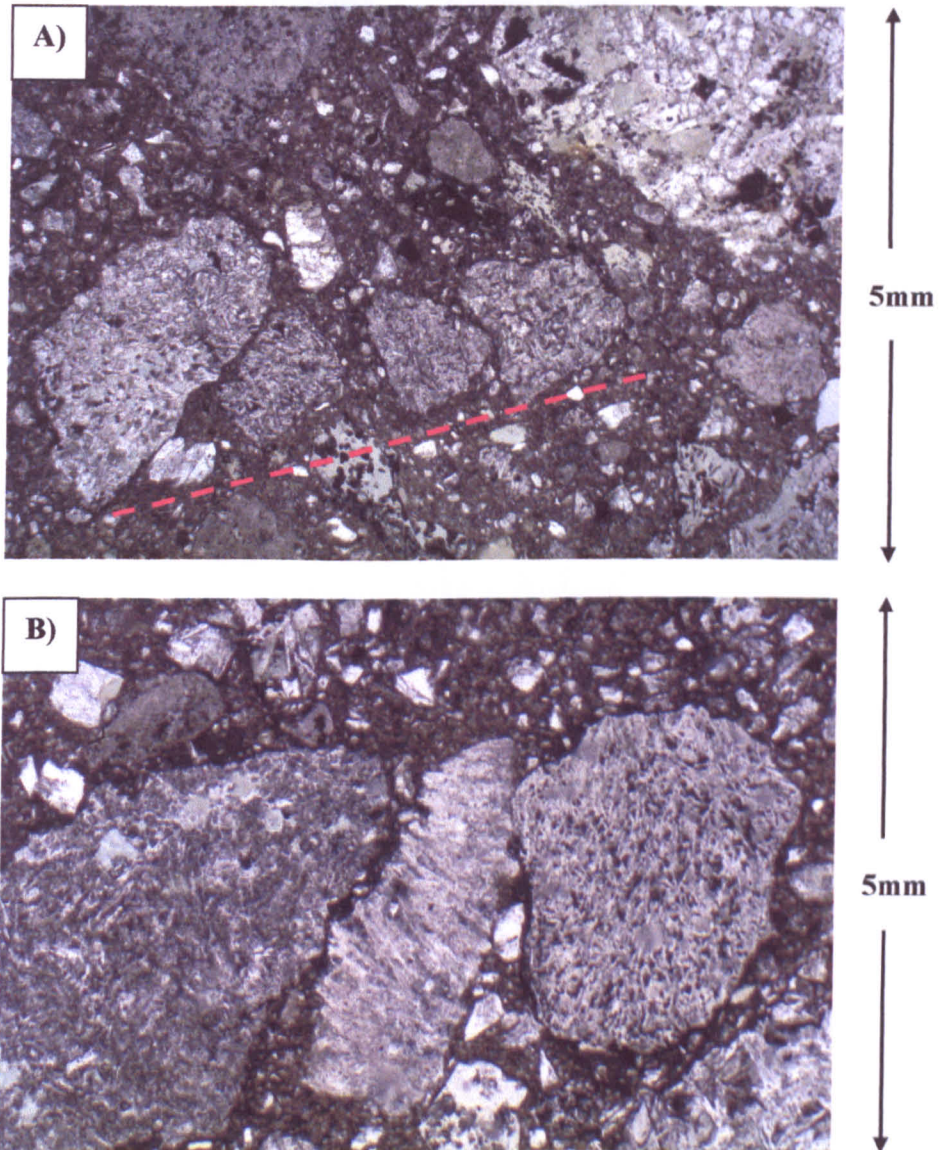
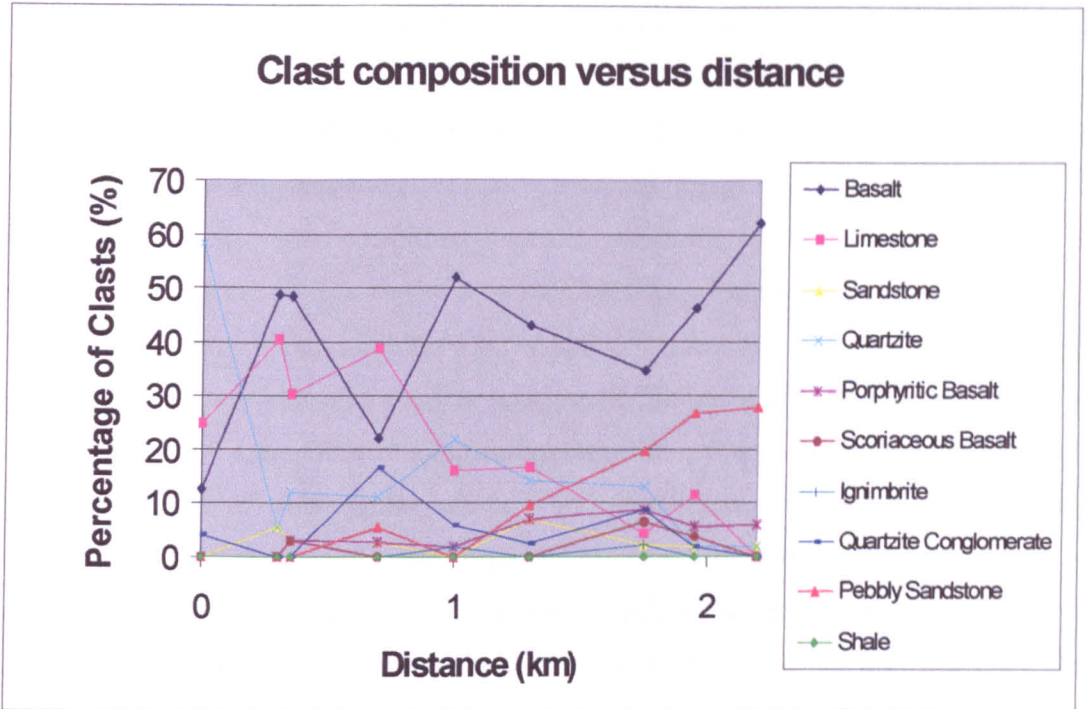
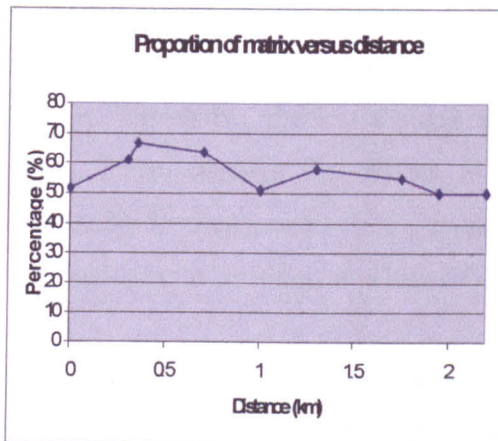


**Figure 7.14 – Photomicrograph displaying sedimentary textures in the Kilchrist breccias, collected from NG58172360. Both views in xpl. a) Sub-rounded grains of basalt displaying sub-horizontal alignment (highlighted). The base of the image is aligned horizontally. b) Sub-rounded to sub-angular ‘vertically stacked’ grains of basalt with well aligned boundaries. The base of the image is aligned horizontally.**

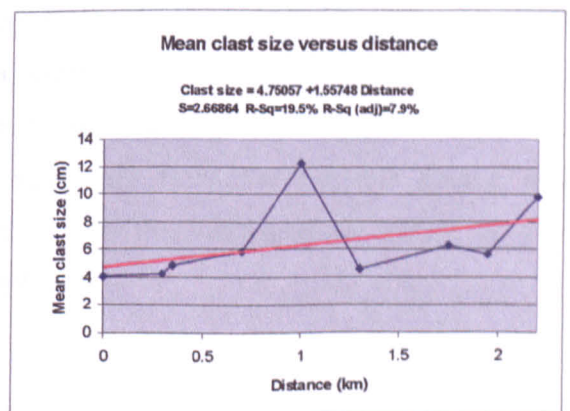
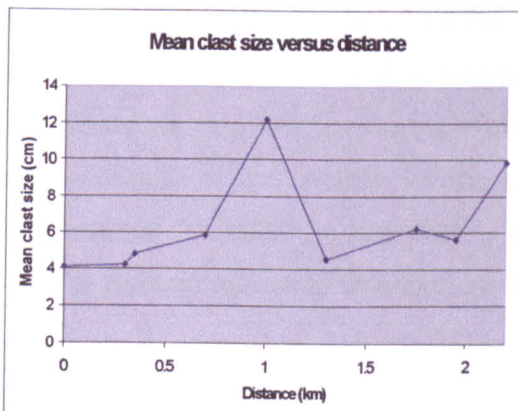
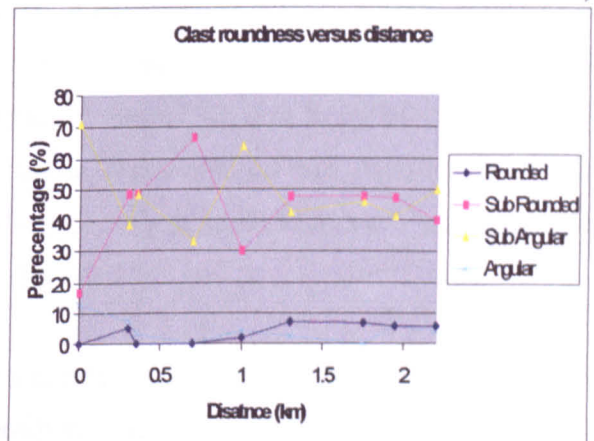
A)



B)



C)



D)

E)

Figure 7.15 – Cnoc nam Fiteach to Meall Coire Forsaidh Clast Count Analysis, Kilchrist, Skye. a) Clast composition versus distance. b) Proportion of matrix versus distance. c) Clast roundness versus distance. d) Mean clast size versus distance. e) Linear regression showing relationship between mean clast size and distance.

Clasts of this pebbly sandstone were derived from the reworking and redeposition of the breccia, and their steady increase to the east may provide evidence of a westerly transport direction, as clasts are eroded from source. Figure 7.15b plots the proportion of matrix versus distance. Along this traverse, matrix typically forms *ca.* 50% of the deposit. No particular trends are recorded, although at one point matrix forms nearly 70% of the breccia, indicating the diverse clast-matrix relationships within the Kilchrist deposits. The degree of roundness of clasts is highly variable and the results are plotted in Figure 7.15c. Clasts do not appear to become more or less rounded in any particular direction and peaks within the data are apparently lithologically controlled. For example, the appearance of large proportions of sub-angular clasts (>65%) at 0km and 1km is due to high concentrations of quartzite and basalt respectively. These are both resistant lithologies and less susceptible to rounding. The appearance of pebbly sandstone/breccia clasts to the eastern end of the traverse suggests a westerly transport direction that is supported by a population of rounded clasts (*ca.* 5%) in the area around Meall Coire Forsaidh. Mean clast size is typically 4-6cm and these results are plotted in Figure 7.15d. A mean clast size of 12cm is recorded at 1km, and this is due to a population of coarse basalt clasts at this locality. Otherwise, there is a slight increase in mean clast size in an easterly direction. Figure 7.15e displays the results of a linear regression on the significance of the relationship between mean clast size and distance. These studies however, indicate a poor relationship with confidence values of less than 20%.

In summary, this traverse suggests that clast composition within the breccia was controlled by country rock geology at the time of deposition. The increasing appearance in an easterly direction of clasts of breccia, of similar appearance to the main breccia mass, indicates reworking, and suggests a westerly transport direction. The proportion of matrix is highly variable and the degree of roundness of clasts appears lithologically controlled. Mean clast size increases in an easterly direction, decreasing from the possible source area. Relationships however are not strong, and due to the heterogeneous nature of these deposits, interpreting transport directions is difficult.

### 7.3.4 Conclusion

The Kilchrist breccias were deposited before the emplacement of the Eastern Red Hills Centre. These deposits were originally interpreted as 'vent agglomerate' (Harker 1904) before being re-classified by Bell (1982, 1985) & Bell & Harris (1986). The identification of ignimbrites, intrusive brecciated rhyolites and pyroclastic debris within the breccia suggests that they formed by surface or near surface explosions in a ring-dyke bounded, subsiding caldera. The breccias were then subject to surface reworking and lateritised, erosion surfaces formed (Bell 1985). Recent fieldwork has provided further evidence to support these conclusions. Sedimentary structures including stratification, reverse grading, and channels have been recognised and an intercalated, cross-bedded volcanic sandstone has been identified. A westerly transport direction has been tentatively proposed. These features demand that the breccias should be re-classified as epiclastic deposits (Cas & Wright 1987).

## **8 Discussion: Palaeotopography, environments and modes of formation of breccia deposits of the British Tertiary Igneous Province**

Chapters 5, 6 and 7 provide detailed accounts of a diverse range of breccias and conglomerates from the Hebridean area of the British Tertiary Igneous Province (BTIP). Detailed descriptions of these coarse deposits and associated rocks have been provided from each locality, together with interpretations of modes of deposition and, where possible, palaeoenvironment and palaeotopography. This chapter aims to bring these observations together to apply a more general model for the nature and origin of the breccias of the BTIP, and to contribute further ideas on the early Tertiary environments and topography.

### **8.1 Modes of formation**

#### **8.1.1 Epiclastic deposits in the British Tertiary Igneous Province**

Breccias and conglomerates from Ardnamurchan, Mull and Skye display textures resembling epiclastic, mass flow deposits. From Ardnamurchan, two formations, the Ben Hiant Conglomerate Formation (BHCF) and the Northern Conglomerate Formation (NCF) are recognised and described in Chapter 5. The BHCF is a *ca.* 150m thick deposit of coarse, stratified conglomerates interbedded with fine-grained siltstone and sandstone sedimentary units. The base of the formation overlies early Tertiary basaltic lavas, with an irregular contact, typically at low angles (<40°). The conglomerates are generally clast supported with sub-rounded clasts, ranging in size from 2cm to 5m across, set in a fine-grained sand grade matrix of comminuted material. Shattered basalt typically forms larger blocks within the conglomerate. No primary pyroclastic material is recognised. The Northern Conglomerate Formation is much thinner, but laterally more extensive. Its base overlies Moine and Mesozoic country rocks, typically with low angle, undulating contacts. The NCF conglomerates are typically clast supported with sub-rounded clasts, ranging in size from 2cm to 5m. Large 'megablocks' (up to 30m across) of shattered and fractured basalt are recognised within the conglomerate and form a distinctive present-day hummocky topography. Megablocks of calcareous sandstone (*ca.* 30m across) and broken shale (*ca.* 15m across) have also been identified.

Sedimentary structures (grading and channels) and surface features (weathered surfaces) are preserved throughout and indicate a sub-aerial mode of deposition for the BHCF and NCF deposits. No primary pyroclastic material is recognised.

Debris flows and avalanches are common epiclastic, mass flow modes of deposition whose characteristics are described in detail in Chapter 4 (Ui 1985; Glicken 1986, 1991; Smith & Lowe 1991; Yarnold 1993; Blair & McPherson 1994, 1998; Coussot & Meunier 1996; Schneider & Fisher 1998; Bertran & Texier 1999; Kessler & Bedard 2000). Many of the features of the BHCF and NCF deposits suggest a combination of debris flow and avalanche processes.

Figure 8.1 is a reconstruction of the palaeogeography of these areas during the formation of the conglomerates. In the BHCF the succession of coarse conglomerates and fine-grained sedimentary units, indicates cyclic deposition of high-energy debris flow conglomerates, interspersed with low-energy sedimentation to form sandstones and siltstones. At least 5 debris flows, of *ca.* 20m thickness each, are identified in the Ben Hiant section. In the NCF, a large avalanche event appears to have been initiated, detaching megablocks of basalt from the early Tertiary lava field. This material slid downslope, fracturing and shattering the megablocks, whilst entraining surface material from country rocks. Later, smaller flows displaying overlapping geometries filled small channels. The BHCF displays increasing clast heterogeneity, support, roundness and size in a southerly direction, whilst the same trends are recognised in a northerly direction in the NCF. A 'sedimentary watershed' between the two is proposed, reflecting a topographic high from which the conglomerates were sourced. Centre 1 intrusions of the Ardnamurchan Central Complex (ACC) cut the conglomerates and the early uplift associated with these was responsible both for the formation of the high and the initiation of the debris flows/avalanches. In both the BHCF and NCF, the presence of ignimbrite and microgranite clasts has been attributed to small, localised vents and intrusions (which may be linked to the early uplift) that are nowhere exposed by the current topography.

Evidence of mass flow processes is also identified from localities on Mull. The Loch Ba Breccia Formation (LBBF) lies within the Loch Ba Ring Dyke, which bounds Centre 3 of the Mull Central Complex (MCC) and is described in detail in Chapter 6.2. The Loch Ba breccias are coarse, stratified deposits interbedded with sandstone sedimentary units. They are poorly sorted, with clasts ranging in size from 2-50cm across, with occasional

larger basaltic megablocks up to 10m in size. Sedimentary structures (grading and channels) are preserved throughout and indicate a sub-aerial mode of deposition. No primary pyroclastic material is identified within the breccia.

The textures and sedimentary features of the Loch Ba Breccia Formation are consistent with large-scale collapse to form debris flows and avalanches. The Loch Ba Breccia Formation lies within the Loch Ba Ring Dyke and forms part of a fault-bounded subsiding block (Bailey *et al.* 1924). It appears that large masses of rock (megablocks) were detached from steep slopes (possibly the caldera walls) and from the Central Lava Group basalts within the ring dyke, (Section 6.2.4.1) and were transported by mass flow. At least two pulses of deposition are reflected in depositional surfaces with channels, with intervening quieter periods of sedimentation and reworking of surface materials. Figure 8.2 is a schematic reconstruction of these environments and the associated palaeogeography at the time of deposition.

Further breccias on Mull at Coire Mor (Section 6.3) and Barachandroman (Section 6.4) lie just outside the Mull Central Complex, in association with early Tertiary basaltic lavas. Textures again resemble those of debris flow deposits. At Barachandroman, the superposition of breccia on lava suggests that the lavas were breaking up under sub-aerial decay as the breccias were deposited. This equates with the idea of blocks of basalt being detached from a lava field by instability, possibly collapse, accumulating as basaltic debris and subsequently being transported within a mass flow. There is no evidence of primary pyroclastic processes.

At Salen on Mull (Section 6.5), a trachytic lava overlies lavas of the Plateau Formation of the Mull Lava Field. A breccia mass at the northern end of this flow seems to have formed by the collapse of basaltic and trachytic material into a small depression at the head of the flow with little subsequent transport. The break up of lava field lithologies, and their incorporation into breccia deposits suggests local instability on the early Tertiary lava field.

Two large outcrops of breccia are present on Skye (Chapter 7). The Srath na Creitheach Breccia Formation (SNCBF, Chapter 7.2), was deposited after the intrusion of the Cuillin Centre and before the Srath na Creitheach Centre of the Skye Central Complex (SCC) (Jassim & Gass 1970). The breccias are preserved within a ring faulted mass, which has undergone central subsidence. The breccias are poorly sorted, stratified deposits with sub-

rounded to sub-angular clasts ranging in size from 2cm to 50cm, set in a matrix of fine-grained, comminuted material. Intercalated with the breccia are two, well-bedded, sandstone units. Gabbro slabs (of Cuillin Centre origin) within the breccia are typically fractured towards their bases, and overlie cataclastic layers, but form present-day hummocky topography. The sandstones appear to have undergone soft-sediment deformation. No primary pyroclastic material is preserved.

The breccias are thought to have formed in a caldera that underwent central subsidence along ring-faulted margins. Within this caldera, there is strong evidence for epiclastic mass flow deposition. The gabbro megablocks are interpreted as representing large blocks of material detached from the caldera wall. As they were transported, they became fractured and brecciated, and the present-day hummocky topography reflects their projection from the surfaces of the flows. Smaller blocks broken off the gabbro slabs and additional surface material was also entrained within the flows. Pauses in debris flow activity are reflected in interbedded laterally discontinuous sandstones and siltstones. Subsequent debris flow deposition caused soft sediment deformation in the sandstones. Figure 8.3 is a schematic reconstruction of these environments and the palaeogeography at the time of deposition.

The Kilchrist breccias are found in the Eastern Red Hills Centre of the Skye Central Complex and are described in detail in Section 7.3. These heterogeneous, poorly sorted breccias are set within a matrix of fine-grained, comminuted material and are associated with a series of *in situ* extrusive ignimbrites, intrusive brecciated rhyolite stocks and volcanic sandstones (Ray 1962; Bell, B. R. 1985; Bell & Harris 1986). The Kilchrist breccias were the products of surface or near surface volcanism in a ring-faulted, subsiding caldera. Subsequent transport by collapse, erosion and surface reworking is associated with this instability and explosivity, forming lateritised breccia layers. Channel fills of stratified breccias showing reverse grading and clast imbrication provide additional evidence of surface reworking. The distribution of clasts suggests a westerly transport direction. Figure 8.4 is a schematic reconstruction of these environments and the associated palaeogeography at the time of deposition.

Localities from Ardnamurchan, Mull and Skye provide evidence for epiclastic deposition in the BTIP. Debris flow and debris avalanche textures are common and are typically linked to large-scale collapse. Features such as stratification, grading, imbrication, channel

formation, erosion surfaces and weathering are widespread, and interbedded sedimentary units indicate periods of low-energy deposition and reworking of surface materials.

Most of these breccias were originally interpreted as 'vent agglomerates' and little research has been carried out on them since. Over the years, however, our understanding of volcanoclastic breccias has broadened and developed. Agglomerates must contain certain primary pyroclastic features such as volcanic bombs (Cas & Wright 1987) and that term is not, therefore, appropriate for these deposits. Volcanic eruptions are typically short-lived, and the intervening periods (that may be hundreds or even thousands of years) are marked by surface collapse (including landslides, debris flows and debris avalanches), weathering, erosion and sedimentation. This, therefore, indicates the important role of epiclastic transport and deposition (Figs. 8.1, 8.2, 8.3 and 8.4).

Due to time and weather restrictions, only two of the major breccia outcrops within the BTIP were not studied: 1) The Sgurr Dearg 'Vents' located at the margin of Centre 1 of the Mull Central Complex; and, 2) Belig, at the margin of the Western and Eastern Red Hills centres of the Skye Central Complex. The various breccias on Rum were not considered due to recent research on these deposits. However, epiclastic deposition has been suggested for these deposits (Bell & Emeleus 1988; Troll *et al.* 2000; Donaldson *et al.* 2001). The recognition of widespread mass flow textures suggests that epiclastic modes of deposition were common within the BTIP, and that surface rather than intrusive or explosive processes were the dominant breccia-forming mechanism. A bias towards pyroclastic processes has meant that the role of epiclastic deposition within the BTIP has in the past been greatly underestimated.

The initiation of epiclastic deposition appears to have been linked to instability associated with uplift and/or central subsidence. The BHCF and NCF deposits from Ardnamurchan pre-date the emplacement of the Ardnamurchan Central Complex, and are cut by Centre 1 cone sheets and intrusions (Fig. 8.1). However, examples from Loch Ba on Mull and Srath na Creitheach and Kilchrist on Skye, formed within ring-faulted subsided masses during the emplacement of their respective central complexes (Bailey *et al.* 1924; Jassim & Gass 1970; Bell 1982; Sparks 1988) (Figs. 8.2, 8.3 and 8.4). The age of formation of the Coire Mor and Barachandroman breccias on Mull is not well constrained but may be approximately contemporaneous with, or later than, folding developed as a result of early intrusion of the Mull Central Complex. At Salen on Eastern Mull, breccia comprises a

small outcrop outwith the Mull Central Complex, and is most likely older than or approximately contemporaneous with early intrusive events. In all these examples there is a strong link between the emplacement of the central complexes of the BTIP and breccia formation.

In Ardnamurchan, the BHCF and NCF deposits formed by debris flows and debris avalanches before the emplacement of the Centre 1 intrusions. The cause of this instability has been linked to a topographic high produced by early Centre 1 uplift. This formed a sedimentary watershed from which the conglomerates were derived (Fig. 8.1). The presence of clasts of microgranite, not now exposed *in situ*, suggests the intrusion of silicic magma, that may have formed shallow domes, and ignimbrite clasts, sourced from vents that are not exposed, indicate early explosive volcanic activity. The emplacement of the Central Complexes is linked to the location of major structural faults (Fyfe *et al.* 1993). Ardnamurchan lies near the Moine Thrust Plane, towards the eastern margin of the Inner Hebrides Trough, whilst the BHCF and NCF deposits are associated with the Loch Mudle Fault and the Allt Fascaidale Fault. Faults are structurally unstable and active faulting, in conjunction with intrusion-associated uplift, and possibly small-scale localised vents, provides a mechanism for the collapse and mass flow seen in the Ardnamurchan area.

The breccias of Coire Mor and Barachandroman may be associated with the early stages of emplacement of the Mull Central Complex that led to localised uplift and folding of the country rocks. The breccias subsequently formed by the break-up of the lava field and surrounding country rocks, and transport by mass flow. The Salen breccias may represent localised lava field collapse or remnants of instability and brecciation due to the emplacement of the Mull Central Complex.

At Loch Ba on Mull and Srath na Creitheach and Kilchrist on Skye, breccias are preserved within ring-faulted subsiding blocks. At Loch Ba and Kilchrist these blocks are bounded by fault controlled mixed magma ring dykes (Bell 1982; Sparks 1988), whilst the ring faulted margin of the Srath na Creitheach deposits is defined by a zone of gabbro crushing (Jassim & Gass 1970). The Loch Ba Breccia Formation is located within Centre 3 of the Mull Central Complex, the Srath na Creitheach Breccia Formation formed between the Cuillin Centre and Srath na Creitheach Centre of the Skye Central Complex, and the Kilchrist breccias pre-date the Eastern Red Hills Centre of the Skye Central Complex. The breccia-forming events are all later stages in the development of the central complexes, at

which point intrusion and associated uplift were common and caldera-forming processes may have occurred.

Caldera-formation is complex. Originally attributed to the collapse of a magma chamber roof following evacuation of the underlying magma chamber (Williams 1941; Smith & Bailey 1968), alternative mechanisms suggested include: magma chamber tumescence (Komuro 1987), chaotic subsidence (Scandone 1990), downsagging (Walker, G. P. L. 1984), resurgence (Lipman 1984), and regional tectonism (Moore & Kokelaar 1997). Ring fractures can form due to underpressure by magma chamber evacuation (Lipman 1997) or overpressure due to doming and chamber inflation (Komuro 1987). Doming creates initial inward-dipping reverse faults and only small volumes of magma escape as lithostatic pressure exceeds magma chamber pressure (Druitt & Sparks 1984). These inward-dipping fractures may be reactivated during collapse to inward-dipping normal faults in order to accommodate subsidence (Komuro 1987; Branney 1995). Caldera evolution cannot always be explained by a single mechanism.

Troll *et al.* (2000) and Donaldson *et al.* (2001) proposed a multi-stage model for Rum that outlines the evolution of the caldera and its fill. An early, 'proto-caldera' stage includes tumescence associated with large shallow magma chambers that may cause doming, and tensile stresses, which result in caldera formation (Komuro 1987; Marti *et al.* 1994). Doming leads to the formation of ring fractures and radial tension until the central region of the dome begins to subside (Marti *et al.* 1994). This collapse depression subsequently fills with sedimentary breccias (Komuro *et al.* 1984) without the eruption of volcanic material (Donaldson *et al.* 2001). The generation of collapse breccias in a non-eruptive caldera, may explain the association of a subsiding caldera with the Srath na Creitheach and Loch Ba breccias, where no primary explosive pyroclastic material is preserved. As the calderas begin to subside, material collapses into the caldera floor by mass flow. Evidence of a caldera structure is, however, incomplete from these localities and collapse processes may simply occur due to high elevation and steep slopes.

In summary, it appears that two stages of breccia formation can be recognised related to the emplacement of central complexes. On Ardnamurchan and at Coire Mor and Barachandroman on Mull, lava field material is broken up due to the early emplacement of intrusions. On Ardnamurchan, an area of uplift formed a watershed from which a series of debris flows and avalanche conglomerates were produced. This uplift was associated with

the beginnings of Centre 1 emplacement and created instability in the early Tertiary lava field, causing block detachments and initiating mass flows (Fig. 8.1). Similar processes were involved at Coire Mor and Barachandroman. Breccias at Loch Ba, Srath na Creitheach and Kilchrist are all associated with later stages of central complexes and lie within ring faults (Figs. 8.2, 8.3 and 8.4). Mass flows related to collapse may be due to subsidence of the central ring fault block. This would create instability and collapse of material onto the caldera floor. However, evidence of a caldera structure from these localities, is incomplete, and these later stage breccias may simply be related to collapse reflecting elevation and steep slopes rather than a caldera.

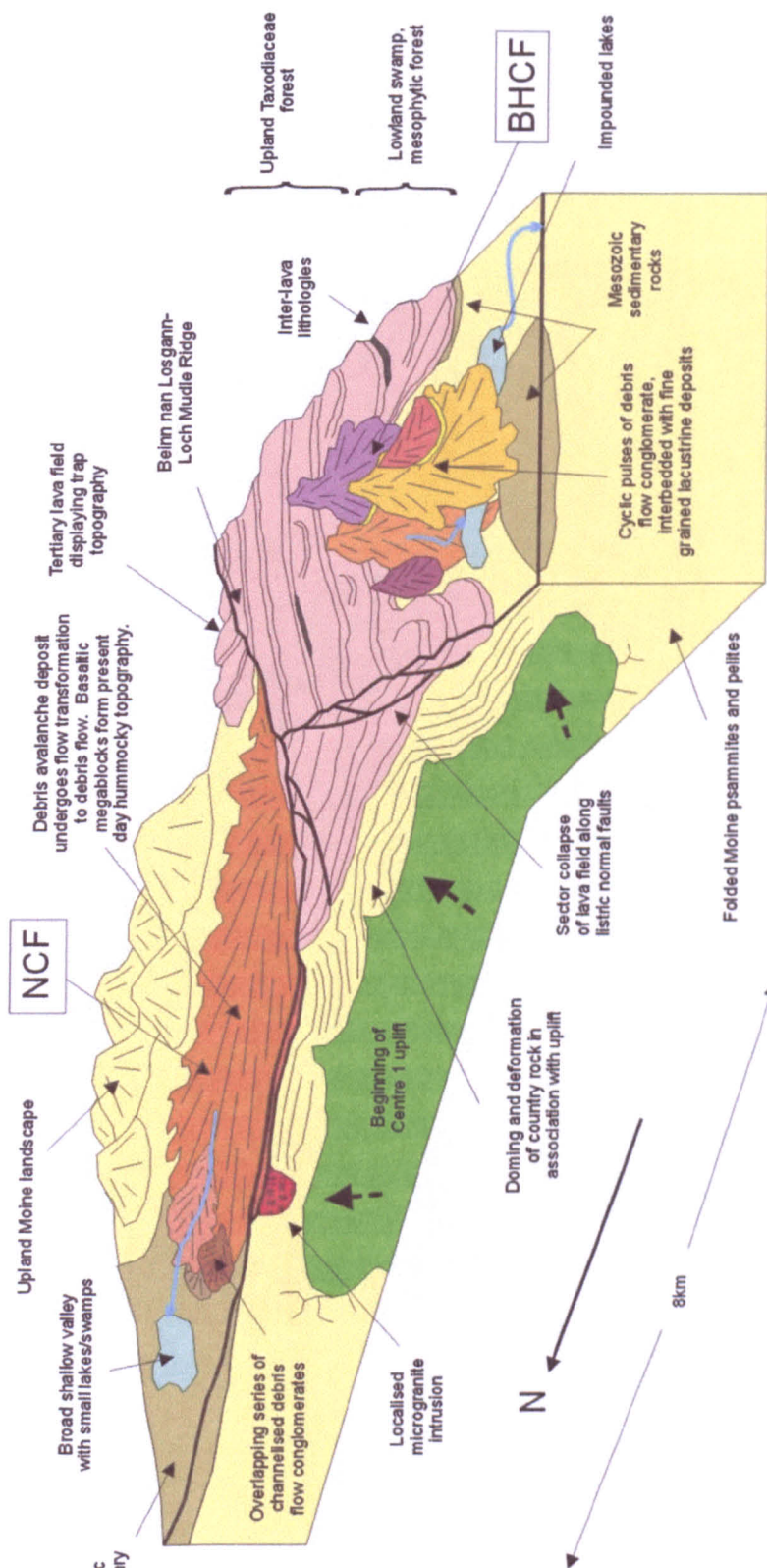


Figure 8.1 - Schematic block diagram showing a reconstruction of the palaeogeography of the Ardnamurchan area during the early Tertiary. See main text for details.

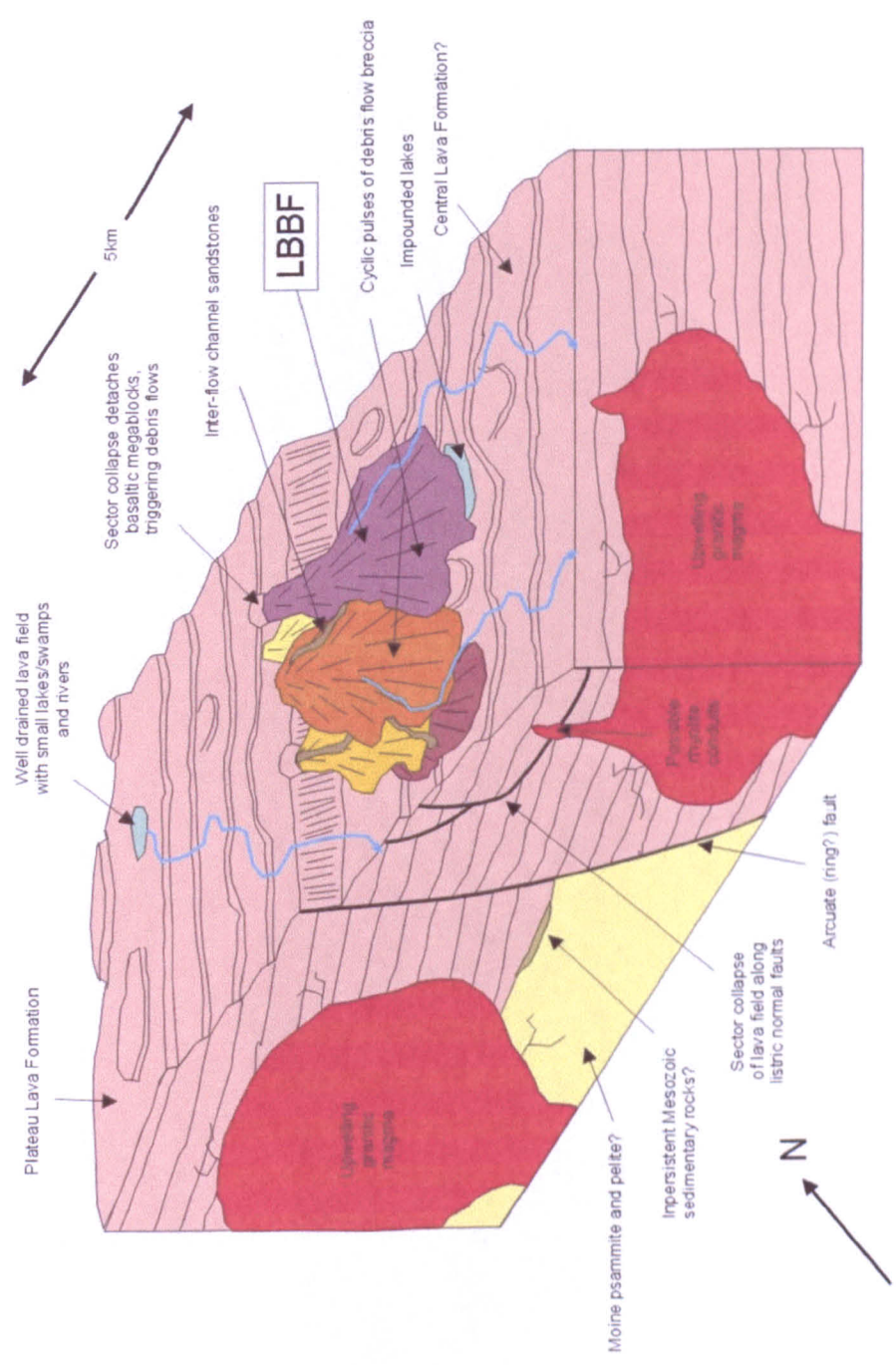


Figure 8.2 Schematic block diagram showing a reconstruction of the palaeogeography of the Loch Ba area during the early Tertiary. See main text for details.

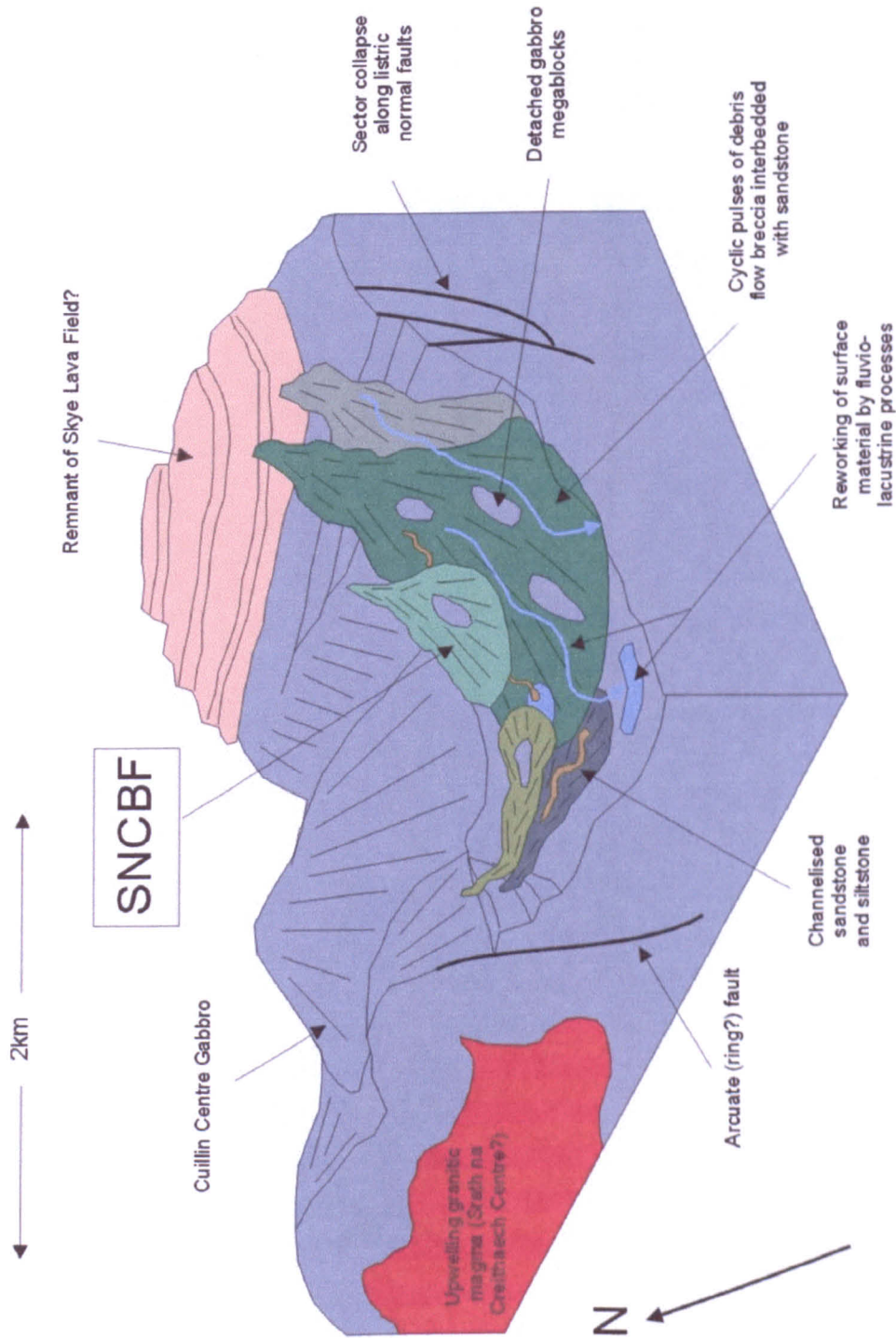


Figure 8.3 Schematic block diagram showing a reconstruction of the palaeogeography of the Strath na Creitheach area during the early Tertiary. See main text for details.

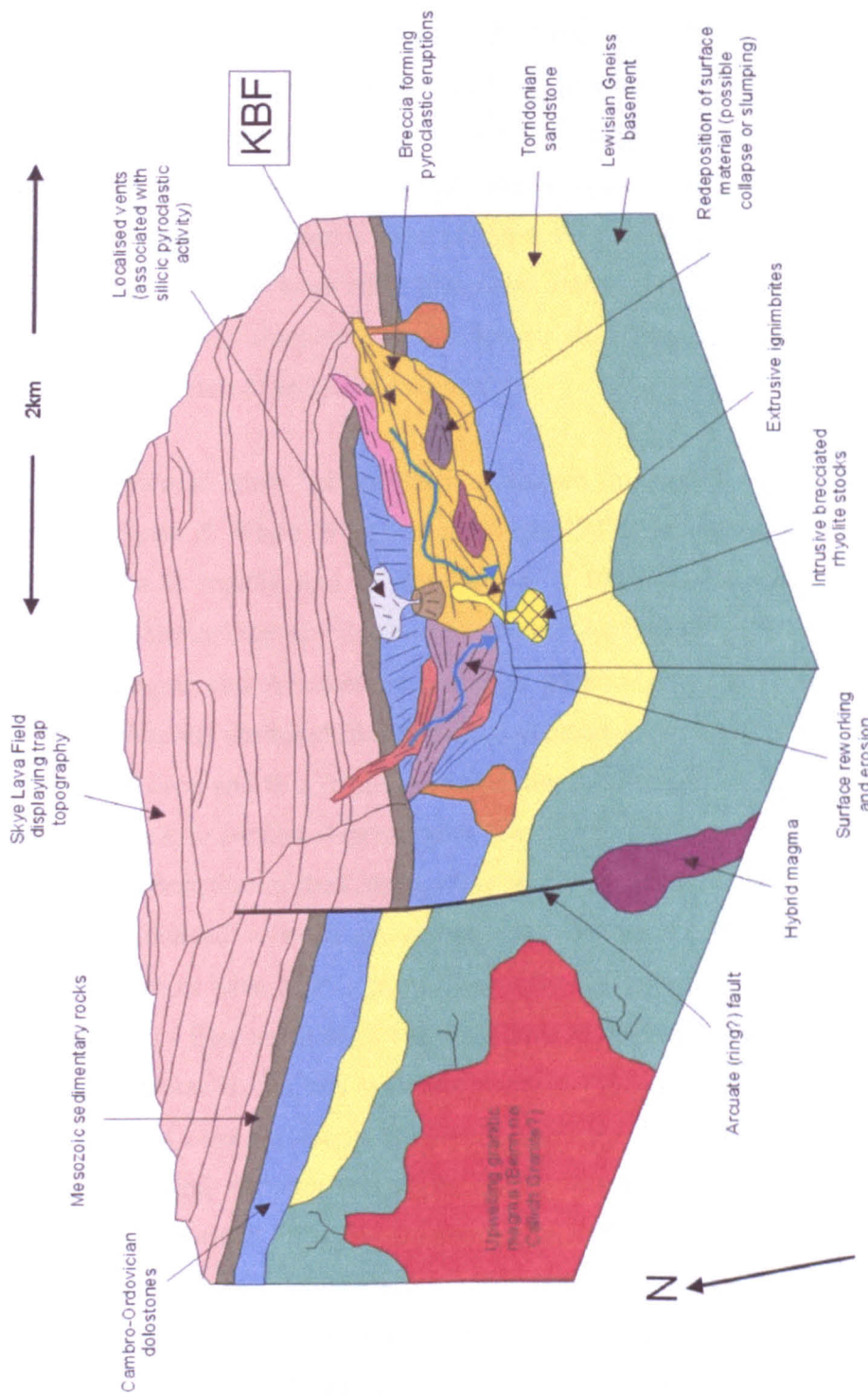


Figure 8.4 Schematic block diagram showing a reconstruction of the palaeogeography of the Kilchrist area during the early Tertiary. See main text for details.

### 8.1.2 Peperite formation in the British Tertiary Igneous Province

In addition to the epiclastic breccias described in Section 8.1.1, outcrops of peperite breccia are present in localities on Mull and Ardnamurchan. These formed early in the Tertiary and are related to the lava fields in the areas in which they are found. At Carraig Mhor, east of Carsaig Bay, Mull a series of breccias are described, with complex morphologies and relationships with sedimentary rocks (Section 6.1). The breccias comprise clasts of altered igneous material, ranging in size from 2cm to 50cm across, set in a fine-grained sedimentary matrix. Four principal clast types can be identified: (i) elongate finger-like structures; (ii) large fluid flame-like clasts; (iii) sub-rounded clasts, and (iv) small angular clasts. A complex graded sequence, displaying progressive changes in clast type and the proportion of sediment, is described.

Peperites are formed when hot magma is emplaced into wet sediment (Kokelaar 1982, 1986; Busby-Spera & White 1987; Cas & Wright 1987; Doyle 2000; White *et al.* 2000). The magma cools rapidly and as it quenches it forms clasts with parallel margins, producing an interlocking or 'jigsaw fit' texture (Kokelaar 1982). Turbulent mixing between the magma and the sediment occurs as pore-water is flash heated to steam, and blocks are explosively shattered (Bulk Interaction Steam Explosivity, Kokelaar 1986). The sediment is fluidised and fills fractures in the now solid magma, wrapping around clasts, causing lamination to parallel clast margins. Similar processes can occur in both sills and lava flows. The peperites of the Carraig Mhor foreshore were formed by the intrusion of a sill into unconsolidated, water saturated sediment. Intrusions in the same area with simple planar contacts must have been intruded when the sediment was at least partly lithified. The Lower Blocky Brecciated Lava and the Upper Graded Breccia represent a lava flow that has been emplaced into wet sediment ponded within surface channels. The Lower Blocky Brecciated Lava represents the blocky core of a lava flow whose outer margins have been brecciated, forming the Upper Graded Breccia. The grading in the Upper Graded Breccia is formed from the sinking of clasts within hot sediment, in conjunction with changes from ductile to brittle fracturing (Busby-Spera & White 1987; Squire & McPhie 2002). As magma comes into contact with wet sediment the magma behaves in a ductile manner and turbulently mixes, forming spectacular fluidally-shaped clasts. As heat is dissipated, interaction between magma and sediment is reduced and the magma simply fractures into small angular clasts, without fluidising and mobilising the sediment.

Similar morphologies are developed on the eastern side of the Loch Mudle valley, near Ben Hiant, on Ardnamurchan (Section 5.8). Within the lava field a channel *ca.* 30m across and 10m deep formed between two lava flows. The base of the channel is filled with mudstone, overlain by a breccia consisting of brown clasts of basaltic material with irregular crenulate margins set in a dark, fine-grained, matrix. This is a peperite similar to that at Carraig Mhor and formed by the inter-mingling of magma and unconsolidated, water saturated sediment (White *et al.* 2000).

The presence of peperites at Carraig Mhor and Loch Mudle provides further evidence for lava field environments in the BTIP during the early Tertiary. The peperites are restricted to small channels filled with water-saturated, unconsolidated sediments, and the mudstones and laminated siltstones reflect quiescent deposition in low-energy environments, such as impounded lakes and/or swamps. At Carraig Mhor, a thick sequence of sedimentary rocks was deposited at an early stage in the formation of the lava field.

Fossilised plant material was recovered from a siltstone towards the base of this sequence, indicating an influx of organic material. A sequence of laterally discontinuous channelised siltstones in the Carraig Mhor sequence suggests periodic fluvial deposition. An irregular topography formed due to the filling of channels with basalt lava forming peperites and well-developed columnar-jointed flows (Long & Wood 1986; Lyle 2000). Sedimentary rocks interbedded with the lavas including the mudstone at Loch Mudle, indicate deposition during hiatuses in the formation of the lava field, when the land surface was well-drained. As volcanism resumed, peperites formed locally within impounded channels. Peperites therefore represent useful environmental indicators. They are formed by autoclastic processes (quench fragmentation) and can be produced by interaction of both sills and lava flows with wet sediment. The peperites at Carraig Mhor and Loch Mudle are the first documented occurrences of such material in the BTIP. Given the abundant volcanism of the early Tertiary and the environments associated it is surprising that more of these distinctive deposits have not been recognised.

Three ignimbrites are interbedded with the sedimentary sequence at Carraig Mhor and were deposited early in the formation of the lava field. Their significance will be discussed in Section 8.4 below.

## 8.2 Palaeoenvironments of the British Tertiary Igneous Province

The identification of breccias, conglomerates and associated interbedded finer-grained sedimentary units in the BTIP, provides information on early Tertiary lava field environments. The peperites reflect the presence of small ponded channels. Tertiary sedimentation early in the formation of the Mull Lava Field comprised a series of siltstones and mudstones (Section 6.1), indicating quiet, low-energy conditions in shallow lacustrine or swamp environments, whereas the channellised sandstones and siltstones suggests a periodic fluvial input. The area was characterised by a warm, wet climate and the landscape included small lakes and abundant vegetation, indicated by fossil trees and other plant remains (Bailey *et al.* 1924; Bell & Williamson 2002). A substantial thickness of sub-aerial basaltic flows developed. Many exhibit well-developed columnar jointing, invasive lava tubes and features indicating lava ponding (Saemundsson 1970; Long & Wood 1986; Lyle 2000; Bell & Williamson 2002). The Gribun Mudstone Member marks the base of the Mull volcanic sequence, and hiatuses in volcanic activity are marked by units such as the Ardtun Conglomerate Member, which preserves leaves from ginkgo, hickory, plane, ash, redwood and swamp cypress trees (Boulter & Kvacek 1989; Jolley 1997). Spectacularly preserved leaves are also recognised from the Ardtun Leaf Beds (Duke of Argyll 1851). Fossil trees, such as Macculloch's Tree (Macculloch 1819), and the newly discovered Carsaig Tree (Bell & Williamson 2002) indicate a rich and varied flora of swamp plants and trees. Carbonised wood/plant remains have been identified from the low tide foreshore sedimentary sequence at Carraig Mhor, and provide additional evidence for such environments.

The Ardnamurchan lavas are interbedded with mudstones and rarer sandstone units and, towards Loch Mudle, a peperite. This suggests similar low-energy shallow lacustrine or swamp environments, corroborating the suggestion that the Ardnamurchan lavas are part of the Mull-Morvern lava field (Bailey *et al.* 1924). Material from interbedded siltstones and sandstones from the Ben Hiant Conglomerate Formation (Sections 5.3.4, 5.3.5, 5.3.6 and 5.3.8) has yielded a moderate amount of organic matter and palynological analysis provides information on palynofloras and environments at the time of deposition. Pollen from the BHCF is listed in Table 8.1. It is dominated by *Pityosporites* derived from pine trees and reflects input from upland sources (*ca.* 1000m relief) (Jolley 1997). Pines are

typically seen next to bounding faults, or in proximal drainage system areas. A large amount of *Inaperturopollenites hiatus*, derived from Taxodiaceae trees, probably *Metasequoia* or *Glyptostrobus*, was included. Grains of *Nyssapollenites kruschi subsp. analepticus* (Nyssaceae, *Nyssa*) and a grain of *Cupuliferoipollenites liblarensis* (Fagaceae, probably *Castanea*-type) were also identified (D. Jolley, pers. comm). *Inaperturopollenites hiatus* is a swamp cypress (Jolley 1997), whilst Taxodiaceae such as *Metasequoia* are equivalent to modern day coniferous trees such as redwoods, and represent the most common flow top vegetation throughout the lava field, forming upland forests (ca. 500m) with an understorey of ferns (Jolley 1997). The *Nyssa*- and *Castanea*-type pollens are common throughout the BTIP and the parent plants grew in swampy conditions, such as lowland swamp forests (Jolley 1997).

	BHLSM	SMMCM	BHUSM	SDSM
<b><i>Pollen &amp; Spores</i></b>				
<i>Inaperturopollenites hiatus</i>	27	22	25	24
<i>Inaperturopollenites distichforme</i>	0	0	1	0
<i>Pityosporites</i> spp.	62	72	123	150
<i>Piceapollis</i> spp.	0	0	2	1
<i>Alnipollenites verus</i>	0	2	0	1
<i>Caryapollenites circulus</i>	1	0	0	0
<i>Corrusporis</i> spp.	0	1	0	0
<i>Cupuliferoipollenites cingulum fusus</i>	0	1	0	0
<i>Cupuliferoipollenites cingulum pusillus</i>	1	0	0	0
<i>Deltoidospora adriennis</i>	4	4	4	9
<i>Laevigatosporites haardti</i>	1	2	4	2
<i>Lycopodiumsporites rotundoides</i>	0	0	2	0
<i>Momipites</i> cf. <i>tenuipolus</i>	0	0	1	0
<i>Momipites</i> spp.	0	0	2	3
<i>Momipites tenuipolus</i>	0	0	1	0
<i>Monocolpopollenites tranquilis</i>	2	2	1	1
<i>Nyssapollenites kruschii subsp. anelep</i>	1	0	3	3
<i>Stereisporites</i> (S) <i>stereoides</i>	0	1	0	0
<i>Triporopollenites coryloides</i>	0	4	1	1
<b><i>Algae</i></b>				
<i>Botryococcus braunii</i>	2	2	1	2

Table 8.1 – Summary of palynological analysis of material collected from interbedded units of the Ben Hiant Conglomerate Formation (D. Jolley, pers. comm). BHLSM = Ben Hiant Lower Siltstone Member; SMMCM = Sron Mhor Middle Conglomerate Member (collected from lenticular bodies of siltstone); BHUSM = Ben Hiant Upper Siltstone Member; SDSM = Stallachan Dubha Sandstone Member.

Minor amounts of fern material were collected. *Laevigatosporites haardti* is a typical early swamp colonist, and *Deltoidospora adriennis* is a Cyathaceae tree fern, representing early colonising vegetation. *Corrusporis*, *Stereisporites*, (a Bryophyte) and *Lycopodiumsporites rotundoides* are low frequency ferns. *Momipites* and *Caryapollenites* species are derived from swamp dwelling angiosperms of the Juglandaceae (Walnuts, Hickories, Pecans). *Alnus* (Alder) is another swamp/marsh plant. *Monocolpopollenites tranquilis* (Ginkgo), *Triporopollenites coryloides* (Myricaceae – myrtles etc.) and *Cupuliferoipollenites* (Fagaceae) imply a dryer, more stable habitat. *Botryococcus braunii* is a chlorophycean algae, implying static freshwater (lacustrine) conditions (D. Jolley, pers. comm). No evidence of any marine or estuarine influence is preserved. A minor amount of pollen derived from reworking of Jurassic material is preserved. Taken together, this evidence suggests a palynoflora of swamp trees in lowland basins and lakes, flanking an upland area dominated by Taxodiaceae and Pine forests (Fig. 8.1). Similar environments are recognised on Skye (Jolley 1997).

Correlations can be made between these results and information from localities on Mull and Ardnamurchan. Simpson (1961) collected material from Ardslnish at the bottom of the Ardnamurchan lava pile. A coal seam from a sedimentary sequence at the base of the lavas, contains abundant *Nyssa* grains. *Nyssa* is common in the BTIP but only occurs in large quantities in interbedded units high up in the Staffa Formation (Bailey *et al.* 1924; Kerr 1995) of Mull (D. Jolley, pers comm). Williamson *et al.* (in prep.) have identified a series of Palaeogene surfaces, labelled A1 (pre-Staffa Formation surface) to A6 (pre-Plateau Formation surface). *Nyssa*-type grains are only common at the A6 horizon (D. Jolley, pers comm), and this therefore suggests a similar age for the material collected by Simpson (1961) from Ardslnish. This material is closely comparable with that collected from the Ben Hiant Conglomerate Formation and indicates similar environments and palynofloras in both Ardnamurchan and Mull at the time.

The presence of swamp palynofloras and impounded lakes suggests that the early Tertiary land surfaces were well-drained. Debris flow and avalanche deposits are common in the BTIP (Sections 5,6,7 and 8.1.1) and the collapse of material to initiate these mass flows can be assisted with heavy rain (Caine 1980; Innes 1983; Pierson 1986; Smith & Lowe 1991). Loose surface material becomes more mobile under such wet conditions (Pierson & Scott 1985; Smith & Lowe 1991). Eruptive activity, sector collapse, earthquakes, breaching of crater lakes and uplift may also contribute to the initiation of debris flows and

avalanches (Smith & Lowe 1991). Caine (1980) and Innes (1983) attempted to quantify the amount of rainfall required to initiate these events. Caine (1980) suggested a threshold for debris flow initiation could be expressed in terms of a limiting curve:

$$I = 14.82D^{-0.39}$$

where  $I$  = rainfall intensity ( $\text{mm hr}^{-1}$ )

$D$  = duration of rainfall (hr)

When  $I < 14.82D^{-0.39}$ , debris flow activity is unlikely to occur, although this is only a limiting curve and more rainfall may be required. Innes (1983) developed a similar curve illustrating the rainfall amount-duration relationship that has been reported as triggering a debris flow:

$$T = 4.9355D^{0.5041} \quad (2)$$

where  $T$  = total rainfall in period (mm)

$D$  = rainfall duration (hr)

Results indicate that anything between 10 to 75mm of rainfall per hour may be required to initiate flows. Current annual rainfall in Britain ranges from 1000 mm to 5000mm (Meteorological Office) and these figures therefore represent significant amounts of rain, falling in a short time. The early warning system in California suggests that for a rainfall of ~15 mm per hour the threshold time for the onset of mud/debris flows varies from 8 to 14 hours depending on slopes and material available (Bryant 1991). In summary, the identification of debris flow and avalanche deposits in the BTIP is indicative of prolonged periods of heavy rainfall, suggesting a relatively wet environment in the early Tertiary.

## 8.3 Palaeotopography of the British Tertiary Igneous Province

Analysis of clast/matrix relationships and distributions provides evidence for a sedimentary watershed in the Ardnamurchan conglomerates. This watershed between Beinn nan Losgann and the Loch Mudle area represents a high point from which the conglomerates have been derived, a topography broadly reflected in the current land surface and coincident with the 'long axis' of the Ardnamurchan Central Complex. It has been suggested that the beginning of emplacement of the Centre 1 intrusions of the Ardnamurchan Central Complex provided uplift that resulted in doming of the country rocks (Section 5.7). The area around Loch Mudle and Beinn nan Losgann therefore formed a topographic 'high' from which the conglomerates were derived by mass flow. This may not have been the highest point or the focus of intrusion and uplift, and there is no evidence to suggest that there was a single point source of intrusion. However, the area does appear to have provided significant relief (Fig. 8.1).

To the north of the watershed, conglomerate (NCF) currently fills the Achateny valley as far as the northern coastline, covering an area of approximately 10km<sup>2</sup>, dipping at *ca.* 5° to the north. The conglomerate is confined within this present day valley, but to the east a landscape of undulating hills composed of Moine psammities and pelites, up to 350m above sea level is present. Therefore, these Moine outcrops are considerably higher than the Moine preserved in the Achateny valley at approximately 110m, which are in places overlain by Mesozoic sedimentary lithologies. This suggests that a valley (or basin) broadly approximating to the current topography controlled the deposition of conglomerates in this area during the early Tertiary. Debris flows and avalanches moved down this valley under gravity and appear to be relatively confined, although relationships are obscured to the west of Achateny valley by Centre 2 and 3 intrusions (Fig. 8.1).

In the BHCF, the most northerly exposure of conglomerate, in the East Ben Hiant Gully area, lies 250m above sea level and forms a thin veneer (of conglomerate) proximal to the Beinn nan Losgann-Loch Mudle watershed. Over a distance of 2.5km the conglomerate descends in a series of oversteps in a southerly direction, to sea level. There is no evidence of faulting to explain this descent. Such slopes represent a 1:10 incline, which is a significant gradient. The BHCF lies unconformably on country rocks and if this unconformity is drawn in cross section a series of 'steps' are recognised, forming, in

places, more precipitous slopes ( $>45^\circ$ ) that would be prone to structural collapse (Fig. 8.5). Scree and other debris collect easily on steep slopes and would be available for accumulation into debris flow deposits.

Therefore, the early Tertiary topography of Ardnamurchan consisted of relatively steep slopes forming north- and south-trending drainage basins. The numerous clasts of angular basalt in the conglomerates indicate that the catchment was most likely the lava field around the Beinn nan Losgann-Loch Mudle area. Palynological evidence suggests that this catchment was of significant relief supporting upland Taxodiaceae and Pine forests. The drainage basins formed broad valleys, which were drained by rivers and small lakes. There is no evidence of any marine or estuarine influence (Fig. 8.1).

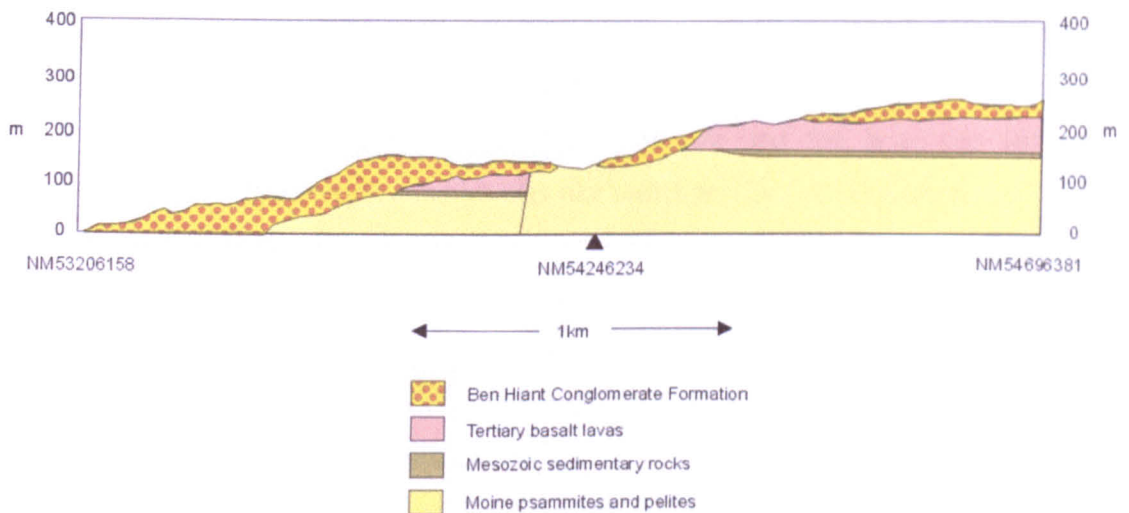


**Figure 8.5 – Simplified cross section showing the relationships of the Ben Hiant Conglomerate Formation with country rock lithologies.**

The BHCF and NCF of Ardnamurchan were developed in the infancy of the Ardnamurchan Central Complex. Breccias from Loch Ba on Mull and Srath na Creitheach and Kilchrist on Skye however, were developed much later in the emplacement of their respective central complexes. Debris flow and avalanche structures have been identified from these localities (Sections 6.2, 7.2 and 7.3) and therefore mechanisms of central collapse and landslides are associated with their development (Figs. 8.2, 8.3 and 8.4).

These mass movements require significant relief to develop and uplift and central subsidence have been suggested as possible sources. The intrusion of a central complex is a source of uplift that has been estimated at *ca.* 1km on Skye (Bell & Harris 1986; Jolley 1997). Models of caldera subsidence resulting from uplift have been suggested for Loch Ba (Bailey *et al.* 1924), Srath na Creitheach (Jassim & Gass 1970) and Kilchrist (Bell 1982). Caldera walls are steep (commonly near-vertical), fault-controlled surfaces, and due to the instability caused by subsidence, would provide an appropriate topography for the initiation of sector collapse and mass movement. However, evidence for caldera subsidence is incomplete at these localities and the initiation of mass flow processes may simply be due to the break up of surface materials on steep slopes.

## 8.4 Magmatic Processes in the British Tertiary Igneous Province

The lava fields of the BTIP are fissure fed continental flood basalts (Bell & Williamson 2002) and represent the early stages of rifting and plume impact in the NE Atlantic. Volcanism is typically effusive rather than explosive and the lavas are commonly unevolved alkali olivine basalts and MORB-like tholeiites (Bell & Williamson 2002). The most evolved lavas are the tholeiitic basalts, mugearites and trachytes of the Coire Gorm Group (Kerr 1995), formerly the Pale Group of the Central Lava Formation of Mull (Bailey *et al.* 1924). Silicic magma and associated volcanism has, however, also been identified in the deposits described in this study. Rhyolitic ignimbrite is recognised from localities on Ardnamurchan, Mull and Skye and an *in situ* ignimbrite is recognised at Carraig Mhor, near Carsaig Bay, Mull. The latter lies below the Plateau Formation of the Mull Lava Field and is evidence of silicic pyroclastic activity early in the lava field development. Ignimbrite clasts in the Ben Hiant conglomerates of Ardnamurchan, suggest the presence of small, localised vents in this area, before the conglomerates were deposited. The Ben Hiant ignimbrites are not exposed in the current topography. Trachyte clasts have also been identified in the Ben Hiant conglomerates. Only one minor flow of trachyte is exposed in the Ben Hiant area, but clasts of this lithology in the conglomerates suggest that abundant trachytic material may have been erupted previously, but is not preserved. Rhyolites and ignimbrites from Kilchrist, Skye (Ray 1962; Bell 1985; Bell & Harris 1986) indicate continuing silicic pyroclastic activity throughout the early Tertiary.

The association of basaltic and silicic magmas in the early Tertiary has long been recognised (Bell, J. D. 1966; Walker, G. P. L. 1975) and the presence of silicic magma throughout the evolution of the BTIP is explained in terms of fractional crystallisation and crustal melting. The eruption of silicic magma before the onset of continental flood basalt volcanism, however, has only recently been recognised (Mitchell *et al.* 1999), and small-scale crustal melts are tentatively proposed as the source of this evolved magma.

## 9 Conclusions

The objective of this thesis has been to describe the nature of breccias associated with central complexes and lava fields of the British Tertiary Igneous Province (BTIP). These descriptions allow models to be developed to elucidate surface and near surface processes of breccia formation that have important implications for palaeoenvironments and palaeotopography during the formation of the BTIP. Studies were carried out by means of extensive fieldwork in conjunction with petrography and laboratory research. Localities studied included the Ben Hiant and Achateny Valley areas of Ardnamurchan; Barachandroman, Carraig Mhor, Coire Mor, Loch Ba and Salen on Mull; and Kilchrist and Srath na Creitheach on Skye. The rocks in many of these were classically defined as 'vent agglomerates,' implying an explosive, pyroclastic, mode of formation close to a vent. However, detailed re-examination and interpretation of these deposits, has suggested the importance of epiclastic processes to their fragmentation, transportation and deposition. New localities provide evidence on the formation of breccias displaying peperite textures. Together, these breccias provide new insights into the palaeoenvironments and palaeotopography of the BTIP.

### 9.1 Debris flows and avalanches

'Breccias' on Ardnamurchan were identified as the 'Ben Hiant Vents' and 'Northern Vents' by Richey & Thomas (1930). Richey (1938) suggested that these Ben Hiant agglomerates were the fillings of vents undergoing a rhythmic series of eruptions and that interbedded fine-grained units represented volcanic ashes, or 'tuffs.' The presence of similar clast types in the Northern Vents was used to suggest a comparable origin.

The 'breccias,' however, are typically conglomerates comprising sub-rounded to rarer angular clasts of various lithologies, set in a fine-grained matrix of comminuted but similar material, in both clast- and matrix-supported relationships. Two formations, the Ben Hiant Conglomerate Formation (BHCF) and the Northern Conglomerate Formation (NCF) are recognised. The conglomerates are stratified and display sedimentary features such as grading, imbrication and erosional surfaces. Interbedded siltstone and sandstone members commonly fill channels on the conglomerate surface and exhibit muddy laminae, cross bedding and sandy layers, indicative of fluvio-lacustrine deposition. In the NCF shattered

megablocks (up to 30m across) form the present-day hummocky topography. These were previously identified as *in situ* remnants of the lava field.

The textures of the BHCF and NCF are typical of debris flow and avalanche deposits and indicate surface deposition. These mass flow deposits comprise typically rounded clasts and contain sedimentary structures such as grading, imbrication and channels. Coarser material is pushed to the front of the flows due to dispersive shear pressures, and the transition from small, angular clasts to large, rounded clasts indicates flow direction. The BHCF displays increasing clast heterogeneity, degree of clast support, roundness and size in a southerly direction, whereas the NCF shows similar trends to the north. A sedimentary watershed in the Beinn nan Losgann-Loch Mudle area forms a topographic high from which the conglomerates were derived. This may be linked to uplift and doming associated with the early emplacement of Centre 1 intrusions of the Ardnamurchan Central Complex. There is no evidence to suggest a single point of intrusion. Sandstones and siltstones interbedded in the BHCF indicate quiet lacustrine deposition between debris flow events. Shattered basaltic megablocks in the NCF reflect catastrophic collapse of the lava field (possibly along faults) initiating debris avalanche events. As flows spread out, blocks became fractured and surface materials were entrained by 'bulking.' Overlapping flows, indicate episodic deposition. No primary pyroclastic material is recognised and, therefore, these are not agglomerates.

Breccias from Barachandroman, Coire Mor, Loch Ba and Salen on Mull, display similar debris flow textures. Examples from Barachandroman, Coire Mor and Salen from the Mull Lava Field are typically poorly stratified deposits comprising sub-rounded clasts set in a fine-grained matrix. Larger blocks of shattered basalt are also present and were detached from the lava field by collapse, accumulating as loose debris before transport as mass flows. Sector collapse may reflect uplift beginning the emplacement of the Mull Central Complex (MCC). No evidence of primary pyroclastic activity is preserved. Loch Ba lies in Centre 3 of the MCC, within a ring dyke thought to define an area of central subsidence and comprising outcrops of Central Lava Group basalts, breccias and (rare) rhyolite. Debris flow features including stratification, grading, and shattered megablocks, are abundant in the breccia and lenticular bodies of sandstone indicate surface reworking of fines. These features reflect episodic collapse of the margins of the lava field and transportation by mass flows. Uplift or subsidence or both may initiate collapse, perhaps associated with caldera subsidence. Mass flow may be initiated simply by instability on a

steep topography. No primary pyroclastic material is recognised and, therefore, these are not agglomerates.

Breccias from Srath na Creitheach and Kilchrist lie within ring fault bounded structures in the Skye Central Complex, and their formation has also been attributed to central subsidence in conjunction with explosive activity. At Srath na Creitheach, stratified breccias, channels and erosion surfaces are interpreted as reflecting debris flow deposition. Interbedded sandstones indicate surface reworking of fines from the breccias. Large gabbro blocks have probably detached from the nearby Cuillin Centre, within mass flows. Flow initiation may have been due to caldera collapse and subsidence, although evidence for a caldera is not complete, or may simply reflect instability on steep slopes. The Kilchrist breccias have been regarded as forming from the reworking and redeposition of pyroclastic breccias. Sedimentary features such as grading, channels, imbrication of clasts, slump structures and intercalated cross-bedded sandstones, have provided further evidence for such a mode of deposition.

Together, these localities indicate that epiclastic deposition was common in the BTIP. The numerous sedimentary structures and debris flow textures indicate a surface mass flow origin. No primary pyroclastic material is present and these are not agglomerates. Deposition was episodic with periods of debris flow activity interspersed by periods of quiescent sedimentation. Mass flows are high-energy events linked to sector collapse caused by uplift or subsidence, or both, by faulting and also related to heavy rainfall.

## 9.2 Peperites

Breccias cropping out at Carraig Mhor, east of Carsaig Bay on the south coast of Brolass, Isle of Mull, show a complex interaction between pale igneous clasts with a variety of morphologies, and a dark, finely laminated, sedimentary matrix. These breccias are 'peperites' formed by the inter-mingling of magma with unconsolidated, water-saturated sediments. The igneous clasts were originally of glassy basic material, now thoroughly altered, and display margins ranging from angular through curvilinear to crenulate. Four clast populations are identified. Large flame-like clasts have highly irregular margins and bulbous and finger-like projections. Some clasts show an interlocking or 'jigsaw' fit. As magma and sediment interact, pore-water within the sediment is heated and explosively expands, quenching and shattering the basaltic magma. The sediment becomes fluidised,

filling fractures and voids between clasts. Lamination within the sediment parallels some clast margins.

Peperites are present near to the top of the Staffa Lava Formation at Carraig Mhor. On the foreshore they intrude a series of siltstones and mudstones, and represent sills or shallow sheets whose margins have inter-mingled with wet, unconsolidated sediment. Two distinct units are present in the overlying cliff section. The Lower Blocky Brecciated Lava (LBBL) is a blocky, fractured unit that represents the core of a lava flow. The Upper Graded Breccia (UGB) represents the brecciated margins of the LBBL. The base of the LBBL rests in a sequence of channels, indicating emplacement of the lava into a series of small lakes filled with water-saturated clastic deposits, mainly silts and muds.

The UGB fines upwards, from large sub-horizontally aligned, irregular, flame-shaped clasts set in a fine-grained matrix forming *ca.* 50% of the unit, to a 'network' breccia of small angular clasts with sediment comprising *ca.* 25% of the unit. Grading formed by the sinking of clasts within hot wet sediment, in conjunction with a change from ductile to brittle fracturing. The magma reacts in a ductile fashion with wet sediment, and mixes turbulently, to produce highly irregularly-shaped clasts. Heat is quickly lost however, preventing this interaction between the magma and sediment. The sediment is no longer fluidised and the magma simply fractures into small angular clasts.

A peperite also fills a 50m by 10m channel in the Ardnamurchan lava field forming brown clasts with irregular crenulate margins set in a dark brown, silt grade matrix.

### 9.3 Palaeoenvironments and topography

Palynological analysis of interbedded siltstones from the BHCF recovered large amounts of organic matter. Pollens provide information on floras and environments at the time of deposition. These are dominated by *Pityosporites*, derived from Pine trees, reflecting input from upland sources (*ca.* 1000m) and more common next to bounding faults or supposed steeper slopes. Samples are also rich in material derived from Taxodiaceae trees, which were the dominant vegetation of the lava fields and formed upland (*ca.* 500m) forests with an understorey of ferns. *Nyssapollenites kruschi subsp. analepticus* and *Cupuliferoidapollenites liblarensis* indicate lowland swampy conditions nearby. No evidence of any marine or estuarine influence is preserved.

Peperites in the lava fields of both Ardnamurchan and Mull provide further evidence of standing water, reflecting small, impounded channels filled with silt and mud. Plant remains from siltstones towards the base of the Carraig Mhor sequence on Mull reflect a diverse flora.

Evidence of debris flows/avalanches in the BTIP is abundant. Mass flows are high-energy events linked to catastrophic sector collapse caused by uplift or subsidence or both, and are typically initiated by periods of heavy rainfall, up to 75mm per hour. Such high rainfall values provide further evidence of wet environments in the BTIP during the early Tertiary. These flows spread out over wide areas and indicate high-energy events during hiatuses in volcanic activity. No primary pyroclastic material is recognised and, therefore, these deposits are not 'agglomerates'.

Debris flows and avalanches are associated with steep slopes. Clast-matrix relationships indicate an elevated area around Beinn nan Losgann-Loch Mudle on Ardnamurchan, from which debris flows were derived. This elevation may reflect doming and uplift associated with emplacement of the Ardnamurchan Central Complex. The BHCF fills a topography of sheer slopes dropping towards sea level. Together, these features indicate relatively steep slopes and a significant topography at the time of deposition. Pond deposits are found only in distal parts of flows that were initiated in areas of high relief and spread out into gently sloping valley floors in lowland areas. Details of the early Tertiary topography of Ardnamurchan can be seen around the Achateny Valley. The NCF is confined within the present valley floor, but to the east Moine rocks form a landscape of undulating hills, up to 240m above. Therefore, the present landscape broadly exhumes the early Tertiary topography of this area.

Debris flow deposits on Mull and Skye indicate transport of material from steep slopes formed by sector collapse and faulting. A model of caldera subsidence has been suggested for breccias from Loch Ba in Mull and Srath na Creitheach and Kilchrist on Skye, due to their location within ring-faults. Debris flows could have been initiated by collapse of caldera walls surrounding a rapidly subsiding central block, or simply by instability on a steep topography.

## **9.4 Ignimbrites and silicic intrusions**

Clasts of ignimbrite within the BHCF and less commonly in the NCF provide evidence for silicic pyroclastic activity on Ardnamurchan early in the volcanic episode, although such rocks are not now exposed. However, outcrops of ignimbrite are present at Carraig Mhor, close to the top of the Staffa Lava Formation, on SW Mull and indicate similar early silicic pyroclastic activity. Microgranite clasts in the conglomerates on Ardnamurchan suggest early intrusions of silicic magma that may be linked to doming and uplift of the Central Complex.

## 10 Appendix A: Ignimbrites

A number of ignimbrites and tuffs have been identified throughout the British Tertiary Igneous Province (BTIP) (Bell, B. R. 1985; Bell & Harris 1986; Bell & Emeleus 1988; Donaldson *et al.* 2001). These pyroclastic deposits are useful marker units, which assist with understanding the stratigraphy and evolution of ancient volcanic settings, as they indicate the nature of the volcanism and can commonly be traced over wide areas to correlate eruptive events. Furthermore, the mineralogy and chemistry of these deposits allow accurate age dating to be carried out using radiogenic isotope techniques, and therefore aid our knowledge of geological history. Volcanism in the BTIP was dominated by basaltic magma, forming the Eigg, Mull and Skye lava fields. Determining the ages of these lava fields can be difficult due to the shortage of appropriate material, and as a result of intense weathering and alteration. However, suitable material from these lava fields has recently been dated using a variety of appropriate techniques. The following data were obtained:

Eigg Lava Field:  $60.6 \pm 0.1$  Ma (Chambers & Pringle 1999)

Mull Lava Field:  $60.56 \pm 0.3$  Ma (Chambers & Fitton 2000)

Skye Lava Field:  $58.91 \pm 0.18$  Ma (Bell & Williamson 2002)

The Eigg Lava Field was dated using the Ar-Ar technique from a sanidine bearing tuff at the base of the lava field sequence on the Isle of Muck (Chambers & Pringle 1999). The Mull Lava Field was dated using the Ar-Ar technique from a lava sample close to the base of the lava pile (Chambers & Fitton 2000). The Skye Lava Field was dated using the Ar-Ar technique from a trachytic tuff close to the top of the sequence (Bell & Williamson 2002). These results provide good age constraints for lava field events in the BTIP. Accurate dating was difficult in the past when the K-Ar technique was applied, but now, using Ar-Ar and U-Pb methods, results are more accurate and precise. Significantly, ignimbrites and tuffs have been identified from both near the base and high up in the BTIP lava fields and their mineralogy and chemistry enable these precise methods to be used. Therefore, a more accurate picture of the chronology of the BTIP can be developed.

Samples collected as part of this thesis can be used to accurately date events in the early Tertiary (Palaeogene). Material for analysis has been collected from the following localities.

As described in Section 6.1.4, three ignimbrite deposits are identified from Carraig Mhor on the south coast of Mull, and are located below the Mull Plateau Lava Formation at the base of a 10m thick sequence of sandstones and mudstones. Pale brown to yellow, with well-developed fiamme (*ca.* 2mm across) and eutaxitic texture, the Carraig Mhor ignimbrites contain alkali feldspar phenocrysts (*ca.* 1mm across). The feldspar is fresh and zircon crystals are common. Sparse lithics of basalt are also present. The upper two ignimbrite deposits grade vertically into quartz-rich, laminated siltstone. These ignimbrites indicate silicic pyroclastic activity early in the construction of the Mull Lava Field, and should yield an age for the initiation of volcanism on Mull.

Blocks of ignimbrite are recognised in the conglomerate deposits of Ben Hiant (see Chapter 5). The Ben Hiant conglomerate was formed after the eruption of the Ardnamurchan Sector of the Mull Lava Field. This material weathers pink-brown to grey, with a purple to grey eutaxitic texture. Sparse lithics of basalt are present. It contains relatively fresh phenocrysts of anorthoclase (1-3mm across), and occasional microphenocrysts, typically 1mm in length, of quartz and biotite. Zircon crystals are common. Fiamme range from 0.05 to 0.5mm across and surround and drape the anorthoclase phenocrysts. Some layers consist of fine-grained randomly aligned plagioclase laths. Although this ignimbrite occurs only as clasts within the conglomerate it again indicates silicic pyroclastic activity in the early Tertiary.

Ignimbrite has been collected in situ from Carraig Mhor, Mull and as clasts from the conglomerates of Ben Hiant, Ardnamurchan. The relatively fresh nature of these deposits, and the presence of abundant fresh feldspar and zircon crystals, should enable precise dates to be obtained using Ar-Ar and U-Pb methods. These dates can be used to determine the ages of the lava fields, and, as a result, this will considerably increase our understanding of the chronology of the BTIP.

## 11 Appendix B: Samples List

All samples are housed in the Hunterian Museum Annexe, Thurso Street, University of Glasgow. A further collection of hand specimens is housed in the rock store of the Division of Earth Sciences, Gregory Building, Lilybank Gardens, University of Glasgow.

### Ardnamurchan

Sample No.	Description	Location
BH1.2	Ben Hiant Conglomerate Formation Hand Specimen, comprising sub-rounded to sub-angular clasts (2cm to 20cm across), typically of basalt, set in a dark, fine grained matrix	Loose block from MacLean's Nose, SW of Ben Hiant, Ardnamurchan (NM533616)
BH1.2a	Ben Hiant Conglomerate Formation (BH1.2) Thin Section	
BH1.2b	Ben Hiant Conglomerate Formation (BH1.2) Thin Section	
BH1.11	Ben Hiant Lower Siltstone Member Hand Specimen. Light grey, bedded siltstone, with muddy laminae	In the cliff section NE of MacLean's Nose, Ben Hiant, Ardnamurchan. See Figure 5.6. (NM53706196)
BH1.11a	Ben Hiant Lower Siltstone Member (BH1.11) Thin Section	
BH1.14	Ben Hiant Conglomerate Formation Thin Section, comprising sub-rounded to sub-angular clasts (up to 3cm across), typically of basalt and siltstone, set in a dark, fine grained matrix	Loose block from MacLean's Nose, SW of Ben Hiant, Ardnamurchan (NM533616)
BH1.15	Ben Hiant Upper Siltstone Member Hand Specimen. Light grey siltstone with muddy laminae	In the cliff section NE of MacLean's Nose, Ben Hiant, Ardnamurchan. See Figure 5.6. (NM53706197)
BH1.15a	Ben Hiant Upper Siltstone Member (BH1.15) Thin Section	
BH1.15b	Ben Hiant Upper Siltstone Member (BH1.15) Thin Section	
BH1.17	Calcified, white sandstone clast from the Ben Hiant Upper Siltstone Member	
BH1.17a	Thin section of calcified, white sandstone clast (BH1.17) from the Ben Hiant Upper Siltstone Member	
BH1.17b	Cathodoluminescence section of calcified, white sandstone clast (BH1.17) from the Ben Hiant Upper Siltstone Member	

BH1.20	Ben Hiant Conglomerate Formation Thin Section, comprising sub-rounded to sub-angular clasts (up to 3cm across), typically of basalt and siltstone, set in a dark, fine grained matrix	Loose block from MacLean's Nose, SW of Ben Hiant, Ardnamurchan (NM533616)
BH1.22	Moine psammite clast from the Ben Hiant Conglomerate Formation	<i>In situ</i> clasts from the cliff section NE of MacLean's Nose, Ben Hiant, Ardnamurchan. See Figure 5.6. (NM53656191)
BH1.22a	Thin section of Moine psammite clast (BH1.22) from the Ben Hiant Conglomerate Formation	
BH1.23	Amygdaloidal basalt clast from the Ben Hiant Conglomerate Formation	<i>In situ</i> clasts from the cliff section NE of MacLean's Nose, Ben Hiant, Ardnamurchan. See Figure 5.6. (NM53656191)
BH1.23a	Thin section of amygdaloidal basalt clast (BH1.23) from the Ben Hiant Conglomerate Formation	
BH1.24	Plagioclase megacrystic basalt clast from the Ben Hiant Conglomerate Formation	
BH1.24a	Thin section of plagioclase megacrystic basalt clast (BH1.24) from the Ben Hiant Conglomerate Formation	
BH1.25	Porphyritic basalt clast from the Ben Hiant Conglomerate Formation	
BH1.25a	Thin section of porphyritic basalt clast (BH1.25) from the Ben Hiant Conglomerate Formation	
BH1.27	Ignimbrite clast from the Ben Hiant Conglomerate Formation	
BH1.27a	Thin section of ignimbrite clast (BH1.27) from the Ben Hiant Conglomerate Formation	
F1.1	Northern Conglomerate Formation (NCF) Hand Specimen from Fascaidale Bay comprising microgranite and basalt clasts	West of Fascaidale Bay in the Northern Conglomerate Formation, Ardnamurchan (NM49717097)
F1.1a	Northern Conglomerate Formation Thin Section from Fascaidale Bay comprising microgranite and basalt clasts (F1.1)	
MNC1	Porphyritic dolerite with granitic net veining from 'Centre 3 Breccias,' Meall nan Con	From the summit of Meall nan Con, Ardnamurchan (NM50396807)
MNC1a	Thin section of porphyritic dolerite with granitic net veining from 'Centre 3 Breccias,' Meall nan Con (MNC1)	
PB3	Calcareous sandstone clast from the Northern Conglomerate Formation	Tidal pond east of Portban, west of Kilmory Bay, in the NCF, Ardnamurchan (NM52067085)
PB3a	Thin section of calcareous sandstone clast (PB3) from the Northern Conglomerate Formation	

PB7	Laminated siltstone clast from the Northern Conglomerate Formation	From the Portban area, west of Kilmory Bay, in the NCF, Ardnamurchan (NM516705)
PB7a	Thin section of laminated siltstone clast (PB7) from the Northern Conglomerate Formation	
PB8	Spherulitic microgranite clast from the Northern Conglomerate Formation	
PB8a	Thin section of spherulitic microgranite clast (PB8) from the Northern Conglomerate Formation	
PB9	Siltstone clast from the Northern Conglomerate Formation	
PB9a	Thin section of siltstone clast (PB9) from the Northern Conglomerate Formation	
PB10	Trachyte clast from the Northern Conglomerate Formation	
PB10a	Thin section of trachyte clast (PB10) from the Northern Conglomerate Formation	
PB11	Northern Conglomerate Formation Matrix Hand Specimen, comprising pale sand grade matrix	
PB11a	Northern Conglomerate Formation Matrix Thin Section (PB11)	
PB15	Northern Conglomerate Formation Hand Specimen from Rubha a' Gharaidh Leith, comprising bedded, fine conglomerate/pebbly sandstone	
PB17	Northern Conglomerate Formation Hand Specimen from Kilmory Bay, showing sub-rounded basalt clasts in conglomerate	From sea stacks at Kilmory Bay, NCF, Ardnamurchan (NM52477057)
RC1.3	Calcareous sandstone unit from the Rubha Carrach area, Northern Conglomerate Formation	From cliff section at Rubha Carrach, west of Fascaidale Bay, NCF, Ardnamurchan (NM46177053)
RC1.3a	Thin section of calcareous sandstone unit from the Rubha Carrach area, Northern Conglomerate Formation (RC1.3)	
RC1.5	Conglomerate unit from the Rubha Carrach area, Northern Conglomerate Formation, comprising sub-rounded to sub-angular clasts (up to 5cm across), typically of basalt, quartzite, ignimbrite and sandstone, set in a pale, fine grained matrix	
RC1.5a	Thin section of conglomerate unit from the Rubha Carrach area, Northern Conglomerate Formation (RC1.5)	

## Mull

CAR1.1	Foreshore block from Carraig Mhor, comprising fine sandstone with occasional clasts of pale igneous material	From Carraig Mhor coastal section, east of Carsaig Bay, South Mull (NM55532105).
CAR1.1a	Thin section of foreshore block from Carraig Mhor, comprising fine sandstone with occasional clasts of pale igneous material (CAR1.1)	
CAR1.2	Foreshore block of Carraig Mhor peperite displaying small, sub-rounded to sub-angular pale igneous clasts (typically 1-2cm across) set in a dark fine-grained sedimentary matrix. Sediment forms <i>ca.</i> 33 vol. % of the rock. Representative of material towards the top of the Upper Graded Breccia	From Carraig Mhor coastal section, east of Carsaig Bay, South Mull (NM55532105). Upper Graded Breccia Unit located at NM55652118.
CAR1.2a	Thin section of Carraig Mhor peperite displaying small, sub-rounded to sub-angular pale igneous clasts (typically 1-2cm across) set in a dark fine-grained sedimentary matrix (CAR1.2). Sediment forms <i>ca.</i> 33 vol. % of the rock. Representative of material towards the top of the Upper Graded Breccia	
CAR1.3	Foreshore block of Carraig Mhor peperite comprising igneous clasts displaying irregular margins ranging from crenulate, through sub-rounded, to sub-angular. Jigsaw fit texture of clasts is preserved.	From Carraig Mhor coastal section, east of Carsaig Bay, South Mull (NM55532105).
CAR1.3a	Thin section of Carraig Mhor peperite comprising igneous clasts displaying irregular margins ranging from crenulate, through sub-rounded, to sub-angular (CAR1.3) Jigsaw fit texture of clasts is preserved	
CAR1.3b	Thin section of Carraig Mhor peperite comprising igneous clasts displaying irregular margins ranging from crenulate, through sub-rounded, to sub-angular (CAR1.3). Jigsaw fit texture of clasts is preserved	

CAR1.4	Foreshore block of ignimbrite from Carraig Mhor with well-developed eutaxitic texture	From Carraig Mhor coastal section, east of Carsaig Bay, South Mull (NM55532105) (Unit C of Figure 6.6).
CAR1.4a	Thin section of ignimbrite from Carraig Mhor with well-developed eutaxitic texture (CAR1.4)	
CAR1.5	Foreshore block of laminated quartz- and feldspar-rich siltstone from Carraig Mhor	From Carraig Mhor coastal section, east of Carsaig Bay, South Mull (NM55532105) (Unit D of Figure 6.6).
CAR1.5a	Thin section of laminated quartz- and feldspar-rich siltstone from Carraig Mhor (CAR1.5)	
CAR1.6	Foreshore block of ignimbrite unit from Carraig Mhor grading vertically upwards into a laminated siltstone	From Carraig Mhor coastal section, east of Carsaig Bay, South Mull (NM55532105) (Unit C/D of Figure 6.6).
CAR1.6a	Thin section of ignimbrite unit from Carraig Mhor (CAR1.6) grading vertically upwards into a laminated siltstone	
CAR1.7	Foreshore block of peperite from Carraig Mhor displaying igneous clasts with irregular margins and jigsaw fit textures	From Carraig Mhor coastal section, below Top Sill of Figure 6.5, east of Carsaig Bay, South Mull (NM55692110)
CAR1.8	Foreshore block of 'layered peperite' from Carraig Mhor displaying sub-horizontal alignment of highly irregular, fluidally-shaped clasts of igneous material	
CAR1.9	Foreshore block of peperite from Carraig Mhor, displaying large, bulbous projections of igneous material (up to 15cm across) into host sediment. Representative of material towards the base of the Upper Graded Breccia	From Carraig Mhor coastal section, east of Carsaig Bay, South Mull (NM55532105). Upper Graded Breccia Unit located at NM55652118.
CAR1.10	<i>In situ</i> ignimbrite unit from Carraig Mhor grading vertically upwards into laminated siltstone. Carbonaceous, organic material is preserved	Unit E of the Carraig Mhor foreshore platform, east of Carsaig Bay, South Mull. See Figure 6.6. (NM55642110)
CAR1.11	<i>In situ</i> laminated siltstone unit from Carraig Mhor with carbonaceous plant remains.	Top of Unit E of the Carraig Mhor foreshore platform, east of Carsaig Bay, South Mull. See Figure 6.6. (NM55642110)
CAR1.12	<i>In situ</i> poorly laminated siltstone unit from Carraig Mhor	Unit F of the Carraig Mhor foreshore platform, east of Carsaig Bay, South Mull. See Figure 6.6. (NM55642110)
CAR1.13	<i>In situ</i> thin ignimbrite unit from Carraig Mhor, grading vertically upwards into laminated siltstone	Unit G of the Carraig Mhor foreshore platform, east of Carsaig Bay, South Mull. See Figure 6.6. (NM55642110)

CAR1.14	Foreshore block from Carraig Mhor displaying peperite grading vertically upwards into laminated siltstone and ignimbrite with well-developed eutaxitic texture	Units A, B & C of the Carraig Mhor foreshore platform, east of Carsaig Bay, South Mull. See Figure 6.6. (NM55642110)
CM1.1	Coire Mor Breccia Hand Specimen comprising sub-rounded to sub-angular clasts (1-5cm across), typically of basalt, sandstone and Moine psammite, set in a dark, fine-grained matrix.	Coire Mor, west of Craignure, Eastern Mull (NM695355)
LB1.5	Loch Ba Breccia Formation Hand Specimen, comprising sub-rounded to sub-angular clasts (1-2cm across), typically of basalt, sandstone, rhyolite and Moine psammite, set in a dark, fine grained matrix.	Lower unit of the Loch Ba Breccia Formation, south of Salen, Eastern Mull (NM55593724)
LB1.5a	Loch Ba Breccia Formation Thin Section of LB1.5	
LB1.5b	Loch Ba Breccia Formation Thin Section of LB1.5	

## Skye

K1	Kilchrist Breccia Hand Specimen comprising sub-rounded to sub-angular clasts (1-2cm across), typically of basalt, mudstone, granite, limestone and sandstone, set in a green, fine grained matrix	SW of Creagan Dubh, NW of Beinn Dearg Mhor, Kilchrist, west of Broadford, Southern Skye (NG58302371)
K1a	Kilchrist Breccia Thin Section of K1	
K3	Kilchrist Breccia Hand Specimen comprising sub-rounded to sub-angular clasts (1-2cm across), typically of sandstone, granite and basalt, set in a pale, fine grained matrix	SW of Creagan Dubh, NW of Beinn Dearg Mhor, Kilchrist, west of Broadford, Southern Skye (NG58172360)
K3a	Kilchrist Breccia Thin Section of K3	
K8	Kilchrist Breccia Hand Specimen comprising sub-rounded to sub-angular clasts (1-5cm across), typically of sandstone, basalt and limestone	Breccia unit to the north of Cnoc nam Fitheach, Kilchrist, west of Broadford, Southern Skye (NG59322134)

SNC1.12	Srath na Creitheach Breccia Formation Hand Specimen comprising sub- rounded to sub-angular clasts (1-5cm across), typically of gabbro and basalt	Srath na Creitheach area, north of Loch na Creitheach, Cuillin Hills, Southern Skye (NG50202173)
SNC1.12a	Srath na Creitheach Breccia Formation Thin Section of SNC1.12, comprising sub-rounded to sub-angular clasts (1- 5cm across), typically of gabbro and basalt	
SNC1.13	Srath na Creitheach Breccia Formation laminated tuffaceous siltstone hand specimen	Laminated siltstone unit from the Srath na Creitheach area, north of Loch na Creitheach, Cuillin Hills, Southern Skye (NG50642157)
SNC1.13a	Srath na Creitheach Breccia Formation laminated siltstone thin section of SNC1.13	
SNC1.13b	Srath na Creitheach Breccia Formation laminated siltstone thin section of SNC1.13	

## 12 Appendix C: Statistics

### NCF Traverses (South-North)

#### Allt an Doire Dharaich to Ardtoe Island

Distance (km)	0	1	2	3.5	4
Mean Clast Size (cm)	3.80	7.95	4.05	16.73	16.35
Standard Deviation	2.15	9.68	5.09	25.01	43.82

#### Camphouse to Portban

Distance (km)	0	2.25	4	5.75	6	6.25
Mean Clast Size (cm)	4.78	7.15	4.05	13.10	13.30	16.75
Standard Deviation	4.30	7.01	5.09	14.85	11.95	29.75

#### Rubha Carrach

Distance (km)	0	0.25	0.5	0.75
Mean Clast Size (cm)	12.85	11.85	11.8	14.35
Standard Deviation	12.04	15.33	8.22	12.15

#### Tom na Gainmheich to Swordle Cave

Distance (km)	0	0.5	1.75	3.25	3.75
Mean Clast Size (cm)	7.35	14.95	12.25	16.73	24.60
Standard Deviation	10.32	16.63	18.12	25.01	65.25

### BHCF Traverses (South-North)

#### MacLean's Nose to Gribble's Gully

Distance (km)	0	0.25	0.5	0.75	1	1.5	2	2.25	2.5	2.75
Mean Clast Size (cm)	31.35	26.30	27.10	14.10	8.20	3.95	3.93	6.33	5.45	7.30
Standard Deviation	27.83	25.21	31.65	11.12	11.15	3.69	3.88	6.14	5.32	12.90

### East-West Traverses

#### Allt na Mi Chomhdhail to Tom na Gainmheich

Distance (km)	0	2	3	4
Mean Clast Size (cm)	3.30	7.15	3.80	6.85
Standard Deviation	2.45	7.01	2.15	9.91

#### Rubha Carrach to Swordle Cave

Distance (km)	0	3	3.75	4.75	5.5	6	6.25	7.25	7.75
Mean Clast Size (cm)	11.85	6.80	17.90	14.15	10.70	14.50	22.50	16.35	24.60
Standard Deviation	15.33	4.12	26.01	17.85	11.14	19.76	30.25	43.82	65.25

## Vertical

### Ben Hiant

Height (m)	110	170	190	220	240
Mean Clast Size (cm)	27.10	31.95	21.05	16.50	11.75
Standard Deviation	31.65	25.10	21.27	17.64	13.29

The table above displays the mean clast size and standard deviation of the data from the traverses carried out in this thesis (see Section 5-5 for more information).

In the NCF, mean clast size increased from south to north, and in the very north the deposits typically comprised coarse blocks and occasional megablocks of several metres diameter. The standard deviation in the traverses from Allt an Doire Dharaich to Ardtoe Island, Camphouse to Portban, and Tom na Gainmheich to Swordle Cave, is clearly much larger in the more northern (distal) parts of traverses. These figures reflect the appearance of such large clasts, as is observed in the coarser distal parts of debris flows (Sections 5.5 and 5.7). This is a result of the shear stresses and bulking discussed in Section 4. The standard deviations of the four sample sites from Rubha Carrach are in close agreement because of the short distance of this traverse (<1km). In the BHCF, mean clast size increases from north to south (distal), and as in the NCF the standard deviations are much larger in the distal parts of flows.

East-west traverses (across flows) show broadly similar standard deviations, indicating a lack of trends across flows. The exception is the Swordle Cave area where standard deviations reach up to 65. This is explained by the presence of numerous megablocks in this area.

The vertical traverse of Ben Hiant shows a fall in standard deviation with increasing height. This reflects the appearance of a well sorted, fine-grained, matrix-supported unit at the top of this section. (Section 5.3.9).

---

## **13 Appendix D: Optical Microscopy and Cathodoluminescence**

From covered thin sections, optical microscopy images (photomicrographs) were acquired using a Zeiss Axioplan petrological microscope. The images were captured using a Nikon DN100 Digital Net Camera. Cathodoluminescence images were obtained from uncovered thin sections using a CITL Technosyn 8200 Mk 4 system, mounted on a Zeiss Axioplan petrological microscope. The images were also captured using a Nikon DN100 Digital Net Camera.

## 14 References

- ALLABY, A. & ALLABY, M. 1990. *Concise Dictionary of Earth Sciences*. Oxford.
- ALLEN, J. R. L. 1970. *Physical processes of sedimentation an introduction*. Allen & Unwin.
- ALLEN, J. R. L. 1982. *Developments in sedimentology*. Vols 30A & B: *Sedimentary structures. Their character and physical basis*. Amsterdam: Elsevier.
- ALLEN, J. R. L. 1984. *Sedimentary structures; Their Character and Physical Basis*. Vol. I, Amsterdam: Elsevier.
- BAGNOLD, R. A. 1954. Experiments on a gravity-free dispersion of large solid spheres in a Newtonian fluid under shear. *Proceedings of the Royal Society of London, Series A* **225**, 49-63.
- BAILEY, E. B., CLOUGH, C. T., WRIGHT, W. B., RICHEY, J. E. & WILSON, G. V. 1924. Tertiary and Post-Tertiary geology of Mull, Loch Aline, and Oban. *Memoirs of the Geological Survey, Scotland*.
- BELL, B. R. 1982. The evolution of the Eastern Red Hills Tertiary igneous centre, Skye, Scotland. *Unpublished PhD thesis, University of London*.
- BELL, B. R. 1985. The pyroclastic rocks and rhyolitic lavas of the Eastern Red Hills district, Isle of Skye. *Scottish Journal of Geology* **21**, (1), 57-70.
- BELL, B. R. & HARRIS, J. W. 1986. An Excursion Guide To The Geology of the Isle of Skye. *Geological Society of Glasgow*.
- BELL, B. R. & EMELEUS, C. H. 1988. A review of silicic pyroclastic rocks of the British Tertiary Volcanic Province. In: MORTON, A. C. & PARSON, L. M. (eds). *Early Tertiary volcanism and the opening of the NE Atlantic*. Geological Society of London, Special Publication. **39**, 365-379.

- BELL, B. R. & WILLIAMSON, I. T. 2002. Tertiary volcanism. In: TREWIN, N. H (ed) *The Geology of Scotland*. 4th Edition. Geological Society of London.
- BELL, J. D. 1966. Granites and associated rocks of the eastern part of the Western Red Hills Complex, Isle of Skye. *Transactions of the Royal Society of Edinburgh*. **66**, 307-343.
- BERTRAN, P., HETU, B., TEXIER, J.-P & VAN STEIJN, H. 1997. Fabric characteristics of sub-aerial slope deposits. *Sedimentology*. **44**, 1-16.
- BERTRAN, P. & TEXIER, J.-P. 1999. Facies and microfacies of slope deposits. *Catena*. **35**, 99-121.
- BEVERAGE, J. P. & CULBERTSON, J. K. 1964. Hyperconcentrations of suspended sediment. *Journal of the Hydraulics Division, American Society of Civil Engineers*. **90**, 117-126.
- BLAIR, T. C. & MCPHERSON, J. G. 1994. Alluvial fans and their natural distinction from rivers based on morphology, hydraulic processes, sedimentary processes, and facies. *Journal of Sedimentary Research*. **A64**, 451-490.
- BLAIR, T. C. & MCPHERSON, J. G. 1998. Recent debris flow processes and resultant form and facies of the dolomite alluvial fan, Owens Valley, California. *Journal of Sedimentary Research*. **68**, no. 5, 800-818.
- BOUMA, A. H. 1962. *Sedimentology of some flysch deposits*. Amsterdam: Elsevier.
- BOULTER, M. C. & KVACEK, Z. 1989. The Palaeocene Flora of the Isle of Mull. *Special Papers in Palaeontology*. **42**, 1-149.
- BRANNEY, M. J. 1995. Downsag and extension at calderas: new perspectives on collapse geometries from ice-melt, mining and volcanic subsidence. *Bulletin of Volcanology*. **57**, 303-318.
- BRANNEY, M. J. & KOKELAAR, B. P. 1992. A reappraisal of ignimbrite emplacement: progressive aggradation and changes from particulate to non-particulate flow during emplacement of high grade ignimbrite. *Bulletin of Volcanology*. **54**, 504-520.

- BRITISH GEOLOGICAL SURVEY. 1992. Mull. Sheet 44W and part of 44E. Solid. 1:50000. (Keyworth, Nottingham: British Geological Survey).
- BROOKS, E. R., WOOD, M. M. & GARBUTT, P. L. 1982. Origin and metamorphism of peperite and associated rocks in the Devonian Elwell Formation, northern Sierra Nevada, California. *Geological Society of America Bulletin*. 93, 1208-1231.
- BRYANT, E. 1991. *Natural Hazards*. Cambridge University Press.
- BULL, W. B. 1972. Recognition of alluvial fan deposits in the stratigraphic record. In: HAMBLIN, W. K & RIGBY, J. K. (eds.) *Recognition of ancient sedimentary environments*. Society of Economic Palaeontologists and Mineralogists, Special Publication. 16, 63-83.
- BULL, W. B. 1977. The alluvial fan environment. *Progress in Physical Geography*. 1, 222-270.
- BUSBY-SPERA, C. J. & WHITE, J. D. L. 1987. Variation in peperite textures associated with differing host-sediment properties. *Bulletin of Volcanology*. 49, 765-775.
- BUTLER, R. W. H. & HUTTON, D. H. W. 1994. Basin structure and Tertiary magmatism on Skye, NW Scotland. *Journal of the Geological Society of London*. 151, (6), 931-944.
- CAINE, N. 1980. The rainfall intensity-duration control of shallow landslides and debris flows. *Geografiska Annalerum*. 62A, 23-27.
- CAPPACCIONI, B. & SARROCHI, D. 1996. Computer-assisted image analysis on clast shape fabric from the Orvieto-Bagnoreggio ignimbrite (Vulsini district, central Italy): implications on the emplacement mechanisms. *Journal of Volcanology and Geothermal Research*. 70, 75-90.
- CAREY, S. N. & SIGURDSSON, H. 1984. A model of volcanogenic sedimentation in marginal basins. In: KOKELAAR, B. P. & HOWELLS, M. F. (eds.) *Marginal basin geology: volcanic and associated sedimentary and tectonic processes in modern and ancient marginal basins*. Geological Society of London, Special Publication. 16, 37-58.

- CARR, J. M. 1952. An investigation of the Sgurr na Stri, Druim Hain sector of the basic igneous complex of the Cuillin hills, Isle of Skye. *Unpublished D.Phil Thesis, University of Oxford*.
- CAS, R. A. F. 1979. Mass-flow arenites from a Palaeozoic interarc basin, New South Wales, Australia: mode and environment of emplacement. *Journal of Sedimentary Petrology*. **49**, 29-44.
- CAS, R. A. F & WRIGHT, J. V. 1987. *Volcanic successions, modern and ancient*. Allen and Unwin, London
- CAS, R. A. F., EDGAR, C. & SCUTTER, C. R. 1998. Peperites of the Late Devonian Bunga Beds, southeastern Australia: a record of syn-depositional high level intrusion, dome emergence and resedimentation. *International Volcanological Congress, Cape Town, South Africa*.
- CHAMBERS, L. M. & PRINGLE, M. S. 1999. Eruption of the British Tertiary Volcanic Province in ~2 m.y. during Chron 26R. *Goldschmidt Meeting, Cambridge, MA, USA*.
- CHAMBERS, L. M. & PRINGLE, M. S. 2001. Age and duration of activity at the Isle of Mull Tertiary igneous centre, Scotland, and confirmation of the existence of subchrons during Anomaly 26r. *Earth and Planetary Science Letters*. **193**, (3-4), 333-345.
- CHAMBERS, L. M. & FITTON, J. G. 2000. Geochemical transitions in the ancestral Iceland plume: evidence from the Isle of Mull Tertiary volcano, Scotland. *Journal of the Geological Society of London*. **157**, (2), 261-263.
- COSTA, J. E. 1988. Rheologic, geomorphic and sedimentologic differentiation of water floods, hyperconcentrated flows, and debris flows. In: BAKER, V. R. (ed.) *Fluvial Geomorphology*. Wiley.
- COSTA, J. E. & WILLIAMS, G. P. 1984. Debris flow dynamics (videotape). *U.S. Geological Survey Open File Report*. 84-6606, 22.5 min.

- COUSSOT, P. & MEUNIER, M. 1996. Recognition, classification and mechanical description of debris flows. *Earth Science Reviews*. **40**, 209-227.
- CRUDEN, D. M. & HUNGR, O. 1986. The debris of the Frank Slide and theories of rockslide-avalanche mobility. *Canadian Journal of Earth Sciences*. **23**, 425-432.
- DAVIES, I. C. & WALKER, R. G. 1974. Transport and deposition of resedimented conglomerates, The Cap Enrage Formation, Cambro-Ordovician, Gaspé, Quebec. *Journal of Sedimentary Petrology*. **44**, 1200-1216.
- DAVIS, J. C. 1986. *Statistics and data analysis in geology*, 2<sup>nd</sup> edition. New York, John Wiley.
- DONALDSON, C. H., TROLL, V. R. & EMELEUS, C. H. 2001. Felsites and breccias in the Northern Marginal Zone of the Rum Central Complex: changing views, c. 1900-2000. *Proceedings of the Yorkshire Geological Society*. **53**, (3), 167-175.
- DOYLE, M. G. 2000. Clast shape and textural associations in peperite as a guide to hydromagmatic interactions: Upper Permian basaltic and basaltic andesites from Kiama, Australia. *Australian Journal of Earth Sciences*. **47**, 167-77.
- DRUITT, T. H. & SPARKS, R. S. J. 1984. On the formation of calderas during ignimbrite eruptions. *Nature*. **310**, 679-681.
- DUKE OF ARGYLL. 1851. On Tertiary Leaf-Beds in the Isle of Mull. With a Note on the Vegetable Remains from Ardtun by E. FORBES. *Quarterly Journal of the Geological Society of London*. **7**, 89-103.
- EDINBURGH GEOLOGICAL SOCIETY. 1976. Map of Tertiary Igneous Complex of Ardnamurchan. (Bartholomew and Son, Edinburgh).
- EISBACHER, G. H. & CLAGUE, J. J. 1984. Destructive mass movements in high mountains: Hazard and management. *Geological Society of Canada Papers*. 84-16.
- EMELEUS, C. H. 1982. Tertiary igneous activity: the central complexes (British Isles). In: SUTHERLAND, D. S. *Igneous rocks of the British Isles*. Wiley.

- EMELEUS, C. H. 1997. Geology of Rum and the adjacent islands. *Memoirs of the British Geological Survey (Scotland)*. Sheet 60.
- FISHER, R. V. 1960. Classification of volcanic breccias. *Geological Society of America Bulletin*. **72**, 973-982.
- FISHER, R. V. 1961. Proposed classification of volcanoclastic sediments and rocks. *Geological Society of America Bulletin*. **72**, 1409-1414.
- FISHER, R. V. 1983. Flow transformations in sediment gravity flows. *Geology*. **11**, 273-274.
- FISHER, R. V. & SCHMINCKE, H.-U. 1984. *Pyroclastic rocks*. Springer Verlag
- FISHER, R. V., ORSI, G., ORT, M. & HEIKEN, G. 1993. Mobility of a large-volume pyroclastic flow-emplacment of the Campanian Ignimbrite, Italy. *Journal of Volcanology and Geothermal Research*. **56**, 205-220.
- FRANCIS, E. H. 1983. Magma and sediment – II. Problems of interpreting palaeovolcanics buried in the stratigraphic column. *Journal of the Geological Society of London*. **140**, 165-183.
- FYFE, J. A., LONG, D. & EVANS, D. 1993. The geology of the Malin-Hebrides sea area. *United Kingdom offshore regional report*. London: HMSO.
- GASCOYNE, P. 1978. Mudflow, debris flow deposits. In: FAIRBRIDGE, R. W. & BOURGEOIS, J. (eds.) *The encyclopaedia of sedimentology; Encyclopaedia of earth sciences*. **7**, 488-492.
- GATES, O. 1959. Breccia pipes in the Shoshone Range, Nevada. *Economic Geology*. **54**, 790-815.
- GLICKEN, H. 1986. Study of the rockslide avalanche of May 18, 1980, Mount St. Helens volcano. *Unpublished PhD thesis, University of California, Santa Barbara*.

- GLICKEN, H. 1991. Sedimentary architecture of large volcanic-debris avalanches. In: FISHER, R. V. & SMITH, G. A. (eds.) *Sedimentation in volcanic settings*. SEPM Special Publication. **45**, 99-106.
- GRABAU, A. W. 1924. *Principles of stratigraphy*, 2<sup>nd</sup> edition. New York.
- HANSEN, M. J. 1984. Strategies for classification of landslides. In: BRUNSDEN, D. & PRIOR, D. P. (eds.) *Slope instability*. Wiley.
- HARKER, A. 1904. The Tertiary Igneous Rocks of Skye. *Memoirs of the Geological Society of the United Kingdom*.
- HARRISON, J. V. & FALCON, N. L. 1937. An ancient landslip at Saidmarreh in southwestern Iran. *Geography Journal*. **89**, 42-47.
- HEWITT, K. 1988. Catastrophic landslide deposits in the Karakoram Himalaya. *Science*. **242**, 64-67.
- HOOKE, R. L. 1987. Mass movements in semi-arid environments and the morphology of alluvial fans. In: ANDERSON, M. G. & RICHARDS, K. S. (eds.) *Slope stability: Geotechnical engineering and geomorphology*. Wiley.
- HSU, K. J. 1975. Catastrophic debris streams (Sturzstorms) generated by rockfalls. *Geological Society of America Bulletin*. **86**, 129-140.
- HUDSON, J. D. & TREWIN, N. H. 2002. Jurassic. In: TREWIN, N. H. (ed) *The Geology of Scotland*. 4th Edition. Geological Society of London.
- HUGUET, D., KARATSON, D. & TEBLISZ, T. 2001. Paleoflow directions and emplacement mechanisms in Miocene lahar deposits of the Cantal Stratovolcano, Massif Central, France, as inferred from a photo-statistical method (abstract). *Strasbourg, 11<sup>th</sup> European Union of Geosciences Congress, Abstract volume* p505.
- INNES, J. L. 1983. Debris flows. *Progress in Physical Geography*. **7**, 469-501.

- JASSIM, S. Z. 1970. The Loch na Creitheach Volcanic Vent and the Surrounding Area, Isle of Skye. *Unpublished PhD Thesis, University of Leeds*.
- JASSIM, S. Z. and GASS, I. G. 1970. The Loch na Creitheach Volcanic Vent, Isle of Skye. *Scottish Journal of Geology*. 6, 285-294.
- JERRAM, D. A. & STOLLHOFEN, H. 2002. Lava/sediment interaction in desert settings; are all peperite-like textures the result of magma-water interaction? *Journal of Volcanology and Geothermal Research*. 114, (1-2), 231-249.
- JOHNSON, A. M. 1970. *Physical Processes in Geology*. Freeman, Cooper, San Francisco.
- JOHNSON, A. M. 1984. Debris flow. In: BRUNSDEN, D & PRIOR, D. B. (eds.) *Slope instability*. Wiley.
- JOLLEY, D. W. 1997. Palaeosurface palynofloras of the Skye lava field and the age of the British Tertiary volcanic province. In: WIDDOWSON, M. (ed.) *Palaeosurfaces: Recognition, Reconstruction and Palaeoenvironmental Interpretation*. Geological Society Special Publication. 120, 67-94.
- JONES, J. G. 1969. A lacustrine volcano of central France and the nature of peperites. *Proceedings of the Geological Association*. 80, 177-188.
- KARATSON, D., SZTANO, O. & TELBISZ, T. 2002. Preferred clast orientation in volcanoclastic mass-flow deposits: Application of a new photo-statistical method. *Journal of Sedimentary Research*. 72, (6), 823-835.
- KERR, A. 1995. The geochemical stratigraphy, field relations and temporal variation of the Mull-Morvern Tertiary lava succession, NW Scotland. *Transactions of the Royal Society of Edinburgh, Earth Sciences*. 86, (1), 35-47.
- KESSLER, L. G. & BEDARD, J. H. 2000. Epiclastic volcanic debrites-evidence of flow transformations between avalanche and debris flow processes, Middle Ordovician, Baie Verte Peninsula, Newfoundland, Canada. *Precambrian Research*. 101, 135-161.

- KOBAYASHI, Y. 1992. *Travel dynamics of large debris avalanches*. Vol. 2. Interpraevent, Bern.
- KOKELAAR, B. P. 1982. Fluidization of wet sediments during the emplacement and cooling of various igneous bodies. *Journal of the Geological Society of London*. **139**, 21-33.
- KOKELAAR, B. P. 1986. Magma-water interaction in sub aqueous and emergent basaltic volcanism. *Bulletin of Volcanology*. **48**, 275-289.
- KOMURO, H. 1987. Experiments on cauldron formation fractures. *Journal of Volcanology and Geothermal Research*. **31**, 139-149.
- KOMURO, H., FUJITA, Y. & KODAMA, K. 1984. Numerical and experimental models on the formation mechanism of collapse breccias during the Green Tuff Orogenesis, Japan. *Bulletin of Volcanology*. **47**, 649-666.
- KRIEGER, M. H. 1977. Large landslides, composed of megabreccia, interbedded in Miocene basin deposit, southeastern Arizona. *U.S. Geological Survey Professional Paper*. 1008.
- LACROIX, A. 1903. Sur les principaux resultats de la mission de la Martinique. *C. R. Academie de Science, Paris*. **135**, 871-876.
- LAJOIE, J. 1984. Volcaniclastic rocks. In: WALKER, R. G. (ed.) *Facies models*. 2<sup>nd</sup> edn. Geological Association of Canada. Geoscience Canada Reprint Series 1.
- LEEDER, M. R. 1982. *Sedimentology. Process and product*. London: George Allen & Unwin.
- LEWIS, J. D. 1968. Form and structure of the Loch Ba ring-dyke, Isle of Mull. *Proceedings of the Geological Society of London*. **1646**, 110-111.
- LIPMAN, P. W. 1984. The roots of ash flow calderas in North America: windows into the tops of granitic batholiths. *Journal of Geophysical Research*. **89**, 8801-8841.

- LIPMAN, P. W. 1997. Subsidence of ash flow calderas: relation to caldera size and magma chamber geometry. *Bulletin of Volcanology*. **59**, 198-218.
- LISITZIN, A. P. 1962. Bottom sediments of the Antarctic. *American Geophysical Union, Geophysics Monthly*. **7**, 81-88.
- LONG, P. E. & WOOD, B. J. 1986. Structures, textures and cooling histories of Columbia River basalt flows. *Geological Society of America Bulletin*. **97**, 1144-1155.
- LONGWELL, C. R. 1951. Megabreccia developed downslope from large faults. *American Journal of Science*. **249**, 343-355.
- LOWE, D. R. 1982. Sediment gravity flows: II, depositional models with special reference to the deposits of high density turbidity currents. *Journal of Sedimentary Petrology*. **52**, 279-297.
- LYLE, P. 2000. The eruption environment of multi-tiered columnar basalt lava flows. *Journal of the Geological Society of London*. **157**, 715-722.
- LYLE, P. & PRESTON, J. 1993. Geochemistry and volcanology of the Tertiary basalts of the Giant's Causeway area, Northern Ireland. *Journal of the Geological Society of London*. **150**, 109-120.
- MACCULLOCH, J. A. 1819. *A description of the Western Isles of Scotland including the Isle of Man*. London.
- MAJOR, J. J. & VOIGHT, B. 1986. Sedimentology and clast orientations of the 18<sup>th</sup> May 1980 Southwest-Flank Lahars, Mt. St. Helens, Washington. *Journal of Sedimentary Petrology*. **56**, 691-705.
- MARTI, J., ABLAY, G. J., REDSHAW, L. T. & SPARKS, R. S. J. 1994. Experimental studies of collapse calderas. *Journal of the Geological Society of London*. **151**, 919-929.
- MICHEL, R. 1948. Etude geologique du plateau de Gergoria. *Review de Science et Nature, Auvergne*. **14**, 1-68.

- MICHEL-LEVY, A. 1890. Compte rendu de l'excursion du 16 septembre a Gergovie et Veyre-Monton. *Bulletin de la Societe Geologique de France*. **18**, 891-897.
- MIDDLETON, G. V. & HAMPTON, M. A. 1976. Subaqueous sediment transport and deposition by sediment gravity flows. In: STANLEY, D. J. & SWIFT, D. J. P. (eds.) *Marine sediment transport and environmental management*. Wiley.
- MILLS, A. A. 1984. Pillow lavas and the Leidenfrost effect. *Journal of the Geological Society of London*. **141**, 183-186.
- MILLS, H. H. 1976. Estimated erosion rates on Mount Rainier, Washington. *Geology*. **4**, 401-406.
- MITCHELL, W. I., COOPER, M. R., HARDS, V. L. & MEIGHAN, I. G. 1999. An occurrence of silicic volcanic rocks in the early Palaeogene Antrim Lava Group of Northern Ireland. *Scottish Journal of Geology*. **35**, (2), 179-185.
- MOORE, I. & KOKELAAR, B. P. 1997. Tectonic influences in piecemeal caldera collapse at Glencoe volcano, Scotland. *Journal of the Geological Society of London*. **154**, 765-768.
- MUDGE, M. R. 1965. Rockfall-avalanche and rockslide-avalanche deposits at Sawtooth Ridge, Montana. *Geological Society of America Bulletin*. **76**, 1003-1014.
- NARDIN, T. R., HEIN, F. J., GORSLINE, D. S. & EDWARDS, B. D. 1979. A review of mass movement processes, sediment and acoustic characteristics, and contrasts in slope and base-of-slope systems versus canyon-fan-basin floor systems. In: DOYLE, L. J. & PILKEY, O. H. (eds.) *Geology of continental slopes*. SEPM Special Publication. **27**, 61-73.
- NEALL, V. E. 1976. Lahars – Global occurrence and annotated bibliography. *Victoria University Wellington, New Zealand, Publication 5*.
- NEMEC, W. 1990. Aspects of sediment movement on steep delta slopes. In: COLLELLA, A. & PRIOR, D. B. (eds.) *Coarse-grained deltas*. Special Publication of the International Association of Sedimentologists. **10**, 29-73.

- NEMEC, W. & STEEL, R. J. 1984. Alluvial and coastal conglomerates; their significant features and some comments on gravelly mass flow deposits. In: KOSTER, E. H. & STEEL, R. J. (eds.) *Sedimentology of gravels and conglomerates*. Canadian Association of Petroleum Geologists. **10**, 1-31.
- NILSEN, T. H. 1982. Alluvial fan deposits. In: SCHOLLE, P. A. & SPEARING, D. (eds.) *Sandstone depositional environments*. American Association of Petroleum Geologists. **31**, 49-86.
- PACK, F. J. 1923. Torrential potential of desert waters. *Pan-American Geology*. **40**, 349-356.
- PAITHANKAR, M. G. 1967. Tuffsite and volcanic phenomena associated with the Glas Eilean Vent, Ardnamurchan, Argyllshire, Scotland. *Geologiska Föreningens i Stockholm Förhandlingar*. **89**, 15-28.
- PALMER, H. C., ALLOWAY, B. V. & NEALL, V. E. 1991. Volcanic-debris avalanche deposits in New Zealand – Lithofacies organisation in unconfined wet-avalanche flows. In: FISHER, R. V. & SMITH, G. A. (eds.) *Sedimentation in volcanic settings*. SEPM Special Publication. **45**, 89-98.
- PERRET, F. A. 1937. *The eruption of Mt. Pelee 1929-1932*. Carnegie Institute, Washington, 458.
- PICHLER, H. 1965. Acid hyaloclastites. *Bulletin of Volcanology*. **28**, 293-310.
- PIERSON, T. C. 1985. Initiation and flow behaviour of the 1980 Pine Creek and Muddy River lahars, Mount St. Helens, Washington. *Geological Society of America Bulletin*. **96**, 1056-1069.
- PIERSON, T. C. 1986. Flow behaviour of channelised debris flows, Mount St. Helens, Washington. In: ABRAHAMS, A. D. (ed.) *Hillslope processes*. Allen & Unwin.

- PIERSON, T. C. 1995. Flow characteristics of large eruption-triggered debris flows at snow-clad volcanoes: constraints for debris flow models. *Journal of Volcanology and Geothermal Research*. **66**, 283-294.
- PIERSON, T. C. & COSTA, J. E. 1987. A rheologic classification of subaerial sediment water flows. *Reviews in Engineering Geology*. **VII**: 1-12.
- PIERSON, T. C. & SCOTT, K. M. 1985. Downstream dilution of a lahar: transition from debris flow to hyperconcentrated streamflow. *Water Resources Research*. **21**, 1511-1524.
- PLAFKER, G. 1978. Avalanche deposits. In: FAIRBRIDGE, R. W. & BOURGEOIS, J. (eds.) *The encyclopaedia of sedimentology, Encyclopaedia of earth sciences*. **6**, 24-27.
- PRESTON, J. 1982. Explosive volcanism. In: SUTHERLAND, D. S. *Igneous rocks of the British Isles*. Wiley.
- RAY, P. S. 1960. Ignimbrite in the Kilchrist vent, Skye. *Geological Magazine*. **97**, 229-238.
- RAY, P. S. 1962. A Note on Some Acid Breccias in the Kilchrist Vent, Skye. *Geological Magazine*. **99**, 420-427.
- REUBI, O. & HERNANDEZ, J. 2000. Volcanic debris avalanche deposits of the upper Maronne valley (Cantal Volcano, France): evidence for contrasted formation and transport mechanisms. *Journal of Volcanology and Geothermal Research*. **102**, 271-286.
- REYNOLDS, D. L. 1954. Fluidisation as a geological process and its bearing in the problems of intrusive granites. *American Journal of Science*. **252**, 577-613.
- RICHEY, J. E. 1932. Tertiary Ring Structures in Britain. *Transactions of the Geological Society of Glasgow*. **19**, (1), 42-140.
- RICHEY, J. E. 1938. The rhythmic eruptions of Ben Hiant, Ardnamurchan, a Tertiary volcano. *Bulletin of Volcanology*. Serie II, Tome III.

- RICHEY, J. E. 1961. The Tertiary Volcanic Districts of Scotland. *British Geological Survey. Third Edition.*
- RICHEY, J. E. and THOMAS, H. H. 1930. The Geology of Ardnamurchan, North-west Mull and Coll. *Memoirs of the Geological Survey, Scotland.*
- RITTMANN, A. 1962. *Volcanoes and their activity.* New York: Wiley
- SAEMUNDSSON, K. 1970. Interglacial lava flows in the lowlands of southern Iceland and the problem of two-tiered columnar jointing. *Jokull (Journal of the Iceland Glaciological Society).* **20**, 62-77.
- SCANDONE, R. 1990. Chaotic collapse of calderas. *Journal of Volcanology and Geothermal Research.* **105**, 395-416.
- SCHMINCKE, H.-U. 1967. Fused tuff and peperites in south central Washington. *Geological Society of America Bulletin.* **78**, 319-330.
- SCHNEIDER, J.-L. & FISHER, R. V. 1998. Transport and emplacement mechanisms of large volcanic debris avalanches: evidence from the northwest sector of Cantal Volcano (France). *Journal of Volcanology and Geothermal Research.* **83**, 141-165.
- SCOTT, K. M. 1988. Origins, behaviour, and sedimentology of lahars and lahar-runout flows in the Toutle-Cowlitz river system. *U.S. Geological Survey Professional Paper.* 1447-A.
- SCROPE, G. P. 1858. *The geology of extinct volcanoes of central France.* London: John Murray
- SEGERSTROM, K. 1950. Erosion studies at Paricutin, State of Michoacan, Mexico. *U.S. Geological Survey Bulletin.* **965a.**
- SHALLER, P. J. 1991. Analysis and implications of large Martian and terrestrial landslides. *Unpublished PhD thesis, California Institute of Technology.*

- SHREVE, R. L. 1968. The Blackhawk landslide. *Geological Society of America Special Paper*. 108.
- SHULTZ, A. W. 1984. Subaqueous debris flow deposition in the Upper Palaeozoic Cutler Formation, western Colorado. *Journal of Sedimentary Petrology*. **54**, 759-772.
- SIEBERT, L. 1984. Large volcanic debris avalanches: characteristics of source areas, deposits and associated eruptions. *Journal of Volcanology and Geothermal Research*. **22**, 163-167.
- SIGURDSSON, H., SPARKS, R. S. J., CAREY, S. & HUANG, T. C. 1980. Volcanogenic sedimentation in the Lesser Antilles arc. *Journal of Geology*. **88**, 523-540.
- SIMPSON, J. B. 1961. The Tertiary pollen flora of Mull and Ardnamurchan. *Transactions of the Royal Society of Edinburgh*. **64**, 421-468.
- SKELHORN, R. R. 1969. *Field excursion guide to the Tertiary volcanic rocks of Mull*. Geologists' Association Guides, **20**
- SMITH, G. A. 1986. Coarse-grained non-marine volcanoclastic sediment: Terminology and depositional process. *Geological Society of America Bulletin*. **97**, 1-10.
- SMITH, G. A. & FRITZ, W. J. 1989. Volcanic influences on terrestrial sedimentation. *Geology*. **17**, 375-376.
- SMITH, G. A. & LOWE, D. R. 1991. Lahars: Volcano-hydrologic events and deposition in the debris flow - hyperconcentrated flow continuum. In: FISHER, R. V. & SMITH, G. A. (eds.) *Sedimentation in volcanic settings*. SEPM Special Publication. **45**, 99-106.
- SMITH, R. L. & BAILEY, R. A. 1968. Resurgent cauldrons. *Geological Society of America Memoir*. **116**, 613-662.
- SPARKS, R. S. J. 1976. Grain size variations in ignimbrites and implications for the transport of pyroclastic flows. *Sedimentology*. **23**, 147-188.

- SPARKS, R. S. J. 1988. Petrology of the Loch Ba ring dyke, Mull (NW Scotland): an example of the extreme differentiation of tholeiitic magmas. *Contributions to Mineralogy and Petrology*. **100**, 446-461.
- SPARKS, R. S. J. & WALKER, G. P. L. 1973. The ground surge deposit: a third type of pyroclastic rock. *Nature, Physical Sciences*. **241**, 62-64.
- SPARKS, R. S. J. & WRIGHT, J. V. 1979. Welded air-fall tuffs. In: CHAPIN, C. E. & ELSTON, W. E. (eds.) *Ash flow tuffs*. Geological Society of America Special Paper. **180**. 155-166.
- SPARKS, R. S. J., SELF, S. & WALKER, G. P. L. 1973. Products of ignimbrite eruptions. *Geology*. **1**, 115-118.
- SQUIRE, R. J. & MCPHIE, J. 2002. Characteristics and origin of peperite involving coarse-grained host sediment. *Journal of Volcanology and Geothermal Research*. **114**, 45-61.
- STEARNS, H. T. & MACDONALD, G. A. 1947. Geology and ground-water resources of the Island of Molokai, Hawaii. *Hawaii Division of Hydrography Bulletin*. **11**, 113.
- TAKAHASHI, T. 1978. Mechanical characteristics of debris flow. *Journal of the Hydraulics Division, American Society of Civil Engineers*. **104**, 1153-1169.
- THOMPSON, R. N. 1969. Tertiary granites and associated rocks of the Marsco area, Isle of Skye. *Quarterly Journal of the Geological Society of London*. **124**, 349-385.
- THOMPSON, R. N. & GIBSON, S. A. 1991. Subcontinental mantle plumes, hotspots and pre-existing thinspots. *Journal of the Geological Society of London*. **148**, 973-977.
- THORARINSSON, S. 1954. *The eruption of Hekla 1947-1948. II, 3, the tephra-fall from Hekla on March 29<sup>th</sup>, 1947*. Visindafelag Islendinga. Reykjavik: Leiftur.
- TROLL, V. R., DONALDSON, C. H. & EMELEUS, C. H. 2000. The Northern Marginal Zone of the Rum igneous centre: formation of the early caldera. *Bulletin of Volcanology*. **62**, 306-317.

- UI, T. 1983. Volcanic dry avalanche deposits. Identification and comparison with non-volcanic debris streams deposits. *Journal of Volcanology and Geothermal Research*. **18**, 135-150.
- UI, T. 1985. Debris avalanche deposits associated with volcanic activity: *Proceedings 14<sup>th</sup> International Conference and Field Workshop on Landslides, Tokyo, Japan*. 405-410.
- UI, T. & GLICKEN, H. 1986. Internal structural variations in a debris avalanche deposit from ancestral Mount Shasta, California, USA. *Bulletin of Volcanology*. **48**, 189-194.
- UI, T., KAWACHI, S. & NEALL, V. E. 1986. Fragmentation of debris avalanche material during flowage. Evidence from the Pungarehu Formation, Mount Egmont, New Zealand. *Journal of Volcanology and Geothermal Research*. **27**, 255-264.
- VAN BEMMELEN, R. W. 1949. *Geology of Indonesia*. The Hague.
- VARNES, D. J. 1978. Slope movement types and processes. In: *Landslides analysis and control*. National Academy of Sciences, Washington D.C. Transport Research Board Special Report. **176**, 11-33.
- VESSELL, R. K. & DAVIES, D. K. 1981. Non-marine sedimentation in an active fore-arc basin. In: ETHRIDGE, F. G. & FLORES, R. M. (eds) *Recent and ancient non-marine depositional environments: models for exploration*. SEPM Special Publication. **31**, 31-45.
- VOIGHT, B., GLICKEN, H., JANDA, R. J. & DOUGLASS, P. M. 1981. Catastrophic rockslide avalanche of May 18. In: LIPMAN, P. W. & MULLINEAUX, D. R. (eds.) *The 1980 eruptions of Mount St. Helens*. U.S. Geological Survey Professional Paper. **1250**, 347-377.
- WAGER, L. R., VINCENT, E. A., BROWN, G. M. & BELL, J. D. 1965. Marscoite and related rocks from the Western Red Hills Complex, Isle of Skye. *Philosophical Transactions of the Royal Society of London*. **A257**, 273-307.
- WALKER, B. H. & FRANCIS, E. H. 1987. High level emplacement of an olivine-dolerite sill into Namurian sediments near Cardenden, Fife. *Transactions of the Royal Society of Edinburgh, Earth Sciences*. **77**, 295-307.

- WALKER, G. P. L. 1971. Distribution of amygdale minerals in the Mull and Morvern (western Scotland). In: MURTY, T. V. V. G. R. K & RAO, S. S. (eds) *Studies in earth sciences*, West commemoration volume, 181-194.
- WALKER, G. P. L. 1973. Explosive volcanic eruptions - a new classification scheme. *Geologische Rundschau*. **62**, 431-446.
- WALKER, G. P. L. 1975. A new concept of the evolution of the British Tertiary intrusive centres. *Journal of the Geological Society of London*. **131**, 121-141.
- WALKER, G. P. L. 1984. Downsag calderas, ring faults, caldera sizes and incremental growth. *Journal of Geophysical Research*. **89**, 8407-8416.
- WALKER, G. P. L. 1993a. Basaltic-volcano systems. In: PRICHARD, H. M., ALABASTER, T., HARRIS, N. B. W. & NEARY, C. R. *Magmatic Processes and Plate Tectonics*. Geological Society Special Publication. **76**, 3-38.
- WALKER, G. P. L. 1993b. Re-evaluation of inclined intrusive sheets and dykes in the Cuillins volcano, Isle of Skye. In: PRICHARD, H. M., ALABASTER, T., HARRIS, N. B. W. & NEARY, C. R. *Magmatic Processes and Plate Tectonics*. Geological Society Special Publication. **76**, 589-597.
- WALKER, G. P. L. & BLAKE, D. H. 1966. The formation of a palagonite breccia mass beneath a valley glacier in Iceland. *Journal of the Geological Society of London*. **122**, 45-61.
- WALKER, G. P. L. & SKELHORN, R. R. 1966. Some associations of acid and basic igneous rocks. *Earth Science Reviews*. **2**, 93-109.
- WALKER, R. G. 1975. Generalised facies models for resedimented conglomerates of turbidite association. *Geological Society of America Bulletin*. **86**, 737-748.
- WALKER, R. G. (ed.) 1984. *Facies models*. 2<sup>nd</sup> edn. Geological Association of Canada, Geoscience Canada, Reprint Series 1.

- WATANABE, K. K. & KATSUI, Y. 1976. Pseudo-pillow lavas in the Aso caldera, Kyushu, Japan. *Journal of the Japanese Association of Mineralogy, Petrology and Economic Geology*. **71**, 44-49.
- WATSON, R. A. & WRIGHT, H. E. 1969. The Saidmarreh landslide, Iran. In: *U.S. contributions to Quaternary research*. Geological Society of America Special Paper. **123**, 115-139.
- WENTWORTH, C. K. & WILLIAMS, H. 1932. The classification and terminology of the pyroclastic rocks. *National Research Council, Report of the Committee on Sedimentation, Bulletin*. **89**, 19-53.
- WHITE, J. D. L., MCPHIE, J. & SKILLING, I. 2000. Peperite: a useful genetic term. *Bulletin of Volcanology*. **62**, 65-66.
- WILLIAMS, H. 1941. Calderas and their origin. *University of California Publication, Bulletin of the Department of Geological Sciences*. **25**, 239-346.
- WILLIAMS, H. 1956. Glowing avalanche deposits of the Sudbury basin. *Ontario Department of Mines, 65<sup>th</sup> Annual Report*. **65**, (3), 57-89.
- WILLIAMS, H. & MCBIRNEY, A. R. 1979. *Volcanology*. Freeman Cooper
- WILLIAMSON, I. T. & BELL, B. R. 1994. The Palaeocene lava field of west-central Skye, Scotland: Stratigraphy, palaeogeography and structure. *Transactions of the Royal Society of Edinburgh, Earth Sciences*. **85**, 39-75.
- WILLIAMSON, I. T., BELL, B. R. & JOLLEY, D. W. In prep. The Staffa Formation of the Palaeogene Mull Lava Field, NW Scotland.
- WILSON, L., SPARKS, R. S. J., HUANG, T. C. & WATKINS, N. D. 1978. The control of eruption column heights by eruption energetics and dynamics. *Journal of Geophysical Research*. **83**, 1829-1836.
- WOOLLEY, R. R. 1946. Cloudburst floods in Utah 1850-1938. *U.S. Geological Survey Water Supply Paper* 994.

- WRIGHT, J. V. & MUTTI, E. 1981. The Dali Ash, Island of Rhodes, Greece: a problem in interpreting submarine volcanogenic sediments. *Bulletin of Volcanology*. **44**, 153-167.
- WRIGHT, J. V., SMITH, A. L. & SELF, S. 1980. A working terminology of pyroclastic deposits. *Journal of Volcanology and Geothermal Research*. **8**, 315-336.
- YAMAGISHI, H. 1991. Morphological features of Miocene submarine coherent lavas from the 'Green Tuff' basins: examples from basaltic and andesitic rocks from the Shimokita Peninsula, northern Japan. *Bulletin of Volcanology*. **53**, 173-181.
- YARNOLD, J. C. 1993. Rock-avalanche characteristics in dry climates and the effect of flow into lakes: Insights from mid-Tertiary sedimentary breccias near Artillery Peak, Arizona. *Geological Society of America Bulletin*. **105**, 345-360.
- YARNOLD, J. C. & LOMBARD, J. P. 1989. A facies model for large rock-avalanche deposits formed in dry climates. In: ABBOTT, P. & COLBURN (eds.) *Conglomerates in basin analysis: a symposium dedicated to A. O. Woodford*. Society of Economic Palaeontologists and Mineralogists. **62**, 9-31.
- ZINOVIEFF, P. 1958. The basic layered intrusion and the associated igneous rocks of the central Cuillin Hills, Isle of Skye. *Unpublished D.Phil Thesis, University of Oxford*.